Design, Synthesis and Applications of Tyrosine-Derived Chiral Functionalised Polymers

Sarah A. Barron

Ph.D. Chemistry

The University of Edinburgh

September 2001

Dedicated to my parents, for their long-standing immense support.

Acknowledgements

I would like to thank my academic supervisor Dr. Alison N. Hulme for her advice and encouragement throughout my postgraduate studies and for her thorough proof-reading of this thesis. I would also like to thank my industrial supervisor Dr. Andrew Walker for his continuous input and the Engineering and Physical Sciences Research Council and Glaxo Wellcome for providing funding and giving me the opportunity to carry out this research.

In addition, I am grateful to Dr. Ian Sadler, John Millar, Wesley Kerr and Dr. David Reed for their excellent service in running the various NMR machines within the department. Thanks also go to Alan Taylor and Harry McKenzie for providing an efficient mass spectrometry service, Simon Parsons for his x-ray diffraction skills and Lorna Eades for running numerous elemental analysis samples.

I would also like to thank all the members of labs 54 and 55, both past and present, who I have been privileged to study and enjoy the odd excursion to the pub with. In particular, Karen Curley for much arm waving and general entertainment over the years, Ed Rosser for keeping me up to date with the latest cricket scores and Jenny Aird for her contribution to one of the more memorable Christmas parties.

Finally, a huge special thanks must go to my fiancé Tim for his love, support and encouragement (cooking, soothing noises, patience (?) and much needed humorous distraction) during the writing of this thesis.

Abstract

This thesis documents the design and synthesis of chiral amino alcohol monomers **161**, **162**, **167**, chiral oxazolidine monomer **168** and chiral oxazolidinone monomers **203** and **204**. The synthetic strategy relies on the key Suzuki coupling of aryl triflates derived from tyrosine with *p*-vinylphenylboronic acid where the resultant vinyl monomers are further modified to provide the desired functionality.

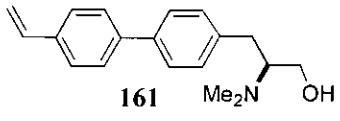

161

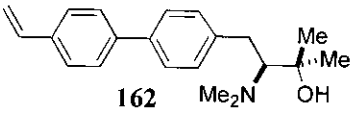

162

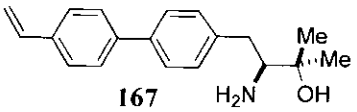

167

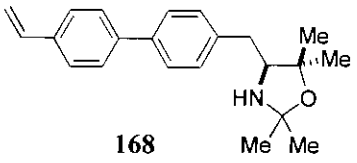

168

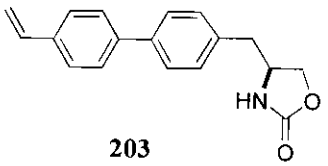

203

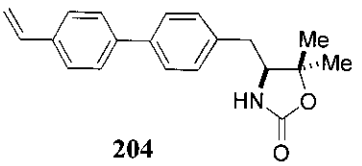

204

Model gel and macroporous-type suspension copolymerisations of styrene, divinylbenzene and vinylbenzyl chloride are investigated to allow modification of the experimental conditions to produce chloromethylpolystyrene beads **3** in optimum yield, size, shape and uniformity.

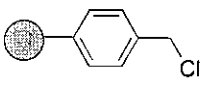

3

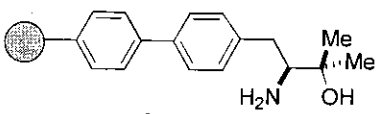

217

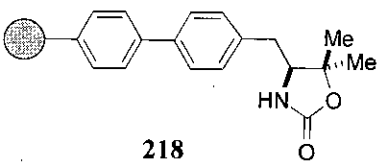

218

The chiral amino alcohol **167** and oxazolidinone **204** monomers are subsequently polymerised utilising the previously optimised suspension protocol. Characterisation of the resultant gel-type polymers **217** and **218** confirms that the functionalised monomers are successfully incorporated with the desired loading. This versatile approach to the synthesis of chiral functionalised polymers ensures that only the chiral moiety is polymer-bound thus affording complete control.

Finally, the utility of the polymer-bound amino alcohol **217** as a catalyst in the addition of dialkylzinc reagents to aldehydes and the application of the supported auxiliary **218** in asymmetric alkylation and aldol reactions are evaluated.

Contents

Chapter 1 : Introduction

Synthesis and Application of Chiral Polymers

The techniques for solid phase synthesis are mainly based on the pioneering work of Merrifield who developed a chloromethylated polystyrene resin for use in solid phase peptide synthesis.[1] Following this revelation the use of functionalised polymers has undergone a steady growth to encompass a broad range of chemistry on the solid phase.[2] Within the field of organic synthesis polymers have been employed as stoichiometric reagents,[3] catalysts and protecting groups,[4] but a continuing challenge remains to adapt solution phase reactions to work equally well on the resin.

Clearly the solid phase approach offers several distinct advantages over the analogous solution phase chemistry:

i) The reagent or catalyst can be separated from the reaction mixture thus simplifying work-up and purification procedures.
ii) Expensive ligands and transition metal catalysts can be recovered and recycled.
iii) Excess reagents can be employed to drive a solid phase reaction to completion resulting in high yields of cleaved product material.
iv) Handling of air-sensitive complexes is improved as they are frequently stabilised by attachment to a solid support.
v) Process is amenable to automation enabling the synthesis of large numbers of compounds for biological evaluation.[5]

It is clear that solid phase chemistry greatly simplifies reaction procedures providing a clean synthetic route to a wide variety of compounds, yet notable disadvantages include:

i) The reaction conditions are restricted in that the solvent must swell the polymer and the reagents / reaction temperature must be compatible with the support.
ii) The inability to directly monitor the progress of a reaction on the solid phase.

iii) Problems are also associated with characterisation of the functionalised polymer product as the normal methods of analysis are not applicable.

The scope of solid phase organic synthesis has been widely documented as a means to generate both single compounds and extensive combinatorial libraries,[6] with expanded reviews incorporating the development of linker design and cleavage strategies.[7]

1.1 Definition of Main-Chain and Side-Chain Chirality

The synthetic approach to chiral polymers can be divided into two main categories. Main-chain chiral polymers incorporate chirality within the main-chain of the polymer where such inherent chirality results from secondary structure. In this instance the chirality is established prior to polymer formation with the use of chiral precursor monomer species. The second important class of side-chain chiral polymers incorporates chirality within the polymer pendant side-chains. As the area of main-chain chirality has recently been reviewed,[8] this introduction focuses on the previously unexamined field relating to the synthesis and application of side-chain chiral polymers.[4c]

1.2 Side-Chain Chiral Polymers

Side-chain chiral polymers can be prepared *via* the direct polymerisation of chiral vinyl monomer units or alternatively chirality can be induced at a post polymerisation stage by anchoring a chiral species to an achiral polymer-support.

1.2.1 Polymerisation Route to Side-Chain Chiral Polymers

This method of polymer preparation is defined as the addition of unsaturated molecules through their multiple bonds. In the context of side-chain chiral polymers the most commonly used unsaturated compounds contain carbon-carbon double

bonds in the form of functionalised chiral styrene monomers. As such styrene compounds will be used to illustrate the concepts of polymerisation where the chiral functionality will be represented by the pendant side-chain group, R.

A distinct advantage of this polymerisation approach results from the ability to analyse and unambiguously ascertain the structure of the chiral functionalised monomer prior to polymerisation. In addition the loading of the chiral monomer can be controlled by varying the molar ratio of comonomers employed. For example, direct homopolymerisation of the chiral monomer **1** allows the synthesis of a polymer where each segment carries the chiral moiety. Whereas, copolymerisation with styrene **2** affords a product where only a fraction of the segments possess the chiral pendant group, **scheme 1**.

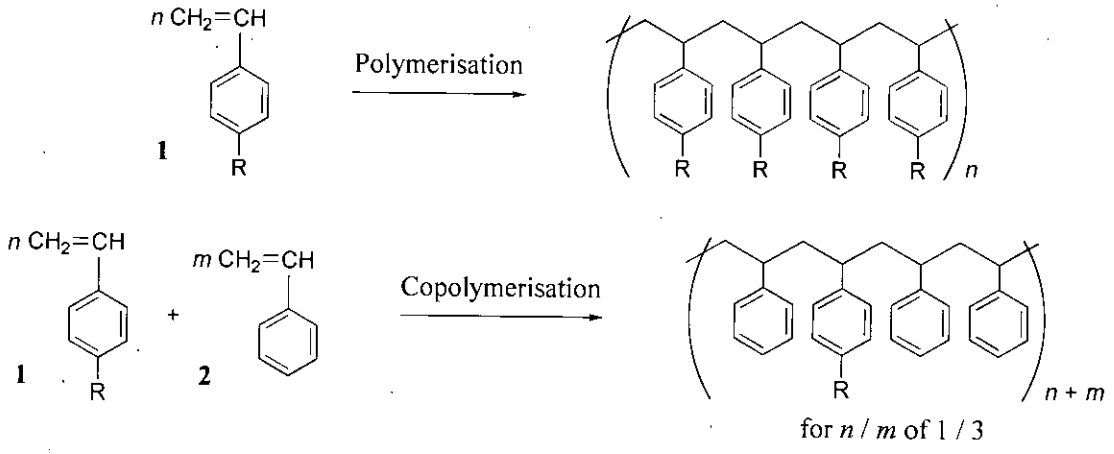

Scheme 1

Unfortunately the copolymerisation procedure often requires considerable manipulation to optimise the yield and form of the required copolymer beads.

Styrene monomers are frequently polymerised to high molecular weight polymers using free radical, cationic or anionic[9] initiators where the nature of the active species determines the method of polymerisation,[10] **scheme 2**.

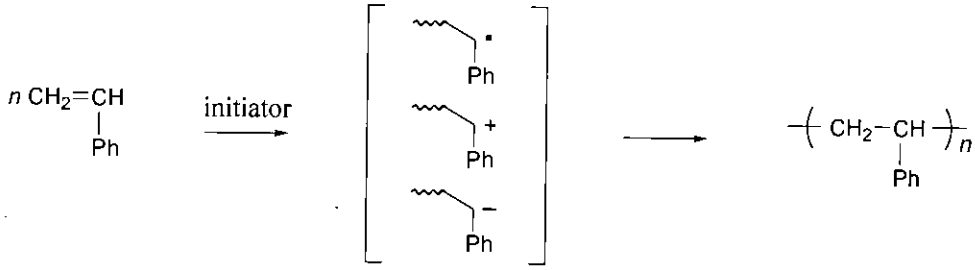

Scheme 2

In each case the initiator converts the unreactive styrene monomer to an active species which is capable of starting the polymerisation. Propagation then follows to generate the high molecular weight polymer with termination causing deactivation to produce the final stable polymer. These elementary reactions which constitute the mechanism of polymerisation will be illustrated employing azobisisobutyronitrile as a typical free radical initiator in **chapter 4**.

The degree of cross-linking and the conditions employed during the polymerisation reaction determine the structure and properties of the functionalised polymer. The polymer can broadly be categorised as either a linear polymer, or as a gel / macroporous polymer where the linear chains are essentially interconnected to generate an insoluble resin.

1.2.1.1 Linear Polymers

Linear polymers are capable of dissolution in an appropriate solvent as they are produced *via* the addition copolymerisation of a vinyl monomer in the absence of a cross-linking reagent.

Advantages associated with the use of linear soluble polymers arise from the fact that their reactions are carried out in solution as a homogenous system, which results in good diffusion of solvents and reagents with equal accessibility to all of the functional groups on the polymer. However, subsequent separation of the polymer from the reaction mixture requires membrane filtration or addition of a poor-solvent to precipitate the polymer which is often difficult to achieve.

1.2.1.2 Gel Resins

Gel resins are generally prepared by the suspension copolymerisation of a vinyl monomer in aqueous medium in the presence of a suspension stabiliser and a cross-linking reagent. This methodology will be discussed in more detail in **chapter 4**. Critically low levels of the divinyl comonomer (0.5-2.0%) are employed to ensure that the polymer chains remain very mobile with extensive swelling being observed in appropriate solvents. This results in the inner reactive groups being exposed to the soluble reagents allowing the functional groups on the polymer beads to essentially react as if they were in solution. Thus, the insolubility of the resin does not translate to a lack of reactivity and is beneficial as the spherical beads can simply be isolated by filtration and washing with various solvents. However, one of the limitations involves the poor mechanical strength of the lightly cross-linked resins where degradation can occur to produce soluble linear fragments.

1.2.1.3 Macroporous Resins

The synthesis of macroporous resins differs from that of gel resins in that notably higher levels of cross-linking reagent (up to 60%) are employed. This results in a more rigid network where the mobility of the chains and hence the swelling capability is reduced. However, the reactivity of the polymer is unaffected due to the inclusion of an inert solvent which acts as a template during the polymerisation process to create porous beads on removal of the solvent. The large surface area which results from this process is essential for reactivity allowing penetration of solvents and reagents throughout the pores in a homogeneous manner. The increased cross-link ratio improves the mechanical stability of the polymer matrix allowing it to retain large solvent volumes, yet macroporous resins remain prone to disintegration forming undesirable fine particles on repeated handling.

1.2.2 Polymer Functionalisation Route to Side-Chain Chiral Polymers

Functionalised side-chain chiral polymers are frequently prepared *via* the chemical modification of pre-formed polymers. This approach has the advantage of not requiring the synthesis of an elaborate comonomer, nor the problem of producing a suitable product by polymerisation of this. The ease of chemical modification of a resin can often depend on the physical properties of the resin itself, and the support and solvent medium must be carefully chosen to ensure adequate diffusion of reagents into the reactive sites. Negative aspects of this route include the inability to accurately control the loading of the modified resin, particularly where conversions are not quantitative or unwanted side-reactions occur. In addition it can also be difficult to adequately characterise those structural changes which have taken place, with some chemical transformations being notoriously unreliable and capricious to reproduce.

The vast majority of side-chain chiral polymers have been synthesised by the chemical modification of pre-formed cross-linked polystyrene as it meets many of the requirements of a solid support:

i) Very pure polystyrene resins in bead form with good mechanical stability and well defined physical characteristics are available commercially.

ii) Polystyrene resins can be used with a wide range of polar and apolar solvents withstanding reaction temperatures from -78 °C to 155 °C, and the support is also compatible with a broad range of reagents.[6a]

iii) The aliphatic backbone of the polymer is unreactive and thus the polymer is not overly susceptible to degradative chain scission, whereas in contrast the reactive aromatic rings readily undergo functionalisation.

The two most versatile routes in the chemical modification of styrene resins are *via* chloromethylation and lithiation.[11] Together these two routes provide a method of attaching a wide variety of both nucleophilic and eletrophilic species, thus introducing a diverse range of functionality onto the solid support, **scheme 3**.

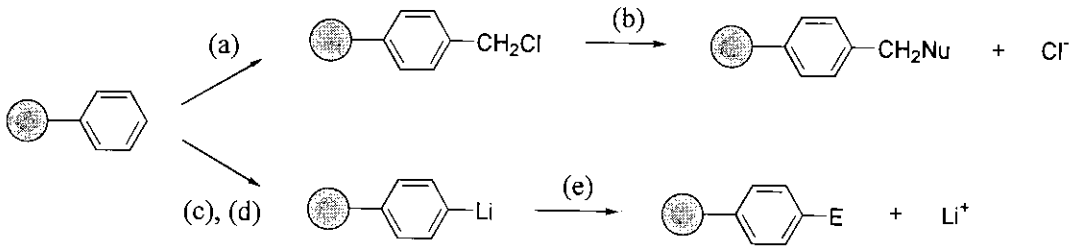

(a) $ClCH_2OCH_3$, $SnCl_4$; (b) Nu^-; (c) Br_2, $Tl(OAc)_3$; (d) *n*-BuLi; (e) E^+.

Scheme 3

In addition to chloromethylated Merrifield resin **3** a range of other supports are commercially available.[5] Wang resin **4** prepared by the treatment of Merrifield resin with 4-hydroxybenzyl alcohol is frequently used to attach carboxylic esters by esterification with a coupling reagent. The Rink amide resin **5** is also used to anchor carboxylic acids generating a carboxamide linkage. In each case cleavage of the modified component is effected with trifluoroacetic acid, **figure 1**.

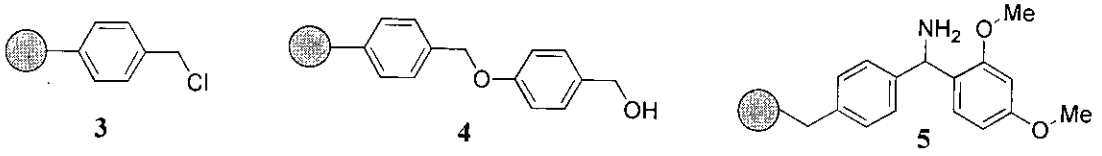

Figure 1

Poly(ethylene glycol) **6** commonly named PEG resin provides a support which is freely permeable to larger molecules and enzymes. Poly(ethylene glycol) has also been adapted to the role of a flexible cross-linker in the development of novel resins.[12] Tentagel **7** is synthesised by grafting poly(ethylene glycol) onto a polystyrene resin through an ether linkage. Due to the hydrophilic nature of the support it is particularly useful for biotransformation reactions that occur in water. Silicon traceless linkers **8** are invaluable where the modified group can be cleaved with acid to leave no clue as to the point of resin attachment, **figure 2**.

Inorganic oxides such as silica **9** have an abundance of surface hydroxyl groups which can be utilised in attaching other functional groups to the support. Functionalised silicates provide a chemically and mechanically stable support which

is especially useful for catalytic reactions that must be carried out under severe reaction conditions, **figure 2**.

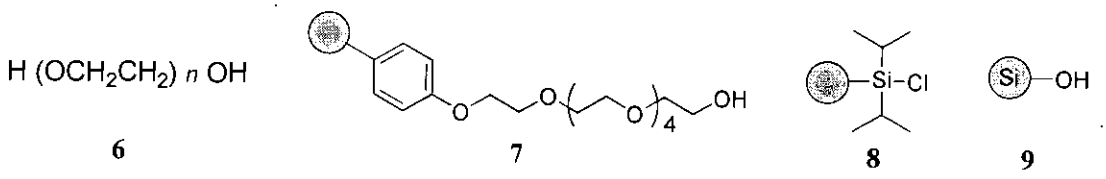

6 **7** **8** **9**

Figure 2

1.2.3 Polymer-Supported Chiral Auxiliaries

The attachment of a chiral auxiliary to the solid support effectively converts the polymer into an asymmetric carrier species. The substrate is covalently bound to the solid support and the asymmetric transformation is then determined by the inherent chirality of the auxiliary. Cleavage releases the chiral product to leave the polymer which can potentially be removed and recycled.

The first report of a functionalised polymer being utilised as a chiral auxiliary was published in 1972 by Kawana *et al.*[13] The polymer-support **10** was prepared by attaching a xylofuranose sugar to polymeric equivalent of trityl chloride, reaction with phenyl glyoxyl chloride gave the fully protected sugar **11**. Asymmetric Grignard addition of a methyl group to the ketone carbonyl and subsequent hydrolytic cleavage afforded the optically active (*R*)-atrolactic acid **12**, **scheme 4**. The acid was obtained in higher chemical and optical yield than was possible with a similar reaction performed in solution, thus indicating that the conformational rigidity of the polymer-bound material had contributed to the enhancement of stereochemical selectivity.

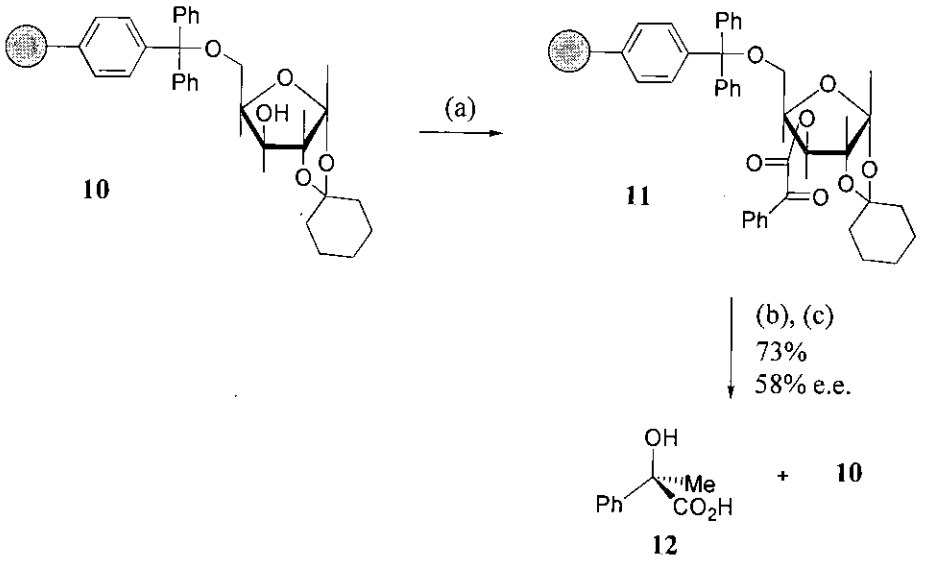

(a) PhCOCOCl; (b) MeMgI; (c) aqueous KOH followed by treatment with H^+.

Scheme 4

The concept of asymmetric synthesis on the solid phase was further developed by Leznoff *et al.* who used a polymer-bound chiral amine **13** prepared from Merrifield resin to synthesise chiral 2-alkylcyclohexanones.[14] Reaction of the chiral auxiliary **13** with cyclohexanone under dehydrating conditions gave the chiral alkoximine **14**. After alkylation with lithium diisopropylamide and methyl iodide followed by cleavage under acidic conditions, (*S*)-2-methylcyclohexanone **15** was obtained in high yield with excellent enantioselectivity, **scheme 5**. The chiral polymer **13** was isolated by filtration and although the e.e. of the product **15** remained unchanged in subsequent reaction cycles, reduced yields were obtained.

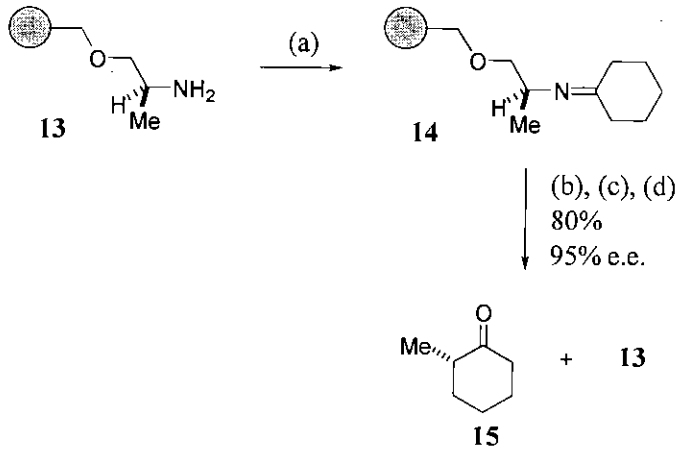

(a) Cyclohexanone; (b) LDA; (c) MeI; (d) aqueous H^+.

Scheme 5

1.2.3.1 Oxazoline Auxiliaries

Enantiopure oxazolines have been utilised as chiral auxiliaries for the synthesis of optically active carboxylic acids and other functional derivatives.[15] McManus *et al.* investigated the possibility of transferring the auxiliary to the solid phase by attaching a chiral oxazoline to Merrifield resin **16**.[16] Metallation with *n*-butyllithium followed by alkylation with benzyl chloride and acid catalysed ethanolysis afforded (*S*)-ethyl-2-methyl-3-phenylpropanoate **17** in lower chemical and optical yield than the analogous solution phase reaction, **scheme 6**. The reduced yield resulted from incomplete hydrolysis of the chiral ester from the support, where harsher conditions were found to also cleave the amino alcohol residue *via* the benzylic ether linkage, thus the recycling of **18** was not feasible.

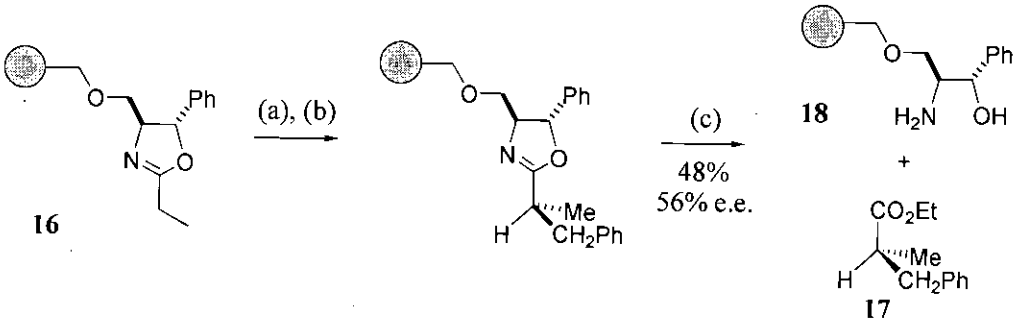

(a) *n*-BuLi; (b) $PhCH_2Cl$; (c) H_2SO_4, EtOH.

Scheme 6

1.2.3.2 Pyrrolidine Auxiliaries

Kurth *et al.* superseded prior publications by preparing chiral auxiliaries which could be repeatedly used over a number of cycles without compromising activity. The *N*-acylated chiral pyrrolidine **19**[17a] and C_2-symmetric pyrrolidine **20**[17b] auxiliaries underwent enolate alkylation with deprotection by iodolactonisation to afford the non-racemic γ-butyrolactones in moderate yield and high diastereoselectivity, **figure 3**.

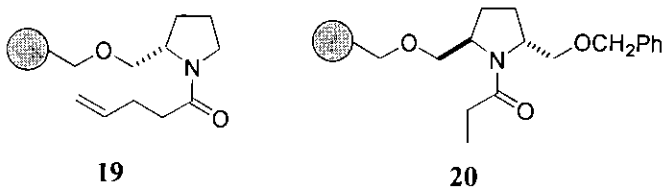

Figure 3

1.2.3.3 Oxazolidinone Auxiliaries

The asymmetric transformation of acyl fragments is most commonly achieved using the highly versatile chiral oxazolidinone auxiliary pioneered by Evans.[18] Analogous polymer-auxiliaries have also been used to carry out asymmetric enolate alkylation, aldol condensation, conjugate addition and Diels-Alder reactions on the solid phase.[19] Deprotection under mild non-destructive conditions allowed cleavage of the optically pure products as acids, esters or alcohols depending on the conditions

employed. Results comparable with the corresponding solution phase work have been obtained although few attempts were made to recycle the auxiliaries.

The following discussion focuses on the applications of polymer-bound chiral auxiliaries rather than their synthesis. In general the chiral oxazolidinones are formed by cyclisation of an enantiopure α-amino alcohol with either phosgene or diethyl carbonate providing the carbonyl functionality. Similarly *N*-acylation is achieved by reacting the oxazolidinone with an acyl chloride or an acid anhydride. However, there appears to be no specific stage in the synthesis when the chiral moiety is attached to the solid support.

1.2.3.3.1 Alkylation Reaction

The first preparation and application of a polymer-bound chiral oxazolidinone was reported in 1996 by Allin *et al.*[19a] The Merrifield supported auxiliary **21** was prepared in six steps from commercially available *L*-serine methyl ester. Treatment of the propionylated resin with lithium diisopropylamide gave the chelated *Z*-enolate which was quenched with benzyl bromide affording the alkylated adduct **22**. Base hydrolysis provided the chiral α-alkyl carboxylic acid **23** and effectively regenerated the auxiliary **24**, **scheme 7**. The mechanistic details of the asymmetric alkylation reaction will be detailed in **chapter 7.1.2.**

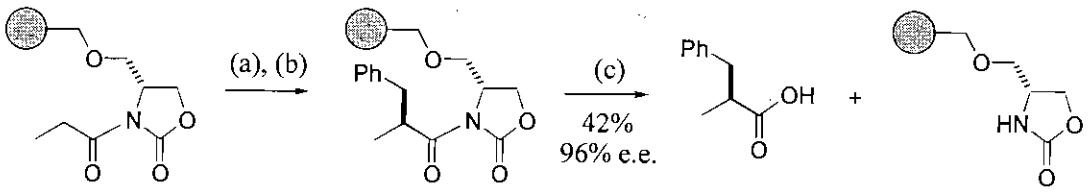

(a) LDA; (b) $PhCH_2Br$; (c) aqueous $LiOH{\bullet}H_2O$ followed by treatment with H^+.

Scheme 7

Burgess *et al.* prepared a polymer-bound chiral auxiliary derived from *L*-tyrosine where the phenolic hydroxyl group was used to anchor the auxiliary

directly to the support **25**.[19b] In order to investigate how the resin type affects the yield and stereoselectivity of the asymmetric alkylation reaction the auxiliary was attached to Merrifield, Wang and Tentagel resins. Deprotonation with lithium diisopropylamide and reaction with benzyl bromide was chosen as the model transformation with reductive cleavage affording the α-alkylated alcohol **26**, **figure 4**. It was concluded that Wang resin gave superior performance in terms of yield (66%) and enantioselectivity (90%), where this support also offered the highest loading capacity. Furthermore, the length of alkylation time was found to be significant, as a general decrease in yield was observed after prolonged reaction which was ascribed to premature release of some material from the resin.

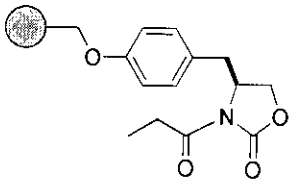

25

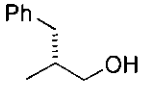

26

Figure 4

1.2.3.3.2 Aldol Reaction

The solid-supported chiral auxiliary **27** was used for the enantioselective aldol synthesis of the α-substituted-β-hydroxy ester **28**.[19c] The *L*-tyrosine derived auxiliary was again attached to Wang resin by means of a Mitsunobu coupling reaction *via* the phenolic hydroxyl group. The auxiliary was enolised by treatment with *n*-dibutylboron triflate and diisopropylethylamine before being condensed with isovaleraldehyde to furnish the aldol adduct **29**. Cleavage with sodium methoxide generated the ester **28** in 90% d.e. (yield not quoted) as determined by ^{1}H NMR and chiral HPLC analysis, **scheme 8**. The major component was the expected Evans *syn* diastereomer, thus the stereochemical integrity of the oxazolidinone auxiliary is maintained on the solid phase. The mechanistic details of the asymmetric aldol reaction will be detailed in **chapter 7.1.1**.

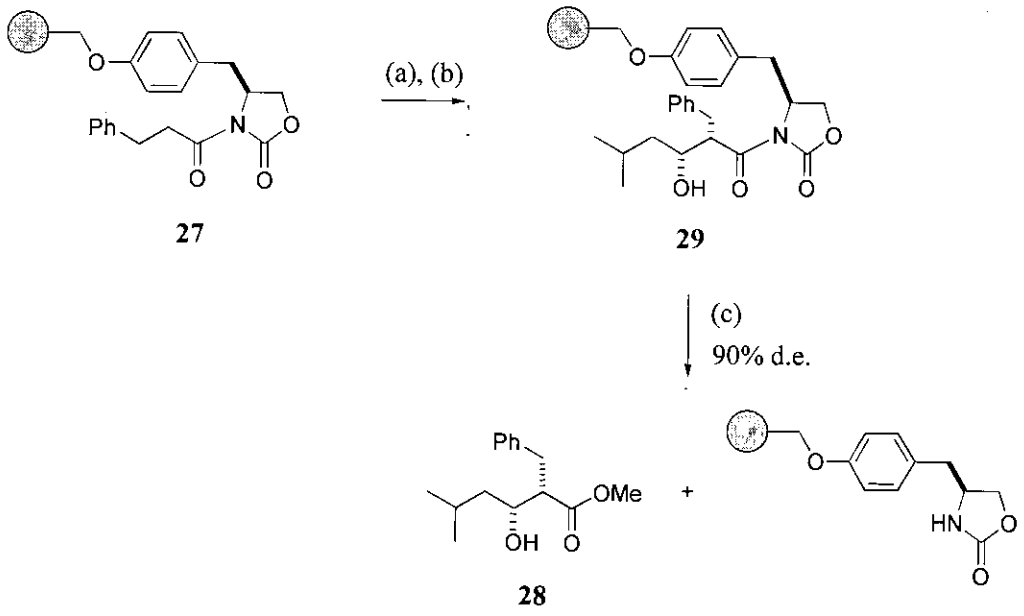

(a) n-Bu_2BOTf, DIPEA; (b) $(CH_3)_2CHCH_2CHO$; (c) NaOMe.

Scheme 8

Abell *et al.* reported the application of a similar *L*-tyrosine derived auxiliary bound to hydroxymethyl resin **30**.[19d] Enolisation of the *N*-acylated polymer was driven to completion using an excess of *n*-dibutylboron triflate and triethylamine, where the surplus reagents were removed by washing the resin prior to condensation with benzaldehyde. Treatment of the resulting aldol adduct **31** with lithium hydroxide afforded the acid **32** in 63% yield where only the *syn* diastereomer was detected by ^{1}H NMR. The acid **32** was further derivatised by reaction with (*S*)-1-phenylethylamine[20] to generate the amide **33** which was shown to be a single diastereomer by chiral HPLC, thus illustrating the excellent stereoselectivity of the aldol reaction on the solid phase, **scheme 9**.

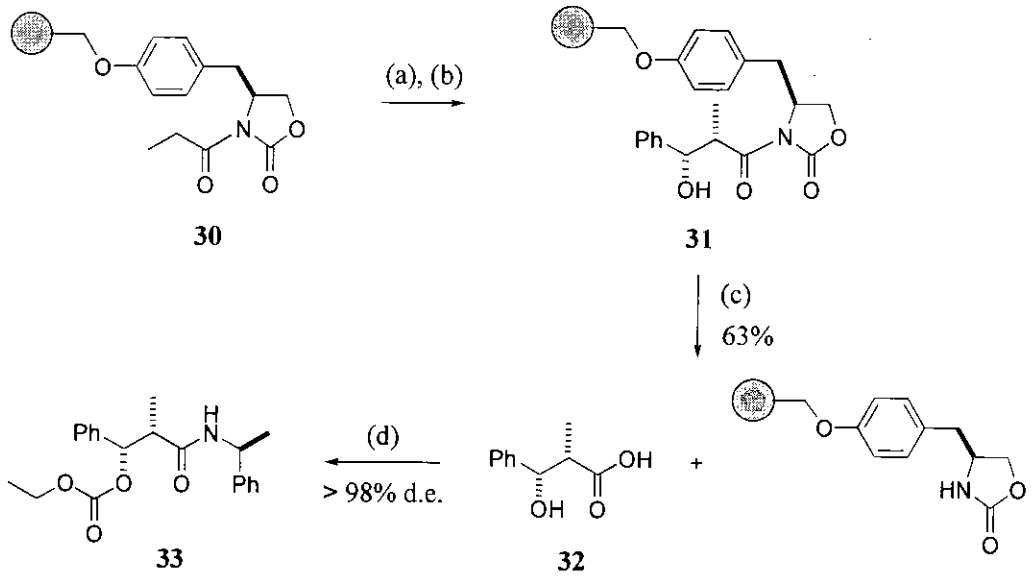

(a) *n*-Bu_2BOTf, Et_3N; (b) PhCHO; (c) LiOH followed by treatment with H^+; (d) $ClCO_2Et$, Et_3N, (*S*)-1-phenylethylamine.

Scheme 9

Polyketide libraries have also been created using asymmetric aldol methodology on the solid phase. This approach involved the reaction of a polymer-bound aldehyde obtained from the oxidation of Wang resin with a chiral oxazolidinone boron enolate. Reductive cleavage of the auxiliary *via* generation of the Weinreb amide provided the key transformation to regenerate the aldehyde functionality.[21] Despite providing an interesting variation of the solid phase aldol reaction, the support functions as a polymer-bound reagent and does not satisfy the criteria of a chiral polymer-bound auxiliary.

1.2.3.3.3 Conjugate Addition Reaction

Abell *et al.* also reported the first instance of a conjugate addition reaction proceeding on the solid phase with stereochemical control.[19d] The previously discussed polymer-bound chiral auxiliary **30** was enolised with excess $TiCl_3$(O*i*-Pr) and diisopropylethylamine before treatment with acrylonitrile. The addition adduct **34** was cleaved from the resin using lithium hydroxide to liberate the chiral acid **35** in moderate yield and 78% enantiomeric excess as determined by conversion to the amide **36** with (*S*)-1-phenylethylamine,[20] **scheme 10**.

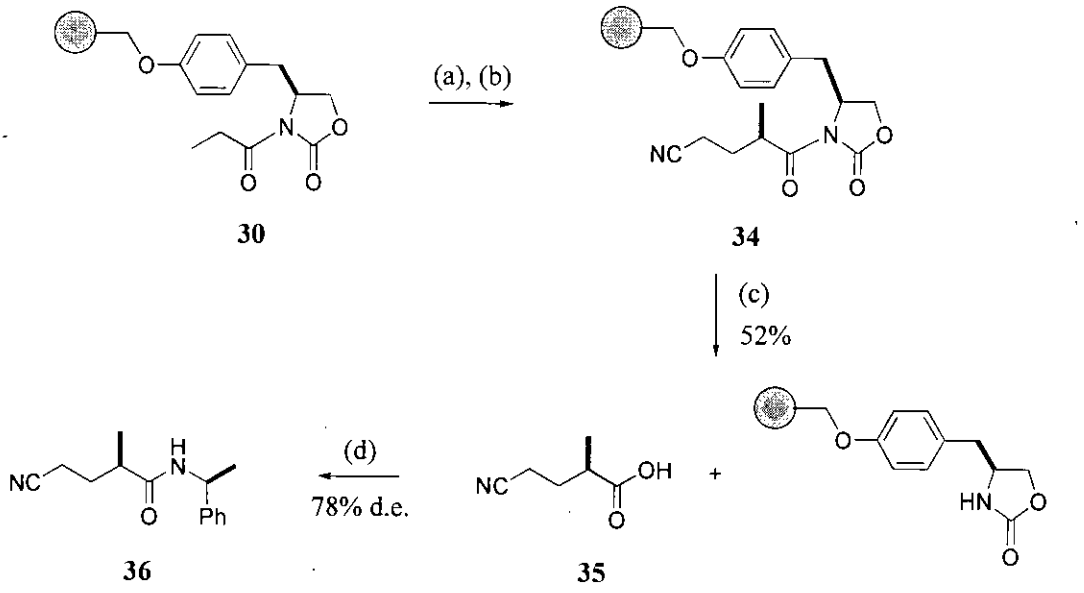

30 **34** **36** **35**

(a) $TiCl_3(O\textit{i}\text{-Pr})$, DIPEA; (b) CH_2CHCN; (c) LiOH followed by treatment with H^+, (d) $ClCO_2Et$, Et_3N, (*S*)-1-phenylethylamine.

Scheme 10

1.2.3.3.4 Diels-Alder Reaction

The hydroxymethyl polymer-bound oxazolidinone crotonate **37** was found to undergo efficient Diels-Alder cycloaddition with cyclopentadiene in the presence of diethyl aluminium chloride.[19e] This illustrates the first application of an asymmetric Diels-Alder transformation on the solid phase. Exposure of the adduct to lithium benzyloxide gave the desired *endo* Diels-Alder adduct **38** in good yield with an enantiomeric excess of 86%, **scheme 11**. These results were found to compare favourably with the analogous solution chemistry.

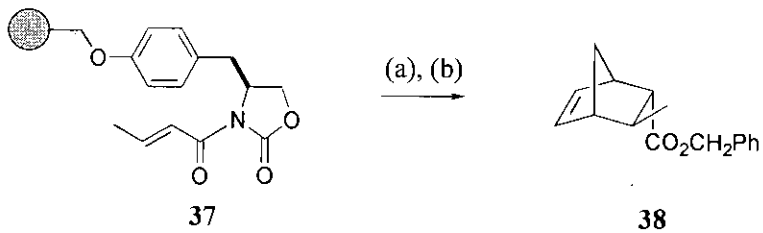

37 **38**

(a) Cyclopentadiene, Et_2AlCl; (b) $LiOCH_2Ph$.

Scheme 11

The nature of the resin was found to be critical to the success of the asymmetric transformation. The analogous Wang supported oxazolidinone crotonate failed to generate any of the desired Diels-Alder adduct due to the instability of the resin to the Lewis acid conditions employed.

Note that all of the previously discussed polymer-bound oxazolidinone auxiliary reports stated the obvious attractions of a recyclable chiral auxiliary, but it is not clear if any attempts were actually made to re-use the various supports.

1.2.3.3.5 1,3-Dipolar Cycloaddition Reaction

It has recently been demonstrated that the chiral resin-bound oxazolidinone can act as a chiral dipolarophile, facilitating asymmetric dipolar addition reactions on the solid support.[19f] The chiral oxazolidinone was again derived from *L*-tyrosine and grafted onto both Merrifield and Wang resin, where the acylated crotonate resin **37** was shown to react with the 1,3-dipoles, mesitonitrile oxide **39** and diphenylnitrone **40**. The cycloadducts **41**, **42**, **43**, and **44** were reductively cleaved from the resin using sodium borohydride conditions that have been shown to result in little racemisation in the solution phase,[22] **scheme 12**.

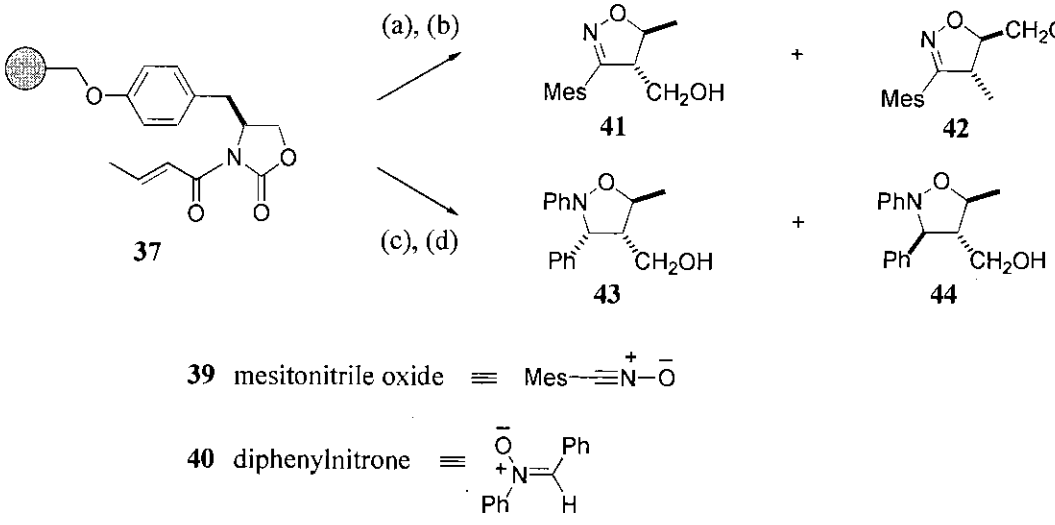

(a) Mesitonitrile oxide; (b) $NaBH_4$; (c) diphenylnitrone; (d) $NaBH_4$.

Scheme 12

The cycloaddition reactions with mesitonitrile oxide **39** were shown to give similar yields and regioisomer product ratios to those of the free auxiliary. In contrast the corresponding reactions with diphenylnitrone **40** gave reduced stereochemical control and considerably lower yields as a result of decomposition of the dipolar reagent. The recovered Merrifield supported chiral oxazolidinone was functionalised and re-used in further cycloadditions with comparable success. However, the Wang supported analogue gave diminished selectivity, thus establishing Merrifield resin as the preferred support for optimum recycling potential.

1.2.4 Polymer-Supported Chiral Catalysts

A polymer-supported catalyst involves a conventional catalytic species being attached to a solid support and subsequently being used in catalytic quantities relative to the reaction substrate. A variety of polymer-supported catalysts that effect unique transformations of various organic substrates have been developed. In some cases it has been shown that these reactions can be carried out more effectively by attachment of the catalytic moiety to the resin.

1.2.4.1 Jacobsen Epoxidation Catalyst

Polymer-supported Jacobsen chiral Mn (III) (salen) complexes have assumed considerable importance as enantioselective catalysts for the epoxidation of internal non-functionalised *cis*-alkenes. This research was necessitated by the expensive and unstable nature of the soluble salen catalysts which are prone to oxidative destruction effectively negating any recycling potential.

Initial attempts to prepare a polymer-bound Jacobsen catalyst focused on the use of styryl derived chiral ligands which resulted in the synthesis of di-styryl monomers due to the inability to prepare non-symmetric salen ligands.[23] Polymerisation afforded functionalised polymers where the ligands were incorporated as the cross-links **45**[23b] and **46**[23d], **figure 5**.

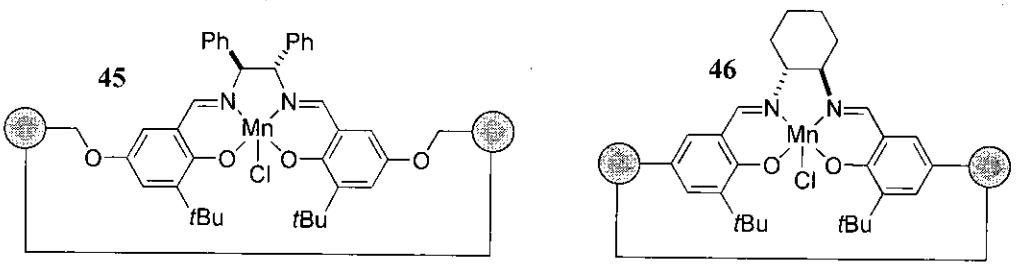

Figure 5

In the latter case the chiral cross-linked polymer **46** was used to induce the asymmetric epoxidation of *cis*-β-methylstyrene **47** using *m*-chloroperbenzoic acid and *N*-methylmorpholine *N*-oxide as the optimised oxidant combination, **scheme 13**.[23d] The activity of the catalyst was not impaired by attachment to the solid support affording predominantly the *cis* epoxide **48** in high yield. However enantiocontrol was poor (41% e.e.) as a result of steric restrictions with the imobile catalytic species situated on the polymer cross-link.

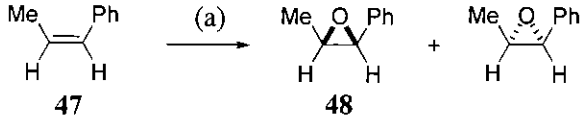

47 **48**

(a) Polymer-bound Jacobsen epoxidation catalyst **46**, *m*-chloroperbenzoic acid, *N*-methylmorpholine *N*-oxide.

Scheme 13

Sherrington *et al.* have developed a number of analogous polymer-supported Jacobsen epoxidation catalysts with the emphasis on ensuring site isolation of the catalyst to minimise deactivation caused by dimerisation to μ-oxo-manganese (IV) species. Pendant chiral attachment of the chiral salen ligand was also a crucial factor considered to improve the activity of the catalyst.[24] These criteria were attained by developing a low loading catalyst where the ligand was essentially constructed on the polymer, **scheme 14**.

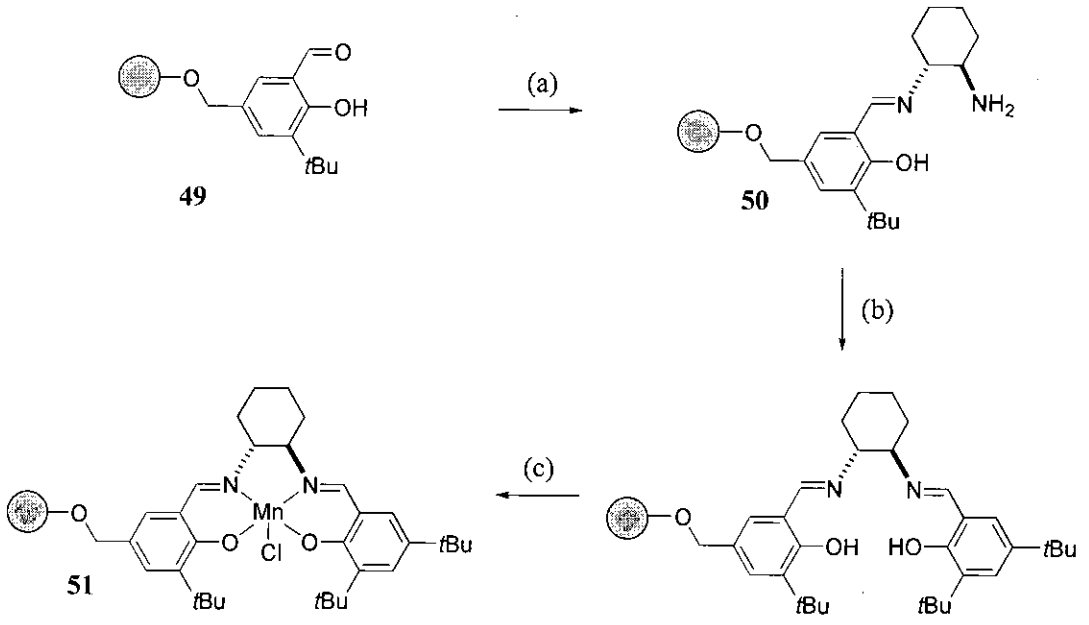

(a) (*R*,*R*)-1,2-Diaminocyclohexane; (b) 2,4-di-*t*-butylsalicylaldehyde; (c) $Mn(OAc)_2 \cdot 4H_2O$, air, LiCl.

Scheme 14

The polymer-bound salicylaldehyde **49** was condensed with enantiomerically pure *trans*-1,2-diaminocyclohexane. The resultant chiral polymer **50** was condensed with di-*t*-butylsalicylaldehyde and complexed with Mn (II) acetate / LiCl to afford the chiral polymer-supported salen epoxidation catalyst **51**. The activity and selectivity of the catalyst were investigated for the epoxidation of 1-phenylcyclohex-1-ene using a range of supports. Optimum yields and enantioselectivities comparable with the solution phase Jacobsen catalyst (72% yield, 92% e.e.) were obtained when a porous methacrylate-based resin was employed (49% yield, 91% e.e.). This result was rationalised by the improved local mobility of the resin relative to styrene-based analogues and the significantly higher polarity of the support.

Unfortunately, the catalysts performance was shown to be very substrate dependant, and a decrease in catalytic activity and selectivity was observed on recycling the resin potentially owing to the fragile nature of the catalyst itself.

Recently, Janda *et al.* attached the known unsymmetrical Mn salen Jacobsen ligand to hydroxymethyl resin through a glutarate spacer **52**, **figure 6**.[25] This spacer unit ensured that the catalyst was positioned away from the polymer backbone

allowing easy access of the alkene substrate to the active metal centre. Another design feature incorporated the use of flexible polytetrahydrofuran cross-linkers which have been shown to increase the swelling capacity of the resultant polymerised resin.[12] The increased interaction between solvent and resin appears to have improved the enantioselectivity of the epoxidation catalyst as results comparable with the homogeneous Jacobsen catalyst were obtained. Furthermore, the catalyst could be re-used in three cycles before a significant decline in enantioselectivity or yield was observed.

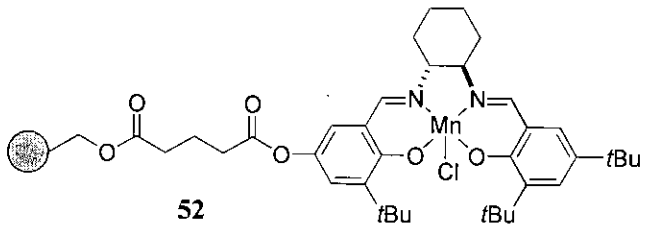

52

Figure 6

1.2.4.1.1 Membrane Immobilised Catalyst

In order to improve recovery of the Jacobsen catalyst, Vankelecom *et al.* have immobilised the Mn salen catalyst in elastomeric polydimethylsiloxane membranes.[26] The heterogeneous catalyst is physically trapped inside a hydrophobic membrane where the pores are too small to permit it to escape. As the catalyst is not covalently bound to the membrane it essentially reacts as if it were in solution providing catalytic activity, product, and enantiomeric selectivity as in the homogeneous case. The membrane immobilised Jacobsen asymmetric epoxidation catalyst does not constitute a main-chain nor a side-chain chiral polymer, but the potential application of the regenerable catalyst in large scale industrial synthesis is noteworthy.

1.2.4.2 Sharpless Epoxidation Catalyst

Sharpless main-chain linear polytartrate esters **53** where the optically active ligand forms a component of the polymer backbone were synthesised *via* the acid

catalysed polycondensation of *L*-(+)-tartaric acid **54** with a range of diols **55**, **scheme 15**.[27a]

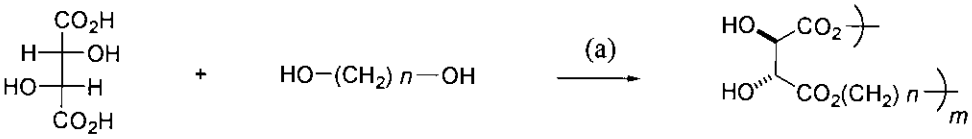

54 **55** **53**

(a) Toluene-*p*-sulphonic acid.

Scheme 15

The model allylic alcohol substrate, *trans*-hex-2-en-1-ol **56** underwent asymmetric epoxidation in the presence of titanium tetraisopropoxide with *tert*-butyl hydropropoxide as the oxidant. The highest yield (92%) and e.e. (79%) of the target epoxide **57** were observed using the polytartrate ester ligand condensed with octane-1,8-diol ($n = 8$), **scheme 16**.

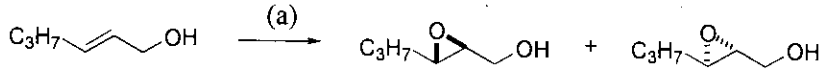

56 **57**

(a) Polymer-bound Sharpless epoxidation catalyst **53**, Ti(O*i*-Pr)$_4$, *t*BuOOH.

Scheme 16

The research was extended to include insoluble branched / cross-linked polyesters **58** generated in a similar manner employing anaerobic and more forcing condensation conditions, **figure 7**.[27b] The branched systems gave higher levels of asymmetric induction than the soluble linear analogues where the heterogeneous nature of the catalyst also facilitated work-up procedures. However, the cross-linked insoluble 3D polyesters afforded the epoxidation product with reduced enantioselectivity as formation of the titanium complex was inhibited.

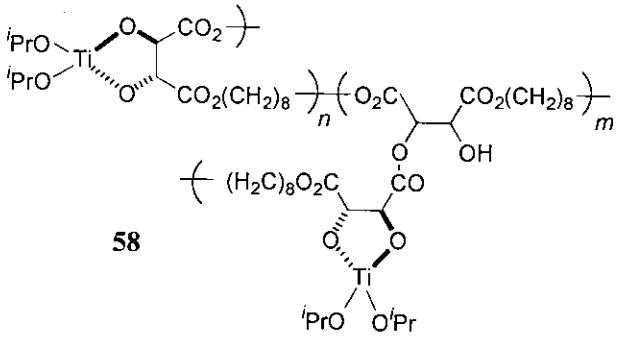

58

Figure 7

In addition to these systems, chiral side-chain epoxidation catalysts were investigated to mimic the Sharpless tartrate ester / Ti (IV) / hydropropoxide system for the epoxidation of allylic and related alcohols. Farrall *et al.* immobilised tartrate residues on 1% cross-linked polystyrene **59** and employed the polymeric ligand in the asymmetric epoxidation of geraniol, **figure 8**. The corresponding epoxide was typically obtained in 60-70% yield and 50-60% enantiomeric excess and the polymer-bound catalyst was amenable to recyling.[28]

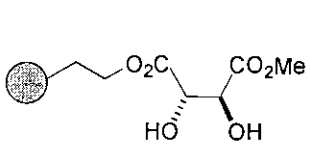

59

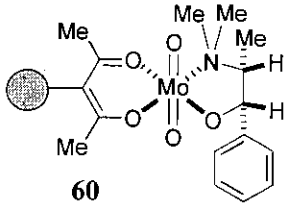

60

Figure 8

A later report by Cazaux *et al.* utilised a polymer-supported chiral Mo (VI) catalyst **60** again selecting geraniol as the allylic epoxidation substrate, **figure 8**. In agreement with analogous solution phase studies the Mo (VI) complex was found to be less selective that the aforementioned Ti-tartrate complexes. The polymer catalyst was also found to be unstable with loss of molybdenum during the epoxidation reaction.[29]

1.2.4.3 Sharpless Dihydroxylation Catalyst

Sharpless later developed the cinchona alkaloid catalytic system for the asymmetric dihydroxylation of alkenes generating optically pure vicinal diols. The main disadvantages associated with this system include the use of toxic osmium tetroxide and the high cost of preparing the catalyst. To address these inherent problems and facilitate recycling of the catalyst several attempts have been made to attach the cinchona alkaloid ligand to an insoluble support. However, initial studies were disappointing exhibiting low yields and poor enantioselectivity with extended reaction times required. A comprehensive review of chiral Sharpless polymer-bound dihydroxylation catalysts from 1990-1997 has been published by Shuttleworth *et al.*[2a] Notable omissions and more recent developments are described below.

Janda *et al.* attached the dihydroquinidine cinchona alkaloid ligand to a soluble polyethylene glycol monomethyl ether support **61**, **figure 9**.[30] It was postulated that the solubility of the PEG-support would improve the activity of the catalyst by enabling all of the reaction components to interact freely with each other in solution.

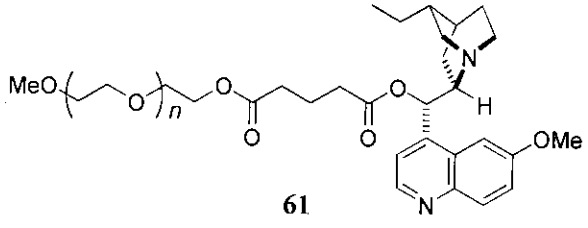

61

Figure 9

The polymer-bound ligand was employed in the asymmetric dihydroxylation of *trans*-β-methylstyrene **62** affording the chiral diol **63** in 80% yield and 84% e.e., **scheme 17**. With a range of alkene substrates the catalyst exhibited similar reactivity and enantioselectivity to the original Sharpless system suggesting that the PEG backbone does not influence or affect the observed asymmetric induction. Furthermore, the polymer could subsequently be recovered by precipitation and recycled with no loss of reaction yield or selectivity.

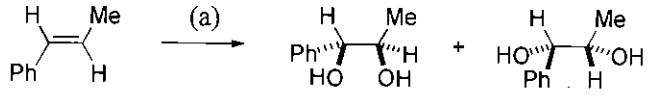

62 63

(a) Polymer-bound Sharpless dihydroxylation catalyst **61**, *N*-methylmorpholine *N*-oxide.

Scheme 17

Bolm *et al.* attached a modified dihydroquinidine-diphenylpyrazinopyridazine based ligand to commercially available chloropropyl functionalised silica *via* an ether linkage, **figure 10**.[31] The polymer-supported ligand **64** was employed with osmium tetroxide in the asymmetric dihydroxylation of styrene affording the chiral vicinal diol in excellent yield and enantioselectivity. The catalyst was recovered quantitatively by direct filtration and reused several times without any detectable loss in function, although it was necessary to add further osmium to compensate for leached material.

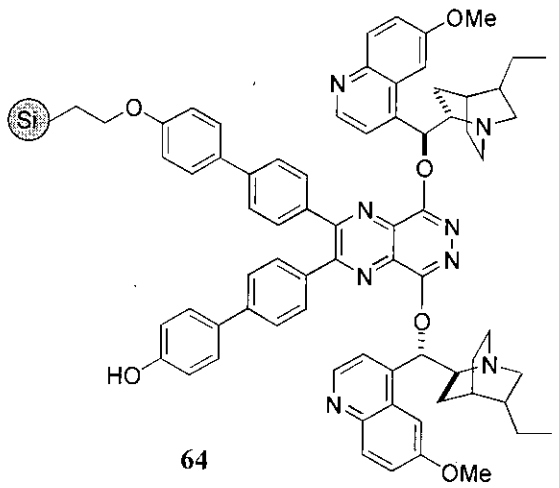

64

Figure 10

Recently Bolm *et al.* reported the synthesis and application of polymer-bound anthraquinone alkaloids as Sharpless dihydroxylation catalysts.[32] Soluble MeO-PEG resin was chosen as the support using ester or ether linkages to attach the alkaloid ligands. In the first instance a remote position of the anthraquinone core was used for attachment resulting in a large distance between the active site of the alkaloid and the polymeric backbone **65** and **66**. The second case utilised the double bonds present in

a system derived from the naturally occurring alkaloid quinidine to generate the polymer-bound catalyst **67**, **figure 11**.

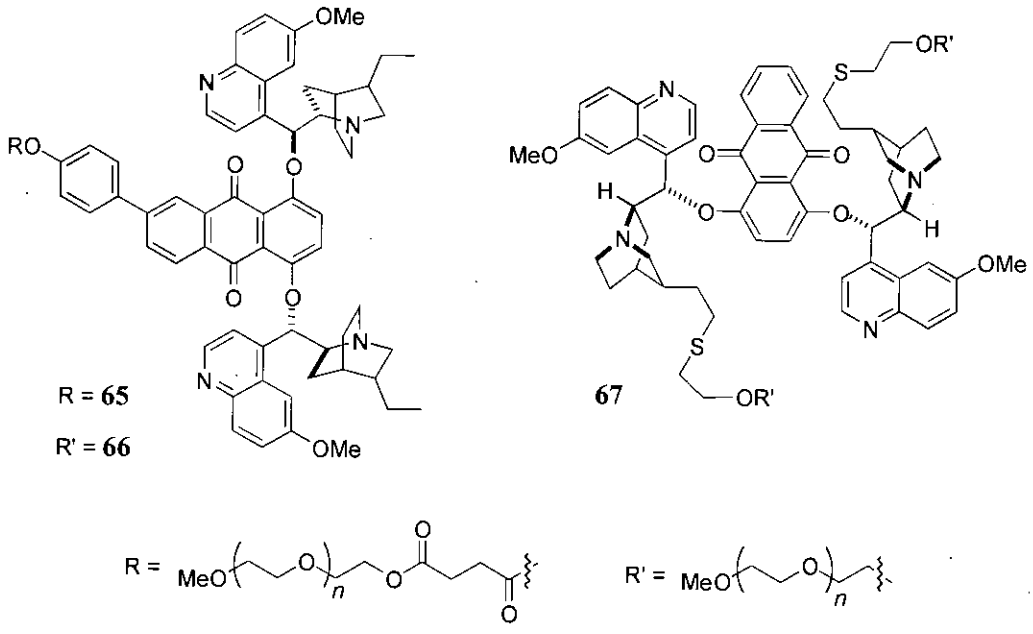

Figure 11

The levels of asymmetric induction imparted by the three catalysts were investigated using allyl iodide and indene as the alkene substrates. Interestingly, there was no significant influence of the attachment type (**65** versus **66**) or binding site (**66** versus **67**) on the enantioselectivity of the dihydroxylation reactions. In each case consistently high levels of selectivity and activity were obtained on recycling.

1.2.4.4 Asymmetric Addition of Dialkylzinc Reagents to Aldehydes

1.2.4.4.1 Polymer-Supported Amino Alcohol Catalysts

A range of polymer-supported chiral amino alcohols have been investigated as catalysts for the enantioselective addition of dialkylzinc reagents to aldehydes producing optically active secondary alcohols. In each case the polymeric catalyst was synthesised by nucleophilic displacement of the functionalised amino alcohol onto a cross-linked chlorinated resin. **Table 1** compares the activity and selectivity

imparted by various polymer-bound catalysts in the asymmetric addition of diethylzinc **68** to benzaldehyde **69** producing 1-phenyl-1-propanol **70**, **scheme 18**.

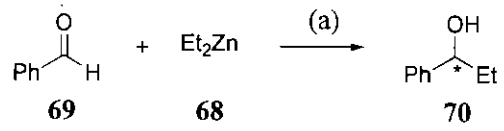

(a) Polymer-bound amino alcohol catalyst.

Scheme 18

Table 1 - Polymer-Supported Amino Alcohol Catalysts

Amino alcohol catalyst	Polymer support	Reaction conditions	Result
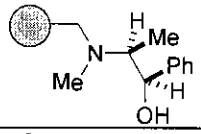	Merrifield resin[33a]	10 mol% catalyst [a] hexane, room temperature, 48 h	R enantiomer 83% yield, 89% e.e.
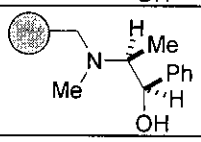	Merrifield resin[33b]	10 mol% catalyst [a] toluene, room temperature, 93 h	R enantiomer 58% yield, 80% e.e.
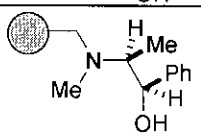	Merrifield resin[33c]	5 mol% catalyst [a] toluene room temperature, 48 h 0 °C, 62 h	R enantiomer 95% yield, 74% e.e. 96% yield, 80% e.e.
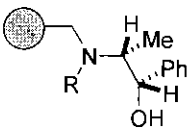	Merrifield resin[33b]	10 mol% catalyst hexane, room temperature R=Et, 117 h R=Pr, 157 h R=Bu, 115 h	S enantiomer 72% yield, 41% e.e. 70% yield, 29% e.e. 64% yield, 17% e.e.
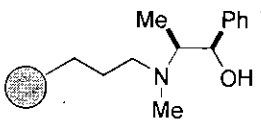	Alumina gel[33d]	2 mol% catalyst hexane, room temperature, 48 h hexane-benzene (1:1.1) room temperature, 72 h hexane, 0 °C, 120 h	R enantiomer 81% yield, 43% e.e. R enantiomer 66% yield, 50% e.e. R enantiomer 79% yield, 59% e.e.

[a] Catalyst can be recycled with slight reduction in subsequent enantioselectivity.

Amino alcohol catalyst	Polymer support	Reaction conditions	Result
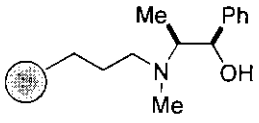	Silica gel[33d]	5 mol% catalyst hexane, room temperature, 48 h hexane, 0 °C, 120 h	R enantiomer 75% yield, 25% e.e. R enantiomer 47% yield, 37% e.e.
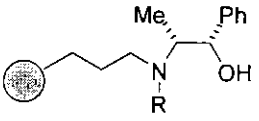	Silica gel[33d]	5 mol% catalyst R=Et, hexane 0 °C, 120 h R=Pr, hexane 0 °C, 120 h	S enantiomer 61% yield, 24% e.e. S enantiomer 59% yield, 29% e.e.
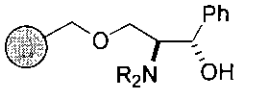	Merrifield resin[33c]	5 mol% catalyst, toluene R=H, 0 °C, 170 h R=Me, 0 °C, 72 h	R enantiomer 76% yield, 9.2% e.e. S enantiomer 85% yield, 9.5% e.e.
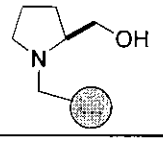	Merrifield resin[33c]	5 mol% catalyst, toluene 0 °C, 65 h	R enantiomer 93% yield, 24% e.e.
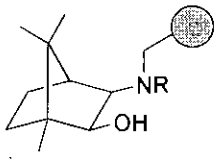	Merrifield resin[33c]	5 mol% catalyst, toluene R=H, 0 °C, 75 h R=Me, 0 °C, 73 h	R enantiomer 90% yield, 10% e.e. S enantiomer 91% yield, 92% e.e.

Various factors influencing the yield and enantiomeric purity of the 1-phenyl-1-propanol product **70** can be deduced from the results in **table 1**:

i) Higher enantioselectivities are obtained at lower temperatures, yet this reduces the reaction rate, and lower yields are often obtained.

ii) Faster reactions rates are observed in hexane than in toluene resulting in higher yields and enantioselectivities.

iii) Amino alcohol ligands bearing *N*-H substituents exhibit poor levels of asymmetric induction in comparison with *N*,*N*-dialkylated analogues. Within this series the yields and enantioselectivities steadily decrease as the length of the *N*-alkyl substituent increases from methyl through to butyl.

iv) (1*R*,2*S*)-1-phenyl-2(*N*-alkyl)amino-propanol systems preferentially produce the *R* enantiomer of the alcohol product **70**, whereas amino alcohols with the opposite stereochemistry favour formation of the *S* enantiomer.

v) The most efficient catalysts are directly bound to Merrifield resin *via* the nitrogen atom of the amino alcohol.

vi) The majority of polymer-supported catalysts are derived from Merrifield resin, immobilising the amino alcohol on alumina gel results in lower activity and selectivity and using silica gel as the solid support further reduces efficiency.

vii) The last entry in **table 1** employing the isoborneol catalyst provides optimum catalytic activity with excellent enantioselectivity suggesting that a hindered amino alcohol ligand is advantageous.

Soai *et al.* developed a polymer-bound catalyst with methylene spacer units to separate the active catalytic site from the polymeric backbone.[34] As optimum enantioselectivities were achieved using the monomeric catalyst possessing butyl and 6-benzyloxyhexyl (six methylene spacer) substituents on the nitrogen atom of the amino alcohol, this system was subsequently attached to Merrifield resin, **figure 12**.

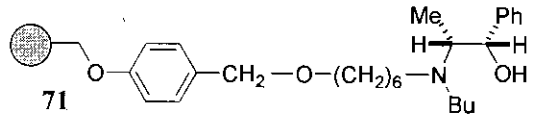

71

Figure 12

The polymer-supported amino alcohol **71** was utilised in the enantioselective ethylation of benzaldehyde affording (*S*)-1-phenyl-1-propanol in 91% yield and 82% e.e. Similarly, the addition of diethylzinc to nonanal produced (*S*)-undecan-3-ol in 75% yield and 69% e.e. To date the polymer-bound catalyst **71** provides optimum levels of asymmetric induction for the alkylation of aliphatic aldehyde substrates.

The polymer was also amenable to recycling with no loss in catalytic activity or selectivity.

Hodge *et al.* prepared polymer-supported ephedrine **72** and camphor **73** derived amino alcohols and examined how the support parameters affect the selectivity of the dialkylzinc addition reaction, **figure 13**. The most important factor promoting high levels of asymmetric induction was found to be a favourable interaction of the polymer matrix with the reaction solvent, thus enabling easy access of reactants to the catalytic sites within the swollen polymer.[35a]

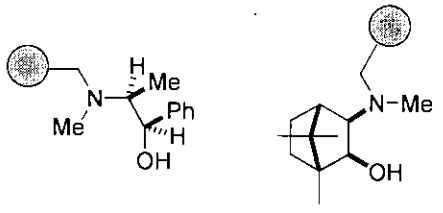

72 **73**

Figure 13

Both of the amino alcohol catalysts **72** and **73** were subsequently adapted to a bench-top flow system where the diethylzinc and benzaldehyde were continuously supplied to a column filled with the chiral polymeric catalysts. This process provided high turnover allowing the synthesis of large quantities of the 1-phenyl-1-propanol product in 97-99% enantiomeric excess.[35b] The polymer-bound ephedrine derived amino alcohol **72** is currently available from Lancaster illustrating the high commercial impact of these polymeric catalytic systems.

Copolymerised chiral ligands derived from norephedrine and ephedrine amino alcohols have also been used for the enantioselective addition of diethylzinc to *N*-diphenylphosphinylimines giving optically pure *N*-diphenylphosphinylamines.[35c]

α,α-Diphenyl-*L*-prolinol was attached to a linear soluble copolymer of octadecyl methacrylate and 2-hydroxyethyl methacrylate affording polymeric amino alcohol **74**, **figure 14**.[35d] The addition of diethylzinc to benzaldehyde was performed using the polymeric catalyst **74** in a continuously operated membrane reactor.

Unfortunately, the levels of asymmetric induction and the dominant configuration of the product were found to be highly dependant on the ratio of substrates employed.

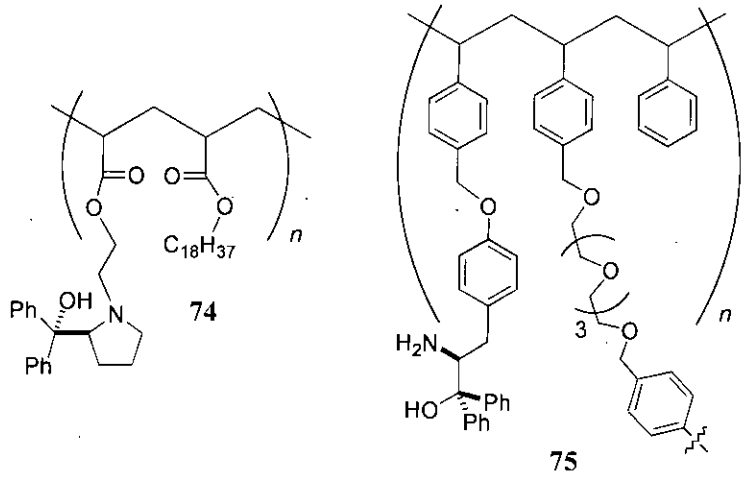

Figure 14

Polymer-bound amino alcohol **75** was prepared by copolymerisation of the corresponding chiral styrene monomer with styrene using a poly(ethylene glycol) derived cross-linking agent, **figure 14**.[35e] The flexible nature of the cross-link was found to enhance the swelling capacity and mechanical stability of the resin when compared with analogous divinylbenzene cross-linked systems. Furthermore, the polymeric catalyst **75** provided superior asymmetric induction during the dialkylzinc addition reactions due to improved solvation and stabilisation of the reaction complex.

1.2.4.4.2 Polymer-Supported Ti-TADDOL Catalysts

The constant stirring of a polymeric reaction mixture ultimately results in breakdown of the resin beads forming fine powders which can no longer be easily removed from the reaction mixture. To circumvent this physical degradation Seebach *et al.* prepared a polymer-bound Ti-TADDOL catalyst **76** which was contained within a polypropylene 'tea bag' and immobilised in a reactor, **figure 15**.[36]

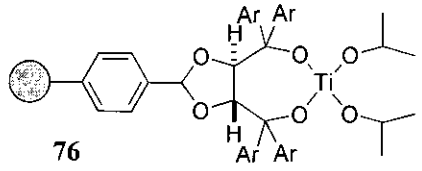

76

Figure 15

The enantioselective addition of dialkylzinc reagents to a range of aldehyde substrates were mediated by the polymer-supported catalyst **76**. Recycling capabilities were excellent as the polymer was re-used without quenching up to 20 times with no appreciable deterioration in yield or enantioselectivity. After a series of reactions the polymer-bound TADDOL was recovered from the 'tea bag' with no apparent degradation or abrasion of the polymer surface.

The dentritically modified TADDOL ligands possessing terminal styrene functionality **77** and **78** were copolymerised with styrene incorporating the ligand as the cross-linking reagent, **figure 16**.[37a] Treatment of the resultant resin with titanium tetraisopropoxide generated polymer-bound diisopropoxy-Ti-TADDOLates which were utilised as catalysts in the asymmetric addition of diethylzinc to benzaldehyde.

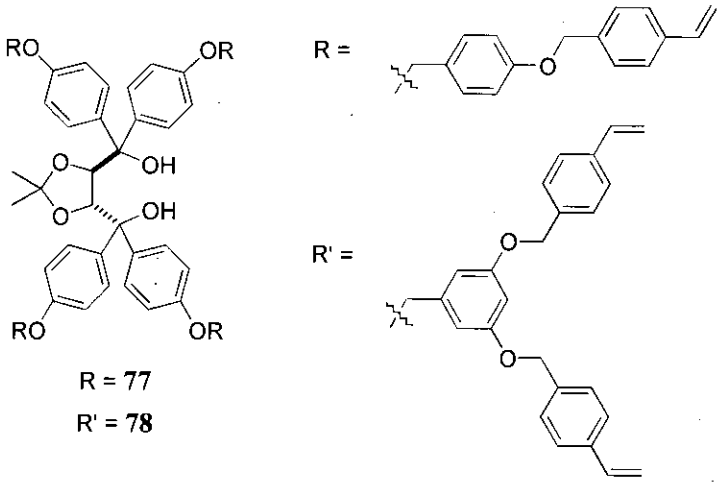

R = 77

R' = 78

Figure 16

The catalysts were recycled 20 times where only the dentritic polymer derived from **78** gave constant selectivity of 96% e.e. in sequential applications with the resin maintaining a high swelling capacity. Furthermore, the rate of reaction was found to

be the same with or without stirring of the reaction mixture indicating free diffusion of reactants and products to and from the active centre. Polymeric **78** actually provided a faster rate of reaction than the analogous soluble dendritic monomer, illustrating the overall excellent performance of this immobilised catalyst.

Seebach *et al.* employed a range of polymer-bound and dendritic TADDOL ligands based on **77** and **78** as stoichiometric reagents and catalysts.[37b] The reactions studied included the enantioselective reduction of ketones, the ring opening of *meso*-anhydrides, Diels-Alder addition and [3+2] cycloaddition of 3-crotonyloxazolidinone **79** to cyclopentadiene **80** and nitrone **81**, **figure 17**. The enantioselectivities reached with most of the polymeric TADDOL ligands were comparable or identical to those observed with the solution phase analogues.

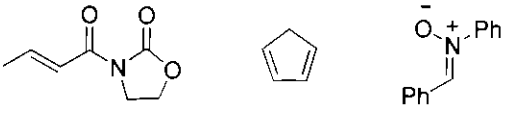

79 **80** **81**

Figure 17

1.2.4.4.3 Polymer-Supported BINOL Catalyst

Wang *et al.* prepared the polymer-bound BINOL **82** by coupling (*S*)-2,2'-dihydroxy-1,1'-binaphthyl-3,3'-dicarboxylic acid with an aminomethyl polystyrene resin, **figure 18**.[38]

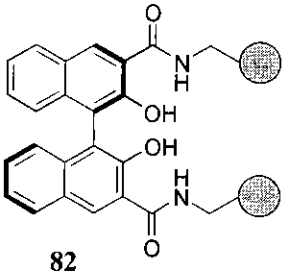

82

Figure 18

The titanium complex of the polymeric catalyst was found to be more enantioselective for the addition of diethylzinc to aldehydes than the homogeneous counterpart. The chiral biaryl axis in combination with the steric bulk of the polymer backbone was thought to provide a rigid ligand with enhanced enantiomeric control.

1.2.4.4.4 Rigid Main-Chain Polymeric Binaphthyl Catalyst

Pu *et al.* developed a rigid main-chain chiral polymeric catalyst **83** for the asymmetric reaction of aldehydes with diethylzinc. The binaphthyl polymer **83** was synthesised in 90% yield from the Suzuki coupling of **84** with **85** followed by hydrolysis, **scheme 19**.[39a]

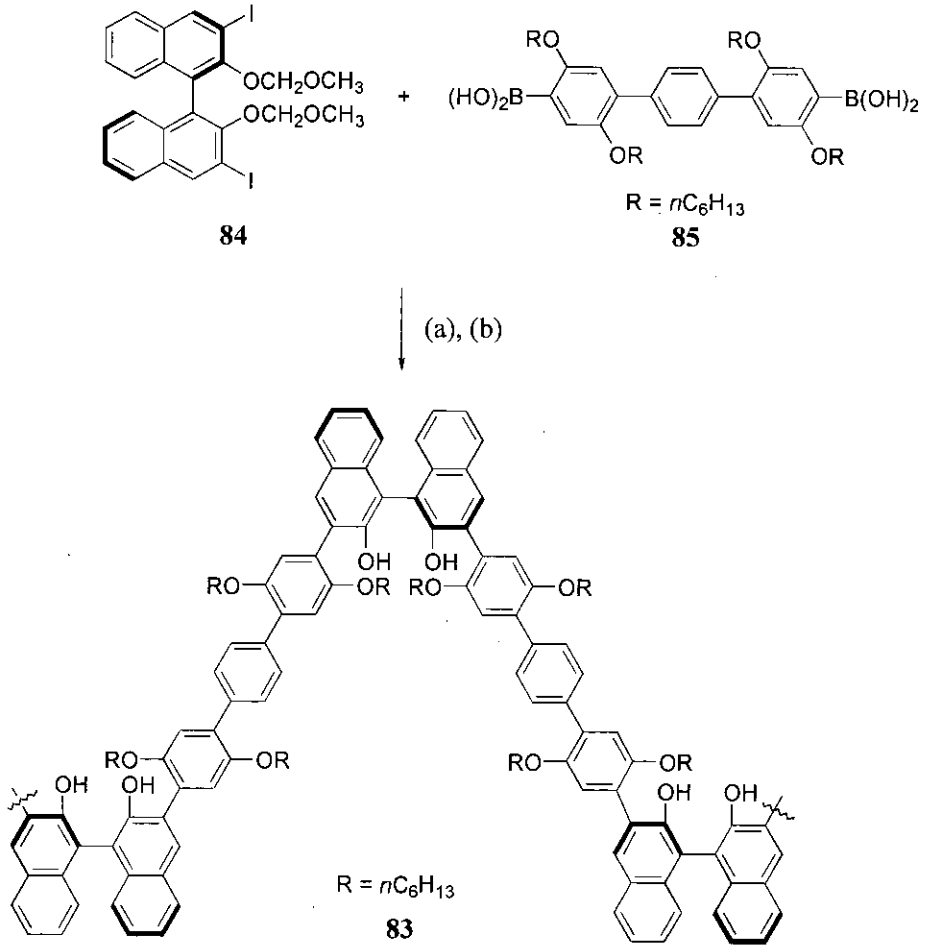

(a) $Pd(PPh_3)_4$, aqueous K_2CO_3; (b) aqueous HCl.

Scheme 19

The high activity and stereoselectivity of the polymeric catalyst **83** closely resembled that of the analogous monomer illustrating that the steric and electronic properties were maintained within the rigid polymer framework. This is in contrast to many functionalised polymer catalysts where the microenvironment of the catalytic sites in a polymer are often significantly altered from those in the monomeric catalyst due to the flexible and sterically irregular polymer chains.

The properties of the rigid and sterically regular polymer ligands were further modified to systematically achieve high enantioselectivities with both aromatic and aliphatic aldehydes.[39b]

1.2.4.4.5 Chiral Homogeneous Catalyst *via* ROMP

The chiral homogeneous polymeric catalyst **86** was prepared by the ring opening metathesis polymerisation of the strained bicyclic olefin **87** using Grubbs catalyst, **scheme 20**.[40]

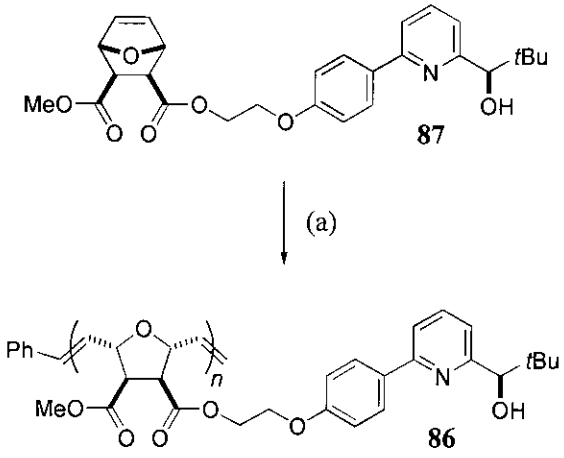

(a) Grubbs catalyst.

Scheme 20

The catalytic activity of the polymer **86** was evaluated in the enantioselective addition of diethylzinc to benzaldehyde. Reaction rates and enantioselectivity were lower than those observed for the monomeric counterpart affording (*R*)-1-phenyl-1-propanol in 78% yield and 71% enantiomeric excess after a prolonged reaction time.

1.2.4.5 Asymmetric Reduction of Ketones

1.2.4.5.1 Polymer-Supported Oxazaborolidine Catalysts

Numerous reports have documented the asymmetric reduction of prochiral ketones **88** to afford optically active secondary alcohols **89** employing polymer-bound chiral oxazaborolidine catalysts, **scheme 21**. In the solution phase a relatively large amount of the oxazaborolidine catalyst (typically 10 mol%) is required to achieve high selectivity, thus it was hoped that use of a heterogeneous system would allow catalyst recovery and recycling to improve the economic viability of the process. The ability to separate the polymeric catalyst prior to work-up of the reaction would also be advantageous in preventing decomposition of the unstable oxazaborolidine ring.

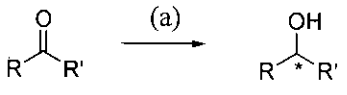

88 **89**

(a) Polymer-bound oxazaborolidine catalyst.

Scheme 21

Early publications by Itsuno *et al.* prepared the polymer-supported amino alcohol **90** by anchoring the phenolic hydroxyl group of a tyrosine derived amino alcohol to Merrifield resin. Subsequent treatment with a borane source afforded the active oxazaborolidine catalyst **91** where effective asymmetric hydride transfer to a range of ketones produced chiral alcohols with the same degree of selectivity as for the monomeric model, **scheme 22**.[41a]

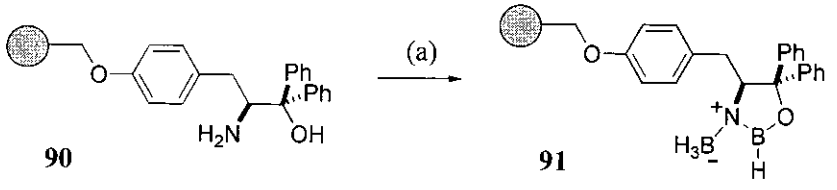

90 **91**

(a) BH_3•THF.

Scheme 22

This catalytic system was further adapted for use in a flow reactor where borane-tetrahydrofuran complex and aromatic ketone were continuously supplied to a column containing the polymer-supported amino alcohol **90**.[41b] The chiral secondary benzylic alcohol was successfully obtained in 90% e.e. allowing the synthesis of large quantities of product material using only small amounts of the polymeric catalyst. The continuous flow method also eliminated any destruction of the resin as stirring was not required.

Franot *et al.* synthesised the polymer-bound oxazaborolidine **92** by reacting cross-linked polystyrene boronic acid **93** and (*S*)-α,α-diphenyl-2-pyrrolidenemethanol **94** with removal of water, **scheme 23**.[42a]

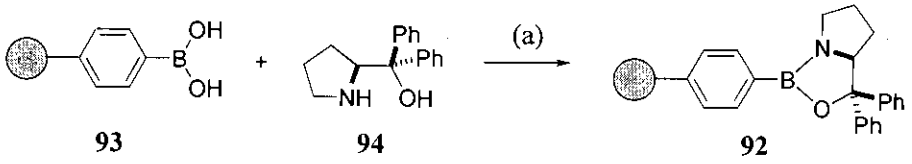

93 **94** **92**

(a) Dean-Stark trap.

Scheme 23

Addition of borane-dimethylsulphide generated the active catalyst and the asymmetric reduction of acetophenone proceeded in 93% yield and 83% enantiomeric excess. An analogous approach of generating a polymer-supported oxazaborolidine catalyst bound *via* the boron atom was adopted by Caze *et al.*, with similar success.[42b]

Recently, Kragl *et al.* prepared the linear soluble oxazaborolidine catalyst **91** for use in the asymmetric reduction of ketones by borane.[43] The polymer-bound catalyst **91** was synthesised by copolymerisation of the chiral styrene monomer **95** with styrene, and subsequent treatment of the resulting polymer with borane-dimethylsulphide, **scheme 24**.

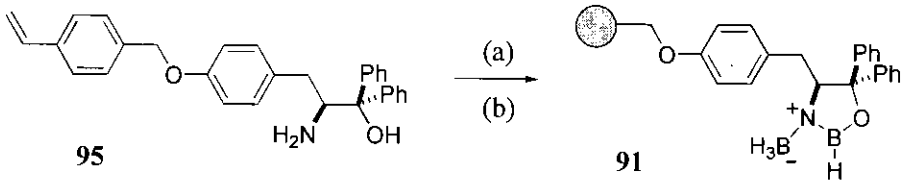

(a) CH_2CHPh, AIBN; (b) $BH_3{\cdot}SMe_2$.

Scheme 24

The homogeneous catalyst was retained within a continuously operated membrane reactor allowing the quantitative reduction of various ketones in 84-99% enantioselectivity. The total turnover number of the soluble catalyst was greatly enhanced (from 10 to 560) illustrating significant advances in the recycling potential of these catalysts.

1.2.4.5.2 Polymer-Supported Ruthenium Catalysts

The enantioselective hydride transfer reduction of prochiral ketones has emerged as a powerful tool in the synthesis of many chiral targets. Common chiral catalysts for this transformation include diphosphine ligands bound to ruthenium.

Lemaire *et al.* prepared a heterogeneous polymeric analogue of Noyori's *N*-(*p*-tolylsulphonyl)-1,2-diphenylethylamine ligand by copolymerising the parent styrene monomer with styrene and divinylbenzene, **figure 19**.[44a] Treatment of the resultant polymer **96** with $[RuCl_2(p\text{-cymene})]_2$ afforded the ruthenium polymer-bound active catalyst. Subsequent application in the asymmetric reduction of acetophenone using isopropyl alcohol as the hydrogen donor afforded (*S*)-1-phenyl-1-ethanol in 23% yield and 84% enantiomeric excess.

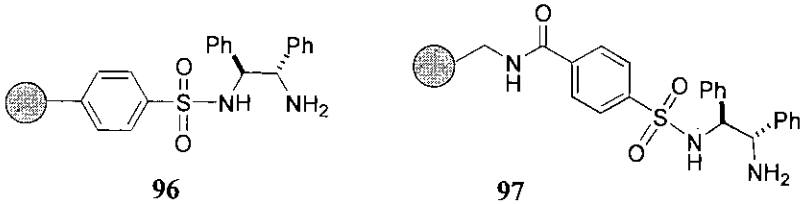

Figure 19

A similar strategy was followed by Polywka *et al.* where a Noyori derived ligand was immobilised on Tentagel amino resin **97**, **figure 19**.[44b] The active hydride transfer catalyst was formed *in situ* again by reaction with $[RuCl_2(p\text{-cymene})]_2$. The polymer-supported catalyst was shown to be highly efficient in the reduction of acetophenone affording the chiral alcohol product in 95% yield and 97% e.e. Unfortunately, reactivity of the polymeric catalyst decreased on re-use and after three cycles the reaction time required for good conversion was impracticably long although selectivity remained high.

1.2.4.6 Polymer-Supported Diels-Alder Catalyst

A number of chiral catalysts have been demonstrated for the enantioselective Diels-Alder reaction in the solution phase, but polymer-bound catalysts for the reaction have not been utilised extensively. A report by Itsuno *et al.* prepared the polymer-supported chiral Lewis acid oxazaborolidine catalyst **98** by copolymerisation of **99** with styrene **2** and a range of cross-linking reagents **100**, **101**, and **102**, followed by reaction with borane-dimethylsulphide, **scheme 25**.[45]

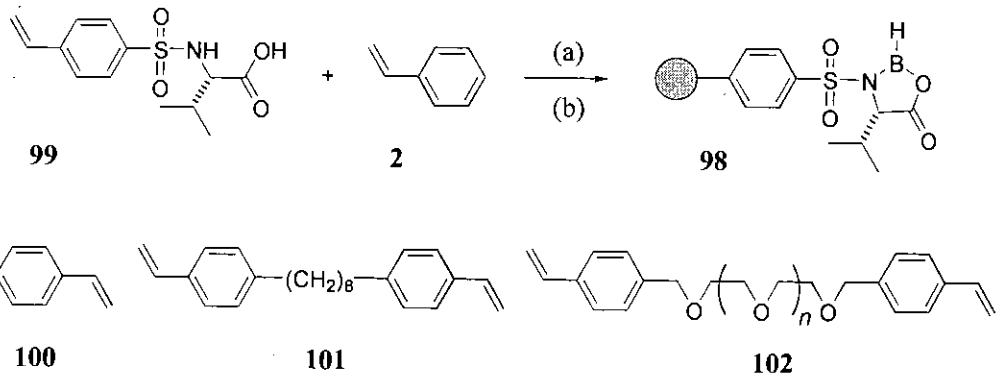

(a) Cross-linking reagent **100**, **101** or **102**, benzoyl peroxide; (b) $BH_3 \cdot SMe_2$.

Scheme 25

The polymer-supported catalyst **98** afforded high *exo* selectivity in the solid-phase Diels-Alder reaction of methacrolein **103** with cyclopentadiene **80** generating predominantly the *R* configuration (up to 95% e.e.) of the cycloaddition product **104** in excellent yield, **scheme 26**.

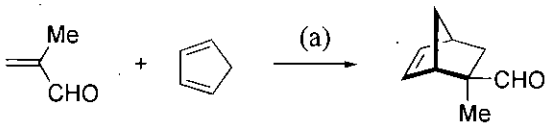

103 **80** **104**

(a) Polymer-bound Diels-Alder catalyst **98**.

Scheme 26

It was reported that the cross-linking structure greatly affected the performance of the polymeric catalyst with the divinylbenzene cross-linked resin affording the lowest enantioselectivity, while resins containing the oxyethylene cross-link **102** afforded the highest. Interestingly, the use of cross-linkage **101**, a hydrocarbon analogue of **102**, resulted in intermediate enantioselectivity. This indicated that both the flexibility and polarity of the cross-link played an important role in enhancing the asymmetric induction.

1.2.4.7 Hydroformylation Catalyst

Copolymerisation of the vinyl monomer **105** with styrene and divinylbenzene, and subsequent treatment of the polymer with bis(benzonitrile)dichloroplatinum (II) followed by an exchange with tin (II) chloride generated the polymer-supported chiral catalyst **106**, **figure 20**.[46]

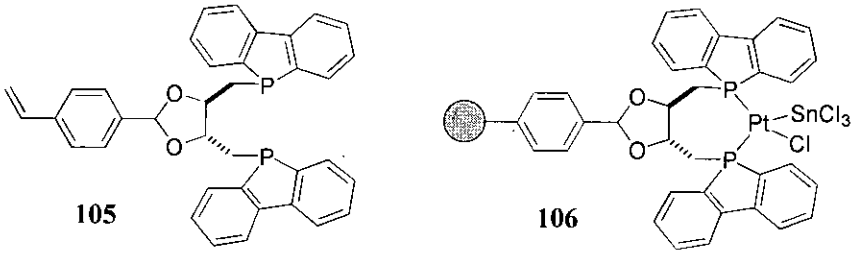

105 **106**

Figure 20

The catalyst **106** was employed in the asymmetric hydroformylation of styrene **2** to yield the branched chiral aldehyde **107** along with the unwanted addition product **108**, **scheme 27**. Unfortunately, the polymer-bound catalyst gave an appreciable decrease in both reaction rate and product ratios when compared to the

analogous solution phase studies. In contrast, the linear soluble polymer catalyst prepared in an identical manner with the omission of divinylbenzene, afforded the aldehyde **107** in moderate yield and 65% enantiomeric excess. It was also possible to recover the polymer by precipitation and re-use the catalyst with no loss in rate or selectivity.

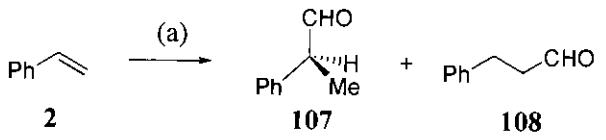

2 **107** **108**

(a) Polymer-bound hydroformylation catalyst **106**, H_2, CO, 2600 psi.

Scheme 27

1.3 Summary of Chapter 1

The emergence of combinatorial chemistry has spurred renewed interest in polymer-assisted synthesis where the use of chiral polymer-supported reagents and catalysts has the potential to allow high levels of automation in the synthesis of libraries of target drug discovery compounds. The explosive growth in combinatorial synthesis is also driven by the ever increasing need to provide environmentally acceptable chemical syntheses to minimise the poor economics of dirty processes and the heavy cost of downstream purifications.

Chapter 1 highlights the fundamental advances within the synthesis and application of chiral side-chain polymers. In addition, a detailed introduction to the specific polymers of interest was made, namely polymer-supported chiral oxazoldinone auxiliaries and polymer-supported amino alcohol catalysts for the asymmetric addition of dialkylzinc reagents to aldehydes. Previous synthetic approaches to these polymeric targets were given with an in-depth discussion of the asymmetric inductions achieved through modification of the chiral species and optimisation of the polymer-support.

Chapter 2 : Results and Discussion Part 1

Polymer Functionalisation Route to Chiral Polymers

As explained in **chapter 1** we have been interested in the synthesis and application of chiral polymers. In particular our goal was to develop a synthetic route to novel robust and recyclable polymer systems which possess side-chain chirality. Initial studies focused on the preparation of polymer-bound chiral amino alcohols **109** as catalysts in the enantioselective addition of dialkylzinc reagents to aldehydes. This methodology was then be expanded to include the preparation of polymer-bound oxazolidinone chiral auxiliaries **110** for carrying out asymmetric aldol and alkylation reactions on the solid phase, **figure 21**.

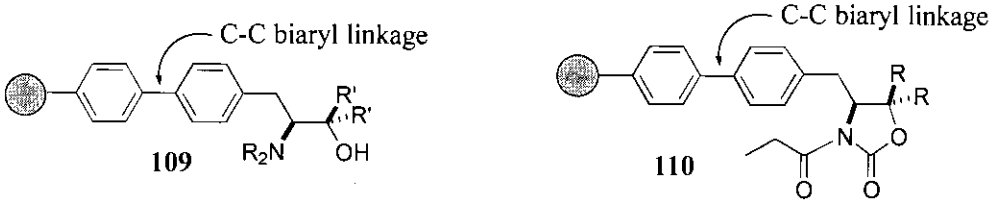

Figure 21

The key feature to be identified in each of these systems is the carbon-carbon bond which will be used to link the chiral moiety to the polystyrene backbone. It was postulated that this strong attachment would offer increased stability enabling the chiral polymers to withstand a wide range of experimental conditions. By reducing the degradation potential of the polymer systems it would then be possible to recover and recycle the chiral polymers efficiently.

Such an attachment will also be advantageous to the polymer-bound chiral amino alcohol catalysts **109** in that unlike the C-O linkages used in previous syntheses of supported amino alcohols,[33c] a C-C based linkage cannot coordinate the reactant zinc metal centre of the dialkylzinc reagent which should result in greater control over the asymmetric induction. The biaryl component will also act as a spacer unit, which could potentially increase the enantiomeric excesses obtained

from the alkylation of aliphatic aldehydes, just as methylene spacers have been shown to assist the stereochemical control of such reactions.[34]

As discussed above, the all-carbon backbone will increase the recycling potential of the polymer-bound oxazolidinone chiral auxiliaries **110**. Currently there are no literature examples involving the re-use of analogous polymer systems. The rigid biaryl unit should also minimise steric repulsion between the active site of the auxiliary and the polystyrene backbone, potentially allowing a faster rate of reaction. Thus reducing the common problem of comparatively slow reaction rates on the solid phase.

2.1 Retrosynthesis of Chiral Polymers

Our initial approach to these target polymer systems was derived from the functionalisation of cross-linked polystyrene. As discussed in **chapter 1.2.2** this strategy routinely involves the reaction of Merrifield resin with a nitrogen or oxygen based nucleophile, or the Mitsunobu coupling of Wang resin with an appropriate alcohol generating C-N and C-O linkages.

Our strategy towards the chiral polymers is unique, necessitated by the requirement to form the crucial C-C bond between the polystyrene and the chiral moiety. Retrosynthesis is illustrated for the polymer-bound amino alcohol **109** case in **scheme 28**, where the polymer-bound oxazolidinone auxiliary **110** would undergo analogous disconnections. The crucial reaction involves the palladium catalysed Suzuki coupling of a polymer-bound aryl boronic acid or ester with a tyrosine triflate derivative. In turn the polymeric boron component is derived from bromo- or iodo-polystyrene where various tyrosine triflate compounds can be synthesised from commercially available *L*-tyrosine.

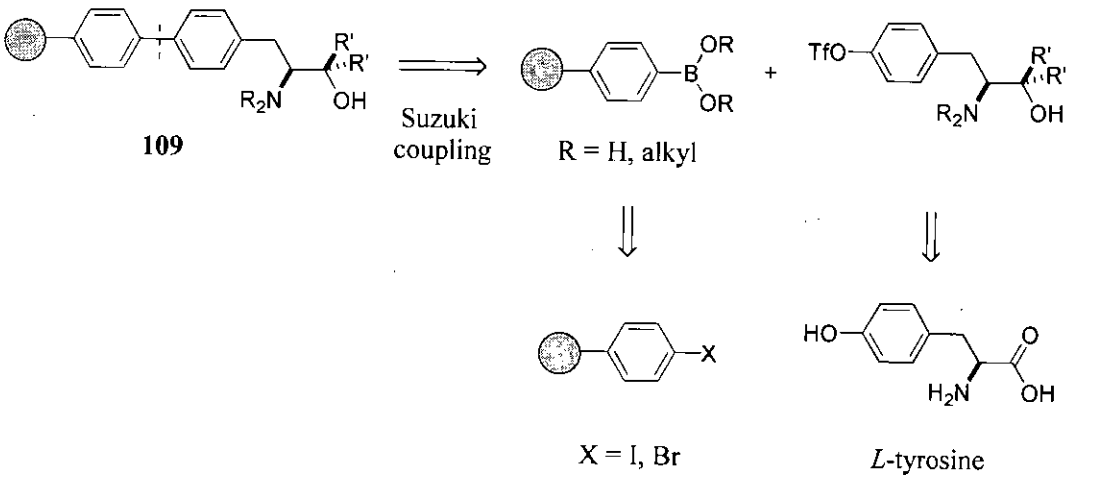

Scheme 28

Biaryl systems have previously been prepared *via* the Suzuki coupling of an aryl boronic ester and an aryl triflate[47, 48] using $PdCl_2$(dppf) as the transition metal catalyst. There is also evidence to suggest that the aryl boronic ester can be prepared on the solid support,[49] and aryl triflate formation in tyrosine derivatives is well-precedented[50, 51] thus indicating the suitability of both components to this reaction.

There are currently no literature examples to support the Suzuki coupling of an immobilised polymer-bound boronic acid **93** with aryl halides or triflates, although this functionalised polymer can be prepared *via* lithiation of bromopolystyrene **111**, followed by reaction with trimethylborate and an acidic work-up, **scheme 29**.[11]

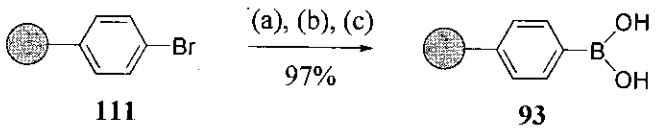

111 **93**

(a) *n*-BuLi, benzene, 65 °C; (b) $B(OMe)_3$, THF, RT; (c) HCl, water, dioxane, 60 °C.

Scheme 29

Due to the problems commonly associated with monitoring reactions on the solid phase and ultimately the characterisation of the functionalised polymer product, initial studies focused on the synthesis of model biaryl systems **112** and **113**, **figure 22**. This approach allowed optimisation of the Suzuki coupling step before

transferring the system to the solid phase, and also provided spectroscopic data for future comparison with the polymer-bound analogous systems **109** and **110**.

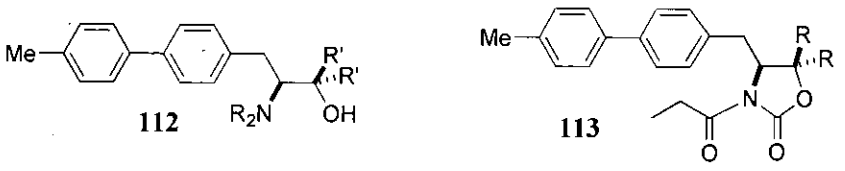

Figure 22

2.2 Alternative Routes to Biaryl Linker on Solid Support

An alternative approach to the chiral polymers might involve the analogous palladium or nickel catalysed Suzuki coupling of the polymeric boronic acid or ester with tyrosine derived phosphates, mesylates or tosylates. Such methodology has been developed in the solution phase using activated vinylic substrates derived from 1,3-dicarbonyl compounds, as a cheaper alternative to the use of vinyl triflates which are often unstable, **scheme 30**.[52] However, we predicted that the use of phosphate, mesylate or tosylate derivatives of tyrosine would result in lower Suzuki coupling yields, as the aromatic tyrosine component would not be sufficiently activated towards oxidative addition due to its lack of electron withdrawing groups.

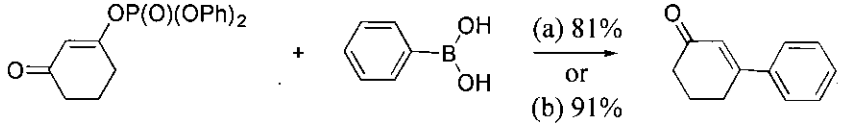

(a) $PdCl_2(dppf)$, 3N aqueous K_2CO_3, DMF, 60 °C; (b) $Ni(PPh_3)_4$, K_3PO_4, THF, 35 °C.

Scheme 30

In a similar manner, the use of either bromo- or iodo-phenylalanine derivatives as coupling partners for the solid support was discarded at the outset of the project due to the prohibitively high cost of such starting materials. Our approach must be amenable to scale-up and therefore cost effective as large quantities of material will ultimately be required for coupling to the solid support. *p*-Bromo-*L*-phenylalanine has been prepared *via* the *N*-acylation of *p*-bromo-*DL*-phenylalanine

with subsequent enzymatic deacylation of the *L*-enantiomer,[53] and *p*-iodo-*L*-phenylalanine from the diazotisation of *p*-amino-*L*-phenylalanine,[53] yet neither of these routes incur lower starting material costs. *p*-Iodo-*L*-phenylalanine **114** has also been produced *via* the direct iodination of *L*-phenylalanine yet this reaction is low yielding due to uncontrollable ortho and para overiodination,[54] **scheme 31**. All of these factors negated any possible advantages to be gained from the increased activity of an aryl bromide or iodide versus that of an aryl triflate in the Suzuki coupling step.

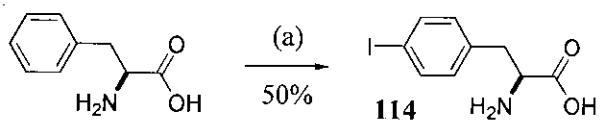

(a) I_2, $NaIO_3$, H_2SO_4, AcOH, 70 °C.

Scheme 31

Further speculative routes to generate the C-C biaryl linkage on the solid phase[55] would allow the use of commercially available bromo- or iodo-polystyrene as the solid phase coupling component:

i) Palladium mediated Stille coupling reactions of polymer-bound aryl iodides with unsaturated organostannanes have been reported with limited success,[56a, 56b] **scheme 32**. The necessary stoichiometric use of tin in the Stille reaction[57] also renders this methodology unsuitable for applications on the solid phase due to the problematic removal of tin residues from the polymer. This approach was ultimately discounted as bromo- or iodo-phenylalanine would be required as a precursor for synthesis of the tyrosine derived tin component which is not cost effective as discussed earlier.

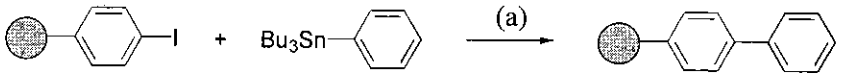

(a) Palladium catalyst.

Scheme 32

ii) There is literature precedent to support the palladium catalysed cross-coupling reactions of aryl zinc bromides with aryl bromides,[58] iodides and triflates[59] on the solid phase, **scheme 33**. However, as the tyrosine derived organozinc component could only be prepared *via* the reaction of bromo-phenylalanine with magnesium and subsequent transmetallation of the Grignard reagent with zinc bromide, the mandatory use of bromo-phenylalanine again translates to a non-viable process.

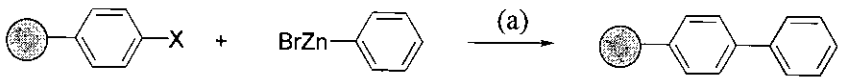

X = I, Br, OTf

(a) Palladium catalyst.

Scheme 33

iii) The final considered approach to the chiral polymers is effectively the reverse of the chosen strategy, whereby the crucial Suzuki coupling step would occur between bromo- or iodo-polystyrene and a tyrosine derived boronic ester, **scheme 34**. Tyrosine triflate[60] and nonaflate[61] derivatives readily undergo palladium catalysed coupling reactions with tetraalkoxydiboron pinacol ester or dialkoxyhydroborane respectively affording the corresponding aryl boronic esters. The subsequent Suzuki coupling of *p*-borono-phenylalanine derivatives with aryl chlorides,[62] iodides, bromides or triflates[63] to produce *p*-aryl-phenylalanine compounds is also well documented in the solution phase.

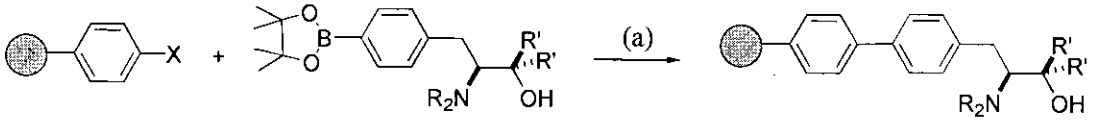

X = I, Br

(a) Palladium catalyst, base.

Scheme 34

This final route is marginally more attractive as bromo- or iodo-phenylalanine are not required, but essentially an extra step is created to convert each of the tyrosine derived triflates to their respective boronic esters prior to Suzuki coupling with the solid support. Our chosen strategy allows direct Suzuki coupling of the tyrosine

derived triflates with a universally applicable polymeric boronic acid or ester, thus condensing the synthesis.

2.3 Synthesis of Tyrosine Triflate Derived Coupling Component

As the *N,N*-dimethylated amino alcohols were found to display optimum catalytic activity on the solid phase (**chapter 1.2.4.4.1**) attempts were made to prepare the analogous biaryl compounds where R = Me (**figure 22**). Appropriate functionalisation of the R' substituents to investigate how steric hindrance affects the enantioselectivity of the dialkylzinc reaction directed us to the synthesis of a range of tyrosine triflate derived amino alcohols where R' = H **115**, R' = Me **116**, R' = Ph **117**.

Similarly in the case of the biaryl oxazolidinone auxiliary the primary target tyrosine triflate derivative possessed R = H **118** (**figure 22**) being consistent with previous oxazolidinone auxiliaries developed on the solid phase (**chapter 1.2.3.3**), **figure 23**.

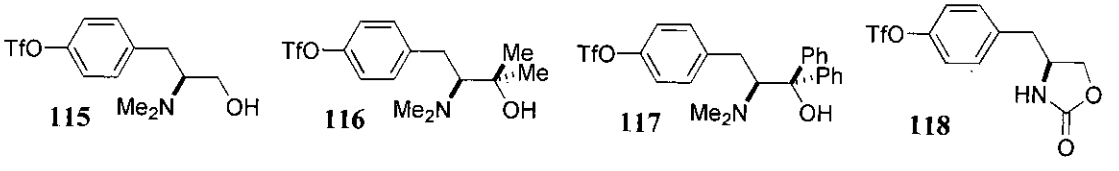

Figure 23

2.3.1 Synthesis of Triflated Amino Alcohol 115

Tyrosine was chosen as the obvious starting material being inexpensive and commercially available in either enantiomeric form. *L*-tyrosine **119** was converted to the methyl ester hydrochloride salt **120** (100%), which afforded the free methyl ester **121** in high yield (89%) upon treatment with aqueous potassium carbonate. Reaction with formaldehyde generated the imine which was reduced *in situ* under hydrogenation conditions to form the *N,N*-dimethylated methyl ester **122** (100%).[64]

The methyl ester was then reduced in moderate yield (57%) using $LiAlH_4$ to afford diol **123**, **scheme 35**.

However, subsequent attempts to selectively triflate the more acidic phenolic hydroxyl group of the diol **123** using triflic anhydride[50] gave a mixture of products including mono- and di-triflated material and we were unable to isolate any of the desired triflated amino alcohol **115**. In contrast, the reduced activity provided by *N*-phenyl triflimide[51a] gave the desired selectivity for this triflation step affording the target compound **115** in low yield (17%), **scheme 35**. ^1H NMR analysis of the product material gave the characteristic singlet signal representing the aromatic protons of the aryl triflate and MS (APCI) determined that the compound was mono-triflated.

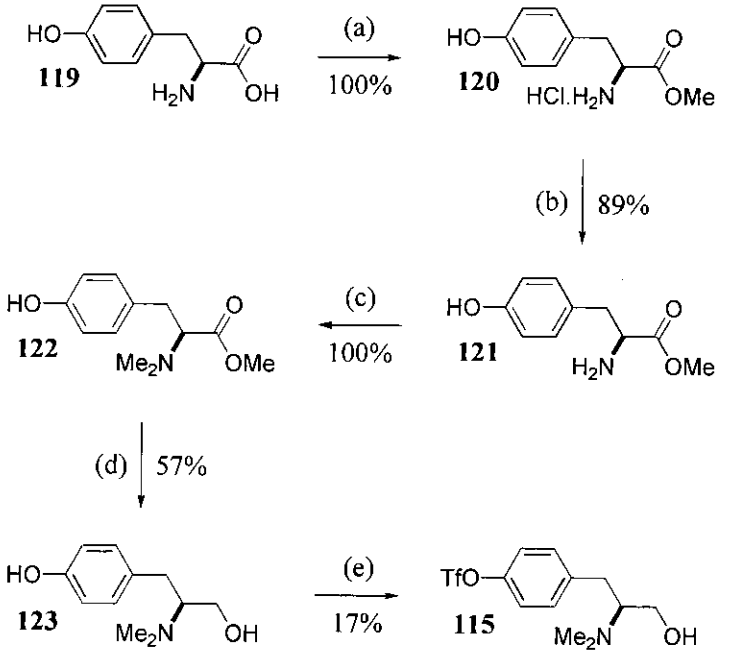

(a) AcCl, MeOH, reflux; (b) K_2CO_3; (c) H_2CO, Pd-C, H_2 (1 atm), MeOH, RT; (d) $LiAlH_4$, Et_2O, -78 °C; (e) $PhN(SO_2CF_3)_2$, Et_3N, DCM, 0 °C→RT.

Scheme 35

An alternative approach was adopted in an attempt to synthesise the unsubstituted triflated *N,N*-dimethylated amino alcohol **115**, effectively reversing the last two stages in the previous synthesis, **scheme 36**.

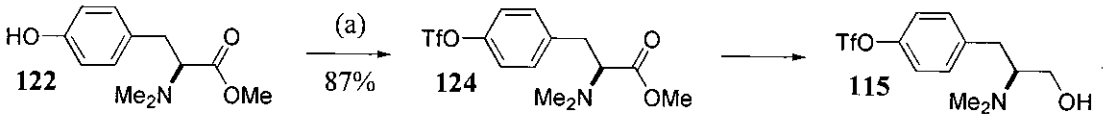

(a) $(CF_3SO_2)_2O$, pyridine, DCM, 0 °C.

Scheme 36

Treatment of the methyl ester **122** with triflic anhydride[50] afforded the triflated amino alcohol **124** in high yield (87%). The ^{19}F NMR spectrum of this compound gave the desired singlet peak at δ = -73.2 ppm, but the expected quartet arising from the triflate group was not detected in the ^{13}C NMR spectrum due to the low relative intensity of this signal. The second step proved infinitely more problematic and a range of hydride reducing agents routinely used for the transformation of esters to primary alcohols were employed as summarised in **table 2**. The inherent instability of the triflate group under these reaction conditions often resulted in S-O bond cleavage thus regenerating the phenol.

Table 2 - Summary of Reaction Conditions Studied to Reduce 124 to 115

Entry	Reagents / Conditions	Main product components [a]
1 [65]	$NaBH_4$, MeOH reflux, 3 h	no reaction, **124** recovered
2 [66]	PMHS, TBAF, THF RT, 48 h	no reaction, **124** recovered
3	DIBAL, toluene -78 °C, 3 h	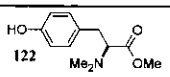
4 [67]	$LiBH_4$, THF RT, 17 h	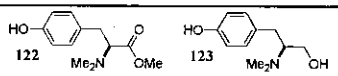
5 [68]	RedAl, THF reflux, 3 h	multiple products, trace **124** recovered
6	$LiAlH_4$, Et_2O -78 °C, 4 h	multiple products, trace **124** recovered
7 [69]	$LiAlH_4$, silica gel, Et_2O RT, 24 h	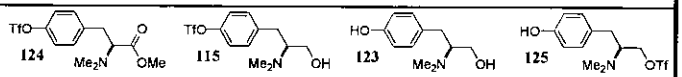
8 [70]	$(CH_3)_2CHCH_2MgBr$ Cp_2TiCl_2, Et_2O RT, 20 h	numerous product components resulting from both hydride transfer and Grignard addition to the methyl ester **124**

[a] Determined from ^1H NMR and MS (APCI) analysis of the crude product reaction mixtures.

Entries 1 and 2 using $NaBH_4$[65] and polymethylhydrosiloxane[66] failed to induce any reduction and the triflated methyl ester **124** was recovered intact. Similarly diisobutylaluminium hydride (entry 3) provided no reduced material with cleavage of the triflate group affording **122** as the main product after chromatography. Using $LiBH_4$[67] as the hydride source (entry 4) caused cleavage of the triflate group **122** along with partial reduction of the methyl ester to afford **123**.

Both reductions using sodium bis(2-methoxyethoxy)aluminium hydride[68] and $LiAlH_4$ (entries 5 and 6) generated several products by t.l.c. and a trace of unreacted methyl ester **124** could be identified. The addition of silica gel (entry 7) was investigated as $LiAlH_4$ on silica gel has been shown to reduce esters in the presence of nitro and cyano groups,[69] suggesting a potentially milder and more selective hydride source. Chromatography of the crude product mixture indicated the presence of unreacted **124**, target product **115**, reduced phenol **123** and a fourth component which was subsequently determined to be **125**. This interesting by-product presumably results from nucleophilic attack of a reduced primary alkoxide onto an adjacent triflate containing molecule where many permutations are possible.

Finally the combination of Cp_2TiCl_2 and isobutylmagnesium bromide (entry 8) which has been shown to effect the Ti-catalysed Grignard reduction of esters to primary alcohols[70] resulted in both hydride transfer and Grignard addition to the methyl ester **124** in various combinations. Ultimately in those cases where the desired triflated amino alcohol **115** was formed it could not be isolated in acceptable yield due to the extensive range of accompanying impurities.

2.3.2 Synthesis of Triflated Amino Alcohol 116

Reaction of the previously prepared methyl ester **122** with either freshly prepared MeMgI or MeLi afforded the α,α-dimethylated amino alcohol **126** in good yield (81% and 77% respectively). *N*-Phenyl triflimide[51a] then allowed selective triflation of the phenol presumably due to the steric bulk introduced by the methyl groups (74%). However, the target tiflated amino alcohol **116** could not be separated from close running impurities *via* chromatography, **scheme 37**.

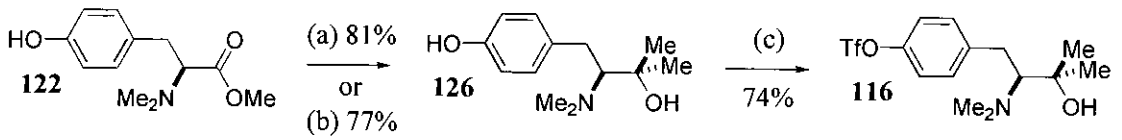

(a) (i) MeI, Mg, I_2, Et_2O, reflux; (ii) **122**, Et_2O, reflux; (b) MeLi, THF, -78 °C→0 °C; (c) $PhN(SO_2CF_3)_2$, Et_3N, DCM, 0 °C.

Scheme 37

An alternative route to the triflated amino alcohol **116** involved treating the already triflated methyl ester **124** with MeLi or MeMgI to incorporate the geminal dimethyl groups, **scheme 38**. However, 2.2 equivalents of MeLi caused cleavage of the triflate group providing 97% yield of a 1:1 ratio of the target compound **116** and the analogous phenol **126** as determined by integration of the aromatic peaks in the ^{1}H NMR spectrum. Reaction with freshly prepared MeMgI afforded the triflated amino alcohol **116** in low yield (14%) due to difficult chromatographic purification, thus a high yielding route to this compound has not been established. (The minor oxazolidine by-product **127** isolated from this reaction (3% yield) will be discussed in greater detail in **chapter 5**).

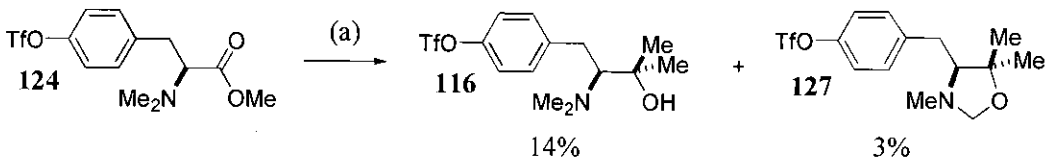

(a) (i) MeI, Mg, I_2, Et_2O, reflux; (ii) **124**, Et_2O, reflux.

Scheme 38

2.3.3 Synthesis of Triflated Amino Alcohol 117

Literature precedent illustrates that PhMgBr Grignard addition to *L*-tyrosine methyl ester hydrochloride salt at 0 °C produces the α,α-diphenyl amino alcohol in 43% yield.[41a] Analogous treatment of the tyrosine triflated methyl ester **124** with freshly prepared PhMgBr under forcing reflux conditions gave no reaction, **scheme 39**. These results can be explained by the increased steric bulk of **124** caused by the

N,*N*-dimethyl groups which hinder the approach of relatively bulky nucleophiles, thus making the target compound **117** not viable synthetically.

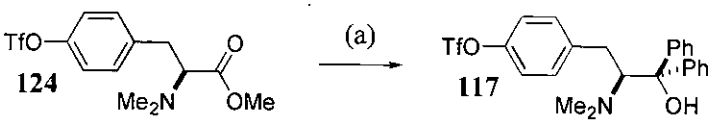

(a) (i) PhBr, Mg, I_2, THF, reflux; (ii) **124**, THF, RT.

Scheme 39

2.3.4 Synthesis of Triflated Oxazolidinone 118

Synthesis of the target oxazolidinone **118** was achieved *via* the direct reduction of tyrosine methyl ester **121** using $LiBH_4$[67] to generate diol **128** (93%), which afforded the oxazolidinone **129** when treated with sodium ethoxide and diethyl carbonate (61%).[71] The final triflation step using triflic anhydride[50] produced the desired Suzuki coupling precursor **118** in moderate yield (69%), **scheme 40**.

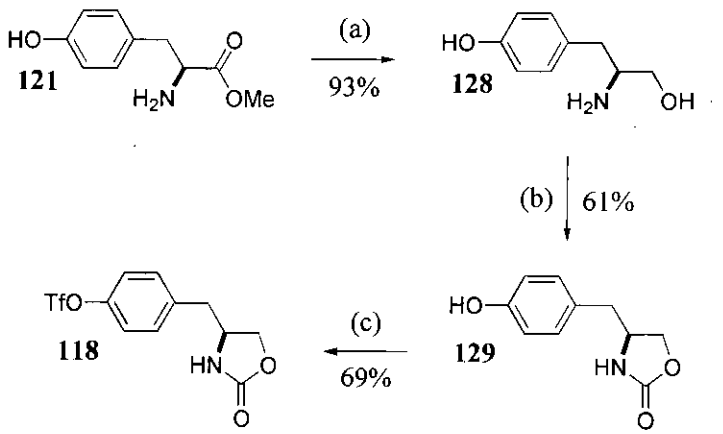

(a) $LiBH_4$, THF, RT; (b) NaOEt, $(EtO)_2CO$, EtOH, 130 °C; (c) $(CF_3SO_2)_2O$, pyridine, DCM, 0 °C.

Scheme 40

2.4 Suzuki Coupling Reaction

The palladium catalysed cross-coupling reaction of two unsaturated carbon centres has become a powerful tool in organic synthesis achieving direct

carbon-carbon bond formation in high yield. The palladium catalysed Suzuki reaction[72] of unsaturated halides or triflates with boronic acids or esters has been well utilised in the solution phase allowing a diverse range of substituents to be introduced onto aromatic systems, **scheme 41**.

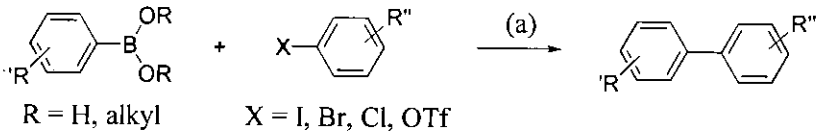

(a) Palladium catalyst, base, solvent.

Scheme 41

The mechanistic cycle for the Suzuki coupling reaction[73] proceeds *via* initial oxidative addition of the aryl halide or triflate **130** to the Pd° complex generating Ar-Pd^{II}-X which forms the rate determining step. Transmetallation with the aryl boronic acid or ester produces Ar-Pd^{II}-Ar'. This step in the sequence proceeds at a faster rate and is feasible as the nucleophilicity of the aryl group is increased and consequently activated by formation of the aryl boron 'ate' complex **131** under the basic aqueous reaction conditions. Rapid *cis* alignment and subsequent reductive elimination of the biaryl product **132** regenerates the Pd° complex thus completing the catalytic cycle, **scheme 42**.

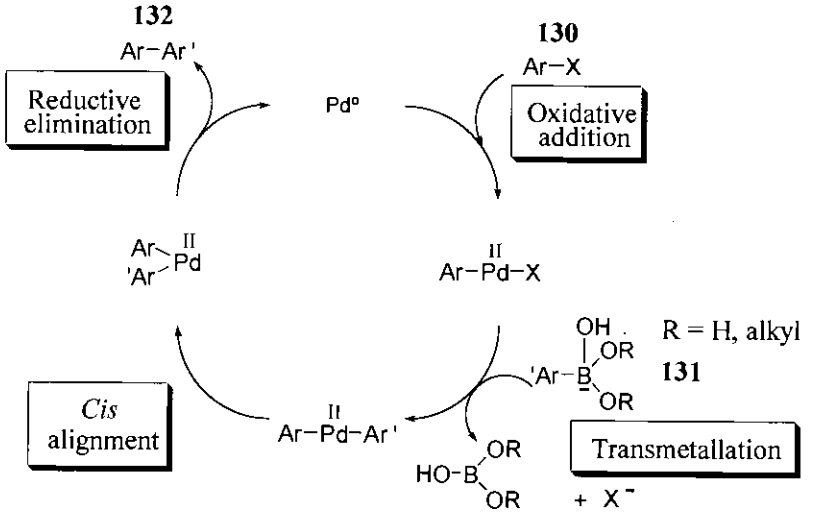

Scheme 42

Relatively few Suzuki reactions have been adapted to the solid phase, such examples include the palladium catalysed cross-coupling reaction of free aryl boronic acids with aryl iodides and bromides that are bound to the solid support.[56] The Suzuki reaction for the formation of biaryl systems *via* this strategy is widely applicable, both in terms of aryl halide and aryl boronic acid coupling partners. A number of conclusions can be drawn from the literature reviews:

i) Aryl bromides are less reactive than aryl iodides with respect to the cross-coupling, although this could be improved by attaching electron withdrawing groups to the aryl bromide. More recently unactivated aryl chlorides have been shown to undergo Suzuki coupling with aryl boronic acids using novel palladium and nickel catalysts.[74]

ii) Both electron deficient and electron rich aryl boronic acids are viable substrates, and using an excess of boronic acid increases the yields obtained.

iii) $Pd(PPh_3)_4$ is an amenable catalyst for all coupling reactions, whereas, $PdCl_2(dppf)$ has been shown to be ineffective in some cases.[56c]

iv) Reaction times of up to 12 h at elevated temperatures are necessary for complete conversion to the polymer-bound biaryl products.

v) Microwave irradiation can be used to enhance the reaction rate with minimal decomposition of the solid support.[56b]

One of the limitations of conducting the coupling reactions between a polymer-bound aryl halide and a free aryl boronic acid is represented by the comparatively limited number of commercially available aryl boronic acids. To circumvent this problem Piettre *et al.*[49] have developed methodology for transforming polymer-bound aryl halides into the corresponding aryl boronic ester **133** by reaction with tetraalkoxydiboron **134**, which can then be Suzuki coupled with a vast range of aryl iodides and bromides, **scheme 43**.

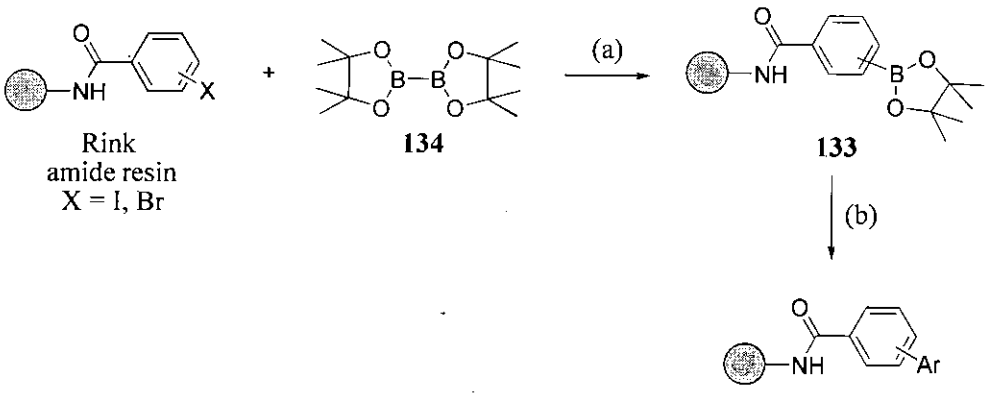

(a) $PdCl_2$(dppf), KOAc, DMF, 80 °C; (b) ArI or ArBr, $Pd(PPh_3)_4$, K_3PO_4, DMF, 80 °C.

Scheme 43

Using analogous methodology Fesik *et al.*[75] prepared the biphenylcarboxylic acid **135** in 44% yield *via* the Suzuki coupling of an immobilised aryl boronic ester on Wang resin **136** with 3-(*N*,*N*-dimethylamino)phenyl triflate **137** and subsequent cleavage using trifluoroacetic acid, **scheme 44**. This is the only reported case involving the use of an aryl triflate for solid phase Suzuki couplings, presumably due to the large number of commercially available aryl iodides and aryl bromides.

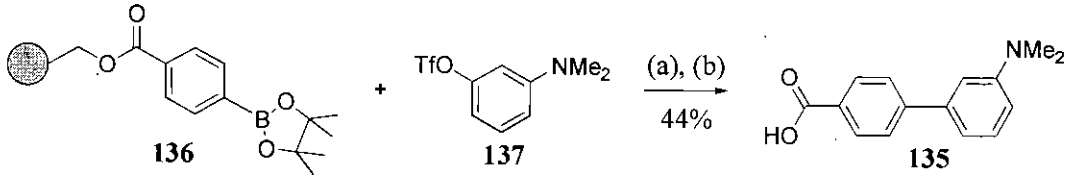

(a) $Pd(OAc)_2$, dppf, 2N aqueous Na_2CO_3, toluene, EtOH, reflux; (b) 95% CF_3CO_2H / H_2O.

Scheme 44

A similar approach, immobilising the aryl boronic ester on the solid support and subsequently coupling it with substituted aryl iodides and bromides, was investigated by Guiles *et al.*[56c] and comparable results were obtained. The principle distinguishing feature of these reactions was that the Suzuki couplings using the polymer-bound boronic ester were shown to proceed at a slower rate than the previously discussed polymer-bound aryl halide systems.[56] $PdCl_2$(dppf) and $Pd(PPh_3)_4$ were once again found to be the optimum catalysts for respective formation of the aryl boronic ester and the subsequent Suzuki coupling reaction.

Both authors also reported successfully coupling functionalised aryl iodides and bromides containing nitro, cyano and methoxy substituents to the polymer-bound aryl boronic ester illustrating the stability of such functional groups to the mild conditions employed.

Giroux *et al.*[47] have developed a one pot biaryl synthesis which eliminates the need to isolate the aryl boronic ester. Initial coupling of tetraalkoxydiboron **134** with a range of aryl halides and triflates using $PdCl_2$(dppf) and potassium acetate in DMF generated the aryl boronic ester, which was reacted *in situ* with various aryl halides and triflates by simply adding further $PdCl_2$(dppf) and aqueous sodium carbonate affording the biaryl systems, **scheme 45**.

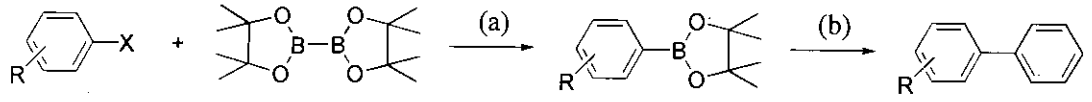

X = Br, I, OTf **134**

(a) $PdCl_2$(dppf), KOAc, DMF, 80 °C; (b) ArBr or ArI or ArOTf, $PdCl_2$(dppf), aqueous Na_2CO_3, 80 °C.

Scheme 45

Our synthetic route requires the Suzuki coupling of a chiral aryl triflate which is effectively substituted with an amino alcohol functional group. An analogy can be drawn with the research undertaken by Shieh *et al.*[50] as they investigated the Suzuki coupling of *N*-Boc-(*S*)-tyrosine triflate **138** with aryl boronic acids. The chiral centre was found to undergo partial racemisation during the palladium catalysed coupling reaction, yet this was eliminated through changing the reaction solvent from DMF to toluene, **scheme 46**.

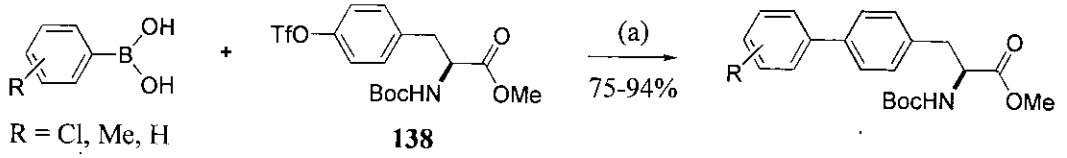

R = Cl, Me, H **138**

(a) $Pd(PPh_3)_4$, K_2CO_3, toluene, 90 °C.

Scheme 46

Optimum results of 94% yield and >99% e.e. were obtained in the aryl boronic acid coupling (R = H) using $Pd(PPh_3)_4$ and potassium carbonate in toluene at 90 °C. Hence, analogous reaction conditions were initially applied in our Suzuki coupling reactions of chiral aryl triflates with aryl boronic esters.

To date, aryl halides have predominantly been used in Suzuki coupling reactions with aryl boronic esters, and the use of aryl triflates is limited. Another example is provided by Giroux *et al.*[47] who reacted phenyltriflate **139** with *p*-methoxyphenyl boronic ester **140** using $PdCl_2$(dppf) and 2N aqueous sodium carbonate in DMF at 80 °C affording the biaryl product **141** in 73% yield, **scheme 47**. As we are also wanting to Suzuki couple aryl triflates and aryl boronic esters these specified reaction conditions were initially investigated.

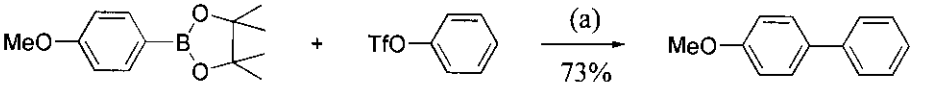

140 + **139** → **141**

(a) $PdCl_2$(dppf), aqueous Na_2CO_3, DMF, 80 °C.

Scheme 47

The nature and substitution of the aryl halides were found to have a strong influence on the yields of the biaryl products obtained. Electron rich aryl boronic esters generated *in situ* from electron rich aryl halides were found to undergo efficient cross-coupling with electron poor aryl halides in high yield. However, lower yields of the biaryl products were obtained when the reactions were carried out in the reverse order.

These observations can be explained by looking at the previously proposed mechanism of the palladium catalysed Suzuki coupling reaction (**scheme 42**). Initial oxidative addition of the aryl halide to the Pd° species is favoured if the aryl halide has electron withdrawing substituents as this effectively activates the Ar-X bond towards the oxidative addition. Therefore it is not surprising that electron poor aryl halides were efficient in the cross-coupling reactions. The rate determining step involves the transmetallation of the aryl boronic ester which is facilitated by

formation of the aryl boron 'ate' complex in the presence of a suitable base. As the rate of transmetallation is increased if the aryl group is nucleophilic we would expect the Suzuki coupling of electron poor aryl halides with electron rich aryl boronic esters to generate the biaryl products in high yield.

2.5 Synthesis of Aryl Boronic Ester Coupling Component

Aryl boronic esters **142** can be formed by the palladium catalysed coupling reaction of either dialkoxyhydroborane **143**[76] or tetraalkoxydiboron pinacol ester **134**[47, 49, 77] with an aryl halide **144** in the presence of a base, **scheme 48**. This methodology was recently expanded to include the direct borylation of aryl triflates and nonaflates utilising dialkoxyhydroborane **143** in an analogous manner.[78]

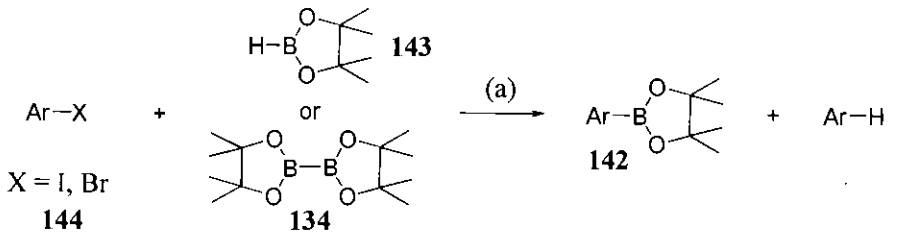

(a) Palladium catalyst, base, solvent.

Scheme 48

As the tetraalkoxydiboron reagent **134** is very expensive and the alternative option of synthesis involves several steps,[79] we decided to use the less expensive dialkoxyhydroborane reagent **143** as a source of the boronic ester.

The coupling reactions of dialkoxyhydroborane **143** with a range of aryl iodides and bromides were investigated by Masuda *et al.*[76] Anhydrous dioxane, toluene, MeCN or CH_2ClCH_2Cl were used as the solvent medium giving similar results, although the use of the polar solvent, DMF, caused decomposition of the dialkoxyhydroborane **143**. The reactions were efficiently catalysed by palladium (II) complexes which had two equivalents of a phosphine ligand, $PdCl_2$(dppf) was typically used. Triethylamine was used in all of the coupling reactions to effectively

convert the $Pd^{II}Cl_2$(dppf) to the Pd°(dppf) complex as the palladium catalyst requires an oxidation state of zero to catalyse the formation of aryl boronic esters, **scheme 49**.

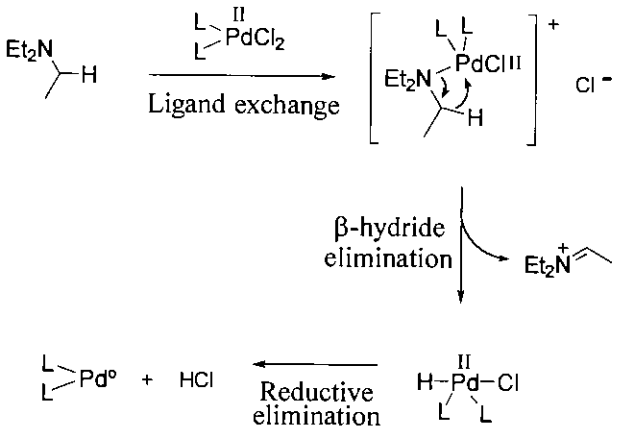

Scheme 49

The mechanism proposed by Masuda for formation of the aryl boronic ester **142**[76] involves initial oxidative addition of the dialkoxyhydroborane **143** to the Pd° complex, this then undergoes σ-bond metathesis with the aryl halide **144** generating aryl boronic ester **142**. Subsequent *cis* alignment and reductive elimination of HX regenerates the Pd° complex thus completing the catalytic cycle, **scheme 50**.

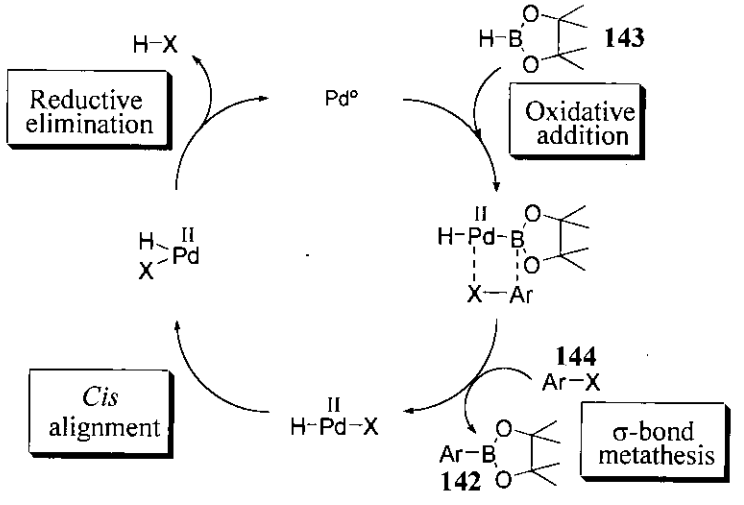

Scheme 50

An alternative catalytic cycle normally observed in palladium catalysed metal hydride reduction would generate the unwanted reduced product Ar-H **145**. This would occur *via* initial oxidative addition of the aryl halide **144** to the Pd° complex

giving Ar-Pd^{II}-X, followed by sequential transmetallation with dialkoxyhydroborane **143** forming Ar-Pd^{II}-H, which undergoes *cis* alignment and reductive elimination of Ar-H **145**, **scheme 51**.

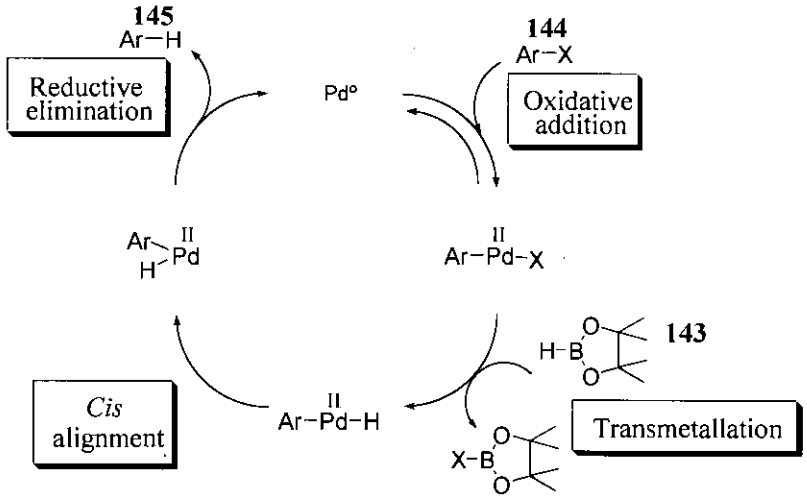

Scheme 51

The anhydrous reaction conditions employed in the synthesis of aryl boronic esters do not allow conversion of the dialkoxyhydroborane **143** to an activated boron 'ate' complex. As a result of this, this second catalytic cycle will be suppressed due to a slow rate of transmetallation with dialkoxyhydroborane **143** resulting from the low nucleophilicity of the hydride. Since the oxidative addition step is reversible, any material which enters this cycle will be released as unreacted Ar-X **144**. Masuda *et al.* illustrated that the undesirable reduction pathway in **scheme 51** can be further suppressed by selectively using electron rich aryl halides which are inactivated to oxidative addition. Thus, the coupling reactions of aryl bromides possessing electron donating groups predominantly afforded the desired aryl boronic ester **142**, although reduced Ar-H **145** was often obtained as a minor component illustrating the feasibility of both catalytic cycles.

Homocoupling of the resultant aryl boronic ester to generate a biaryl product *via* the standard Suzuki coupling cycle (**scheme 42**) is also not observed due to a lack of the required activated boron 'ate' complex.

4-Bromotoluene **146** was chosen as the substrate for the coupling reaction as it most closely models the brominated polystyrene backbone, and the inductive methyl group may suppress the formation of undesirable toluene *via* the reduction pathway. The coupling reaction between 4-bromotoluene **146** and dialkoxyhydroborane **143** using $PdCl_2(dppf)\cdot CH_2Cl_2$ generated 4-(4,4,5,5-tetramethyl-1,3,2-dioxaborolyl) toluene **147** (70%), where the product was purified by Kugelrohr distillation owing to its instability on both silica and alumina observed *via* 2D t.l.c. plates, **scheme 52**.[76]

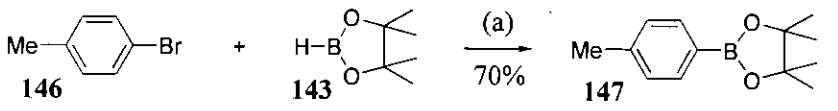

(a) $PdCl_2(dppf)\cdot CH_2Cl_2$, Et_3N, dioxane, 100 °C.

Scheme 52

2.6 Suzuki Coupling Reactions Using Aryl Boronic Ester 147

2.6.1 Suzuki Coupling of Triflated Methyl Ester 124

Since it was not possible to synthesise the triflated amino alcohol **115** directly, it was decided to effect a Suzuki coupling on the triflated methyl ester **124** which can readily be prepared in high yield. It was postulated that reduction of the methyl ester functionality within the biaryl product **148** would be simplified in the absence of the unstable triflate group, allowing generation of the target biaryl amino alcohol **149**.

The aryl boronic ester **147** was successfully coupled with the triflated methyl ester **124** in moderate yield (43%) using the reaction conditions previously optimised by Shieh.[50] The yield of biaryl product **148** was subsequently improved (66%) when those conditions described Giroux[47] were utilised, **scheme 53**.

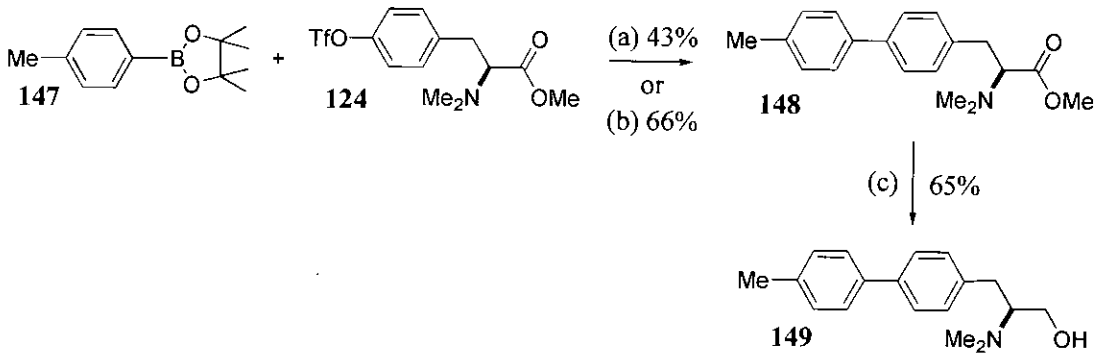

(a) $Pd(PPh_3)_4$, K_2CO_3, DMF, 90 °C; (b) $PdCl_2(dppf)\cdot CH_2Cl_2$, 2N aqueous Na_2CO_3, DMF, 80 °C; (c) $LiBH_4$, THF, RT.

Scheme 53

In retrospect it was noted that Shieh *et al.*[50] used anhydrous conditions for the Suzuki coupling of boronic acids, whereas Giroux *et al.*[47] required an aqueous medium for the Suzuki coupling of boronic ester **140**. It is therefore postulated that our boronic ester **147** requires water to facilitate activation to the boron 'ate' complex resulting in an enhanced rate of transmetallation, thus explaining the difference in yields obtained.

The biaryl methyl ester **148** was subsequently reduced using $LiBH_4$[67] affording the target biaryl amino alcohol **149** in reasonable yield (65%), **scheme 53**. This material was used as a catalyst for the addition of dialkylzinc reagents to aldehydes as discussed in **chapter 6.2.2**.

2.6.2 Suzuki Coupling of Triflated Amino Alcohol 116

The analogous Suzuki coupling of aryl boronic ester **147** and triflated amino alcohol **116** proceeded in moderate yield (50%) using the aqueous Giroux[47] coupling conditions, **scheme 54**. Inevitably some material was lost on purification as the reaction failed to go to completion leading to a difficult separation of biaryl product **150** and unreacted triflate **116** (R_f [DCM:MeOH (90:10)] 0.36 and 0.42 respectively).

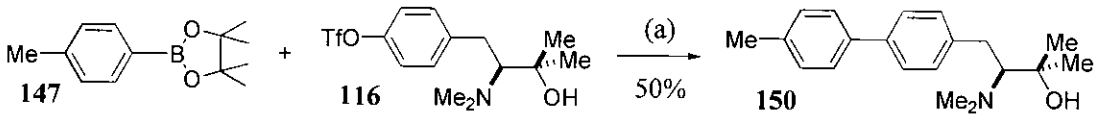

(a) $PdCl_2(dppf)\cdot CH_2Cl_2$, 2N aqueous Na_2CO_3, DMF, 80 °C.

Scheme 54

The disappointing yield could also be attributed to the presence of sodium carbonate deprotonating the free amino alcohol in solution to generate the *N,O*-chelated palladium complex **151**. Formation of the alkoxopalladium (II) complex would effectively consume the palladium catalyst thus reducing the efficiency of the Suzuki coupling reaction, **figure 24**.

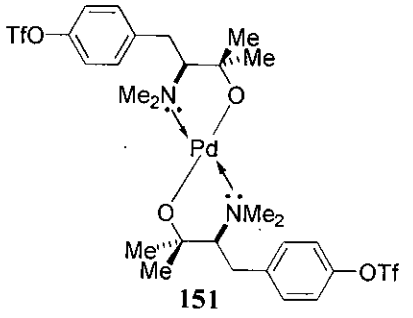

Figure 24

Literature precedent supports the formation of analogous five membered $PdOCH_2CH_2N$ chelate rings from the 2:1 molar reaction of 2,2'-methyliminodiethanol **152** with $Pd(OAc)_2$ in the presence of potassium carbonate, **scheme 55**. The alkoxopalladium (II) complex **153** was isolated and found to be thermally stable thus illustrating the feasibility of this concept.[80]

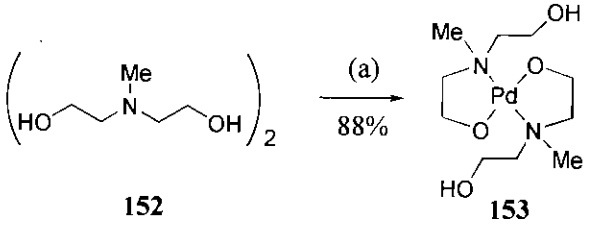

(a) $Pd(OAc)_2$, K_2CO_3, benzene.

Scheme 55

The biaryl amino alcohol **150** was ultimately not studied as a catalyst for the addition of dialkylzinc reagents to aldehydes as it was found to partially cyclise to the monomethylated oxazolidine on standing in $CDCl_3$ as discussed in **chapter 5.4**.

2.6.3 Suzuki Coupling of Triflated Oxazolidinone 118

The attempted Suzuki coupling of boronic ester **147** and triflated oxazolidinone **118** using $Pd(PPh_3)_4$ catalyst in the presence of potassium carbonate and DMF failed to produce any of the desired biaryl oxazolidinone. A black residue was seen to precipitate at an early stage from the reaction mixture which indicates decomposition of the catalyst as palladium black, thus explaining the lack of coupled product. Such a phenomenon is associated with the Suzuki coupling reactions of unsaturated triflates[81] due to the unfavourable interaction generated between the palladium centre (soft acid) and the triflate group (hard base) in the complex **154** generated by oxidative addition. Reaction of **154** with a PPh_3 ligand originating from $Pd(PPh_3)_4$ affords the phosphonium salt **155** and the insoluble Pd (0) species **156**, **scheme 56**.

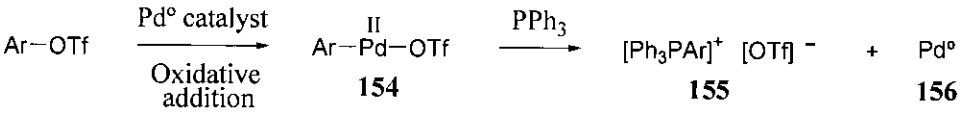

Scheme 56

2.7 Summary of Chapter 2

At this early stage in the research it became apparent that the polymer functionalisation route to chiral polymers posed various problems. Primarily the tyrosine triflate derivatives could not be prepared directly in high yield which would necessitate the premature Suzuki coupling of tyrosine triflate precursors with a polymer-bound boronic acid or ester. As the individual Suzuki coupling reactions and subsequent functional group interconversions only proceeded in moderate yield in the solution phase, these conversions would then be difficult to monitor on the

solid phase. Clearly if such reactions failed to go to completion traces of polymer-bound impurities from previous stages in the synthesis may affect the resultant performance of the chiral polymers. Therefore, in summary the solution phase studies proved invaluable in determining that this approach is not suitable for transferal to the solid support.

In **chapters 3** and **4** an alternative approach to the chiral polymers is presented, whereby tyrosine derived amino alcohol and oxazolidinone vinylic monomers are prepared and subsequently polymerised ensuring that only the chiral moiety is polymer-bound affording complete control.

Chapter 3 : Results and Discussion Part 2

Polymerisation Route to Chiral Polymers

An alternative approach to the target chiral polymer systems **109** and **110** (**figure 21**) involves the synthesis and subsequent copolymerisation of tyrosine derived chiral amino alcohol and oxazolidinone vinylic monomers **157** and **158**, **figure 25**.

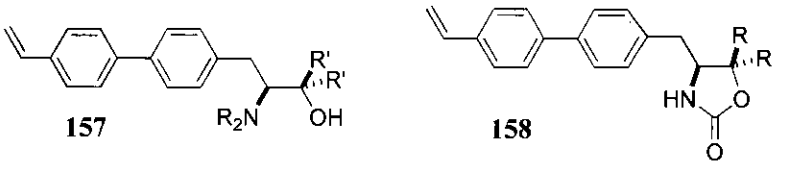

Figure 25

As discussed in **chapter 1.2.1** this strategy involves the copolymerisation of chiral vinyl monomers with styrene where the loading can be controlled by varying the molar ratio of comonomers employed. In addition, the degree of cross-linking can be specified to afford functionalised polymers with the desired sub-structure. This route also allows the polymerisation of a single purified monomer, thus ensuring that only the chiral moiety is polymer-bound providing complete control.

Examples documented throughout **chapter 1** illustrate the general applicability of this approach in the synthesis of polymer-supported amino alcohol catalysts,[35a, 35c, 35e] oxazaborolidine catalysts[43, 45, 82] and a polymeric analogue of Noyori's ligand.[44a]

3.1 Retrosynthesis of Chiral Polymers

Retrosynthesis is illustrated for the chiral polymer-bound amino alcohol **109** case in **scheme 57**, where the polymer-bound oxazolidinone auxiliary **110** would undergo analogous disconnections.

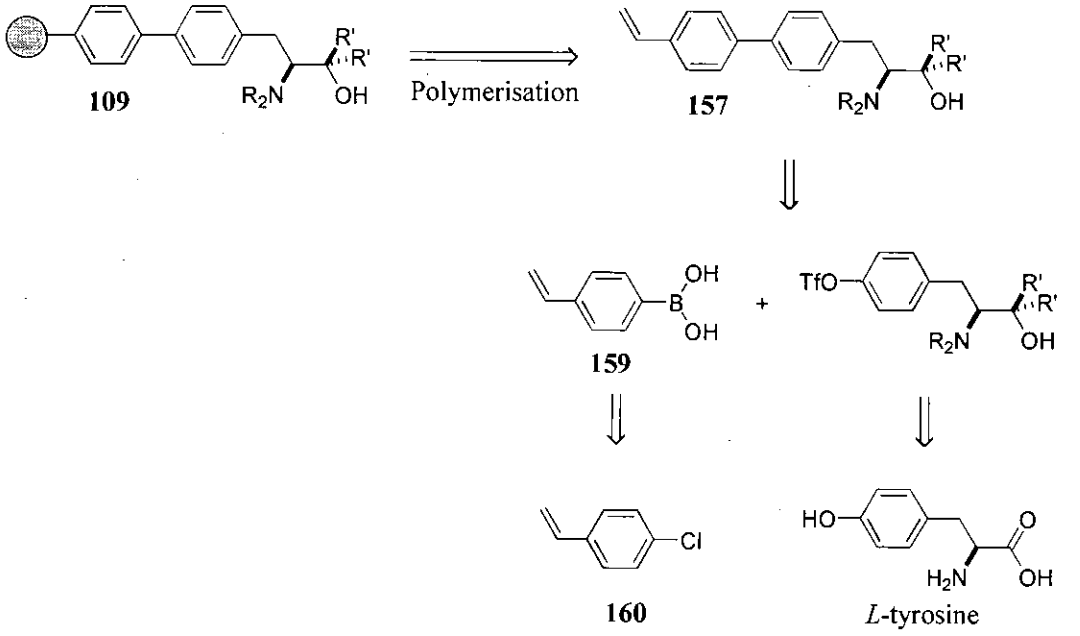

Scheme 57

The proposed strategy aims to generate the crucial C-C biaryl linkage *via* the Suzuki coupling of *p*-vinylphenylboronic acid **159** with a tyrosine triflate derivative. In turn the vinylboronic acid is prepared from *p*-chlorostyrene **160** where various tyrosine triflate compounds can be synthesised from commercially available *L*-tyrosine.

Biaryl systems have previously been prepared *via* the Suzuki coupling of an aryl boronic acid and an aryl triflate[50, 83] using various palladium catalysts in the solution phase. There is also evidence to support the synthesis of vinylboronic acid **159**[84] and aryl triflate formation in tyrosine derivatives is well-precedented[50, 51] thus indicating the suitability of both components to this reaction.

Initial studies focused on the preparation of *p*-vinylphenylboronic acid **159** and its application in the synthesis of vinyl amino alcohol monomers **161** and **162**, **figure 26**.

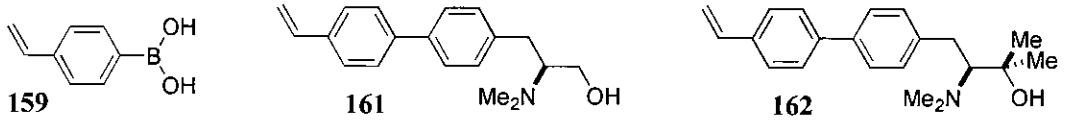

Figure 26

3.2 Synthesis of Vinylboronic Acid 159

Kamogawa *et al.* prepared *p*-vinylphenylboronic acid **159** in 39% yield utilising *p*-bromostyrene as the commercially available starting reagent.[84] Our synthesis of **159** differs in that *p*-chlorostyrene **160** was chosen as the halostyrene component due to availability within the research group. Direct conversion of *p*-chlorostyrene **160** to the corresponding Grignard reagent and *in situ* reaction with trimethylborate, followed by base hydrolysis afforded vinylboronic acid **159** in improved yield (46%), **scheme 58**.

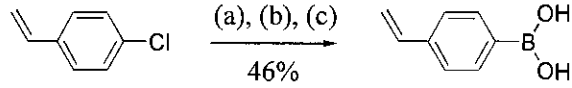

160 **159**

(a) Mg, I_2, THF, reflux; (b) $B(OMe)_3$, -78 °C; (c) aqueous NaOH, RT.

Scheme 58

However, synthesis of *p*-vinylphenylboronic acid **159** proved highly capricious. The necessary inclusion of iodine often required to activate Grignard formation generated the ion pair I^+ I_3^- which subsequently initiated the preferential cationic oligomerisation of *p*-chlorostyrene. This process provided insoluble oligomerised material thus reducing the yield of vinylboronic acid **159**. Alternative approaches designed to activate Grignard formation whilst minimising the use of iodine were investigated with limited success.

1,2-Dibromoethane **163** has been shown to react with magnesium to give 2-bromoethylmagensium bromide **164** which rapidly eliminates activated magnesium (II) bromide **165** with ethene produced as a gaseous by-product, **scheme 59**.[85]

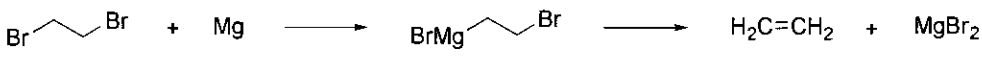

163 **164** **165**

Scheme 59

Yet, despite the addition of one equivalent of **163** to the reaction mixture significant amounts of iodine were still required to initiate formation of

p-styrenemagnesium chloride resulting in a low overall yield (8%) of the target vinylboronic acid **159**. Ultimately the use of rigorously activated magnesium turnings which were washed with ether, dried at 100 °C under reduced pressure and finally stirred under argon for 24 h reduced the iodine requirement and thus the oligomerisation potential. In addition the slow controlled addition of *p*-chlorostyrene **160** proved vital in ensuring that the monomer concentration remained low throughout the course of the reaction, thus again minimising undesirable oligomerisation.[86] These joint modifications afforded the target vinylboronic acid **159** in 46% yield with improved reproducibility.

3.3 Synthesis of Vinyl Amino Alcohol Monomer 161

A similar strategy to that described in **chapter 2.6.1** was followed effecting the Suzuki coupling of triflated methyl ester **124** which can readily be prepared in high yield (**chapter 2.3.1**). It was postulated that reduction of the methyl ester functionality within the vinyl monomer **166** would be simplified in the absence of the unstable triflate group, allowing generation of the amino alcohol monomer **161**.

A range of different reaction conditions were investigated varying the palladium catalyst, base and solvent used in the Suzuki coupling of vinylboronic acid **159** and triflated ester **124** in order to optimise the yield of vinyl monomer **166**, **scheme 60**. In each instance a slight excess of **159** was employed to ensure complete consumption of **124** thus eliminating the difficult chromatographic separation of triflated ester **124** and monomer product **166** which possess similar R_f values, [DCM:MeOH (90:10)] 0.78 and 0.71 respectively. The yields of vinyl monomer **166** obtained employing the various reaction conditions are summarised in **table 3**.

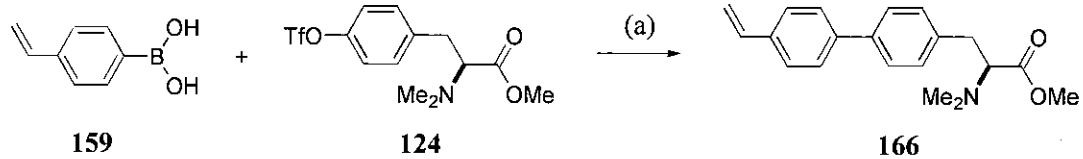

159 **124** **166**

(a) Palladium catalyst, base, solvent.

Scheme 60

Table 3 - Suzuki Coupling Results

Entry	Pd catalyst	Base	Solvent	Result
1 [a]	$Pd(PPh_3)_4$	K_2CO_3	DMF	incomplete reaction
2 [b]	$PdCl_2(dppf)•CH_2Cl_2$	2N aqueous Na_2CO_3	DMF	71% yield
3 [b,c]	$PdCl_2(dppf)•CH_2Cl_2$	2N aqueous Na_2CO_3	DMF	63% yield
4 [b]	$PdCl_2(dppf)•CH_2Cl_2$	$K_3PO_4•H_2O$	DME	82% yield

[a] Analogous protocol to that detailed in **method D** of **chapter 8.2** followed for the experimental and work-up procedures.
[b] Analogous protocol to that detailed in **method C** of **chapter 8.2** followed for the experimental and work-up procedures.
[c] Potassium bromide (1.1 equivalents) added to the reaction mixture.

Utilising the anhydrous reaction conditions optimised by Shieh *et al.*[50] (entry 1) afforded an inseparable 5:1 ratio of product **166** : unreacted triflated ester **124** as deduced from the relative integration of N*Me* signals in the crude ^{1}H NMR spectrum. In contrast, the conditions developed by Giroux *et al.*[47] gave complete conversion to the monomer **166** which was subsequently isolated in 71% yield (entry 2). This result suggests that aqueous activation of vinylboronic acid **159** to the boron 'ate' complex is required to enhance the rate of transmetallation, thus explaining the difference in yields obtained.

The presence of potassium bromide in the Suzuki coupling of unsaturated triflates has been shown to reduce decomposition of the catalyst as palladium black (**scheme 56**).[81] However, in this case addition of potassium bromide (entry 3) reduced the yield of vinyl monomer **166** (63%) and a black residue was still seen to precipitate at an early stage from the reaction mixture.

The optimised yield of vinyl monomer **166** (82%) was ultimately obtained by substituting potassium phosphate monohydrate as the base and DME as the solvent (entry 4). These reactions conditions effectively mimic those developed by Satoh *et al.* for the Suzuki coupling of an aryl boronic ester and an aryl triflate.[48] Overall these results strongly imply that the Suzuki coupling reaction conditions are substrate dependant and must be individually optimised for each specific reaction under investigation.

The vinyl methyl ester **166** was subsequently reduced using $NaBH_4$[65] affording the target amino alcohol monomer **161** in good yield (78%), **scheme 61**. Thus this monomer was produced in 5 steps with 63% overall yield. However, it was not polymerised and investigated as a polymer-supported catalyst for the addition of dialkylzinc reagents to aldehydes, as the analogous solution phase reduced amino alcohol **149** mimic prepared in **chapter 2.6.1** was found to induce poor levels of asymmetric induction as discussed in **chapter 6.2.2**.

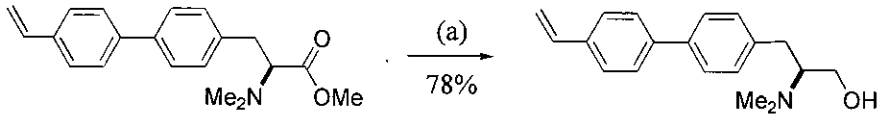

166 **161**

(a) $NaBH_4$, THF, MeOH, reflux.

Scheme 61

Additional monomers **167** and **168** possessing alternative amino alcohol derived functionality were introduced as potential dialkylzinc catalysts to compensate for the inadequate catalytic activity of vinyl amino alcohol monomer **161**, **figure 27**.

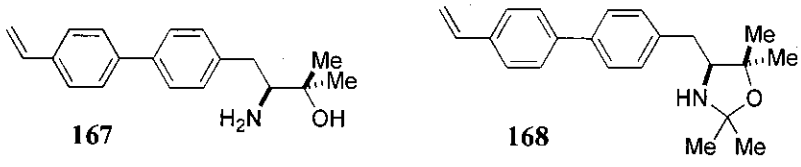

167 **168**

Figure 27

Monomer **167** was investigated as an analogue of the *N,N*-dimethylated system **162** to observe how the asymmetric induction is affected by varying the substitution patterns of the amino alcohol catalyst. Monomer **168** was considered following a report by Joshi *et al.* where a similar oxazolidine system **169** was utilised as a solution phase catalyst for the addition of dialkylzinc reagents to aldehydes with impressive results, **scheme 62**.[87] The synthesis of vinyl monomers **167** and **168** is discussed in **chapters 3.6** and **3.8** respectively.

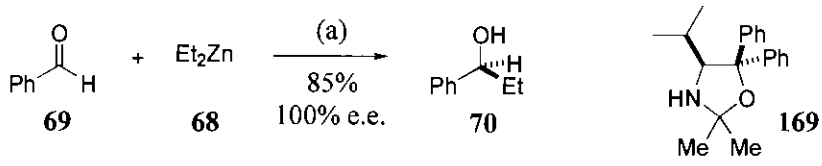

(a) Oxazolidine catalyst **169**.

Scheme 62

3.4 Attempted Synthesis of Vinyl Amino Alcohol Monomer 162

Treatment of vinyl methyl ester **166** with MeMgI or MeLi to incorporate the geminal dimethyl groups routinely afforded the amino alcohol monomer **162** in very poor yield (4-18%), **scheme 63**. The reaction conditions employed and the resulting yields of amino alcohol monomer **162** obtained are summarised in **table 4**.

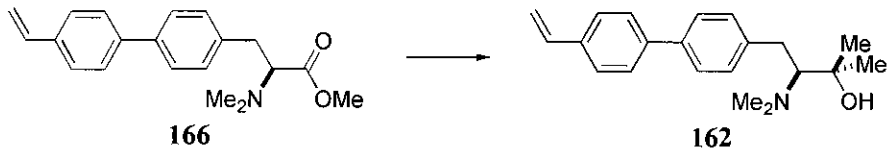

Scheme 63

Table 4 - Summary of Reagents Employed to Convert 166 to 162

Entry	Reagents	Reaction temperature	Result
1	(i) MeI, Mg, I_2, Et_2O, reflux; (ii) **166**, Et_2O	reflux	18% yield
2	**166**, MeLi, THF	-78 °C→0 °C	12% yield
3	**166**, MeLi, Et_2O	-78 °C	4% yield

The Grignard addition of freshly prepared MeMgI to vinyl methyl ester **166** (entry 1) appeared to go to completion as monitored by t.l.c. However, subsequent work-up and chromatographic purification afforded the vinyl amino alcohol **162** in low yield (18%) where unreacted **166** was recovered (60%). This result could be attributed to MeMgI acting as a base to deprotonate the chiral centre of **166**, thus generating the enolate salt **170**, **figure 28**. This process could effectively remove the

reactive methyl ester **166** from solution as the insoluble salt whereby quenching of the reaction mixture would then regenerate racemic vinyl methyl ester *rac*-**166**.

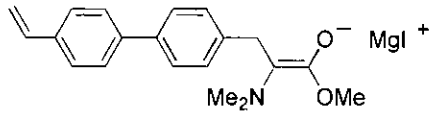

170

Figure 28

Similar deprotonation of the intermediate vinyl ketone **171** generated by addition of a single equivalent of Grignard reagent would result in the generation of enolate salt **172**, **scheme 64**. Clearly if this process is reversible vinyl ketone *ent*-**171** would be exposed to the Grignard reagent resulting in formation of racemic amino alcohol monomer *rac*-**162**, thus casting doubt over the stereochemical integrity of the amino alcohol monomer **162** isolated from this reaction.

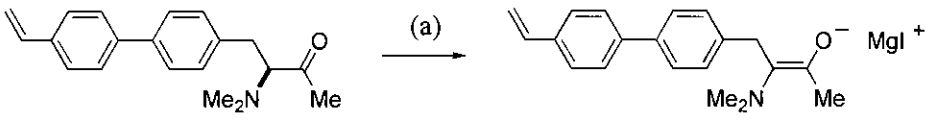

171 **172**

(a) MeMgI.

Scheme 64

Treatment of vinyl methyl ester **166** with MeLi using THF as the solvent (**table 4**, entry 2) allowed chromatographic isolation of the amino alcohol vinyl monomer **162** in only 12% yield (**scheme 63**). The remainder of material eluted from the column gave signals consistent with those expected for the α-methyl protons by ^{1}H NMR analysis, but the vinylic protons were no longer present and all of the signals were very broad suggesting that the product material **162** had oligomerised.

The reaction was repeated using ether as the solvent medium (**table 4**, entry 3) as anionic oligomerisation of styrene systems using organolithium is more common in THF than in ether.[88a] Unfortunately the product **162** was isolated in reduced yield (4%) where the bulk of material was recovered as a soluble jelly which was presumed to be the linear oligomerised material (**scheme 63**).

Note that no discrete product **173** was isolated in either MeLi addition reaction (**table 4**) from the carbolithiation of MeLi to the styrene component of vinyl methyl ester **166**, **scheme 65**.[88b] Presumably the highly reactive lithiated intermediate **174** undergoes rapid oligomerisation with the introduced methyl group providing little steric hindrance to inhibit this process.

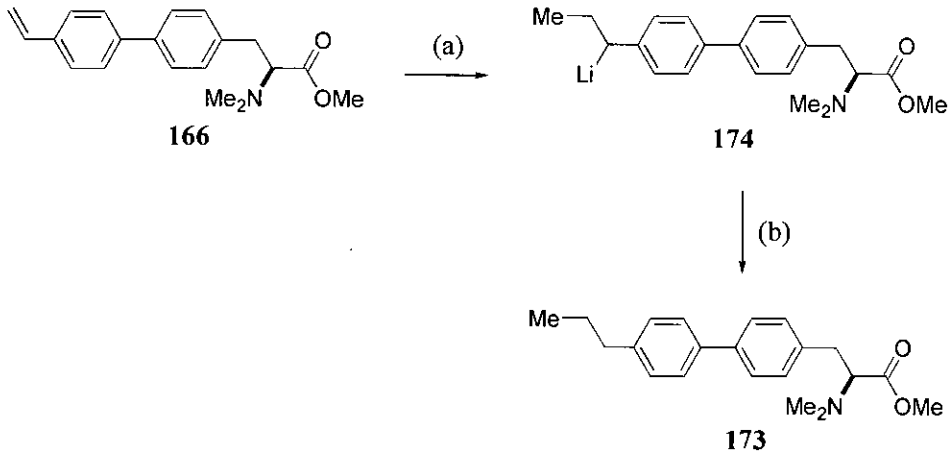

(a) MeLi, THF or Et_2O; (b) aqueous work-up.

Scheme 65

At this stage in the research no high yielding route to amino alcohol monomer **162** had been established due to the problematic introduction of the geminal dimethyl functionality. Use of MeLi was not viable owing to preferential oligomerisation of the styrene group, and MeMgI addition proceeded in low yield with the added concern of stereochemical control.

3.5 Introduction of *N*-Boc Protection in Monomer Synthesis

A report by Davies *et al.* illustrated that the addition of MeMgBr to chiral *N*-Boc methyl esters of α-amino acids afforded *N*-Boc protected amino alcohols with no racemisation of the product chiral centre, **scheme 66**.[89] Introduction of the Boc protecting group was found to be crucial in disfavouring deprotonation of the stereogenic centre by excess Grignard reagent.

The mechanism proposed by Davies *et al.* denotes that initial deprotonation of the acidic carbamate proton results in the formation of an anion α to the chiral centre **175**. The second equivalent of MeMgBr attacks the ester functionality of **175** to afford the intermediate ketone **176** which predominantly undergoes nucleophilic addition of MeMgBr to afford the desired homochiral product **177**. The absence of *ent*-**177** suggests that the minor alternative reaction pathway involving deprotonation of ketone **176** is irreversible due to the inherent stability of enolate **178, scheme 66**.

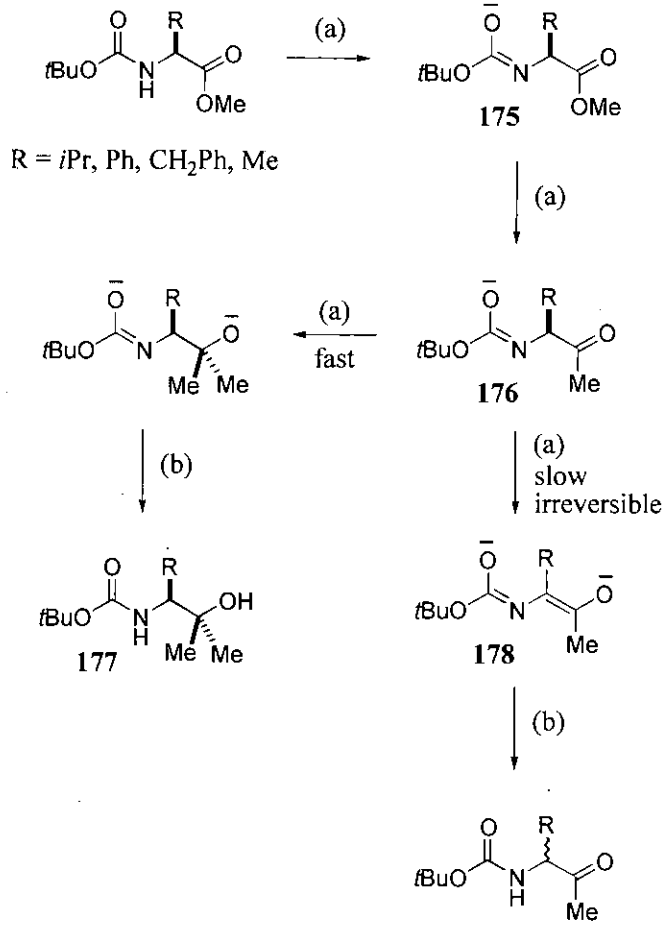

(a) MeMgBr; (b) MeOH.

Scheme 66

A similar approach of subjecting an *N*-Boc protected methyl ester to the Grignard addition reaction was adopted in our synthetic strategy to ensure stereogenic control. Furthermore, it was decided that inclusion of the Boc group at

an early stage in the synthesis would eliminate the possibility of base promoted racemisation in the subsequent triflation and Suzuki coupling steps.

In accordance with this hypothesis *L*-tyrosine methyl ester **121** was initially Boc protected using standard literature conditions to afford **179** in good yield (77%).[90] Subsequent triflation with triflic anhydride provided almost quantitative conversion to the triflated Boc methyl ester **138** (96%), **scheme 67**.[50]

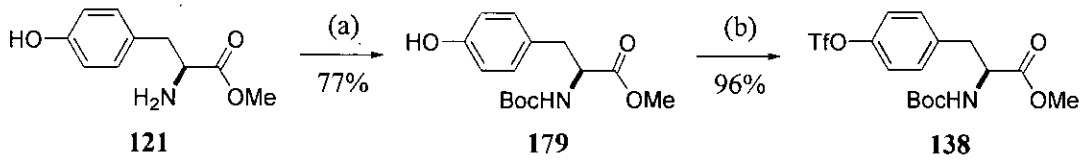

121 **179** **138**

(a) $(Boc)_2O$, Et_3N, DCM, 0 °C→RT; (b) $(CF_3SO_2)_2O$, pyridine, DCM, 0 °C.

Scheme 67

A range of different reaction conditions were then investigated varying the palladium catalyst, base and solvent used in the Suzuki coupling of vinylboronic acid **159** and triflated ester **138** in order to optimise the yield of the coupled product **180**, **scheme 68**.

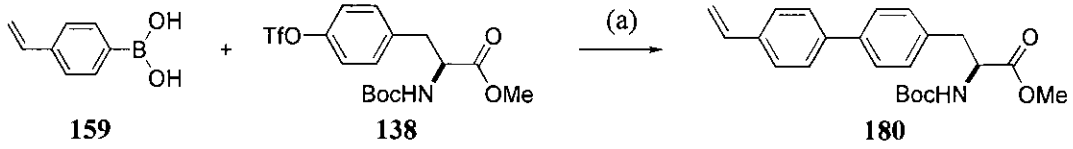

159 **138** **180**

(a) Pd catalyst, base, solvent.

Scheme 68

In each reaction an analogous protocol to that detailed in **method E** of **chapter 8.3** was followed for the experimental and work-up procedures. The reaction parameters were also consistent throughout using a 2:1 excess of vinylboronic acid **159** : triflated ester **138** with anhydrous solvent (unless otherwise stated). The results are summarised in **table 5**.

Table 5 - Suzuki Coupling Results

Pd catalyst	Base	Solvent	Reaction time	Result [a]
$PdCl_2(dppf)•CH_2Cl_2$ (10 mol%) [48]	$K_3PO_4•H_2O$ (4.0 equivalents)	DME	23 h	incomplete reaction
$Pd(PPh_3)_4$ (3 mol%) [50]	K_2CO_3 (1.5 equivalents)	toluene	22 h	36% yield [b]
$Pd(OAc)_2$ (2 mol%) PPh_3 (6 mol%)	K_2CO_3 (1.5 equivalents)	toluene	20 h	61% yield
$Pd(OAc)_2$ (2 mol%) [c] PPh_3 (6 mol%)	K_2CO_3 (1.5 equivalents)	toluene	22 h	incomplete reaction
$Pd(OAc)_2$ (2 mol%) [d] PPh_3 (6 mol%)	K_2CO_3 (1.5 equivalents)	toluene	16 h	no reaction
$Pd(OAc)_2$ (1 mol%) (2-Ph)PhP(tBu)$_2$ (2 mol%) [91a]	$K_3PO_4•H_2O$ (2.0 equivalents)	toluene	16 h	incomplete reaction
$Pd(OAc)_2$ (1 mol%) P(tBu)$_3$ (3 mol%) [91b]	K_2CO_3 (3.0 equivalents)	toluene	32 h	incomplete reaction
$PdCl_2(dppf)•CH_2Cl_2$ [e] (10 mol%) Ph_3As (40 mol%) [91c]	Cs_2CO_3 (3.0 equivalents)	DMF	16 h	incomplete reaction
Pd / C (40 mol%) [f] [83b]	Na_2CO_3 (1.5 equivalents)	DMF	21 h	no reaction
$Pd_2(dba)_3$ (6 mol%) [91d]	KOH (3.0 equivalents)	toluene	72 h	no reaction
$Pd_2(dba)_3$ (2 mol%) Ph_3As (6 mol%)	K_2CO_3 (1.5 equivalents)	toluene	19 h	no reaction

[a] Determined from crude ^{1}H NMR spectra ($CDCl_3$) of residues obtained identifying isolated O*Me* signal of triflated ester **138** (δ = 3.70 ppm) versus that of the coupled product **180** (δ = 3.73 ppm).
[b] Reaction failed to go to completion resulting in difficult separation of triflated ester **138** and coupled product **180**. The residue was chromatographed on silica gel [hexane:EtOAc (92:8)] with further chromatography [DCM] required to allow isolation of pure product material **180**.
[c] Molecular sieves added to the reaction mixture. [d] Water (0.5 cm^3) added to the reaction mixture in addition to toluene (3.0 cm^3). [e] Potassium bromide (1.2 equivalents) added to the reaction mixture. [f] Lithium chloride (2.0 equivalents) added to the reaction mixture.

Initial studies utilised the Suzuki conditions previously optimised for the analogous coupling between vinylboronic acid **159** and triflated *N,N*-dimethylated ester **124** (**chapter 3.3**).[48] However, the combination of $PdCl_2(dppf)\bullet CH_2Cl_2$ catalyst with potassium phosphate as the base in DME gave incomplete conversion. Isolation of the coupled product **180** from unreacted triflated ester **138** by chromatography or crystallisation proved impossible owing to the similar R_f values and solubility properties of **180** and **138**. Addition of further catalyst and base during the reaction or extending the reaction time failed to drive the reaction to completion.

Employing $Pd(PPh_3)_4$ catalyst with potassium carbonate in toluene afforded the coupled product in poor yield **180** (36%) which could potentially be attributed to the air sensitive and unpredictable activity of the commercially available catalyst.[50]

An analogous reaction using $Pd(PPh_3)_4$ prepared *in situ* from $Pd(OAc)_2$ and PPh_3 improved the yield of isolated product **180** (61%). The addition of molecular sieves to ensure anhydrous conditions gave reduced conversion potentially resulting from surface adhesion of the reagents to the molecular sieves, thus effectively removing the reactive species from solution. The alternative approach of including water in the reaction mixture to potentially activate the vinylboronic acid **159** to the boron 'ate' complex gave detrimental results as no reaction was observed.

The remaining experimental conditions detailed in **table 5** were investigated following literature precedent which suggested that specific palladium reagent / ligand combinations could be employed to generate activated palladium catalysts.

$Pd(OAc)_2$ was used in combination with (2-Ph)PhP(tBu)$_2$[91a] and P(tBu)$_3$[91b] where the increased steric bulk of the phosphine ligands would limit their complexation to the palladium centre. $PdCl_2(dppf)\bullet CH_2Cl_2$ was also investigated in combination with Ph_3As ligand which is known to bind less strongly to palladium than the traditional phosphine ligands.[91c] Despite selecting ligands to generate an electronically and co-ordinatively unsaturated palladium centre all three reactions failed to go to completion and no coupled product **180** could be isolated.

Palladium on charcoal represented the inexpensive "ligandless" catalyst[83b] which unfortunately provided no activity in the Suzuki coupling of vinylboronic acid **159** and triflated ester **138** (**scheme 68**). $Pd_2(dba)_3$ was also studied as a "ligandless" catalyst where the dibenzylidene ligands weakly complex the two palladium centres. Clearly $Pd_2(dba)_3$ catalyst with or without[91d] Ph_3As as a co-ligand failed to enhance oxidative addition of triflated ester **138** as no reaction occurred.

Ultimately the optimised yield (61%) of coupled product **180** resulted from the use of $Pd(PPh_3)_4$ generated *in situ* with potassium carbonate as the base in toluene. The unexplainable lack of reactivity observed with many of the other studied reagent combinations again highlights the capricious substrate dependant nature of the Suzuki coupling reaction.

An analogous racemic synthesis of *rac*-**180** using the previously optimised reaction conditions afforded the coupled *rac*-**180** in five steps with 17% overall yield, **scheme 69**.[ξ]

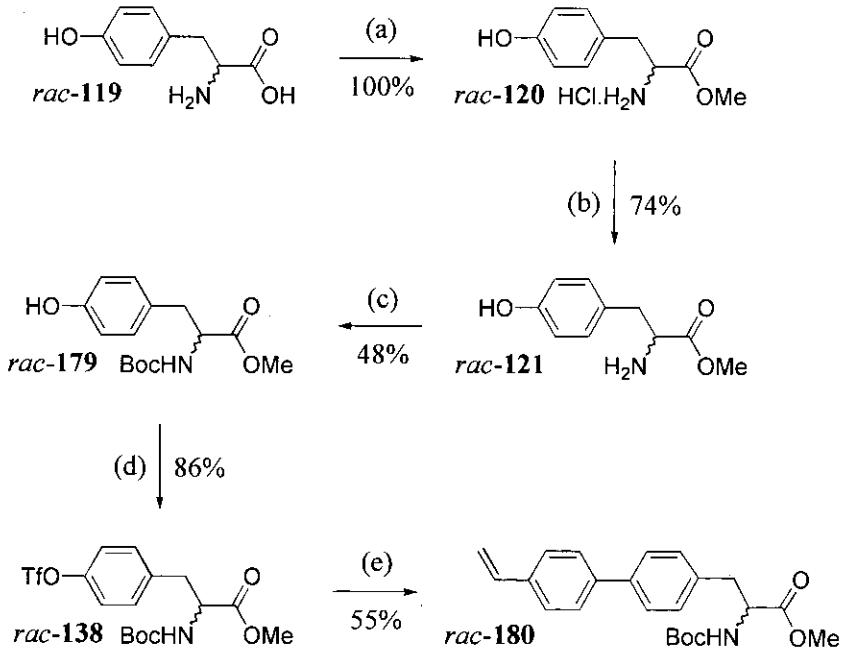

(a) AcCl, MeOH, reflux; (b) K_2CO_3; (c) $(Boc)_2O$, Et_3N, DCM, 0 °C→RT; (d) $(CF_3SO_2)_2O$, pyridine, DCM, 0 °C; (e) (i) $Pd(OAc)_2$, PPh_3, toluene, RT; (ii) $CH_2CHC_6H_4B(OH)_2$, *rac*-**138**, K_2CO_3, 85 °C.

Scheme 69

[ξ] *Rac*-**121** was reacted with 1.5 equivalents of $(Boc)_2O$ resulting in some material being doubly Boc protected on the amine and phenolic hydroxyl positions thus reducing the isolated yield of *rac*-**179**.

Synthesis of *rac*-**180** provided a means to optimise chiral HPLC column conditions to give good baseline separation of the two enantiomer peaks. Freshly prepared chiral non-racemic **180** was then analysed by HPLC under the same conditions. The optical purity of the vinyl ester **180** was measured to be ≥ 99.8% enantiomeric excess, see **appendix** for chiral HPLC traces.

Grignard addition of freshly prepared MeMgI to vinyl methyl ester **180** proceeded smoothly affording the Boc protected amino alcohol monomer **181** (82%), **scheme 70**. On this occasion iodine was omitted from the reaction and forcing reflux conditions were employed as an alternative means of initiating formation of MeMgI Grignard reagent. This was necessary to eliminate possible cationic oligomerisation of the styrene functionality which was observed when iodine was used in a similar context in the preparation of vinylboronic acid **159** (**chapter 3.2**).

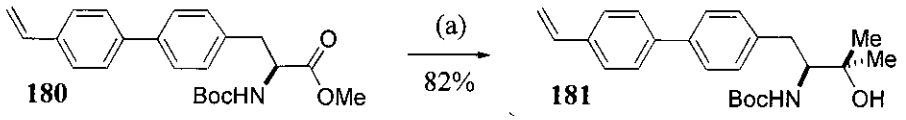

(a) (i) MeI, Mg, Et_2O, reflux; (ii) **180**, Et_2O, reflux.

Scheme 70

The vinyl amino alcohol **181** was subjected to chiral HPLC analysis where the analogous *rac*-**181** was prepared (55%) to provide the retention times of the two enantiomers, **scheme 71**. The optical purity of chiral non-racemic **181** was measured to be ≥ 99.8% enantiomeric excess, see **appendix** for chiral HPLC traces. This result illustrates that introduction of the Boc protecting group was successful in eliminating racemisation of the stereogenic centre during Grignard reaction.

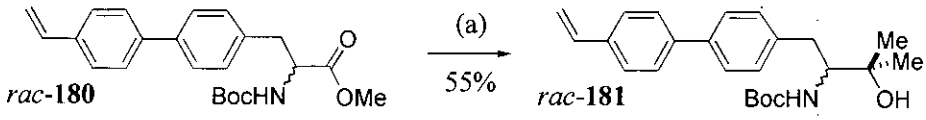

(a) (i) MeI, Mg, Et_2O, reflux; (ii) *rac*-**180**, Et_2O, reflux.

Scheme 71

3.6 Synthesis of Vinyl Amino Alcohol Monomer 167

The Boc protected amino alcohol **181** was treated with aqueous hydrochloric acid to effect removal of the Boc group where MeCN was introduced as a co-solvent for the reaction to eliminate the need for a phase transfer catalyst. This provided the vinyl amino alcohol monomer **167** in good yield (87%), **scheme 72**. This monomer was subsequently polymerised (**chapter 4.5.3**) and investigated as a polymer-supported catalyst for the addition of dialkylzinc reagents to aldehydes (**chapter 6.3**).

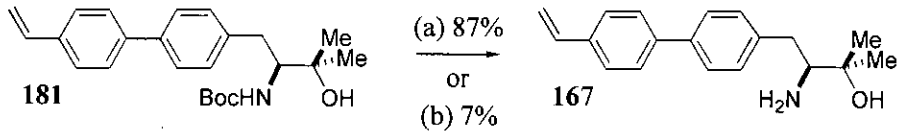

(a) 3N aqueous HCl, MeCN, RT; (b) CF_3CO_2H, DCM, RT.

Scheme 72

In contrast, reaction of Boc protected amino alcohol **181** with trifluoroacetic acid was found to induce extensive cationic oligomerisation of the vinyl functionality resulting in a poor yield of **167** (7%), **scheme 72**.[92] The reaction temperature was reduced to -78 °C in an attempt to promote Boc removal relative to oligomerisation, but this afforded no vinyl amino alcohol **167** despite reducing the rate of oligomerisation.

The differing reactivity of amino alcohol **181** with aqueous hydrochloric acid / MeCN versus trifluoroacetic acid / DCM where the latter reagent combination causes preferential oligomerisation of the vinyl monomer **181**, can be explained by considering the different solvent mediums employed. Potentially H_2O / MeCN forms a biphasic system where the two solvents are not fully miscible. This results in solvation of the polar Boc protected amino ester component of **181** with aqueous hydrochloric acid, thus facilitating removal of the Boc group. However, the non-polar styrene component of **181** being surrounded with MeCN does not come into contact with the acid and as such oligomerisation of the vinyl functionality is not observed, **figure 29**.

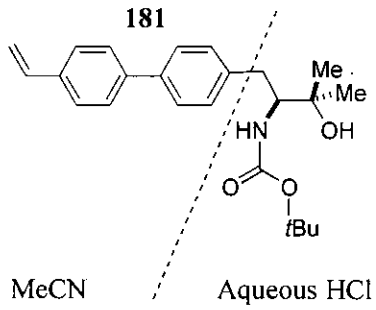

Figure 29

In contrast, reaction of amino alcohol **181** with trifluoroacetic acid in DCM predominantly effects cationic oligomerisation of the monomer. This occurs *via* initial protonation of the vinyl group generating the initiated carbocation chain **182**, subsequent propagation with further monomer **181** proceeds rapidly due to the absence of any other reagents capable of causing chain termination to afford the oligomerised material, **scheme 73**.

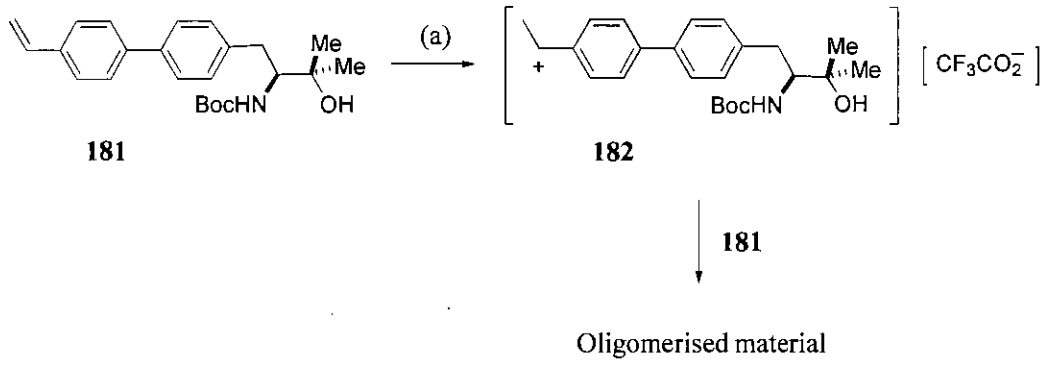

(a) CF_3CO_2H, DCM, RT.

Scheme 73

Clearly, in this case amino alcohol **181** is surrounded by a monophasic solution of acid / DCM with no discrimination between solvation of the polar head and non-polar tail of **181**, thus the acid can either deprotect or oligomerise the Boc protected amino alcohol monomer **181**.

3.7 Attempted Synthesis of Vinyl Amino Alcohol Monomer 162

Amines are routinely methylated by reaction with formaldehyde and formic acid,[93] or formaldehyde and acetic acid in the presence of a hydride reducing agent.[67, 94] Initial studies focused on the reductive amination of vinyl amino alcohol monomer **167** using formaldehyde, acetic acid and sodium cyanoborohydride, **scheme 74**.[94]

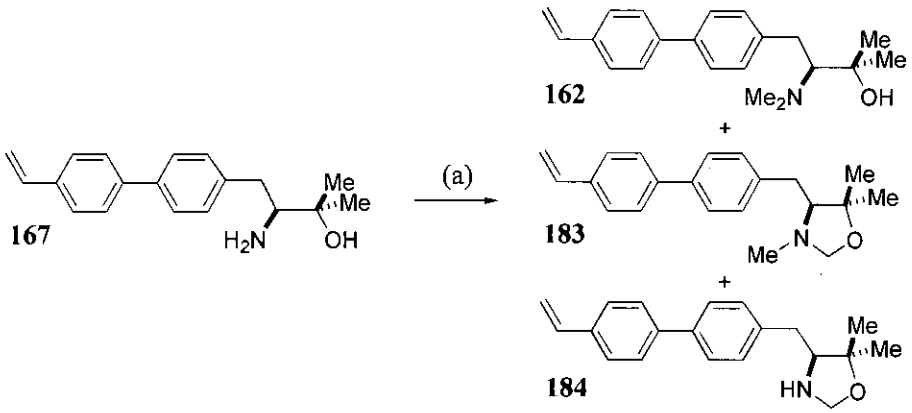

(a) Aqueous H_2CO, $NaCNBH_3$, AcOH, MeCN, RT.

Scheme 74

The crude product mixture was analysed by ^1H NMR and found to contain an 11:1 ratio of the desired *N,N*-dimethylated amino alcohol **162** : *N*-methyl oxazolidine **183** with traces of the *N*-H oxazolidine **184** as determined from the relative intensity and chemical shift values of the various distinctive methyl proton signals, **scheme 74.**

These observations can be explained by considering the reductive amination mechanism, which occurs *via* the sequential generation and hydride reduction of the intermediate iminium ions **185** (R = H, Me), **figure 30**.

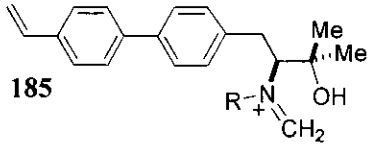

R = H, Me

Figure 30

In this instance competitive intramolecular cyclisation of the hydroxyl group onto the methylene carbon of the respective iminium ions **185** affords the oxazolidine impurities **184** (R = H) and **183** (R = Me). It is also feasible that cyclodehydration of amino alcohol **167** with formaldehyde could generate the *N*-H oxazolidine **184**.

The complex mixture of reaction products prevented isolation of the vinyl amino alcohol **162** by crystallisation or chromatography. However, another possible means of purification documented by Page *et al.*[95] illustrated that oxazolidines derived from formaldehyde undergo reductive cleavage in refluxing formic acid. This process is exemplified in the reductive ring opening of oxazolidine **186** affording *N*-methylpseudoephedrine **187** in excellent yield (90%), **scheme 75**.

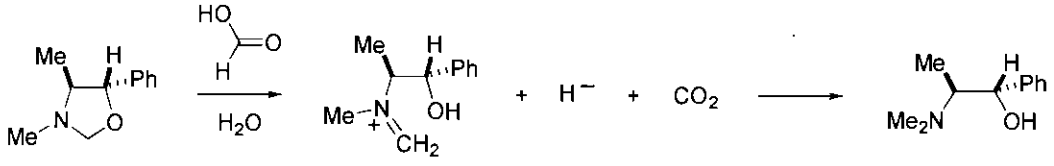

186 **188** **187**

Scheme 75

Initial cleavage of oxazolidine **186** *via* protonation with formic acid generates the methyleneiminium ion **188** with elimination of a formate anion. Decarboxylation of the formate anion produces a hydride ion which in turn effects reduction of the iminium ion **188** to provide the amino alcohol **187**.

In accordance with this report the crude reaction mixture obtained in **scheme 74** containing **162**, **183** and **184** was subjected to the formic acid reflux conditions. ^{1}H NMR analysis of the crude product mixture indicated that reductive ring opening had occurred, but the absence of any vinylic signals suggested oligomerisation of the product vinyl amino alcohol monomer **162**. The main component was postulated to be the dimer **189** (45%) as determined by ^{1}H NMR with a 3 : 16 ratio of protons representing the CH*Me* singlet relative to the aromatic multiplet, **scheme 76**. The presence of two methyl doublets and two hydroxyl protons in a 9:1 ratio denoted the existence of two diastereomers.

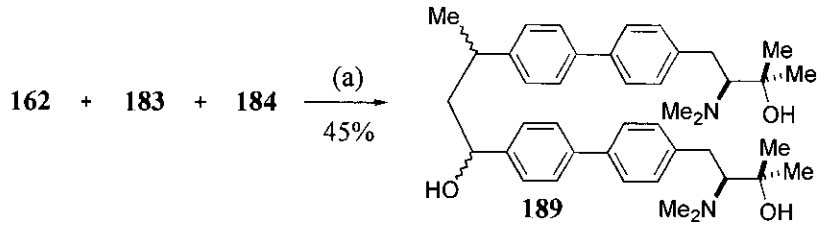

(a) 38% aqueous HCO_2H, reflux.

Scheme 76

The proposed mechanism for formation of dimer **189** involves protonation of the amino alcohol monomer **162** with formic acid to provide the initiated chain **190** where the formate anion functions as the gegenion. Propagation of **190** with another vinyl amino alcohol monomer **162** affords the carbocation dimer **191** which can effectively chain terminate with water present in the formic acid to provide the dimeric product **189** (45%), **scheme 76**. Alternatively, **191** could further propagate with **162** to generate oligomerised product, where this material was presumably lost on work-up, explaining the non-quantitative conversion to dimer **189**, **scheme 77**.

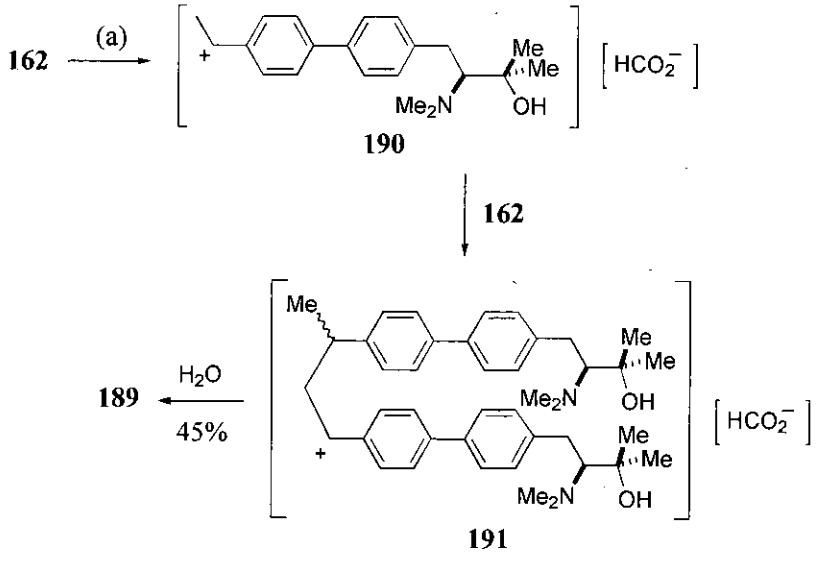

(a) 38% aqueous HCO_2H, reflux.

Scheme 77

The *N*,*N*-dimethylation transformation could also be achieved by reacting the vinyl amino alcohol monomer **167** with formaldehyde in the presence of palladium on charcoal under a hydrogen atmosphere,[64] but these reagents would also result in

hydrogenation of the vinyl group. Similarly, the other amination route involving treatment of **167** with iodomethane and potassium carbonate[96] was discarded as low yields were obtained with the solution phase biaryl model (**chapter 3.9.2**).

Ultimately, the inability to prepare vinyl monomer **162** did not hinder the progression of research, as the analogous biaryl amino alcohol prepared in **chapter 3.9.2** was found not to be the optimum catalyst for addition of dialkylzinc reagents to aldehydes (**chapter 6.2.3**). Therefore, had vinyl amino alcohol **162** been synthetically viable it would not have been polymerised and utilised as a polymer-bound catalyst.

3.8 Synthesis of Vinyl Oxazolidine Monomer 168

The final monomeric oxazolidine catalyst **168** for the enantioselective addition of dialkylzinc reagents to aldehydes was synthesised in quantitative yield (100%) by reaction of vinyl amino alcohol **167** with acetone, **scheme 78**.[87]

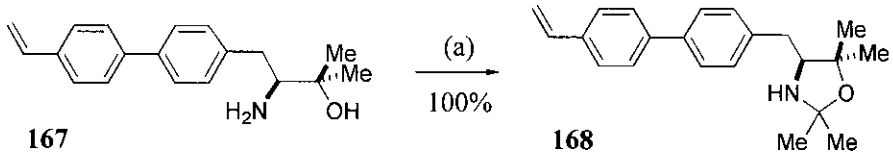

167 **168**

(a) $(Me)_2CO$, RT.

Scheme 78

This conversion was impossible to monitor by t.l.c. as the oxazolidine **168** was found to partially decompose to the amino alcohol starting material **167** as determined by extraction and subsequent MS (APCI) analysis of the two t.l.c. component bands. Similarly, rapid ^1H NMR analysis of the product material was required as the oxazolidine **168** reverted back to the amino alcohol **167** on standing in $CDCl_3$. It was proposed that the inherent acidity of the silica / $CDCl_3$ with possible traces of water lead to the acid hydrolysis of oxazolidine **168**, thus regenerating amino alcohol **167** and acetone. This process was not observed during the cyclodehydration reaction itself (**scheme 78**) due to the large excess of acetone employed.

The instability of the oxazolidine functionality with respect to acid hydrolysis indicated that vinyl monomer **168** may not be an ideal substrate for polymerisation. If hydrolysis were to occur during the dialkylzinc addition reaction the resultant oxazolidine and amino alcohol bound residues could provide conflicting catalytic activity. Ultimately, solution phase studies using the analogous biaryl oxazolidine prepared in **chapter 3.9.3** illustrated that this substrate did not provide optimum catalytic activity for the addition of dialkylzinc reagents to aldehydes (**chapter 6.2.4**). As such vinyl oxazolidine monomer **168** was not polymerised and employed as a polymer-bound catalyst.

3.9 Synthesis of Biaryl Catalysts

A series of model biaryl compounds **192**, **193** and **194** were synthesised and subsequently evaluated as solution phase catalysts for the addition of dialkylzinc reagents to aldehydes (**chapter 6**), **figure 31**.

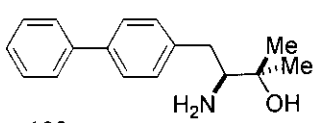

192

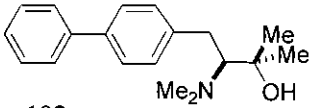

193

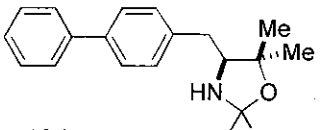

194

Figure 31

This enabled identification of the optimised catalyst substrate which was then transferred to the solid phase by polymerisation of the appropriate modified styrene monomer. In addition, we were also able to study how the catalyst's performance was affected by attachment of the chiral moiety to the resin.

3.9.1 Synthesis of Biaryl Amino Alcohol 192

The Suzuki coupling of phenylboronic acid and previously prepared triflated ester **138** provided the biaryl product **195** in moderate yield (55%) using the reaction conditions previously optimised for the analogous coupling of vinylboronic acid **159** with **138** (**chapter 3.5**). Grignard addition of freshly prepared MeMgI afforded **196**

(77%) and subsequent removal of the Boc group with trifluoroacetic acid[92] furnished the biaryl amino alcohol **192** (87%), **scheme 79**.

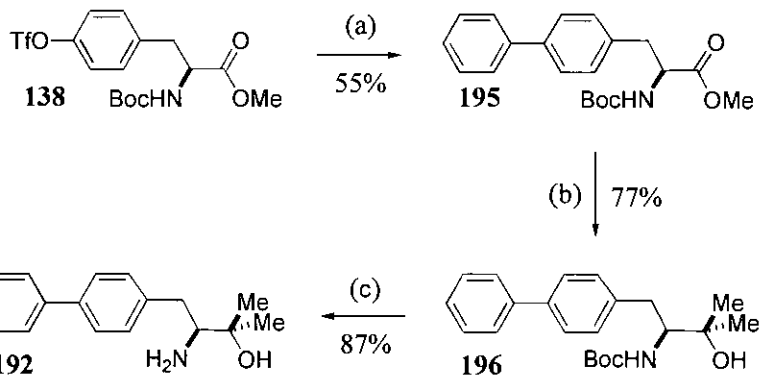

(a) (i) $Pd(OAc)_2$, PPh_3, toluene, RT; (ii) $PhB(OH)_2$, **138**, K_2CO_3, 85 °C; (b) (i) MeI, Mg, Et_2O, reflux; (ii) **195**, Et_2O, reflux; (c) CF_3CO_2H, DCM, RT.

Scheme 79

3.9.2 Synthesis of Biaryl Amino Alcohol 193

Kragl *et al.* reported the *N*-alkylation of amino alcohol **197** using *n*-iodobutane and potassium carbonate, yet no isolated yields were reported for the mono- and di-alkylated products **198** and **199**, **scheme 80**.[96]

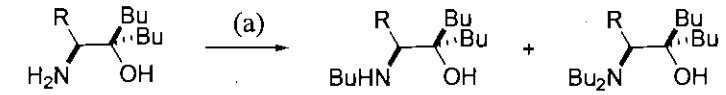

R = $BnOPhCH_2$

197 **198** **199**

(a) *n*-BuI, K_2CO_3.

Scheme 80

This alternative alkylation strategy was adapted to our synthesis whereby biaryl amino alcohol **192** was reacted with iodomethane and potassium carbonate, **scheme 81**. However, ^1H NMR analysis of the crude product mixture indicated quantitative conversion to a 5:1 ratio of *N*,*N*-dimethylated amino alcohol **193** : quaternary ammonium salt **200**. This assignment was deduced from the relative intensities and chemical shift values of the newly introduced distinctive methyl

groups. The six equivalent NMe_2 protons within **193** gave rise to a singlet at $\delta = 2.35$ ppm, whereas the nine equivalent N^+Me_3 protons within **200** gave a singlet further downfield at $\delta = 3.48$ ppm due to the increased electron withdrawing nature of the adjacent nitrogen cation.

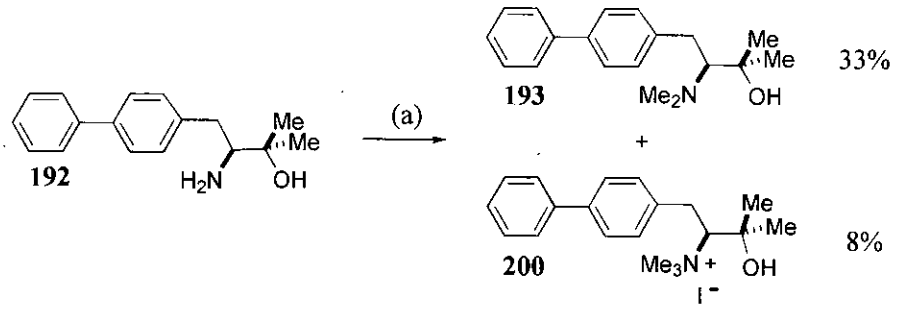

(a) MeI, K_2CO_3, MeCN, RT.

Scheme 81

Chromatographic purification of the reaction mixture was complicated by the polar nature of the two components resulting in a low isolated yield of **193** (33%) and **200** (8%). Lowering the reaction temperature to 0 °C and using fewer equivalents of iodomethane failed to eliminate generation of salt **200**, which ultimately resulted in a reduced overall yield of biaryl amino alcohol **193**. Formation of **200** is presumably unavoidable as **193** would be expected to exhibit enhanced reactivity towards methylation following the normal reactivity pattern of 3° > 2° > 1° amines.

Following the two step methylation protocol employed in the attempted synthesis of vinyl amino alcohol **162** (**chapter 3.7**) which mechanistically does not allow the formation of quaternary ammonium salts, afforded the biaryl amino alcohol **193** in a much improved yield (91%), **scheme 82**.

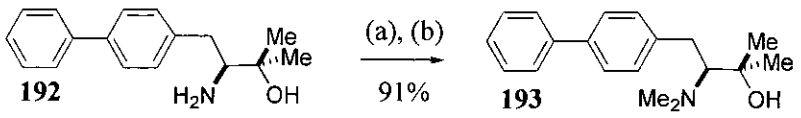

(a) Aqueous H_2CO, $NaCNBH_3$, AcOH, MeCN, RT; (b) 38% aqueous HCO_2H, reflux.

Scheme 82

Initial reductive amination[94] of biaryl amino alcohol **192** generated an 8:1 ratio of the desired *N*,*N*-dimethylated amino alcohol **193** : *N*-methyl oxazolidine **201** with traces of the *N*-H oxazolidine **202** as determined from the relative intensity and chemical shift values of the various distinctive methyl proton signals by ^{1}H NMR, **figure 32**.

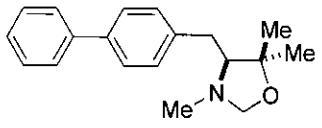

201

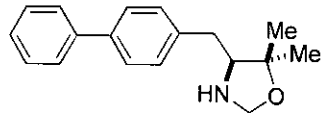

202

Figure 32

The crude reaction mixture was then refluxed with formic acid[95] effectively converting the *N*-methyl oxazolidine **201** to further product material **193**. Traces of the *N*-H oxazolidine **202** which failed to undergo reductive cleavage due to insufficient stabilisation of the intermediate iminium ion were finally removed by chromatography.

3.9.3 Synthesis of Biaryl Oxazolidine 194

Conversion of amino alcohol **192** to the biaryl oxazolidine **194** was achieved in quantitative yield (100%) by reaction with acetone,[87] **scheme 83**.

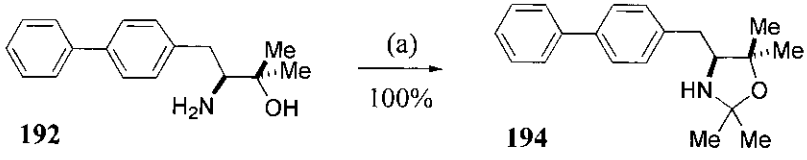

192 **194**

(a) $(Me)_2CO$, RT.

Scheme 83

3.10 Synthesis of Oxazolidinone Auxiliaries

As previously discussed the primary target oxazolidinone monomer possessed R = H **203** (**figure 25**) being consistent with the oxazolidinone auxiliaries already

developed on the solid phase (**chapter 1.2.3.3**). However, our research was later expanded to include the synthesis of vinyl oxazolidinone **204** (R = Me), **figure 33**.

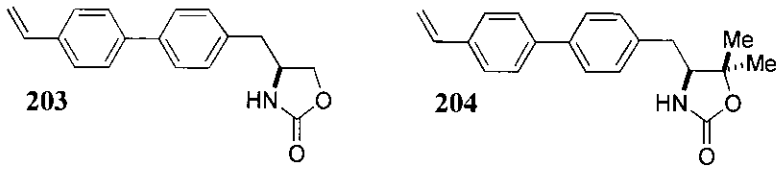

Figure 33

Davies *et al.* originally developed a similar series of novel oxazolidinone auxiliaries termed the "SuperQuat" auxiliaries which effectively incorporated the analogous geminal dimethyl group at the C-5 position **205**, **figure 34**.[97]

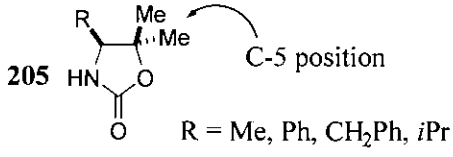

Figure 34

The "SuperQuat" auxiliaries **205** were designed in an attempt to eliminate the endocyclic ring opening of acylated oxazolidinones which is often observed when R = H under hydroxide cleavage conditions, **scheme 84**.[98] This undesirable cleavage pathway reduces the yield of cleaved product and limits the recycling capability of the auxiliary. The problem of endocyclic cleavage may be overcome by deploying the more nucleophilic hydroperoxide species for hydrolysis which is less susceptible to steric hindrance,[98] yet the use of this reagent on a large scale is clearly undesirable.

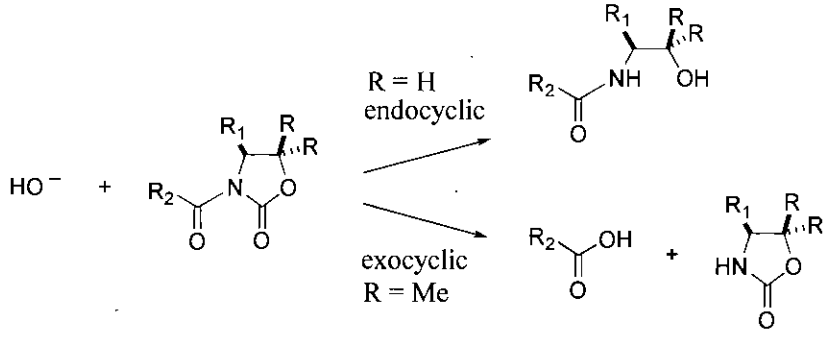

Scheme 84

Solution phase studies using the "SuperQuat" auxiliaries **205** illustrated that inclusion of the geminal dimethyl groups (R = Me) efficiently protected the ring carbonyl from nucleophilic attack, and hence promoted the desired exocyclic cleavage, **scheme 84**.[97] Therefore, it was postulated that adaptation of the new family of "SuperQuat" oxazolidinone based auxiliaries to the solid phase *via* polymerisation of the vinyl oxazolidinone monomer **204** would provide a robust auxiliary with enhanced recyclability. The ability to re-use the polymer-bound auxiliary would represent a significant advance within this field of research as only one report to date documents the recycling of a polymer-bound oxazolidinone system.[19f]

3.10.1 Synthesis of Vinyl Oxazolidinone Monomer 203

Reduction of the previously prepared vinyl methyl ester **180** with $NaBH_4$[99] afforded the Boc protected amino alcohol **206** in high yield (89%). Subsequent cyclisation using thionyl chloride[100] where the Boc group is deployed as a carbonyl equivalent furnished the vinyl oxazolidinone monomer **203** (67%), **scheme 85**.

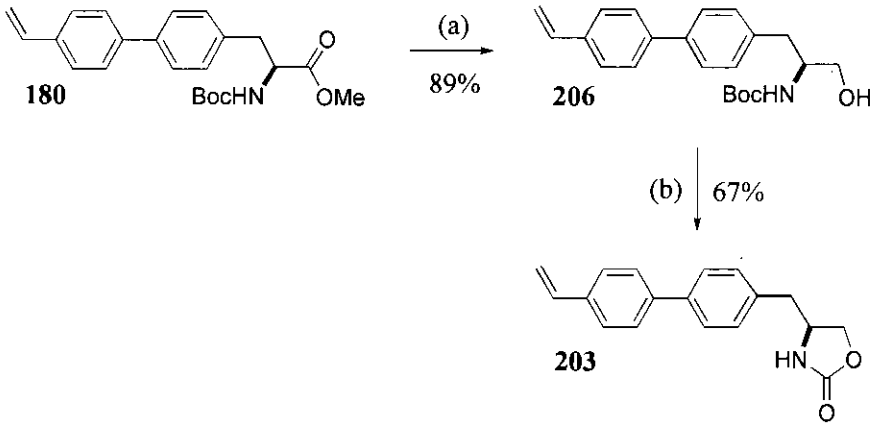

(a) $NaBH_4$, MeOH, THF, reflux; (b) $SOCl_2$, THF, 0 °C.

Scheme 85

Monomer **203** was ultimately not polymerised and employed as a polymer-supported auxiliary as higher priority was given to investigating the applications of the novel "SuperQuat" oxazolidinone system.

3.10.2 Synthesis of Vinyl Oxazolidinone Monomer 204

Vinyl oxazolidinone monomer **204** was synthesised (99%) *via* direct cyclisation of the previously prepared vinyl amino alcohol **181** with elimination of *t*BuOH using potassium *tert*-butoxide,[89] where the Boc functionality again provided the carbonyl group, **scheme 86**.

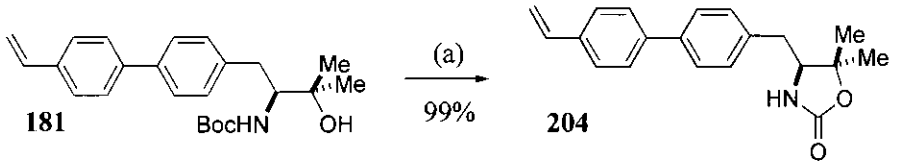

(a) *t*BuOK, THF, 0 °C.

Scheme 86

N-propionylation of the oxazolidinone group was carried out after polymerisation of the vinyl monomer **204** as *n*-butyllithium used in the acylation process would cause anionic oligomerisation or carbolithiation of the vinyl moiety.

3.10.3 Synthesis of Biaryl Oxazolidinone Auxiliary 207

Model biaryl oxazolidinone **207** and *N*-acylated oxazolidinone **208** were prepared to enable the asymmetric alkylation and aldol reactions to be conducted in the solution phase. Infra-red data obtained for **207**, **208** and the alkylated / aldol adducts was then used for comparison with the polymer-bound analogues to facilitate the monitoring of these various transformations on the solid phase. In addition, we were also able to investigate how the levels of asymmetric induction imparted by the "SuperQuat" oxazolidinone were affected by attaching the auxiliary to the resin.

The biaryl auxiliary **207** was synthesised (95%) in an analogous manner to the vinyl oxazolidinone **204**, from the reaction of biaryl amino alcohol **196** with potassium *tert*-butoxide.[89] Deprotonation of **207** with *n*-butyllithium and subsequent acylation with propionyl chloride[101] afforded the *N*-propionylated biaryl oxazolidinone **208** in high yield (85%), **scheme 87**.

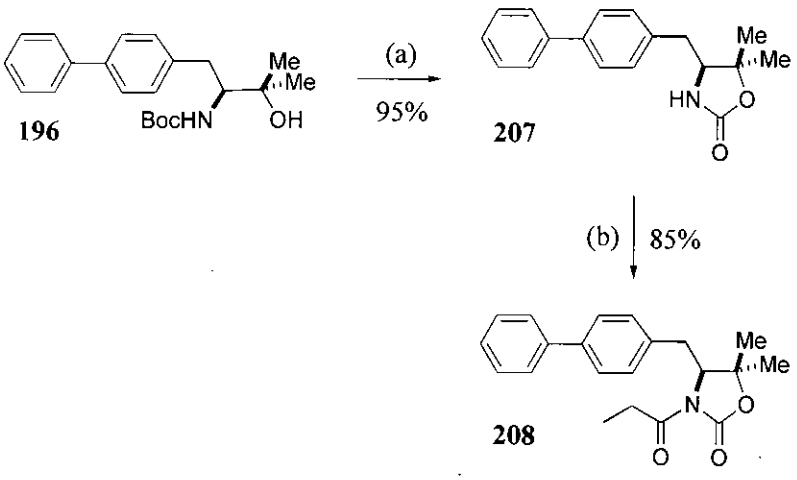

(a) *t*BuOK, THF, 0 °C; (b) *n*-BuLi, EtCOCl, THF, -78 °C→RT.

Scheme 87

3.11 Summary of Chapter 3

Chapter 3 illustrates the versatility of the chosen route in the preparation of a range of amino alcohol and oxazolidinone monomers. The synthetic strategy relied on the key Suzuki coupling of aryl triflates derived from tyrosine with vinylboronic acid **159**. The resultant vinyl monomers were further modified to incorporate the desired functionality as required. Subsequent polymerisation of the monomers to provide the functionalised polymers is detailed in **chapter 4** where the nature of this process ensures that only the chiral moiety is polymer-bound affording complete control.

In addition, the analogous biaryl amino alcohol catalysts and oxazolidinone auxiliary were synthesised to investigate their activity in the solution phase. This allowed the optimum catalyst substrate to be identified prior to polymerisation of the corresponding monomer, and characterisation of the alkylated / aldol oxazolidinone adducts thus facilitating the monitoring of these reactions on the solid phase.

Chapter 4 : Results and Discussion Part 3

Suspension Copolymerisation of Vinyl Monomers

The polymerisation of chiral vinyl monomers allows the synthesis of linear, gel or macroporous functionalised side-chain chiral polymers. **Chapter 1.2.1** highlights the versatility of this approach where the loading of the chiral species, degree of cross-linking and morphology of the polymer can be controlled by variation of the comonomer composition and solvent medium.

Experimentally vinyl monomers are frequently polymerised *via* free radical suspension polymerisation where this process is illustrated pictorially in **scheme 88**. Initially the comonomer mixture and free radical initiator (hatched area) are dispersed in an immiscible aqueous phase which contains a suspension stabiliser, where water acts as the heat transfer agent (**stage 1**). Continuous stirring of the reaction mixture creates a suspension of spherical liquid monomer droplets which are cushioned and separated from one another by the suspension stabiliser (**stage 2**). Subsequent fragmentation of the free radical initiator by thermal, photolytic or chemical reaction produces radicals which in turn initiate polymerisation within the liquid monomer droplets. The resulting spherical solid polymer beads (**stage 3**) are isolated by filtration, washed free of stabiliser and other contaminants and finally dried to remove solvent.

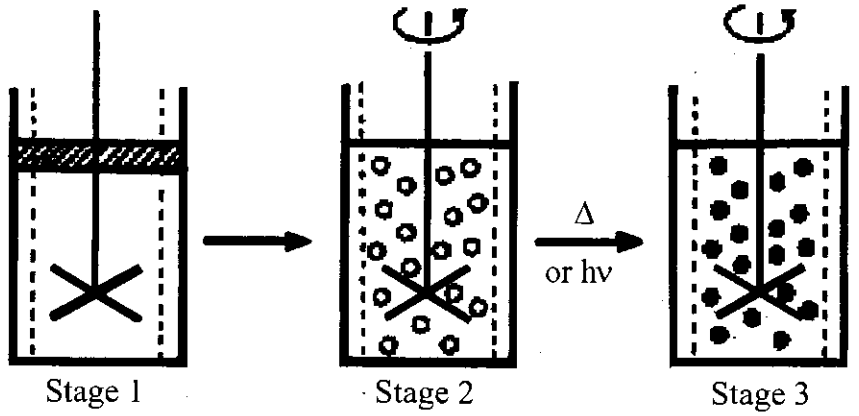

Scheme 88[ξ]

[ξ] Reproduced from reference 102.

The most commonly utilised free radical initiator is azobisisobutyronitrile **209** (AIBN) which undergoes thermal or photolytic fission to produce two identical radicals **210** with loss of nitrogen, **scheme 89**.

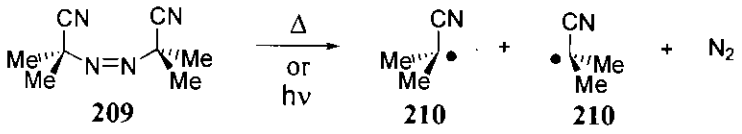

Scheme 89

The polymerisation mechanism proceeds *via* reaction of a free radical R• with a monomer unit **211** where the initiated chain **212** undergoes rapid addition of further monomer units, **scheme 90**. Chain propagation occurs in a head to tail manner thus minimising the steric interaction of the pendant R' side groups and ensuring maximum stability of the intermediate secondary radicals.

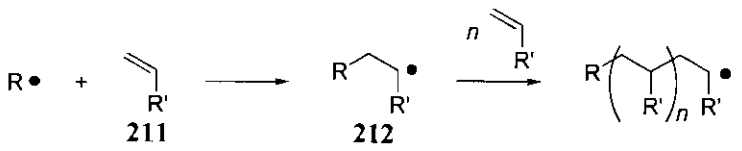

Scheme 90

This series of elementary reactions concludes with the bimolecular interaction between two growing polymer chains **213**. The termination can occur *via* the head to head combination of two chains generating one long chain **214** or by disproportionation with hydrogen abstraction providing an unsaturated polymer terminus **215** and a second saturated polymer chain **216, scheme 91**.

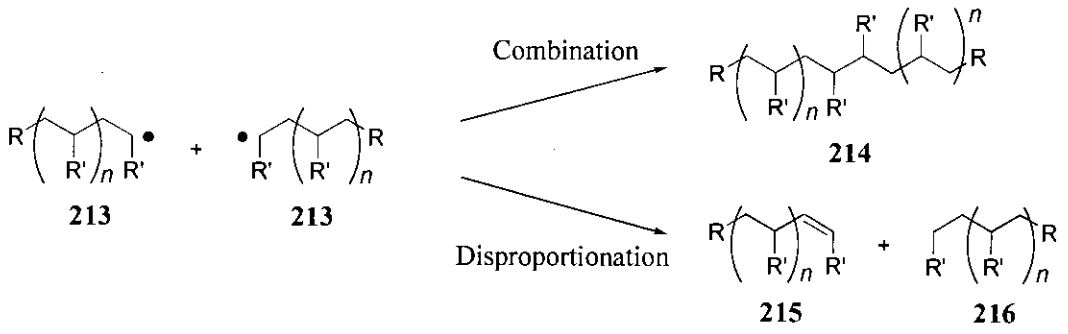

Scheme 91

4.1 Reactor and Stirrer Design

The main difficulty with suspension polymerisation is that at some crucial time into the conversion, corresponding roughly with the onset of the polymer network formation within each liquid monomer droplet, the monomer swollen polymer particles become extremely tacky and the probability of aggregation is maximised. The degree of aggregation which can occur varies enormously from perfectly formed spherical particle which are coagulated to an amorphous mass where the spherical integrity of the particles is completely lost.[103]

As particle collisions cannot be eliminated, appropriate stirring techniques are employed to control the kinetic energy of the collisions thus reducing the tendency for aggregation. The rate of stirring can be minimised whilst maintaining a suspension by using impellers and reaction vessels which provide the optimum top-to-bottom flow turnover required to maintain a suspension. Vertical flow patterns are conveniently achieved using a propeller type impeller and a flattened base cylindrical vessel with baffles spaced around the walls to break up horizontal flow, **figure 35**.[4a]

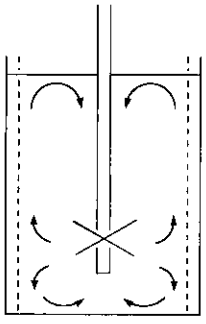

Figure 35

Unfortunately, adapting literature protocol to within our means resulted in the use of a standard round bottomed flask as the reaction vessel with a paddle type impeller powered by an overhead stirrer. This experimental design will encourage horizontal circular motion, with a tendency for vortex formation around the stirrer shaft as the stirrer speed is increased. Forcing the suspended medium against the sides of the reaction vessel also draws gas into the centre of the liquid phases effectively destroying the suspension to yield an aggregated or amorphous product.

4.2 Characterisation of Functionalised Supports

The range of analyses applied to linear soluble polymers is effectively the same as those methods used for the characterisation small molecules. However, with insoluble cross-linked gel or macroporous resins many of these techniques are no longer applicable. One of the most powerful methods of analysis widely performed on insoluble resins is elemental analysis. This technique routinely allows the carbon, hydrogen, nitrogen, halogen, sulphur and phosphorus percentage of the resin to be determined. On some occasions this is the only quantitative measure available and much of the interpretation in the literature depends heavily on this analytical method. Infra-red spectroscopy provides a vital qualitative probe for following the course of a reaction, especially when the synthetic transformation being performed results in a change of absorption frequency.

Conventional NMR methods are of limited use due to the low mobility of the solid phase where line broadening also occurs to give poorly resolved spectra. Furthermore, the signals of the polymer backbone can swamp the area of interest in the spectrum particularly if the loading of the functionalised support is low. Magic angle spinning ^{13}C and ^{1}H gel-phase NMR techniques can be used to analyse solid polymer samples but this instrumentation is not widely accessible.

Destructive techniques requiring cleavage of the compound being examined from the solid phase include maldi-TOF mass spectrometry. Single beads are placed in a stream of trifluoroacetic acid vapour (or ammonia for base labile linkers) before irradiation with a laser beam to ionise the parent compound. This process is ideal for characterising solid phase products allowing the detection of femtomole quantities of cleaved compound.

4.3 Method of Polymerisation for Chiral Functionalised Monomers

From the range of styrene derived chiral functionalised monomers prepared in **chapter 3** two substrates **167** and **204** were selected for polymerisation, **figure 36**. The vinyl amino alcohol monomer **167** was chosen as the biaryl amino alcohol

mimic **192** gave optimum selectivity when employed as a solution phase catalyst in the addition of dialkylzinc reagents to aldehydes (**chapter 6.2.5**). Whereas, the vinyl oxazolidinone monomer **204** was selected to investigate the applications of the novel "SuperQuat" auxiliary on the solid phase (**chapter 3.10**).

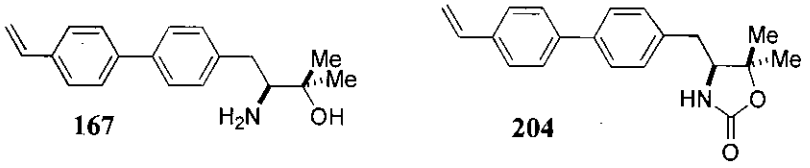

Figure 36

A review of the literature revealed that no oxazolidinone derived monomers have previously been polymerised. However, of the few polymer-supported amino alcohol catalysts prepared by polymerisation of functionalised monomers, the majority were produced using suspension polymerisation methodology. Itsuno *et al.* prepared the macroporous polymer-bound amino alcohol **90** by copolymerisation of the parent vinyl monomer with styrene and divinylbenzene, **figure 37**.[82] In this instance benzoyl peroxide was employed as the free radical initiator and poly(vinyl alcohol) (PVA) as the suspension stabiliser with THF / benzene providing the template solvent medium for formation of the macroporous beads. This procedure was later expanded to introduce alternative cross-linking reagents where AIBN was substituted as the free radical initiator.[35e]

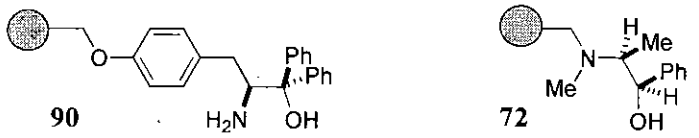

Figure 37

Soai *et al.* applied almost identical experimental conditions in the suspension polymerisation of an ephedrine derived vinyl monomer using AIBN, PVA and THF / benzene in the synthesis of the functionalised macroporous resin **72**, **figure 37**.[35c]

The remainder of the polymer-bound amino alcohol supports were synthesised using solution polymerisation which differs in that water is not included

in the polymerisation process. Instead, the vinyl monomer is dissolved in a suitable organic solvent which acts as a diluent and heat transfer agent, and the polymerisation is initiated as before. If the solvent solvates both monomer and polymer, the latter must be precipitated by addition of a poor solvent. Whereas if the reaction solvent is not compatible with the polymer then precipitation of the polymer occurs as it is formed in solution.

Examples incorporating this technique include the synthesis of linear polymer-bound amino alcohol **90** which was prepared *via* copolymerisation of the appropriate vinyl monomer with styrene using toluene as the diluent and AIBN as the free radical initiator, **figure 38**.[43] Similarly, cross-linked gel resin **96** functionalised with Noyori's ligand was prepared by solution polymerisation with the inclusion of divinylbenzene utilising DCM as the solvent medium with AIBN as the free radical initiator, **figure 38**.[44a]

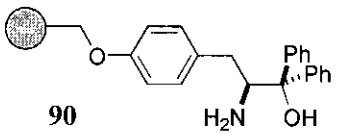

90

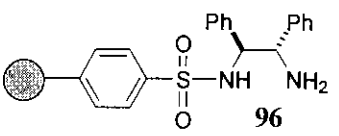

96

Figure 38

Our specifications for the target polymer-bound amino alcohol catalyst **217** and oxazolidinone auxiliary **218** include the ability to remove and recycle the resins, **figure 39**. In view of this requirement, the solution polymerisation approach which necessitates the often problematic precipitation of the resin from the reaction mixture was not very attractive. Therefore, initial studies were directed to the suspension polymerisation methodology where the product polymer beads are readily isolated by filtration whilst maintaining a physical form useful for manipulation.

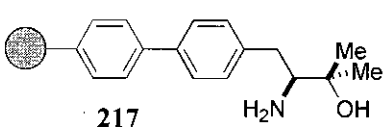

217

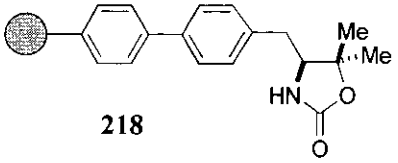

218

Figure 39

4.4 Synthesis of Gel-Type Chloromethylpolystyrene 3

Expertise relating to the synthesis of gel-type resins by suspension polymerisation acquired during an industrial placement provided an appropriate starting point for the polymerisation studies. As discussed in **chapter 1.2.1.2** gel resins are lightly cross-linked and therefore insoluble, but the mobility of the polymer chains and resultant swelling of the resin ensures that the functional groups on the polymer are exposed to the soluble reagents.

Initial research focused on the suspension copolymerisation of styrene **2** with divinylbenzene **100** and vinylbenzyl chloride **219** using AIBN as the free radical initiator with PVA as the suspension stabiliser to afford chloromethylpolystyrene gel resin **3**, **scheme 92**. Vinylbenzyl chloride **219** was substituted as the model functionalised monomer in order to identify the reaction parameters which produce the polymer beads in optimised yield, size, shape and uniformity before incorporating the valuable chiral functionalised monomers.

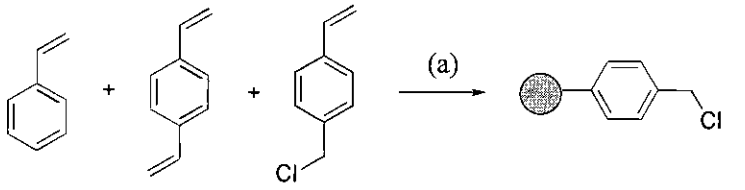

2 **100** **219** **3**

(a) (i) H_2O, PVA, 125 °C→RT; (ii) **2**, **100**, **219**, AIBN, 80 °C.

Scheme 92

The amounts of vinylbenzyl chloride **219** and divinylbenzene **100** employed in the suspension copolymerisation must reflect the desired loading and cross-linking of the resultant chloromethylpolystyrene gel resin **3**. **Calculation 1** depicts the method used to calculate the quantity of reagents required in a typical polymerisation reaction aiming to produce 1% cross-linked chloromethylpolystyrene gel-type resin **3** with 4 $mmolg^{-1}$ loading. These parameters were derived from in house expertise of the industrial sponsor.

Calculation 1

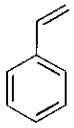

styrene **2**
MW 104.15
d 0.909

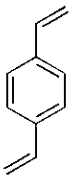

divinylbenzene **100**
MW 130.19
d 0.914
80 % w/w

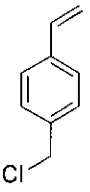

vinylbenzyl chloride **219**
MW 152.62
d 1.083

Assumed: 100% of monomers are consumed in the polymerisation reaction.
Average monomer density = 0.969.

Volume: Aqueous phase : comonomer phase = 10 : 1.

Example

Aqueous phase = 160 cm^3 water.

⇒ Combined volume of monomers = 16 cm^3.

⇒ Total mass of monomers = 0.969 x 16 = 15.5 g.

Loading = 4 $mmolg^{-1}$.

⇒ 4 x 15.5 = 62.0 mmol = 9.46 g = 8.73 cm^3 vinylbenzyl chloride **219**.

Majority of remaining mass constitutes styrene = 15.5 - 9.46 = 6.04 g = 58.0 mmol.

⇒ Approximate total mmol of monomers = 62.0 + 58.0 = 120 mmol.

1% cross-linked system requires 2 mol% of divinylbenzene.

⇒ (2 x 120) / 100 = 2.40 mmol = 312 mg = 0.427 cm^3 divinylbenzene **100**.

Subtracting mmol of divinylbenzene from previously assumed mmol of styrene.

⇒ 58.0 - 2.40 = 55.6 mmol = 6.37 cm^3 styrene **2**.

1 weight % of PVA in water used = 160 / 100 = 1.60 g PVA.

Mass of AIBN = volume of aqueous phase / 640 = 250 mg AIBN.

The suspension polymerisation protocol outlined in **method J** of **chapter 8.4** was followed incorporating the reagent quantities calculated above where the overhead stirrer speed was maintained at 188 RPM. The chloromethylpolystyrene gel resin **3** was produced in 37% yield (**scheme 92**) having defined the quantitative yield of polymer product to be the combined mass of the three comonomers employed in the polymerisation reaction.

The chloromethylpolystyrene beads **3** were found to have a negligible surface area in the dry state as measured by N_2 sorption and application of BET theory. Gel resins typically adsorb less than 10 m^2 of N_2 per gram of dry resin thus confirming that the chloromethylpolystyrene beads **3** were indeed gel-type.[102]

Calculation 2 describes the method used to calculate the expected C, H, N and Cl elemental analysis percentages for the chloromethylpolystyrene gel resin **3** with 4 $mmolg^{-1}$ loading.

Calculation 2

Anal. Calcd. styrene **2**:	C, 92.26;	H, 7.74;	N, 0.00;	Cl, 0.00.
Anal. Calcd. divinylbenzene **100**:	C, 92.26;	H, 7.74;	N, 0.00;	Cl, 0.00.
Anal. Calcd. Vinylbenzyl chloride **219**:	C, 70.83;	H, 5.94;	N, 0.00;	Cl, 23.23.

4 $mmolg^{-1}$ denotes 4 mmol of vinylbenzyl chloride monomer **219** unit per gram of polymer which is equivalent to 610 mg of monomer per gram of polymer. Remainder of mass was attributed to styrene **2** and divinylbenzene **100** (390 mg) which were combined as one entity as they have identical elemental profiles.

Anal. Calcd. for polymer:

C, (0.390 x 92.26) + (0.610 x 70.83) = 79.19%;

H, (0.390 x 7.74) + (0.610 x 5.94) = 6.64%;

N, (0.390 x 0.00) + (0.610 x 0.00) = 0.00%;

Cl, (0.390 x 0.00) + (0.610 x 23.23) = 14.17%.

Therefore Anal. Calcd. for chloromethylpolystyrene beads **3**: C, 79.19; H, 6.64; N, 0.00, found C, 79.33; H, 6.58; N, 0.00. It was assumed that Cl constitutes the remaining 14.09% of material by mass which translates to 141 mg or 3.98 mmol of Cl per gram of resin **3**. Therefore, the loading was determined to be 3.98 $mmolg^{-1}$ which is consistent with the intended loading of 4 $mmolg^{-1}$.

In addition to this measurement, Cl elemental analysis allowed us to directly calculate the loading of the chloromethylpolystyrene gel resin **3** as 4.37 $mmolg^{-1}$. Clearly, the latter loading measurement is more accurate although the two values obtained are not too dissimilar. Unfortunately, due to the time restraints of the technician it was not possible to analyse each batch of polymer product by Cl elemental analysis, and as such the majority of loadings were determined from basic C, H and N analytical data.

Infra-red analysis where the resin **3** was prepared as a KBr disc gave aromatic and aliphatic C-H stretching regions at 3024 and 2922 cm^{-1} with a strong band at 1601 cm^{-1} resulting from C=C stretching. The beads **3** were found to swell to 4.0 times their own volume in DCM where this was recorded by visually measuring the increase in volume of the beads upon addition of DCM in a measuring cylinder.

Final evaluation of the chloromethylpolystyrene beads **3** both in the dry state (**picture 1**) and swollen in DCM (**picture 2**) under a microscope indicated that they were generally discrete spherical free flowing beads. Swollen gel-type beads are typically transparent and glossy but it is evident from **picture 2** that the individual beads contain roughly spherical micro-particles. This internal substructure could be attributed to vapour bubbles which have become trapped within the polymer matrix.

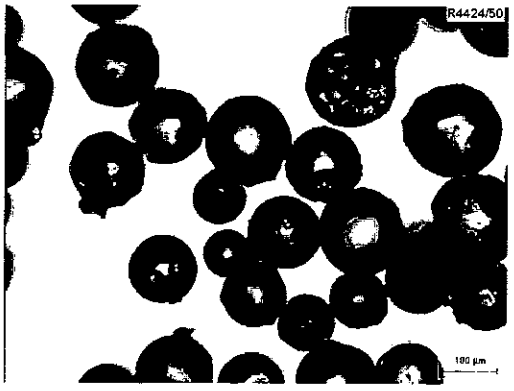

Picture 1

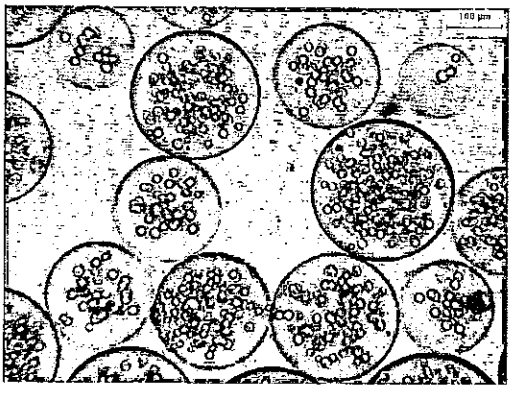

Picture 2

Lightly cross-linked resins (< 1%) are often mechanically weak when swollen and are easily damaged by shear, whereas higher levels of cross-linking (> 2%) yield resins which exhibit insufficient swelling in good solvents. Ultimately we require robust functionalised resins **217** and **218** (**figure 39**) which are amenable to recycling, thus further suspension polymerisations were conducted aiming to produce 2% cross-linked chloromethylpolystyrene gel-type resin.

Therefore, following the protocol outlined in **method J** of **chapter 8.4** further gel-type polymerisations were carried out aiming to prepare a range of 2% cross-linked resins varying the scale of the polymerisation reaction and the desired vinylbenzyl chloride loading. The stirrer speed of the overhead stirrer was also varied to investigate how this affected the yield and quality of polymer beads. A summary of the results are depicted in the **table 6**.

Table 6 - Gel-Type Polymerisation Results

Entry	Volume of water (cm^3) [a]	Desired loading ($mmolg^{-1}$)	Stirrer speed (RPM)	Swelling capacity in DCM [b]	CHN error margin (Δ%) [c]	Loading obtained ($mmolg^{-1}$) [d]	Yield (%)
1	160	0.5	188	2.5	0.26	0.61	35
2	75	0.5	154	2.0	0.52	0.38	19
3	75	0.5	190	2.3	0.20	0.46	33
4 [e]	75	0.5	200	2.5	0.49	0.69	41
5 [f]	75	0.5	200	2.5	0.29	0.45	35
6	75	1.0	200	2.4	0.35	1.03	39
7	75	2.0	200	2.6	0.52	2.20	65
8	75	4.0	200	2.7	0.64	3.81	73

[a] Volume of water used as an indication of reaction scale where the remaining reagent quantities were determined using **calculation 1**. Where the volume of water is 75 cm^3 a 100 cm^3 3-necked flask was used as the reaction vessel unless otherwise stated.
[b] Swelling capacity of resin measured by volume in DCM relative to that of the non-swollen material.
[c] Elemental analysis error margin is expressed as the difference between those percentage compositions calculated and found for carbon or hydrogen whichever has the greater numerical value.
[d] Material unaccounted for from CHN elemental analysis assumed to be chlorine and this percentage was then used to determine the loading of the polymer product.
[e] Experiment carried out using a 250 cm^3 3-necked flask with impeller positioned 2/3 distance below the surface of the suspension medium to minimise horizontal flow.
[f] Impeller positioned ~ 1 cm below surface of suspension medium to visually minimise horizontal flow.

Entries 1-5 lowered the loading of the polymer to 0.5 $mmolg^{-1}$ to ensure even distribution of the vinylbenzyl chloride monomer. Clearly, this will only be possible if the comonomers employed possess similar reactivity ratios. This criteria was designed to enable site isolation of the subsequently introduced chiral monomers **167** and **204** (**figure 36**), thus minimising any interactions between neighbouring chiral species which may affect the selectivity of the polymer-bound catalyst or auxiliary.

The polymer-supported amino alcohol **217** may be used with a low loading as the chiral moiety is required in catalytic quantities. Whereas the loading of the polymer-supported auxiliary **218** critically determines the amount of product material cleaved from the resin after the asymmetric transformation. In view of this factor

entries 6-8 investigated increasing the loading from 1.0 to 4.0 $mmolg^{-1}$ to improve the productivity of resin **218**.

From **table 6** a general pattern in swelling behaviour is observed where the 2% cross-linked gel-type resins consistently swelled to 2.0-2.7 times their own volume in DCM. This is in contrast to the previously prepared 1% cross-linked resin which swelled to a larger extent in DCM (4.0). This expected result is explained by the fact that the swelling of a resin is inversely proportional to the level of cross-linking reagent employed in its synthesis.

A further trend includes the minimal error margins observed between the calculated and found elemental analysis results where the largest difference is 0.64%. In relation to this the loadings were reasonably close to the desired loadings indicating that we are able to accurately control the loading of the vinylbenzyl chloride monomer.

Entry 1 was essentially identical to the previous polymerisation except that the loading was reduced from 4.0 to 0.5 $mmolg^{-1}$. The yield of resin (35%) was very similar to that obtained earlier (37%) and the isolated beads were of comparable quality being spherical and translucent. However, a large proportion of the material was fused together as aggregates with some amorphous material present.

The remaining polymerisations were conducted on a smaller scale to minimise possible loss of valuable functionalised monomers **167** and **204** (**figure 36**) should the reaction fail to produce isolated beads. Unfortunately the tendency for aggregation is exaggerated on a small scale as the ratio of the reaction volume : vessel surface area is reduced resulting in unfavourable surface interactions.

Entry 2 illustrated this point where the reduced scale of the polymerisation resulted in significant aggregation. This in turn lowered the yield (19%) of isolated beads which were typically larger due to the slower stirrer speed employed.

The size of the liquid monomer droplets can be reduced by increasing the impeller size or the rate of stirring which effectively increases the degree of shear. However, the likelihood of vortex formation is also increased which as described earlier can result in the destruction of the controlled suspension.

Entry 3 increased the stirrer speed resulting in a greater yield (33%) of smaller beads but significant amounts of amorphous material were present.

Modifications to the apparatus design were subsequently made in an attempt to reduce the formation of aggregated or amorphous resin by encouraging vertical flow within the suspension medium. Literature precedent states that this can be achieved by positioning the impeller approximately two thirds the distance below the surface of the suspension medium where its diameter should be about one third to one quarter the diameter of the reactor.[4a] In agreement with these stipulations entry 4 altered the position of the impeller accordingly and utilised a larger vessel / smaller diameter impeller. The stirrer speed was also increased to compensate for the reduced shear created by the smaller impeller thus maintaining consistency of particle bead size. Unfortunately, these changes failed to reduce the level of amorphous material although the yield of product material was increased (41%).

The relative size and positioning of the impeller were then altered to visually minimise horizontal flow as the previous suggestions were specific to the use of cylindrical baffled vessels. Positioning the impeller 1 cm below the surface of the suspension medium in a 100 cm^3 flask (entry 5) afforded predominantly spherical beads (35%) and the amount of amorphous material was successfully decreased.

Entries 6-8 used the experimental dimensions and stirrer speed (200 RPM) optimised in entry 5 where the loading of vinylbenzyl chloride monomer was increased from 1.0 to 4.0 $mmolg^{-1}$. The results detailed in **table 6** illustrate that as the loading was increased the yield of polymer product steadily increased (39% to 73%) and the levels of aggregation were reduced. However, microscopic examination of the beads indicated that they were of diminished quality possessing black spots of colouration. In view of this factor, entry 5 was ultimately established as the optimised system for formation of 2% cross-linked, 0.5 $mmolg^{-1}$ loaded gel-type beads on a small scale.

4.5 Macroporous Suspension Polymerisation

At this stage in the research it was discovered that the solid functionalised monomers **167** and **204** (**figure 36**) were insoluble in the comonomer liquid phase and therefore required an organic solvent for solubility. As such we directed our attention to the synthesis of macroporous resins where this process incorporates an inert organic solvent (porogen) within the comonomer mixture as discussed in **chapter 1.2.1.3**.

The processes taking place within an individual bead in the macroporous suspension polymerisation process are illustrated pictorially in **scheme 93**. **Stage 1** represents the liquid monomer droplet which is suspended in the immiscible aqueous phase. The radicals produced by fragmentation of the radical initiator initiate the polymerisation process and the polymer network begins to form in the normal manner (**stage 2**). However, the porogen and network begin to phase separate causing precipitation of the growing polymer within the bead. The point at which phase separation occurs depends on the nature of the porogen, its compatibility with the growing polymer matrix and the level at which it is used. At full conversion each polymer bead is composed of a cross-linked polymer phase (hatched area) and a discrete porogen phase (dotted area), the latter acting as a template for the porous structure of the resin (**stage 3**). Removal of the porogen and drying yields rigid opaque beads which possess a permanent porous structure even in the dry state (**stage 4**).

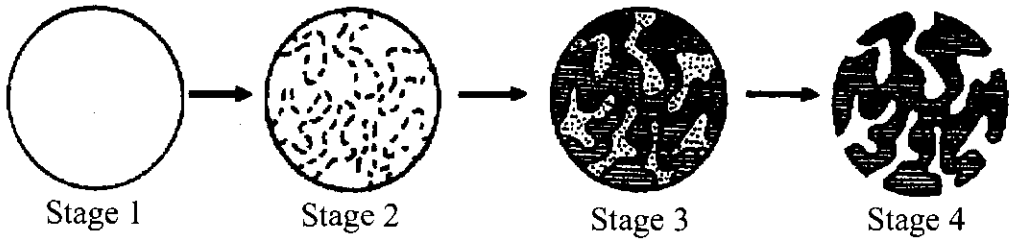

Scheme 93[Ψ]

[Ψ] Reproduced from reference 102.

An additional criteria for producing mechanically stable macroporous polymers in the presence of a porogen is to simultaneously use a higher proportion of difunctional monomer. This reduces the swelling capacity of the resin, but the reactivity of the polymer is unaffected as the porous network ensures that the beads are accessed by both good and bad solvents allowing good diffusion of reagents.

4.5.1 Synthesis of Macroporous-Type Chloromethylpolystyrene 3

Vinylbenzyl chloride **219** was again substituted as the model functionalised monomer in order to identify the reaction parameters which produce the polymer beads in optimised yield, size, shape and uniformity before incorporating the valuable chiral functionalised monomers **167** and **204**.

Following literature precedent a 1:1 ratio of THF : toluene was included in the comonomer phase, utilising the minimum volume of organic porogen which will ultimately be required to solubilise the amino alcohol **167** and oxazolidinone **204** monomers, **scheme 94**.[35c, 35e, 82] The principles applied to the previously optimised gel-type polymerisation procedure (entry 5, **table 6**) were adapted to accommodate the additional porogen. Therefore, experimentally a larger reaction vessel (500 cm^3) was used with the impeller being positioned 3 cm below the surface of the suspension medium to visually minimise horizontal flow.

Further modifications included increasing the level of cross-linking to 12% where the remaining reagent quantities were determined using the general method depicted in **calculation 1**.

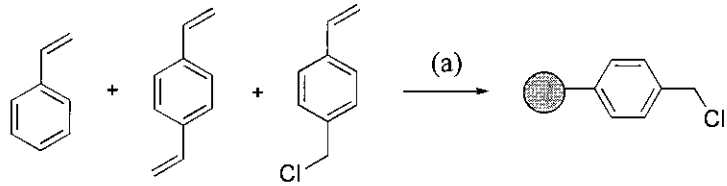

2 **100** **219** **3**

(a) (i) H_2O, PVA, 125 °C→RT; (ii) **2**, **100**, **219**, AIBN, THF, toluene, 80 °C.

Scheme 94

Following the revised protocol outlined in **method K** of **chapter 8.4** a range of polymerisations were investigated aiming to prepare 12% cross-linked macroporous chloromethylpolystyrene **3** with 0.5 $mmolg^{-1}$ loading. The ratio of PVA and stirrer speed employed were subsequently varied to provide control over both the bead size and yield of product. A summary of the results are depicted in the **table 7**.

Table 7 - Macroporous-Type Polymerisation Results

Entry	PVA [a]	Stirrer speed (RPM)	Swelling capacity in DCM [b]	CHN error margin (Δ%) [c]	Loading obtained ($mmolg^{-1}$) [d]	Yield (%) [e]
1	0.0	300	6.0	0.42	0.45	36
2	0.5	350	3.5	0.06	0.51	40
3	1.0	200	8.0	0.44	0.66	7
4	1.0	400	5.5	0.50	0.36	23
5	1.5	350	6.5	0.31	0.43	24

[a] PVA concentration expressed as weight percent in water.
[b] Swelling capacity of resin measured by volume in DCM relative to that of the non-swollen material.
[c] Elemental analysis error margin is expressed as the difference between those percentage compositions calculated and found for carbon or hydrogen whichever has the greater numerical value.
[d] Material unaccounted for from CHN elemental analysis assumed to be chlorine and this percentage was then used to determine the loading of the polymer product.
[e] Yield based on the mass of dried resin when sieved between 500 and 100 micron mesh sieves.

Unlike gel-type resins where the bead response to solvent is solely dependant on the cross-link ratio, the swelling of macroporous beads is also proportional to the volume of porogen employed in their preparation.[104] Therefore, as the level of cross-linking and porogen volume were identical throughout this series of experiments, the variation in swelling capacities exhibited by the resins from 3.5 to 8.0 times their own volume in DCM were unexpected. This result suggests that incorporation of the porogen within the polymer matrix was not consistent, which is feasible when considering that THF can reside in the comonomer or aqueous phase being completely miscible with water.

The elemental analysis error margins were consistently small and the loadings were generally close to the intended 0.5 $mmolg^{-1}$ loading, indicating that we are again able to control the loading of the vinylbenzyl chloride monomer.

PVA is typically employed in suspension polymerisation reactions with a concentration between 0.5-1.5% by weight in water. The water soluble surfactant is crucial in maintaining a suspension as it effectively reduces the surface tension between the liquid monomer droplets and the suspension medium.

Entry 1 illustrated this point where the lack of stabilisation in the absence of PVA generated a large mass of aggregated material which was subsequently broken down to afford amorphous matter (36%).

As the weight percent of PVA was increased from 0.5% to 1.5% (entries 2-5) the yield of polymer product steadily decreased due to excessive emulsification and frothing of the reaction mixture. The major anomaly to this trend was observed for entry 3 where virtually no material (7%) with the desired bead size (500-100 micron) was obtained. This was due to the slow stirrer speed (200 RPM) which resulted in a greater overall yield (76%) of large beads which could not be sieved. Entry 4 provided the extreme case where the increased stirrer rate (400 RPM) produced small particles which were lost through the fine sieve again reducing the final yield (23%).

Entry 5 yielded numerous aggregated clumps of spherical beads (24%) (**picture 3**, dry state resin) which indicated an inadequate stabilising system.

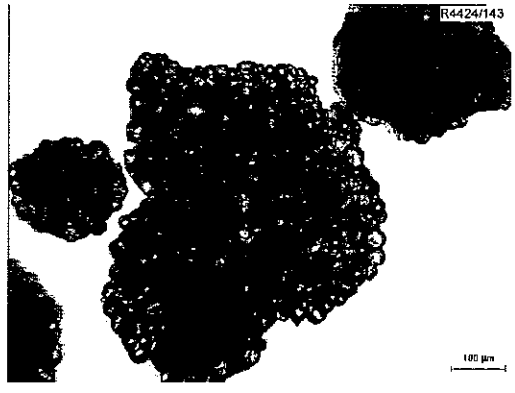

Picture 3

The insufficient stabilisation could be attributed to the inclusion of THF as the co-porogen which will distribute itself between the comonomer phase and the aqueous phase being miscible in all proportions with water, resulting in reduced levels of THF within the comonomer phase. 2-Ethylhexanol was considered as a non-water miscible porogen[105] to eliminate these stabilisation problems but the functionalised monomers **167** and **204** (**figure 36**) were insoluble in this solvent.[§]

Overall entry 2 (**table 7**) afforded the highest yield (40%) of macroporous polymer with an accurate 0.51 $mmolg^{-1}$ loading and negligible elemental analysis error margins. The resin contained a mixture of the desired isolated translucent spherical beads as depicted in **picture 4** (resin swollen in DCM) with negligible aggregated amorphous material as evident in **picture 5** (dry state resin).

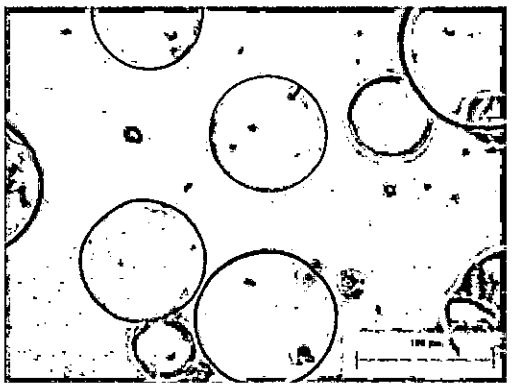

Picture 4

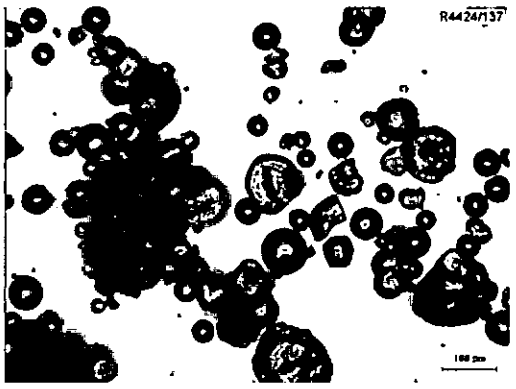

Picture 5

At this stage in the research, the gel-type polymerisations detailed in **table 6** allowed optimisation of the relative impeller dimensions and positioning within the vessel to minimise horizontal flow patterns. Similarly, the macroporous-type polymerisations summarised in **table 7** determined the optimum amount of PVA (0.5%) and stirrer speed (350 RPM) required to prepare the desired bead size in maximum yield with minimum aggregated amorphous material. Interestingly, the preferred stirrer speed varied significantly depending on the type of resin being prepared, gel-type (200 RPM) versus macroporous beads (350 RPM).

§ Solubility of 2-ethylhexanol in water at 20 °C = 0.07 % by weight.[106]

The following series of macroporous polymerisations focused on improving the levels of aggregation and bead morphology as discrete spherical beads are more robust and therefore less prone to mechanical breakdown.

The revised protocol outlined in **method L** of **chapter 8.4** incorporated several modifications in an attempt to limit the formation of aggregated amorphous polymer:

i) In addition to degassing the water prior to addition of PVA, the THF / toluene porogen phase was also degassed to ensure complete removal of the groundstate oxygen diradical which could otherwise interfere with the polymerisation process.

ii) The comonomers were individually purified by washing with aqueous sodium hydroxide to remove the 4-*tert*-butylcatechol stabiliser prior to polymerisation.

iii) The reaction mixture was stirred at 0 °C for 1 h prior to heating which has been shown to regulate particle size.[35c, 35e]

Implementing these adjustments (entry 6, **table 8**) afforded the desired chloromethylpolystyrene in 30% yield with a very accurate loading of 0.50 $mmolg^{-1}$. The surface area of the dry resin was determined to be 178 m^2g^{-1} as measured by N_2 adsorption and application of BET theory. This confirmed that the resin was indeed macroporous where the small adsorption volume and the long equilibration time experienced during the experiment suggested that the pores were very small.[Ψ]

The modifications also visibly enhanced the bead morphology where the majority of beads appeared spherical and isolated with little aggregation in the dry state. However, microscopic examination of the swollen resin indicated that some of the beads were textured as illustrated in **picture 6**.

[Ψ] Typical surface area of macroporous resins in the dry state range from 50-1000 m^2g^{-1}.

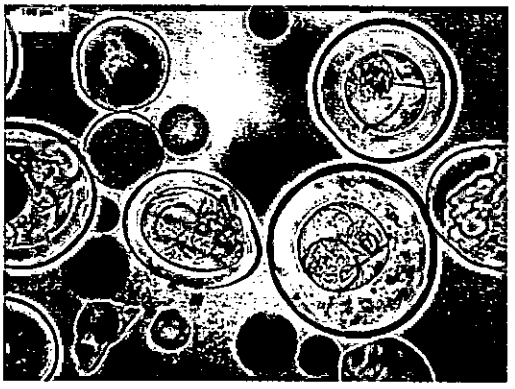

Picture 6

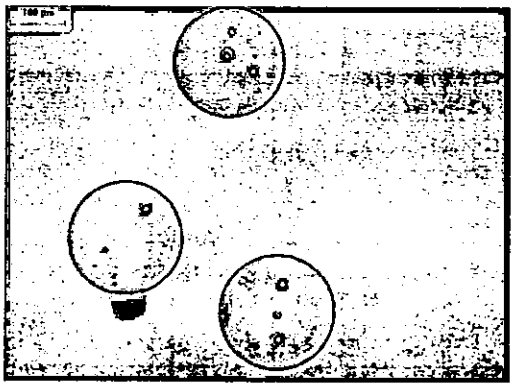

Picture 7

It was postulated that the bead substructure could be attributed to trapped water within the polymer matrix, thus the material obtained from entry 6 was subjected to soxhlet extraction with THF over a 24 h period followed by drying under reduced pressure. Re-examination of the swollen resin (**picture 7**) indicated that the beads were virtually transparent, thus confirming that insufficient washing and drying of the resin had created the textured appearance within the beads.

The remaining entries in **table 8** were conducted following the improved protocol outlined in **method L** of **chapter 8.4**, again aiming to prepare 12% cross-linked macroporous chloromethylpolystyrene **3** with 0.5 $mmolg^{-1}$ loading.

This final series of experiments were designed to investigate how the polymerisation process was affected by varying the AIBN concentration and omitting 2,6-di-*tert*-butyl-4-methylphenol (BHT) **220** which is the stabiliser commonly found in THF. It was postulated that BHT **220** inadvertently incorporated in previous reactions could have acted as a free radical inhibitor to generate the resonance stabilised phenoxy radical **221** which is subsequently unreactive, **scheme 95**.

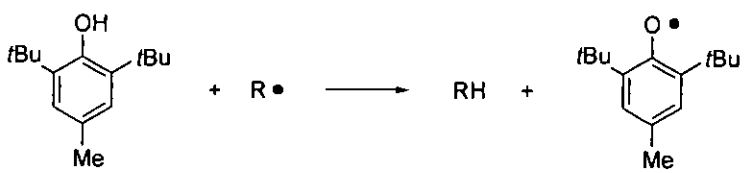

220 **221**

Scheme 95

Table 8 - Macroporous-Type Polymerisation Results

Entry	Mass of AIBN (mg)	BHT stabiliser present in THF	Swelling capacity in DCM [a]	CHN error margin (Δ%) [b]	Loading obtained ($mmolg^{-1}$) [c]	Yield (%) [d]
6 [e]	250	yes	6.7	0.22	0.50	30
7	500	yes	6.3	0.46	0.54	16
8	250	no	6.0	0.64	0.45	20
9	250	no	5.0	0.48	0.55	22
10	125	no	7.8	0.31	0.47	34

[a] Swelling capacity of resin measured by volume in DCM relative to that of the non-swollen material.
[b] Elemental analysis error margin is expressed as the difference between those percentage compositions calculated and found for carbon or hydrogen whichever has the greater numerical value.
[c] Material unaccounted for from CHN elemental analysis assumed to be chlorine and this percentage was then used to determine the loading of the polymer product.
[d] Yield based on the mass of dried resin when sieved between 500 and 100 micron mesh sieves.
[e] N_2 BET adsorption = 178 m^2g^{-1}.

The variation in swelling capacities exhibited by the resins (**table 8**) from 5.0 to 7.8 times their own volume in DCM again indicated that incorporation of the water miscible THF porogen within the polymer matrix was not consistent.

The elemental analysis error margins were typically small and the loadings were accurate when compared to the desired 0.5 $mmolg^{-1}$ loading, again indicating that we were able to control the loading of the vinylbenzyl chloride monomer.

Doubling the concentration of AIBN (entry 7) virtually halved the yield of polymer (16%) when compared to entry 6. The bead quality also deteriorated as a larger proportion of the material was composed of amorphous aggregated clusters.

Employing BHT free THF afforded the polymer in lower yield (20%) but overall the bead morphology was unaffected (entry 8 versus entry 6). This result highlighted the apparent sensitivity of the polymerisation process, where elimination of the stabiliser from the THF porogen reduced the yield of polymer produced.

The experimental conditions detailed in entry 8 were subsequently repeated in an identical manner (entry 9) to investigate the consistency of the polymerisation method. Reassuringly, the two batches of polymer product obtained were similar

both in terms of yield (20% versus 22%) and bead morphology indicating that suspension polymerisation does not constitute an entirely random process.

Finally, comparing entries 8 and 10 an increase in yield (20% to 34%) was generated by halving the concentration of AIBN employed, unfortunately the polymeric material was found to be completely amorphous.

Evaluation of the numerous macroporous polymerisation results established that the polymer beads detailed in entry 6 (**table 8**) possessed the overall optimised yield, size, shape and uniformity. As such the experimental protocol detailed in **method L** of **chapter 8.4** with no further amendments to the AIBN concentration or source of THF was utilised in the subsequent macroporous suspension polymerisation reactions incorporating the functionalised monomers **167** and **204**.

4.5.2 Synthesis of Macroporous-Type Oxazolidinone Polymer 218

The optimised macroporous reaction conditions detailed in **method L** of **chapter 8.4** were employed substituting the chiral oxazolidinone monomer **204** in place of the previously used vinylbenzyl chloride monomer **219**, **scheme 96**.

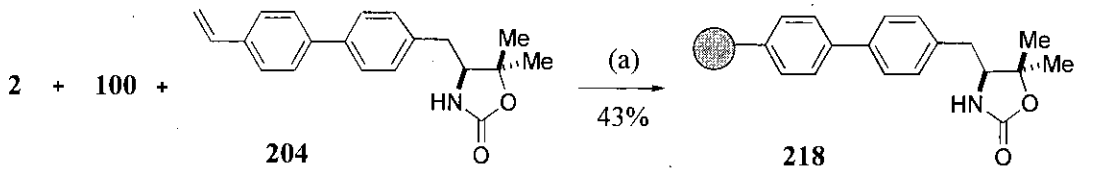

(a) (i) H_2O, PVA, 125 °C→0 °C; (ii) **2**, **100**, **204**, AIBN, THF, toluene, 0 °C→80 °C.

Scheme 96

The polymer-bound "SuperQuat" auxiliary **218** was obtained in 43% yield where the material was sieved between 500 and 100 micron mesh sieves. The resin swelled to 7.4 times its own volume in DCM. Examination of the swollen beads under a microscope indicated that they were predominantly discrete, translucent and spherical with some amorphous material present.

Elemental analysis allowed the nitrogen content of the resin and thus the loading of the polymer to be accurately determined as 0.48 $mmolg^{-1}$. Infra-red

analysis of the resin provided distinct bands at 3421 cm^{-1} (NH) and 1768 cm^{-1} (C=O) (see **appendix**), where the analogous biaryl oxazolidinone solution phase mimic **207** gave similar stretching frequencies at 3441 cm^{-1} and 1753 cm^{-1}. These combined quantitative and qualitative measurements confirmed that the oxazolidinone monomer **204** had been successfully incorporated to produce the functionalised polymer **218**.

The surface area of the dry resin **218** was measured to be 2 m^2g^{-1} as determined by N_2 adsorption and application of BET theory. This clearly classified the resin as gel-type despite incorporating THF / toluene during the polymerisation process. The unexpected result could be explained by extended solvation of the polymer matrix within the droplet due to the increased polarity of the side-chains of the functionalised monomer **204**. Thus resulting in a reduced level of phase separation and hence the development of a gel-type resin.

4.5.3 Synthesis of Macroporous-Type Amino Alcohol Polymer 217

The analogous suspension copolymerisation of chiral amino alcohol monomer **167** with styrene **2** and divinylbenzene **100** was conducted employing the previously optimised experimental protocol outlined in **method L** of **chapter 8.4**, **scheme 97**.

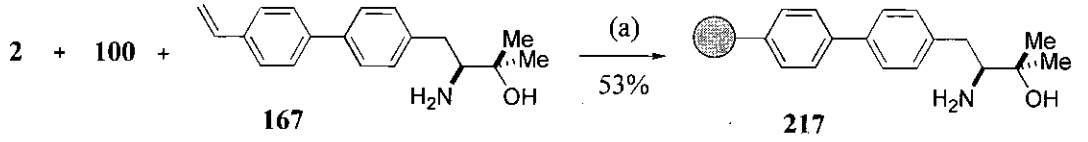

167 **217**

(a) (i) H_2O, PVA, 125 °C→0 °C; (ii) **2**, **100**, **167**, AIBN, THF, toluene, 0 °C→80 °C.

Scheme 97

The polymer-bound amino alcohol catalyst **217** was obtained in 23% yield where the material was sieved between 500 and 100 micron mesh sieves.[ξ] The resin swelled to 5.2 times its own volume in DCM. The swollen resin was composed of free flowing translucent spherical beads with minimal amorphous material evident from microscopic analysis.

Elemental analysis confirmed that the amino alcohol monomer **167** had been successfully incorporated to produce the functionalised polymer **217** where the loading was determined to be 0.48 $mmolg^{-1}$. Infra-red analysis of resin **217** provided a broad band at 3446 cm^{-1} relating to the stretching frequency of the hydroxyl group. It was presumed that the two missing NH stretches observed for the analogous biaryl amino alcohol solution phase mimic **192** at 3341 cm^{-1} and 3270 cm^{-1} were swamped by the intensity of the signal at 3446 cm^{-1}.

Resin **217** was found to have a negligible surface area in the dry state as determined by N_2 adsorption and application of BET theory. Therefore the beads were once again categorised as gel-type despite employing "macroporous" conditions in their synthesis.

Unfortunately, the low loading and high swelling capacity of the functionalised polymers **217** and **218** hindered their analysis by ^{13}C or ^{1}H gel-phase NMR techniques. The resultant low concentration of the chiral moiety within the polymer samples effectively produced spectra which were swamped with signals from the polystyrene backbone.

Magic angle spinning gel-phase NMR and maldi-TOF mass spectrometry techniques could not be used to further characterise the functionalised polymers **217** and **218** due to unavailability of the instrumentation.

[ξ] Additional polymer-bound amino alcohol **217** (30%) was isolated as larger aggregated beads which could not be sieved. However, as this material provided virtually identical data to that of the smaller beads discussed above in terms of swelling capacity, elemental analysis, infra-red spectroscopy and N_2 uptake, the overall yield of polymer was recorded as 53%.

4.6 Summary of Chapter 4

Chapter 4 illustrates the fundamental principles of suspension polymerisation where this process may be regarded as an art rather than a science with successful and reproducible results only being obtained after prolonged experimentation.

Numerous gel and macroporous-type copolymerisations were investigated, where vinylbenzyl chloride **219** was incorporated as the functionalised monomer to afford chloromethylpolystyrene **3**. The employed experimental parameters were improved by modification of the reactor design, stirrer speed and reactant compositions to ultimately yield the polymer beads in optimum size, shape and uniformity.

The chiral oxazolidinone **204** and amino alcohol **167** monomers were subsequently polymerised utilising the previously optimised suspension protocol. Characterisation of the resultant polymer-bound auxiliary **218** and catalyst **217** confirmed that the functionalised monomers were successfully incorporated with the desired loading.

Chapter 5 : Results and Discussion Part 4

Investigation of Oxazolidine Impurity 127 Formation

Chapter 2.3.2 attempted to prepare the α-dimethylated amino alcohol **116** *via* addition of freshly prepared MeMgI Grignard reagent to the triflated methyl ester **124**. ^{1}H NMR analysis of the crude product mixture (> 100% yield) indicated the presence of the target amino alcohol **116** and unreacted methyl ester **124** in an approximate 25:1 ratio with minor baseline impurities. Chromatographic purification of the reaction mixture afforded the desired product **116** (14%) where oxazolidine **127** was isolated as a minor by-product (3%), **scheme 98**. The low recovery of isolated material resulted from the difficult chromatographic separation of **116** and **127** which possess similar R_f values (R_f **116** [DCM:MeOH (90:10)] 0.42 and R_f **127** [DCM:MeOH (95:5)] 0.40).

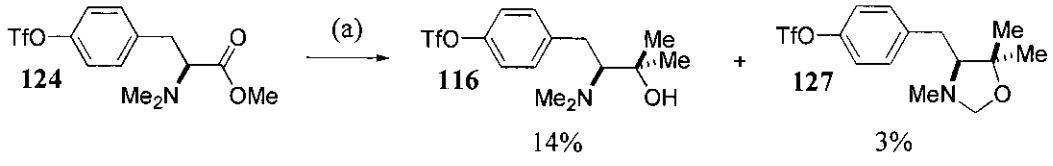

(a) (i) MeI, Mg, I_2, Et_2O, reflux; (ii) **124**, Et_2O, reflux.

Scheme 98

The structure of **127** was determined from ^{1}H NMR and MS (APCI) analysis where the former provided signals indicative of the oxazolidine functionality with the geminal protons at the C-2 position generating a typical AB splitting pattern (δ = 4.59, 3.89 ppm, $J_{H2\text{-}H2'}$ 3.1 Hz).

The coupling constant and chemical shifts of the geminal protons were also consistent with those reported for the closely related 4-ethyl oxazolidine **222** (δ = 4.39, 3.98 ppm, $J_{H2\text{-}H2'}$ 4.3 Hz), **figure 40**.[107]

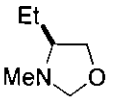

222

Figure 40

To unequivocally prove that the impurity isolated from the Grignard addition reaction had been accurately assigned to be the oxazolidine **127**, the analogous monomethylated biaryl oxazolidine **201** was synthesised, **scheme 99**.

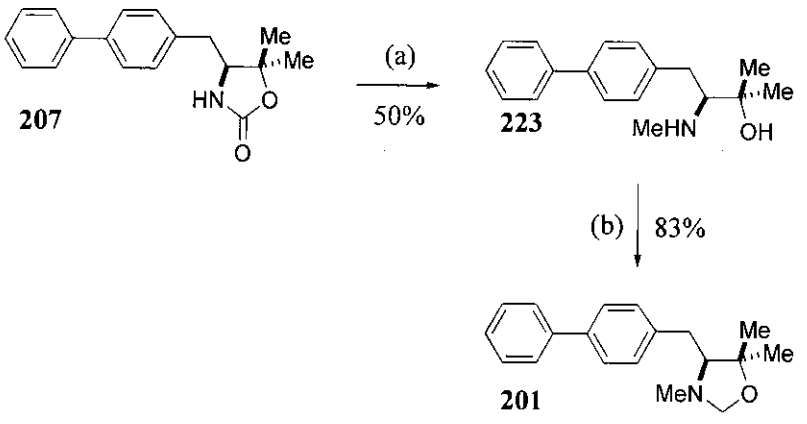

(a) $LiAlH_4$, THF, 0 °C→reflux; (b) aqueous H_2CO, toluene, RT.

Scheme 99

Initial reductive ring-opening of the biaryl oxazolidinone **207** (**chapter 3.10.3**) with lithium aluminium hydride furnished the monomethylated amino alcohol **223** (50%). The low yield of material was attributed to the lengthy aqueous acid / base extraction procedure employed in the isolation of **223** on a small scale. Subsequent cyclisation of **223** with formaldehyde following literature precedent proceeded rapidly to afford the target oxazolidine **201** in good yield (83%).[108]

^{1}H NMR analysis of oxazolidine **201** revealed that the C-2 geminal protons exhibit the previously observed AB splitting pattern (δ = 4.54, 3.81 ppm, $J_{H2\text{-}H2'}$ 2.9 Hz) where the remainder of the aliphatic signals were virtually identical to those of **127**, thus confirming the impurity as the oxazolidine **127**.

5.1 Proposed Mechanism for Oxazolidine 127 Formation

The postulated mechanism for formation of oxazolidine **127** during the Grignard reaction (**scheme 98**) involved initial oxidation of the amino alcohol product **224** to an activated intermediate **225** which could be either the amine *N*-oxide or perhaps the amine *N*-iodo salt, **scheme 100**.

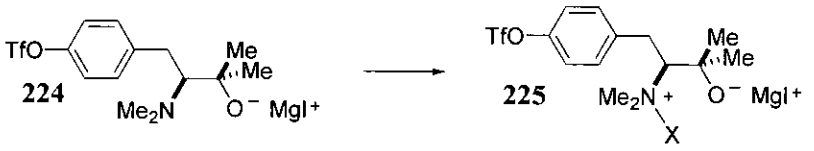

Scheme 100

Subsequent deprotonation of a methylene proton with MeMgI serving as the base generates an intermediate iminium ion **226** which is rapidly trapped by the magnesium alkoxide to afford the cyclised oxazolidine **127**, **scheme 101**.

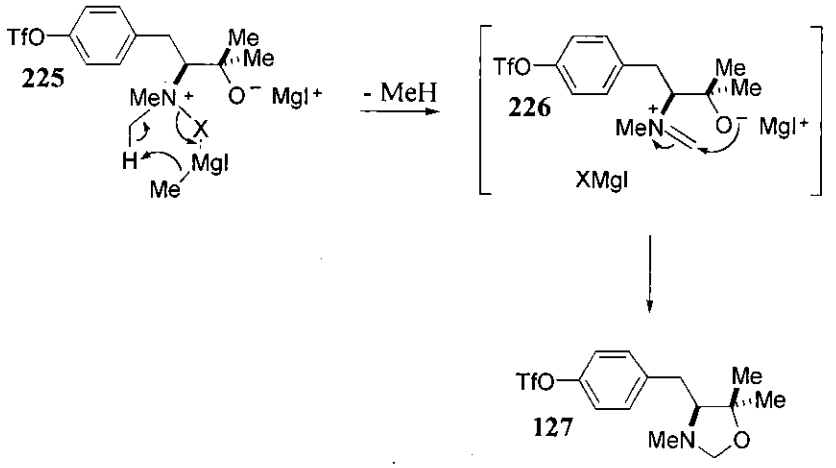

Scheme 101

5.2 Investigation of Amine *N*-Oxide as the Activated Intermediate 225

Although a mechanism for formation of the amine *N*-oxide under the Grignard reaction conditions was unclear, a series of experiments were conducted to determine whether such an activated *N*-oxide species might provide a suitable intermediate for the reaction mechanism detailed in **scheme 101**.

The primary concern with the *N*-oxide mechanistic route was that *N*-oxides which possess a β-hydrogen are often unstable and undergo Cope β-hydride elimination. This well documented process is illustrated in **scheme 102** with an example reported by Fry *et al.* which detailed the thermal decomposition of amine *N*-oxide **227** to the styrene compound **228** with elimination of *N*,*N*-dimethylhydroxylamine **229**.[109]

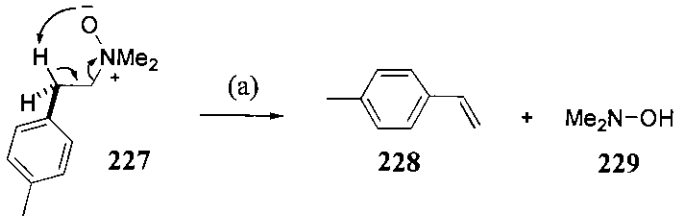

227 **228** **229**

(a) H_2O, DMSO, 65 °C.

Scheme 102

Therefore to investigate the *N*-oxide hypothesis, initial studies focused on preparing and subsequently evaluating the stability of the *N*-oxides derived from the *N*,*N*-dimethylated methyl ester **124** (**chapter 2.3.1**) and *N*,*N*-dimethylated amino alcohol **116** (**chapter 2.3.2**).[ξ]

Following literature precedent, the *N*-oxides were synthesised by equimolar reaction of the corresponding tertiary amines **124** and **193** with *meta*-chloroperbenzoic acid (*m*CPBA) at 0 °C and the reaction mixtures were subsequently allowed to warm to room temperature.[110]

The *N*-oxide of the *N*,*N*-dimethylated methyl ester **124** underwent spontaneous β-hydride Cope elimination where the transition state minimised steric interactions to exclusively afford the (*E*)-α,β-unsaturated ester **230** (91%), **scheme 103**.

[ξ] The analogous biaryl *N*,*N*-dimethylated amino alcohol **193** (**chapter 3.9.2**) was subsequently substituted in place of the triflated amino alcohol **116** due to the comparative ease of preparation of **193**.

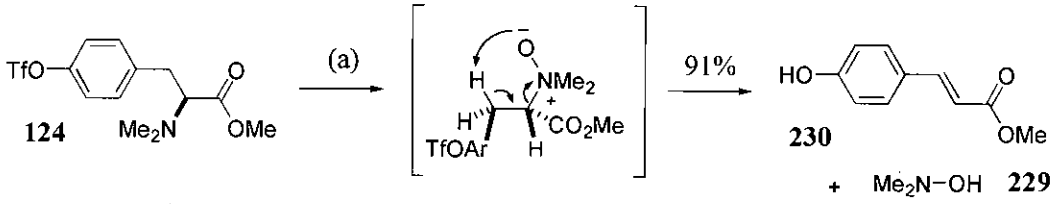

(a) *m*CPBA, DCM, 0 °C→RT.

Scheme 103

Presumably, the *N*-oxide derived from ester **124** did not require reflux conditions for Cope elimination to occur owing to the inherent stability of the product **230** which possesses extended conjugation.

APCI mass spectrometric analysis indicated the presence of the phenol **230** as the molecular ion. This suggested that cleavage of the triflate group in this reaction occurred under the conditions of oxidation and elimination as previous analyses of aryl triflates indicated that the triflate moiety is stable to the APCI conditions. The stereochemistry of **230** was determined by comparison of the ^{1}H NMR spectrum ($J_{H2\text{-}H3}$ 16.1 Hz) with those signals predicted for **230** utilising simple spectroscopic calculations[111] where the spectrum was also consistent with that reported for the analogous methyl (*E*)-cinnamate **231** ($J_{H2\text{-}H3}$ 16.3 Hz), **figure 41**.[112]

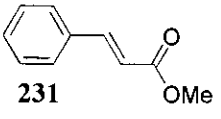

Figure 41

Treatment of the biaryl *N,N*-dimethylated amino alcohol **193** with *m*CPBA also furnished the analogous styrene derived unsaturated product **232** (74%) *via* β-hydride elimination of the intermediate *N*-oxide where the *trans* geometry of the alkene was established from ^{1}H NMR data ($J_{H3\text{-}H4}$ 16.1 Hz). In addition, **232** subsequently underwent acid catalysed dehydration on standing in $CDCl_3$ to afford (*E*)-1-biphenyl-3-methyl-1,3-butadiene **233** with extended conjugation, **scheme 104**.

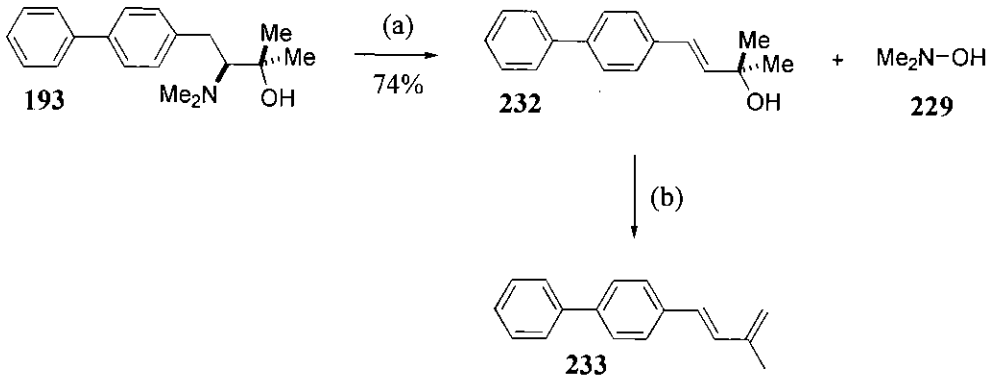

(a) *m*CPBA, DCM, 0 °C→RT; (b) $CDCl_3$.

Scheme 104

It was postulated that the *N*-oxide of amino alcohol **193** similarly underwent spontaneous β-hydride elimination at room temperature to relieve the steric strain of the congested *N*-oxide intermediate.

Further comparisons can be drawn with research by Roussi *et al.* where the α-dimethylated benzylic *N*-oxide **234** prepared by hydrogen peroxide oxidation of the corresponding amine was found to be unstable with respect to spontaneous Cope elimination at 0 °C generating **235**, **scheme 105**.[113]

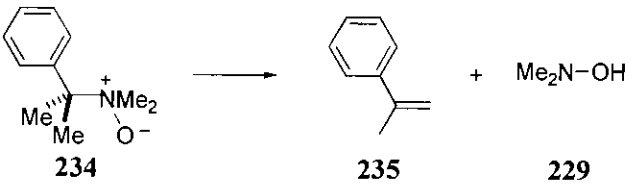

Scheme 105

The aim of the latter report published by Roussi *et al.*[113] was to synthesise pyrrolidines **236** *via* the 1,3-dipolar cycloaddition of an azomethine ylid **237** with an alkene **238**. Ylid **237** formation was proposed to occur by deprotonation of a tertiary amine *N*-oxide **239** with lithium diisopropylamide (LDA) base *via* the intermediate iminium ion **240**, **scheme 106**.

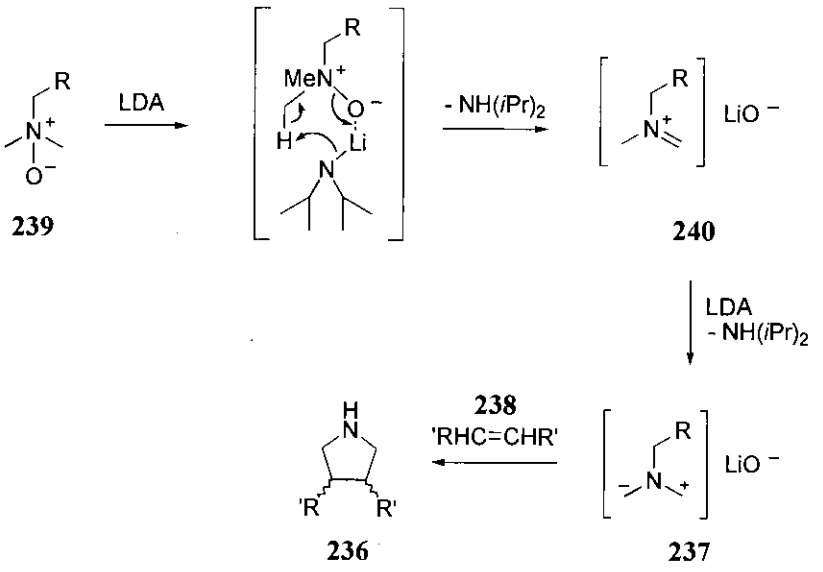

Scheme 106

However, early attempts by Roussi *et al.*[113] to investigate the reaction of the methyl ephedrine *N*-oxide **241** with LDA and *trans*-stilbene **242** afforded the desired diastereomeric pyrrolidine **243** (40%) and oxazolidine **244** (20%) which was generated *via* competitive trapping of the intermediate iminium ion **245** by the lithium alkoxide, **scheme 107**.

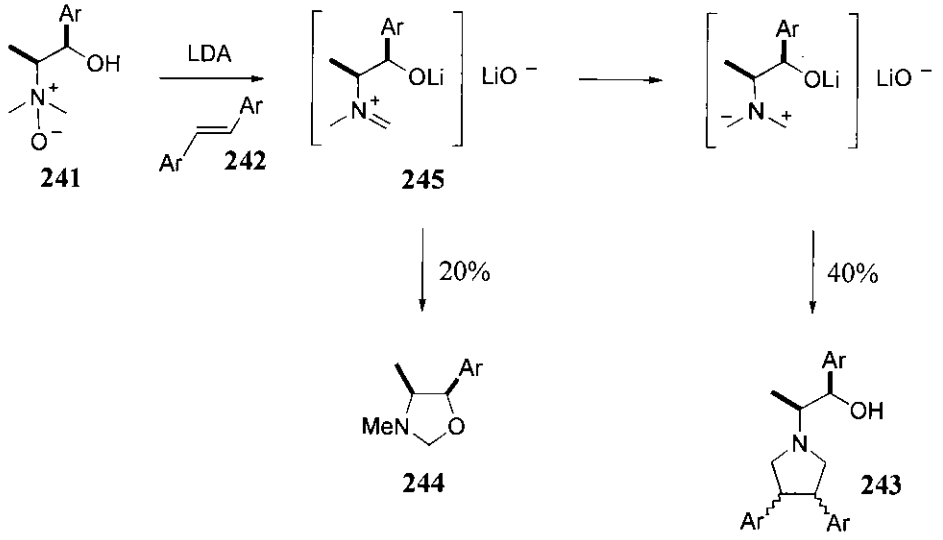

Scheme 107

The proposed mechanism for generation of oxazolidine **244** is therefore essentially identical to that previously postulated within **chapter 5.1** for generation of

the oxazolidine impurity **127** from the original Grignard reaction (**scheme 101**) where LDA base has been substituted in place of the MeMgI. Furthermore, Roussi *et al.*[113] reported that conducting the 1,3-dipolar cycloaddition (**scheme 107**) at -78 °C under kinetic control suppressed oxazolidine **244** formation, thus indicating that the oxazolidine is the thermodynamic product which is also consistent with the original Grignard reaction which was carried out at reflux temperatures (**scheme 98**).

5.2.1 Reaction of Amine *N*-Oxide 246 with MeMgCl Base

Following the research of Roussi *et al.*[113] further experiments were designed to investigate the reactivity of the *N*-oxide derived from amino alcohol **193** in the presence of MeMgCl base. To mimic the experimental parameters detailed in **scheme 107** generation of the *N*-oxide preceded addition of the MeMgCl base, although within the original Grignard reaction (**scheme 98**) prior deprotonation of the hydroxyl group would occur to furnish the magnesium alkoxide.

As the *N*-oxide has already been shown to undergo spontaneous Cope elimination at room temperature (**scheme 104**), *N*-oxide **246** was initially prepared by treatment of the amino alcohol **193** with *m*CPBA at 0 °C. The solvent medium was chosen as CD_2Cl_2 which allowed direct monitoring of the reaction by ^1H NMR analysis, thus confirming quantitative conversion of **193** to the *N*-oxide **246**. The aliphatic signals in **246** predominantly shifted downfield relative to those of **193** owing to the increased electron withdrawing nature of the *N*-oxide moiety, **scheme 108**.

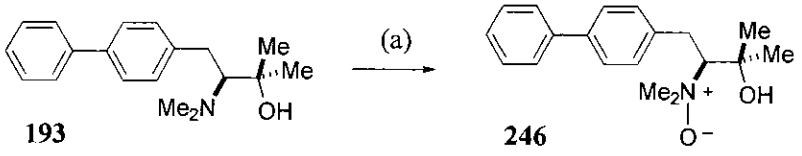

193 **246**

(a) *m*CPBA, CD_2Cl_2, 0 °C.

Scheme 108

The reaction mixture was not subjected to any work-up procedure in an attempt to minimise decomposition of the *N*-oxide **246**. Removal of the CD_2Cl_2 was

simply effected under reduced pressure where the reaction mixture was maintained at 0 °C throughout to again limit spontaneous β-hydride Cope elimination. The crude *N*-oxide **246** was directly treated with MeMgCl in THF at 0 °C. 4.0 equivalents of the Grignard reagent were employed as the first two equivalents would primarily deprotonate the hydroxyl group of the *N*-oxide **246** and the reduced *meta*-chlorobenzoic acid by-product from the prior oxidation step.

^{1}H NMR analysis of the crude product mixture indicated that a range of products were produced and diagnostic isolated signals resulting from the various compounds[Ψ] allowed the ratio of products to be determined as depicted in **scheme 109**.

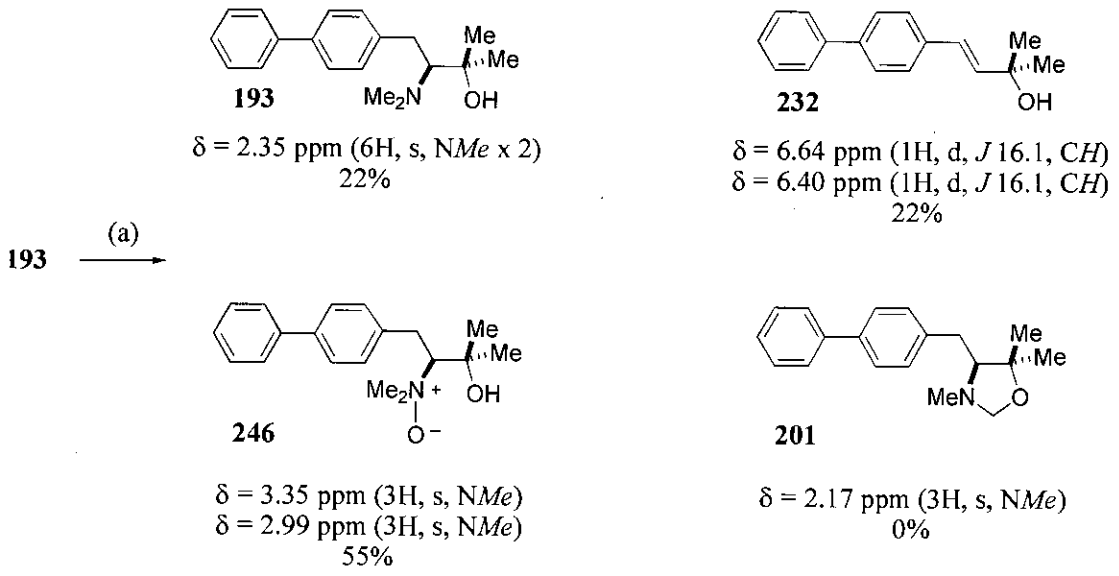

(a) MeMgCl, THF, 0 °C.

Scheme 109

The notable absence of any oxazolidine **201** when the *N*-oxide was treated with MeMgCl base under kinetic control confirmed that **201** is the thermodynamic product of the reaction, thus reinforcing the findings of Roussi *et al.*[113]

[Ψ] The distinguishable signals from the ^{1}H NMR spectrum of the amino alcohol *N*-oxide **246** at δ = 3.61 ppm (3H, s, N*Me*) and δ = 3.35 ppm (3H, s, N*Me*) recorded in CD_2Cl_2 were used to predict those signals relating to the *N*-oxide **246** from the above reaction mixture where the crude ^{1}H NMR spectrum was recorded in $CDCl_3$.

Unfortunately, time constraints did not permit reaction of the amine *N*-oxide **246** with MeMgCl base under thermodynamic control. However, it was postulated that deprotonation of the *N*-oxide **246** with MeMgCl and cyclisation of the resulting iminium ion under reflux conditions would allow partial generation of the oxazolidine **201** as observed by Roussi *et al.* (**scheme 107**).[113]

In summary, these results combined with the findings of Roussi *et al.* suggest that if *N*-oxide **247** formation is achieved within the original Grignard reaction (**scheme 100**) only a small proportion of **247** would be likely to undergo MeMgI base promoted cyclisation to the oxazolidine **127** (**scheme 101**). The remaining *N*-oxide material **247** would preferentially Cope eliminate generating the β-hydride elimination product **248** which could in turn undergo MeMgI base catalysed dehydration to the diene **249**, **scheme 110**.

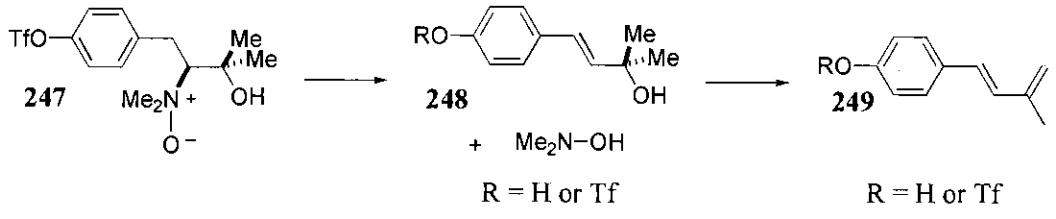

Scheme 110

However, ^{1}H NMR analysis of the crude Grignard product mixture (**scheme 98**) did not contain any alkene signals when compared to the diagnostic isolated signals resulting from the analogous biaryl β-hydride elimination product **232** and diene compound **233** (**scheme 104**), thus discrediting the overall feasibility of an amine *N*-oxide as the proposed activated intermediate **225** (**scheme 100**).

5.3 Investigation of Amine *N*-Iodo Salt as the Active Intermediate 225

Attention was subsequently directed to the alternative proposed mechanistic pathway which involved initial reaction of the Grignard addition product **224** with iodine to generate the activated *N*-iodo salt **250**. Note that iodine was present in the

reaction mixture as it was employed to initiate formation of the MeMgI Grignard reagent (**scheme 98**).

Subsequent deprotonation of a methylene proton with MeMgI serving as the base generates an intermediate iminium ion **251** which is again rapidly trapped by the magnesium alkoxide to afford the cyclised oxazolidine impurity **127**, **scheme 111**.

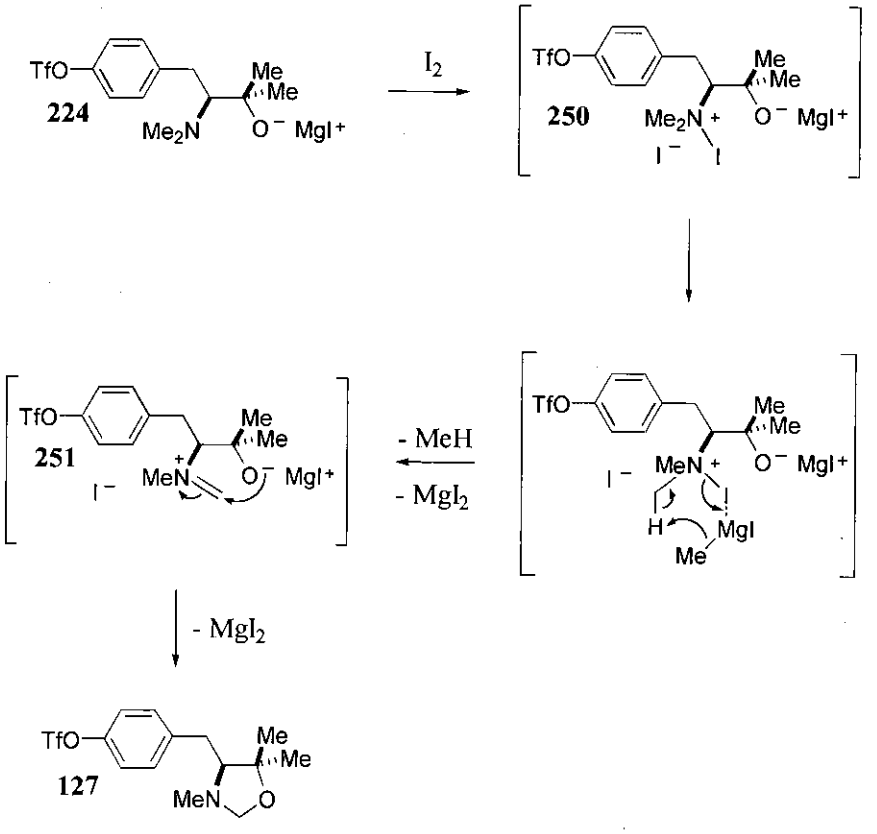

Scheme 111

Literature precedent supports the equimolar iodine oxidation of tertiary amines to afford amine *N*-iodo ionic charge-transfer salt complexes. Subsequent hydro-iodo-elimination furnishes iminium ion intermediates. This elimination step may be base catalysed. The nature of the amine substrate and the reaction medium determine the final products resulting from reaction of the iminium ion.[114]

For example, McCleland *et al.* treated tribenzylamine **252** with iodine where hydrolysis of the resultant iminium ion **253** with water generated dibenzylamine **254** and benzaldehyde **69** as depicted in **scheme 112**.[114]

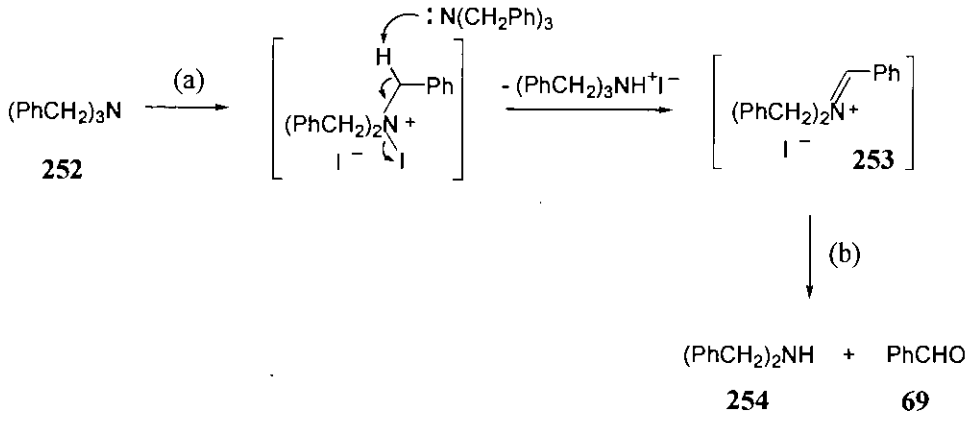

(a) I_2, benzene, reflux; (b) H_2O.

Scheme 112

In this instance, formation of the iminium ion **253** was favoured as **253** possesses extended conjugation. In contrast, base catalysed elimination of the analogous *N*-iodo salt **250** within the proposed mechanism for formation of the oxazolidine **127** (**scheme 111**) cannot create a conjugated intermediate iminium ion. As such, the increased probability of removing one of the six available methylene protons over the single C*H*N proton presumably results in preferential base catalysed removal of the former with MeMgI to generate iminium ion **251**.

Furthermore, the absence of water within the Grignard reaction would prevent subsequent hydrolysis of the iminium ion **251**, thus promoting trapping of **251** by the magnesium alkoxide to furnish the cyclised oxazolidine **127** (**scheme 111**). Finally, the low yield of isolated oxazolidine **127** (3%) was attributed to the negligible amount of iodine present within the Grignard reaction (**scheme 98**).

Further analogies can be drawn with the research by Helquist *et al.* where the reaction of the allylic amine **255** with catalytic iodine in the presence of air and a light source generated of the corresponding aldehyde **256** (66%), **scheme 113**.[115]

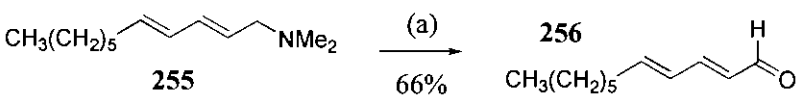

(a) Catalytic I_2, 95% EtOH, reflux, air, light.

Scheme 113

Mechanistic studies were not performed on this reaction although iminium salts were considered as possible intermediates which in turn undergo hydrolysis with water present in the ethanol solvent medium to provide the observed products, thus essentially following the mechanism previously outlined in **scheme 112**. Critically, each of the components (iodine, air, light) were required for significant conversion to occur. This indicates that photochemical oxidation of the liberated iodide anions allows regeneration of iodine which explains the catalytic use of iodine.

Although the level of iodine incorporated within the original Grignard reaction was effectively catalytic (**scheme 98**), the reaction was conducted under argon, thus the absence of air would prevent recycling of the iodine. This factor reinforces the previous suggestion that the low isolated yield of oxazolidine **127** (3%) was ultimately proportional to the trace amounts of iodine employed.

Unfortunately, time constraints did not allow the feasibility of this alternative amine *N*-iodo salt pathway for the generation of the oxazolidine impurity **127** from the original Grignard reaction (**scheme 98**) to be evaluated. The ideal experiment to be performed would involve treatment of the Grignard addition product **224** with both equimolar iodine and MeMgI to potentially furnish the observed oxazolidine by-product **127** *via* the mechanism described in **scheme 111**.

However, in light of the literature reports by McCleland *et al.*[114] and Helquist *et al.*[115] generation of the activated *N*-iodo salt **250** and subsequent MeMgI base promoted elimination to afford the intermediate iminium ion **251** appears viable. In addition, cyclisation of **251** to the oxazolidine **127** under thermodynamic control is substantiated by the previously discussed findings of Roussi *et al.*[113]

Thus, the original proposed mechanism for formation of the characterised oxazolidine impurity **127** discussed in **chapter 5.1** was deduced by systematically conducting a series of related informative experiments with reference to the relevant literature papers.

5.4 Investigation of Stability of Amino Alcohols 193 and 150 in $CDCl_3$

Routine ^1H and ^{13}C NMR analyses of amino alcohols **193** and **150** revealed that they were prone to partial decomposition to the corresponding monomethylated oxazolidines **201** and **257** on standing in $CDCl_3$, **scheme 114**.

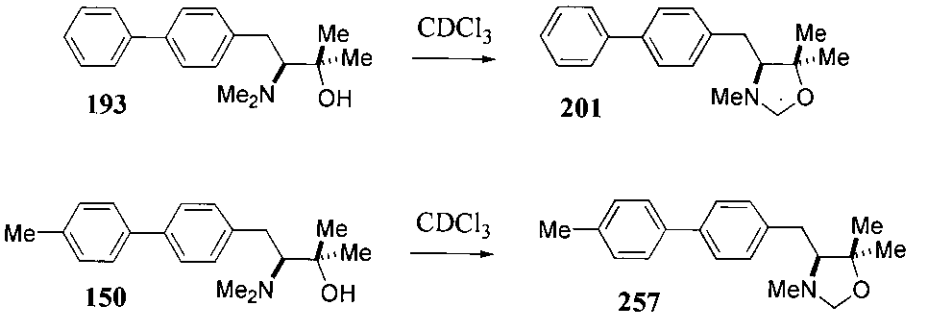

Scheme 114

As the $CDCl_3$ may contain traces of water and the samples were stored under air, hydrogen peroxide generated by photochemical oxidation of the water could be responsible for oxidation of the amino alcohols to the corresponding *N*-oxides.[116] However, oxazolidine formation could not occur *via* deprotonation of the *N*-oxide and subsequent cyclisation of the resulting iminium ion as no base was present. This route was further discredited as the absence of base would in turn promote Cope elimination of the *N*-oxide, yet no alkene signals relating to β-elimination products were evident in the ^1H NMR spectra. Clearly, the *N*-iodo salt pathway is also negated in the absence of iodine.

Alternatively, generation of oxazolidines **201** and **257** (**scheme 114**) could occur *via* initial photochemical oxidation of the *N,N*-dimethylated amino alcohols **193** and **150** with singlet oxygen to afford the Zwitterionic species **258** and **259**, **scheme 115**.[117]

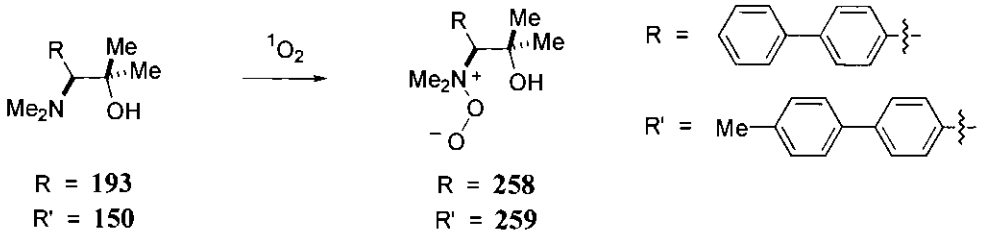

Scheme 115

Formation of the iminium ions **260** and **261** could proceed by direct deprotonation of a methylene proton by the hydroperoxide anion of **258** / **259**, route A, **scheme 116**. Initial intramolecular removal of the more acidic hydroxyl proton within **258** and **259** followed by attack of the resultant oxygen anion onto a methylene proton could also provide the intermediate iminium ions **260** / **261**, route B, **scheme 116**. Alternatively, generation of **260** and **261** could occur *via* an intermolecular process, route C, **scheme 116**.

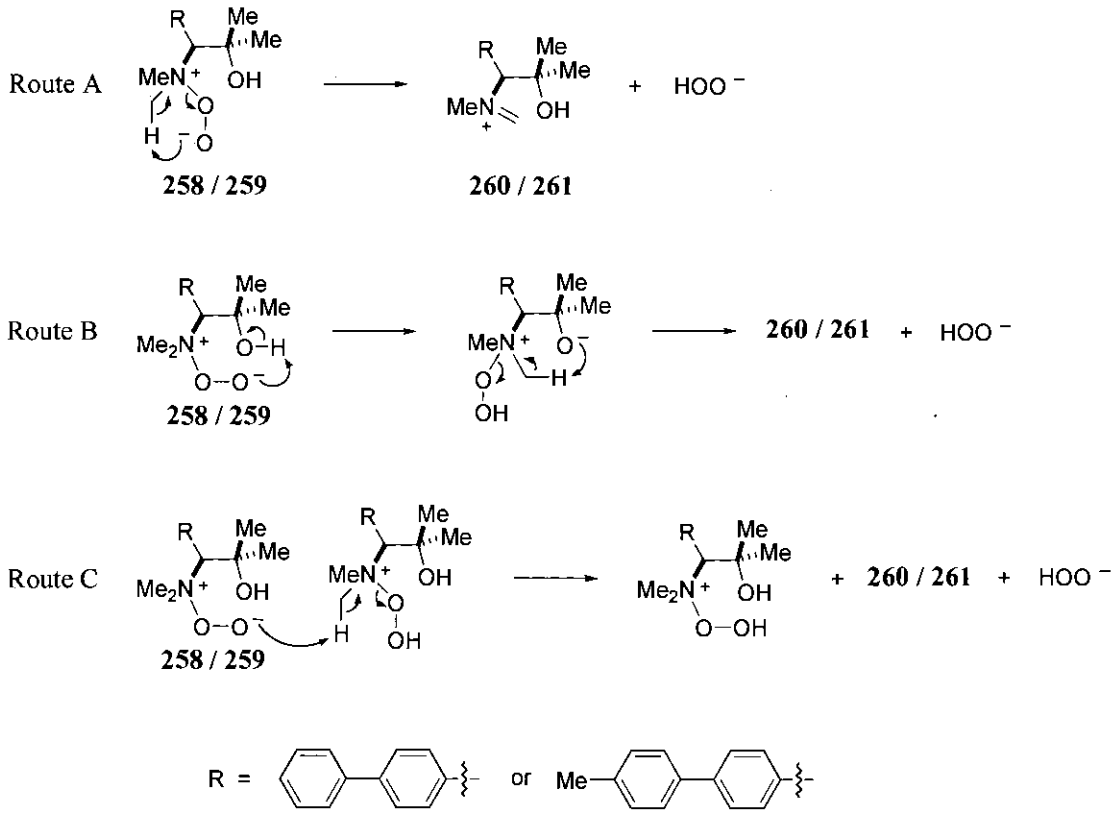

Scheme 116

The liberated hydroperoxide anion would presumably undergo protonation to generate hydrogen peroxide which could in turn oxidise the amino alcohols **193** and **150** (**scheme 114**) to the corresponding *N*-oxides.[116] However, the absence of any Cope elimination products within the amino alcohol $CDCl_3$ samples could be attributed to the relatively low concentrations of hydrogen peroxide resulting in a slow rate of *N*-oxide formation.

Final trapping and cyclisation of iminium ions **260** and **261** (**scheme 116**) would then proceed rapidly with relief of steric strain to furnish the observed oxazolidine compounds **201** and **257**, **scheme 117**.

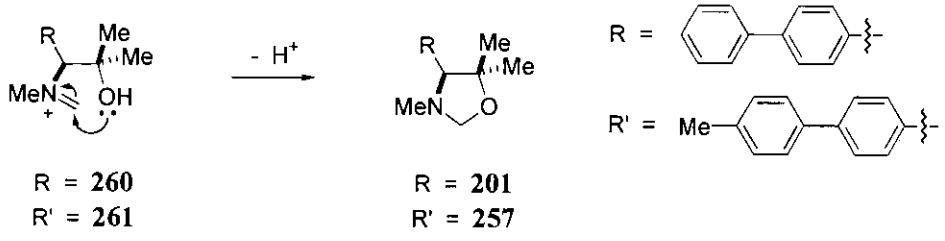

R = **260**
R' = **261**

R = **201**
R' = **257**

Scheme 117

Unfortunately, time restraints did not permit further investigation regarding the nature of the mechanism which effected partial conversion of the amino alcohols **193** and **150** to the oxazolidine compounds **201** and **257** (**scheme 114**).

However, this decomposition process explained the inconsistent selectivity induced by **193** as a catalyst in the addition of dialkylzinc reagents to aldehydes (**chapter 6.2.3**) where the amino alcohol **193** and resultant oxazolidine **201** were proposed to provide conflicting stereocontrol. Therefore, the observed instability of the *N*,*N*-dimethylated-α-dimethylated amino alcohol moiety with respect to oxazolidine formation proved invaluable in determining that the substitution pattern of the amino alcohol catalyst was not an ideal candidate for transferral to the solid phase where such degradation would be impossible to monitor.

Chapter 6 : Results and Discussion Part 5

Catalysed Asymmetric Addition of Dialkylzinc to Aldehydes

Within the domain of asymmetric carbon-carbon bond forming reactions, the enantioselective addition of diorganozinc compounds **262** to aldehydes **263** in the presence of a catalyst has attracted much attention owing to its applicability in the synthesis of chiral secondary alcohols **264**, **scheme 118**.

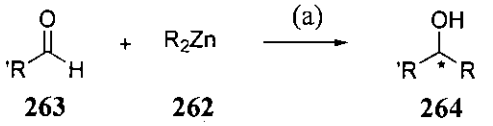

263 **262** **264**

(a) Catalyst.

Scheme 118

As the alkyl group of the organometallic reagent **262** is relatively unreactive towards addition to aldehydes, the role of the catalyst is to activate the alkyl group whilst providing the required enantiocontrol for the transformation. Chiral β-amino alcohols of general type **265** satisfy both of these criteria and have been extensively studied as solution phase catalysts.[118] The amino alcohol functionality effectively acts as a Lewis base by coordinating the zinc atom of the diorganozinc reagent **262** with loss of alkane **266**. The remaining alkyl group within the chiral zincate **267** possesses increased nucleophilicity thus promoting its addition to the aldehyde **263**, **scheme 119**. In addition, the three-dimensional structure of the chiral β-amino alcohol **265** within the transition state controls the stereochemistry of the secondary alcohol product **264**.

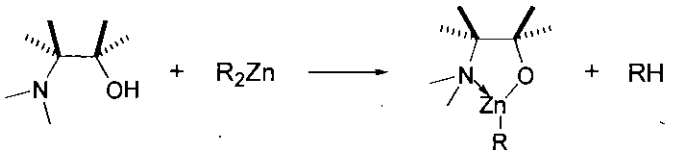

265 **262** **267** **266**

Scheme 119

Mechanistic studies conducted by Noyori *et al.* employed the highly enantioselective sterically congested (-)-3-*exo*-(dimethylamino)isoborneol (DAIB) **268** chiral tertiary amino β-amino alcohol catalyst, **figure 42**.[119]

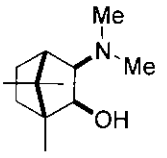

268

Figure 42

Remarkably, a complex formed from equimolar amounts of dimethylzinc and DAIB **268** failed to alkylate benzaldehyde despite the presence of an alkyl-Zn bond. In contrast, the alkylation was found to proceed smoothly if an excess of dimethylzinc was employed. This phenomenon indicated that the alkyl transfer reaction occurs *via* a dinuclear zinc complex containing a chiral amino alkoxide, an aldehyde ligand, and three alkyl groups. The exact mechanism of alkyl transfer from diorganozinc species **262** to aldehydes **263** remains to be elucidated where the proposed related bimetallic transition state models are depicted in **figure 43**.[118]

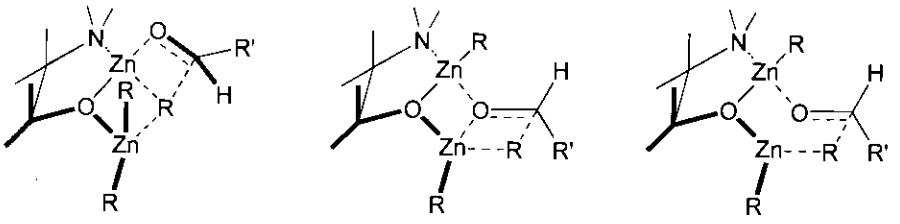

269 **270** **271**

Figure 43

In each case a second molecule of dialkylzinc **262** coordinates to a lone pair of the oxygen atom in the chiral zincate **267**, thus enhancing the nucleophilic properties of the alkyl groups. The zinc centre of the chiral zincate **267** simultaneously behaves as a Lewis acid and coordinates the oxygen atom of the aldehyde **263**, thus activating the latter to nucleophilic attack. These criteria ensure that both reactants are activated and held in close proximity allowing the asymmetric alkyl transfer to occur.

Model **269**[120a] (**figure 43**) involves addition of the tricoordinate bridging alkyl group to the aldehyde where the bulky group of the aldehyde (R') is orientated away from the congested area of the transition state thus affording enantiocontrol.

The 4,4-bicyclic transition state **270**[33c] (**figure 43**) provides an alternative explanation for the observed stoichiometry and stereochemistry of the diorganozinc addition where a dicoordinate terminal alkyl group undergoes migration. Model **271**[120b] (**figure 43**) is closely related with the intramolecular alkyl transfer occurring *via* a six membered ring transition state to generate the carbon-carbon bond. In both cases the asymmetric induction is again controlled by the R' substituent of the aldehyde which is positioned to minimise non-bonded repulsion between itself and the alkyl group of the chiral zincate **267**.

The resultant alkoxide **272** generated after transfer of the alkyl group in the DAIB catalysed addition of dimethylzinc to benzaldehyde is depicted in **scheme 120**. Noyori *et al.*[118] determined the structure of the alkoxide intermediate **272** from ^{1}H NMR analysis which provided a doublet and a quartet at δ = 1.93 and 5.36 ppm respectively due to the methyl and methine protons of the bridged alkoxide with a broad singlet at δ = -0.17 ppm resulting from the Zn(*Me*)$_2$ protons.

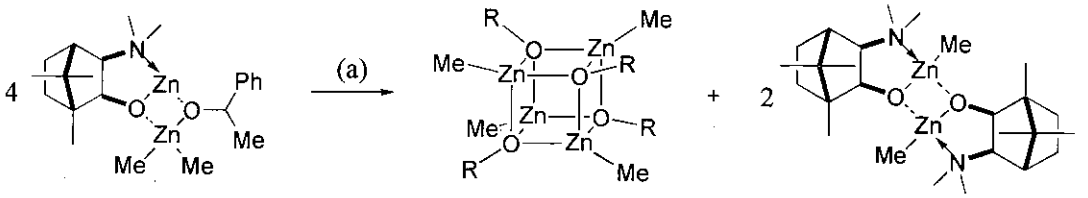

272 **273** **274**

R = CH(Ph)Me

(a) PhCHO or Me_2Zn.

Scheme 120

The alkoxide **272** was found to undergo spontaneous decomposition to the cubic zinc alkoxide tetramer **273** upon exposure to benzaldehyde or dimethylzinc, Structure determination of **273** was ascertained from cryoscopic MW measurements where hydrolysis of **273** on work-up yielded the 1-phenylethanol product.[118]

Finally, conversion of alkoxide **272** to the tetrameric alkoxide **273** generated the dimeric zincoxazine **274**, **scheme 120**. Species **274** is in effect the catalyst precursor as it dissociates to form the chiral zincate monomeric complex as later discussed in **chapter 6.1**, thus completing the catalytic cycle.

The previous mechanistic discussion was specific to the addition of dialkylzinc reagents to aldehydes as catalysed by amino alcohols where the amino moiety is trisubstituted. Itsuno *et al.* postulated a modified reaction pathway for cases where primary amino containing amino alcohol catalysts are employed.[35e]

The proposed mechanism involves initial reaction of the primary amino group of a catalyst with an aldehyde to form the imine Schiff base with elimination of water. This theory was substantiated as reaction of catalyst **275** with benzaldehyde **69** at room temperature generated the Schiff base **276** and oxazolidine **277** in a 2.7 : 1 ratio as determined from ^{1}H NMR analysis, **scheme 121**.

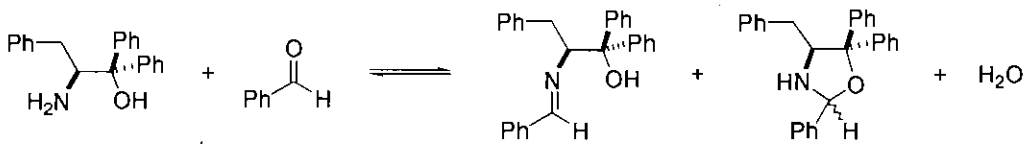

275 **69** **276** **277**

Scheme 121

Itsuno *et al.* predicted that complexation of the Schiff base **276** with diethylzinc and further benzaldehyde **69** would allow the asymmetric alkyl transfer to proceed through a 4,4-bicyclic transition state **278**[35e] in an analogous manner to that previously discussed for model **270**[33c] (**figure 43**), **figure 44**.

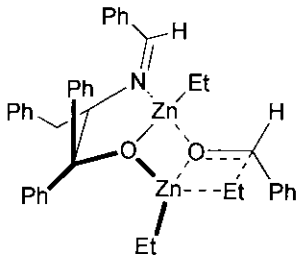

278

Figure 44

The suggested transition state model **278** rationalises the observed sense of asymmetric induction as enantiomerically enriched (*S*)-1-phenyl-1-propanol was consistently obtained. Furthermore, premixing the amino alcohol catalyst **275** with benzaldehyde **69** prior to the addition of diethylzinc **68** provided higher levels of enantiocontrol with reproducible results (90% yield, 85% e.e. *S*) when compared to the reversed order of addition of **69** and **68** (85-95% yield, 22-73% e.e. *S*). This would indicate that formation of the Schiff base **276** prior to zinc complexation plays a significant role in the primary amino alcohol catalysed asymmetric alkylation process.

6.1 Chiral Amplification

As noted in **chapter 6** the coordinatively unsaturated chiral zincate complex **267** exists in equilibrium with the corresponding dimeric zincoxazine species **279**, **scheme 122**. This factor is irrelevant if the amino alcohol catalyst **265** is enantiopure, as the dimer **279** exhibits no catalytic activity and subsequently dissociates to regenerate the chiral monomer **267** which enters the catalytic cycle.

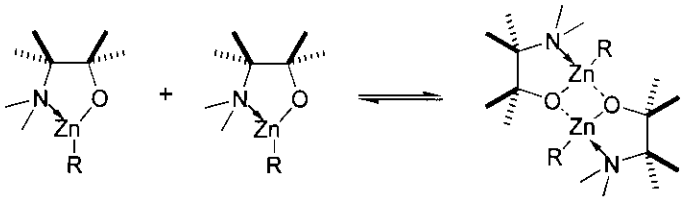

267 **267** **279**

Scheme 122

However, additional dimers are generated if an optically impure catalyst is reacted with a dialkylzinc reagent. This is exemplified with the camphor derived DAIB catalyst which rapidly establishes an equilibrium between the heterochiral (-)-DAIB/(+)-DAIB **280** and homochiral (-)-DAIB/(-)-DAIB **281**, (+)-DAIB/(+)-DAIB **282** dimeric species, **figure 45**.

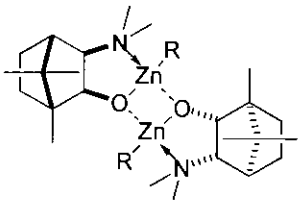

280

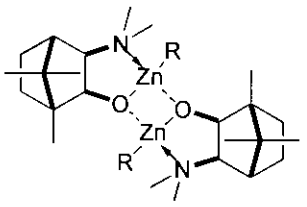

281

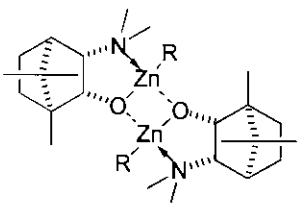

282

Figure 45

The least sterically demanding *meso*-dimer **280** exhibits little tendency to dissociate and is effectively formed irreversibly under the reaction conditions. This results in consumption of the minor enantiomer of the DAIB catalyst leaving the homochiral dimer **281** or **282** which dissociates to generate the major enantiopure zincate, thus the catalytic cycle proceeds in the normal manner.[121] Noyori *et al.* illustrated this point using (-)-DAIB **268** in 15% enantiomeric excess to catalyse the addition of diethylzinc to benzaldehyde where the (*S*)-1-phenyl-1-propanol product was obtained in 92% yield and 95 % e.e.[118]

The amplification of chirality observed between the enantiomeric excess values of the chiral catalysts and the chiral alcohol products in the amino alcohol catalysed enantioselective alkylation process is termed a positive non-linear effect.[122]

Note that chiral amplification did not feature in our catalytic systems as all of the solution phase and polymer-bound amino alcohol catalysts were enantiopure.

6.2 Design and Evaluation of Solution Phase Amino Alcohol Catalysts

The aim of this component of the research was to prepare a novel robust polymer-bound amino alcohol of general type **109** to catalyse the enantioselective addition of dialkylzinc reagents to aldehydes, **figure 46**.

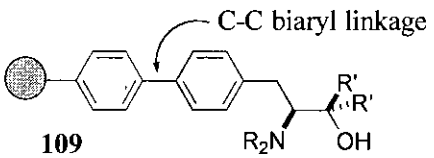

109

Figure 46

Attachment of the chiral amino alcohol catalyst to the solid phase allows simple isolation of the chiral secondary alcohol products where the polymeric catalyst can readily be separated from the reaction mixture and potentially recycled. The design of the support incorporated the carbon-carbon biaryl backbone, this linkage cannot coordinate the reactant zinc metal centre of the dialkylzinc reagent, which should result in greater control over the asymmetric induction. Furthermore, the absence of an ether linkage as typically found in other supported amino alcohol catalysts should offer increased stability, thus maximising the recycling potential of the chiral polymer.

Initial studies focused on a range of model chiral amino alcohol catalysts **283**, **112** and **284** with the R and R' substituents representing H or Me where the syntheses were previously discussed in **chapters 2** and **3**, **figure 47**.

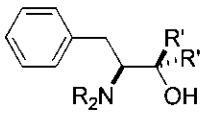

283

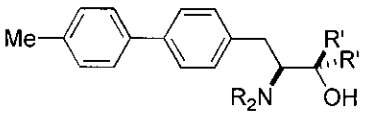

112

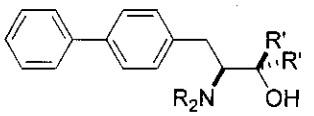

284

Figure 47

Evaluation of the activity and selectivity imparted by these catalysts in the solution phase addition of dialkylzinc reagents to aldehydes allowed identification of the optimum amino alcohol catalytic system. The preferred substitution pattern was subsequently incorporated within the parent vinyl amino alcohol monomer where polymerisation afforded the corresponding functionalised chiral polymeric catalyst. This development process established the extent to which catalyst reactivity and enantioselectivity were affected by introducing the biaryl unit and subsequently binding the amino alcohol to the solid support.

General considerations for the solution phase catalysed alkylation of aldehydes include the nature and stoichiometry of the aldehyde and diorganozinc substrates and the solvent medium. Benzaldehyde **69** and *trans*-cinnamaldehyde **285** were chosen as model aldehyde substrates with diethylzinc **68** as the diorganozinc to afford 1-phenyl-1-propanol **70** and 1-phenyl-1-penten-3-ol **286**, **scheme 123**.

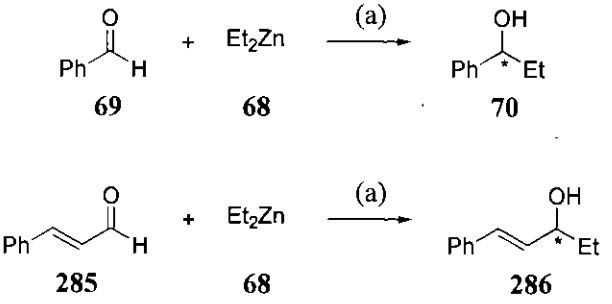

(a) Catalyst, toluene.

Scheme 123

Grignard addition of EtMgBr to benzaldehyde **69** and *trans*-cinnamaldehyde **285** afforded *rac*-**70** and *rac*-**286** in excellent yields (99% and 98% respectively), **scheme 124**. Preparation of the racemic alcohols provided a means to optimise chiral HPLC column conditions to give good baseline separation of the enantiomeric peaks, see **appendix** for chiral HPLC traces. The optical purity of the diethylzinc addition products were subsequently measured by HPLC under the same conditions.

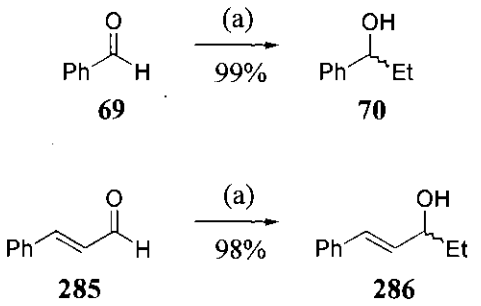

(a) EtMgBr, THF, Et_2O, reflux.

Scheme 124

An analogous experimental protocol to that detailed in **method N** of **chapter 8.6** was undertaken for each of the amino alcohol catalysed reactions whereby the amino alcohol and diethylzinc **68** were premixed prior to addition of the aldehyde. Further diethylzinc **68** was routinely added in an attempt to drive the reactions to completion, as there is literature precedent for an increase in the chemical and optical yields of the alcohol products as the ratio of dialkylzinc : aldehyde is increased.[123]

All of the diethylzinc addition reactions conducted in the solution phase incorporated toluene as the solvent medium as polar solvents (THF) have been shown to reduce the reaction rate and enantioselectivity by interfering in the catalytic cycle. Finally, the influence of reaction temperature, reaction time and catalyst concentration on the yields and enantiomeric excesses of the resultant secondary alcohol products **70** and **286** were examined.

Note that benzyl alcohol **287** was observed as a by-product in all of the benzaldehyde **69** addition reactions from the known reduction of benzaldehyde with diethylzinc *via* β-hydride elimination as depicted in **scheme 125**.[124]

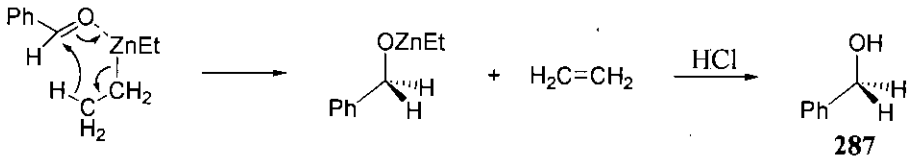

Scheme 125

6.2.1 Diethylzinc Reactions Utilising Amino Alcohol Catalyst 288

Amino alcohol **288** was synthesised within the research group *via* the sodium borohydride / iodine reduction of *L*-phenylalanine[125] and subsequent *N,N*-dimethylation of the resulting *L*-phenylalaninol using formaldehyde / formic acid, **figure 48**.[93]

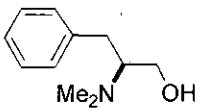

288

Figure 48

Amino alcohol **288** was evaluated as a catalyst for the addition of diethylzinc **68** to benzaldehyde **69** and cinnamaldehyde **285** (**scheme 123**) where the reaction parameters were modified to optimise both chemical and optical yields of the secondary alcohol products **70** and **286** as summarised in **table 9**.

Table 9 - Diethylzinc Results Utilising Amino Alcohol Catalyst 288

Entry	Catalyst (mol %)	Aldehyde substrate	Temperature / time after addition of aldehyde	Temperature / time after addition of further Et_2Zn	yield (%)	e.e. *R* (%)
1	2	**69**	0 °C, 22 h	0 °C, 17 h	13	29 [b]
2	2	**69**	RT, 22 h	RT, 17 h	62	30 [b]
3	2	**69**	RT, 22 h	RT, 17 h [a]	97	36 [b]
4	2	**69**	0 °C, 72 h	RT, 24 h [a]	100	40 [c]
5	2	**285**	0 °C, 72 h	RT, 24 h [a]	76	34 [d]

[a] Fresh batch of diethylzinc reagent used throughout for this reaction.
[b] Determined using Chiracel OD-H HPLC, 0.5 cm^3 min^{-1} [hexane:propan-2-ol (95:5)] (*R* enantiomer) R_t = 14.8 minutes, (*S* enantiomer) R_t = 16.2 minutes [lit.,[126] Chiracel OD-H HPLC, 0.5 cm^3 min^{-1} [hexane:propan-2-ol (95:5)] (*R* enantiomer) R_t = 15.6 minutes, (*S* enantiomer) R_t = 17.7 minutes].
[c] Determined using Chiracel OD HPLC, 0.6 cm^3 min^{-1} [hexane:propan-2-ol (95:5)] (*R* enantiomer) R_t = 12.6 minutes, (*S* enantiomer) R_t = 13.9 minutes [lit.,[127] Chiracel OD HPLC, 0.5 cm^3 min^{-1} [hexane:ethanol (95:5)] (*R* enantiomer) R_t = 14.2 minutes, (*S* enantiomer) R_t = 16.1 minutes].
[d] Determined using Chiralcel OD HPLC, 0.6 cm^3 min^{-1} [hexane:propan-2-ol (95:5)] (*R* enantiomer) R_t = 18.8 minutes, (*S* enantiomer) R_t = 31.2 minutes [lit.,[128] Chiracel OD HPLC, 1.0 cm^3 min^{-1} [hexane:propan-2-ol (95:5)] (*R* enantiomer) R_t = 16.9 minutes, (*S* enantiomer) R_t = 27.2 minutes].

As discussed in **chapter 1.2.4.4.1** (1*R*,2*S*)-1-phenyl-2(*N*-alkyl)amino-propanol catalytic systems preferentially produce the *R* enantiomer of the secondary alcohol product, whereas amino alcohols with the opposite stereochemistry favour formation of the *S* enantiomer. In accordance with this the 2*S* configuration of the chiral catalyst **288** controlled the asymmetric addition to afford the predicted enantiomerically enriched *R* alcohol products.

Entry 1 (**table 9**) afforded 1-phenyl-1-propanol **70** in poor yield (13%) and low enantiomeric excess (29% *R*). Raising the reaction temperature from 0 °C to room temperature (entry 2) significantly improved the yield (62%) but enantiocontrol remained poor (30% *R*). These results suggested that faster reaction rates and subsequently higher yields of alcohol product are obtained at elevated temperatures. However, the expected decrease in enantiocontrol which often results from uncatalysed addition at increased reaction temperatures producing racemic material was not observed in this case.

Employing a fresh batch of diethylzinc reagent **68** (entry 3) further enhanced the yield (97%) and enantioselectivity (36% *R*) illustrating the significant decrease in activity of the diethylzinc reagent over time. Entry 4 employed slightly different reaction temperatures to generate 1-phenyl-1-propanol **70** in optimum yield (100%) and e.e. (40% *R*) confirming the consistency of the diethylzinc addition to benzaldehyde as catalysed by amino alcohol **288**.

Identical reaction conditions were utilised in the addition of diethylzinc to cinnamaldehyde **285** (entry 5, **table 9**) to afford 1-phenyl-1-penten-3-ol **286** in moderate yield (76%) and enantiomeric excess (34% *R*). Cinnamaldehyde **285** was subsequently found to be a poor substrate for diethylzinc addition as the alcohol product **286** is prone to acid catalysed elimination generating 1-phenyl-1,3-pentadiene which could explain the comparatively low yield of **286** obtained in this final entry.[123]

6.2.2 Diethylzinc Reactions Utilising Amino Alcohol Catalyst 149

Amino alcohol catalyst **149** prepared in **chapter 2.6.1** was employed in the addition of diethylzinc **68** to benzaldehyde **69** using identical experimental conditions to those detailed in entry 4 (**table 9**) affording 1-phenyl-1-propanol **70** (78% yield and 34% e.e. *R*). Similarly, following the procedure outlined in entry 5 (**table 9**) substituting **149** as the amino alcohol catalyst provided 1-phenyl-1-penten-3-ol **286** (30% yield, 12% e.e. *R*), **figure 49**.

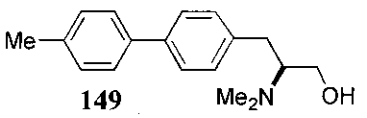

149

Figure 49

These results allowed the performance of catalysts **288** and **149** to be directly compared where the former amino alcohol demonstrated superior activity and selectivity for each of the aldehyde substrates. The reasoning for the poorer levels of asymmetric induction observed on incorporation of the 4-(*p*-tolyl) functionality within the catalyst is unclear. However, it was decided that the analogous vinyl

amino alcohol monomer **161** prepared in **chapter 3.3** would not be polymerised and investigated as a polymer-supported catalyst for the addition of dialkylzinc reagents to aldehydes.

Chapter 2 explored the synthesis of similar *N,N*-dimethylated amino alcohols **150** and **289** where the substitution at the α-position was modified to investigate how increasing the steric bulk of the catalyst affects the enantioselectivity of the dialkylzinc addition reaction, **figure 50**.

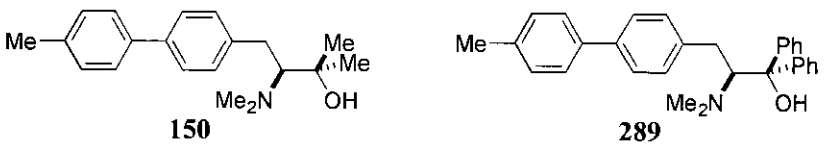

Figure 50

The α-dimethylated amino alcohol **150** was successfully prepared in **chapter 2.6.2** but was ultimately not evaluated as a catalyst for the addition of dialkylzinc reagents to aldehydes as it was found to cyclise to the monomethylated oxazolidine **257** on standing in $CDCl_3$ as discussed in **chapter 5.4**. Unfortunately, the analogous α-diphenyl amino alcohol catalyst **289** was not synthetically viable due to problems incurred in the preparation of the tyrosine triflate Suzuki coupling precursor **117** as detailed in **chapter 2.3.3**.

6.2.3 Diethylzinc Reactions Utilising Amino Alcohol Catalyst 193

Chapter 3 employed an alternative synthetic route in the synthesis of a range of biaryl amino alcohols based on the general template **284** (**figure 47**). Amino alcohol **193** (**chapter 3.9.2**) was initially evaluated as a catalyst for the addition of diethylzinc **68** to benzaldehyde **69** (**scheme 123**) employing an analogous protocol to that described in **method N** of **chapter 8.6**, **figure 51**. The reaction parameters were subsequently modified to optimise both chemical and optical yields of the secondary alcohol product **70** as summarised in **table 10**.

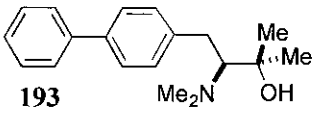

193

Figure 51

Table 10 - Diethylzinc Results Utilising Amino Alcohol Catalyst 193

Entry	Catalyst (mol %)	Temperature / time after addition of benzaldehyde	Temperature / time after addition of further Et_2Zn	yield (%)	e.e. [b] (%)
1	5	0 °C, 112 h	0 °C, 24 h	50	3 *S*
2	2	RT, 92 h	no further Et_2Zn added	41	9 *R*
3	2	RT, 40 h	RT, 72 h [a]	82	6 *R*
4	5	RT, 66 h	RT, 16 h [a]	70	13 *R*

[a] Fresh batch of diethylzinc reagent used throughout for this reaction.
[b] Determined using Chiracel OD-H HPLC, 0.5 cm^3 min^{-1} [hexane:propan-2-ol (95:5)] (*R* enantiomer) R_t = 14.8 minutes, (*S* enantiomer) R_t = 16.2 minutes [lit.,[126] Chiracel OD-H HPLC, 0.5 cm^3 min^{-1} [hexane:propan-2-ol (95:5)] (*R* enantiomer) R_t = 15.6 minutes, (*S* enantiomer) R_t = 17.7 minutes].

Entry 1 provided a spurious result whereby the 2*S* configuration of the chiral catalyst **193** did not afford the predicted enantiomerically enriched *R* alcohol product (50% yield, 3% e.e. *S*). This unexpected inversion of enantioselectivity could be attributed to the instability of catalyst **193** which is known to partially cyclise to the monomethylated oxazolidine **201** which could in turn provide conflicting stereocontrol. This decomposition may become more apparent at 0 °C where the slower reaction rate necessitates a prolonged reaction time, thus explaining why the remaining entries in **table 10** conducted at room temperature furnished the expected enantiomerically enriched *R* alcohol products.

Comparing entries 2 and 3 illustrated that the incorporation of a fresh batch of diethylzinc with a larger number of equivalents improved the yield of isolated 1-phenyl-1-propanol **70** (41% to 82%) but enantiocontrol remained poor (9% *R* versus 6% *R*). Finally, entry 4 increased the catalyst concentration to 5 mol % generating the secondary alcohol **70** in 70% yield and 13% e.e. *R*, allowing the conclusion that catalyst **193** induces consistently poor enantioselectivity.

This result was unexpected as catalyst **193** specifically incorporated bulky α, β and nitrogen substituents to prevent free rotation of the catalyst which is thought to effectively create a rigid catalytic site thus promoting asymmetric alkyl transfer. The concept of analogous sterically hindered polymer-bound β-amino alcohol catalysts providing optimum enantioselectivity in the addition of dialkylzinc reagents to aldehydes was highlighted in **chapter 1.2.4.4.1**.

The poor enantiocontrol exhibited by catalyst **193** combined with its instability with respect to oxazolidine **201** formation which could not be monitored on the solid phase, and the fact that the analogous vinyl amino alcohol monomer **162** (**chapters 3.4** and **3.7**) could not be prepared in high yield, discounted this amino alcohol catalytic system as a candidate for transferral to the solid phase.

6.2.4 Diethylzinc Reactions Utilising Oxazolidine Catalyst 194

Biaryl oxazolidine **194** was introduced as a potential catalyst following a report by Joshi *et al.* where a similar sterically demanding oxazolidine system **169** was employed as a catalyst for the addition of dialkylzinc reagents to aldehydes in the solution phase, **figure 52**.[87] High selectivity was obtained in the oxazolidine **169** catalysed addition of diethylzinc to benzaldehyde affording (*S*)-1-phenyl-1-propanol in 85% yield and 100% e.e.

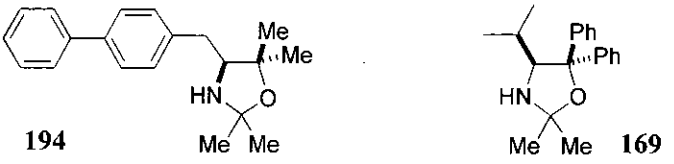

194 **169**

Figure 52

Joshi *et al.* were unable to provide a precise model which explains and predicts the stereochemical outcome of this catalytic system, but postulated that initial reaction of diethylzinc with oxazolidine **169** generates the active zinc amide catalyst. A second molecule of diethylzinc subsequently coordinates to the nitrogen atom of **169** owing to the congested steric environment around the oxygen atom. Coordination and activation of the aldehyde then occurs followed by transfer of an

ethyl group from the diethylzinc as depicted in **figure 53**. Joshi *et al.* recovered the oxazolidine catalyst **169** as its hydrochloride salt in quantitative yield after work-up. The oxazolidine ring was shown to be intact, thus ruling out the possibility that the corresponding imine Schiff base generated by reaction of the hydrolysed primary amino alcohol with benzaldehyde (**chapter 6**) featured as a reactive intermediate.[87]

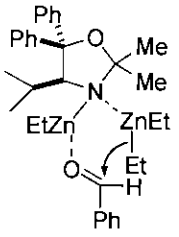

Figure 53

Oxazolidine **194** (**chapter 3.9.3**) was investigated as a catalyst in the addition of diethylzinc **68** to benzaldehyde **69** (**scheme 123**) where the reaction parameters were modified to optimise both chemical and optical yields of the secondary alcohol product **70** as summarised in **table 11**. The employed experimental protocol outlined in **method O** of **chapter 8.6** was derived from the procedures developed by Joshi *et al.*[87] which included initial activation of oxazolidine **194** to the zinc amide catalyst by reaction with diethylzinc **68** at 80 °C for 1 h prior to addition of the benzaldehyde **69**.

Table 11 - Diethylzinc Results Utilising Oxazolidine Catalyst 194

Entry	Catalyst (mol %)	Temperature / time after addition of benzaldehyde	Temperature / time after addition of further Et_2Zn	yield (%)	e.e. [b] (%)
1	5	0 °C, 112 h	0 °C, 24 h	65	20 *R*
2	2	RT, 92 h	no further Et_2Zn added	54	25 *S*
3	2	RT, 40 h	RT, 72 h [a]	86	0
4	5	RT, 66 h	RT, 16 h [a]	100	35 *S*

[a] Fresh batch of diethylzinc reagent used throughout for this reaction.
[b] Determined using Chiracel OD-H HPLC, 0.5 cm^3 min^{-1} [hexane:propan-2-ol (95:5)] (*R* enantiomer) R_t = 14.8 minutes, (*S* enantiomer) R_t = 16.2 minutes [lit.,[126] Chiracel OD-H HPLC, 0.5 cm^3 min^{-1} [hexane:propan-2-ol (95:5)] (*R* enantiomer) R_t = 15.6 minutes, (*S* enantiomer) R_t = 17.7 minutes].

The pattern of results observed in **table 11** followed a similar trend to those previously obtained from utilising the biaryl amino alcohol catalyst **193** (**table 10**).

Entry 1 conducted at 0 °C gave reversal of enantiocontrol to afford 1-phenyl-1-propanol **70** in 65% yield and 20% e.e. *R*, whereas the remaining entries which were carried out at room temperature predominantly provided the predicted *S* alcohol product as determined from the 4*S* stereochemistry of the oxazolidine catalyst **194**. This anomaly could again be attributed to the slower reaction rate and prolonged reaction time at 0 °C causing significant acid hydrolysis of oxazolidine **194** to the biaryl amino alcohol **192** which would favour generation of the *R* alcohol product. Decomposition of oxazolidine **194** was confirmed by washing the polar material from the column using DCM:MeOH (90:10) where ^{1}H NMR analysis of the eluted residue gave only two *Me* signals consistent with those expected for biaryl amino alcohol **192**.

Comparing entries 2 and 3 illustrated that the incorporation of a fresh batch of diethylzinc with a larger number of equivalents improved the yield of isolated 1-phenyl-1-propanol **70** (54% to 86%) but all enantiocontrol was lost (25% *S* versus 0%). Finally, entry 4 increased the catalyst concentration to 5 mol % generating the secondary alcohol **70** in quantitative yield and 35% e.e. *S* concluding that the selectivity induced by catalyst **194** is capricious.

Ultimately the instability of the oxazolidine functionality with respect to acid hydrolysis was a major factor in determining that the analogous vinyl oxazolidine monomer **168** (**chapter 3.8**) was not an ideal substrate for polymerisation. If hydrolysis were to occur during the dialkylzinc addition reaction the resultant oxazolidine and amino alcohol polymer-bound residues would provide conflicting catalytic activity to afford the *S* and *R* alcohol products respectively.

6.2.5 Diethylzinc Reactions Utilising Amino Alcohol Catalyst 192

Biaryl amino alcohol **192** (**chapter 3.9.1**) was finally evaluated as a catalyst for the addition of diethylzinc **68** to benzaldehyde **69** and cinnamaldehyde **285** (**scheme 123**), **figure 54**.

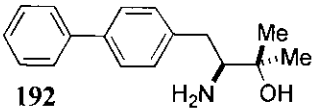

Figure 54

Unaware of the publication by Itsuno *et al.*[35e] regarding the mechanism postulated for the primary amino alcohol catalysed addition of dialkylzinc reagents to aldehydes (**chapter 6**), the order of addition of the diethylzinc **68** and benzaldehyde **69** to catalyst **192** was not reversed within this series of experiments.

As such an analogous protocol to that described in **method N** of **chapter 8.6** was undertaken incorporating a fresh batch of diethylzinc reagent **68** unless otherwise stated. The reaction parameters were subsequently investigated including the toluene and argon source in an attempt to optimise both chemical and optical yields of the secondary alcohol products **70** and **286** as summarised in **table 12**.

Table 12 - Diethylzinc Results Utilising Amino Alcohol Catalyst 192

Entry	Catalyst (mol %)	Aldehyde substrate	Temperature / time after addition of aldehyde	Temperature / time after addition of further Et_2Zn	yield (%)	e.e. *R* (%)
1	2	**69**	RT, 40 h	RT, 72 h	82	15 [c]
2	5	**69**	RT, 66 h	RT, 16 h	77	50 [c]
3	5	**69**	RT, 65 h	RT, 22 h	99	13 [c]
4	5	**69**	RT, 64 h	RT, 24 h [b]	46	7 [c]
5	5 [a]	**69**	RT, 64 h	RT, 24 h [b]	73	4 [c]
6	5	**285**	RT, 65 h	RT, 22 h	90	1 [d]

[a] Anhydrous toluene supplied by Aldrich employed.
[b] Previously unopened bottle of diethylzinc reagent used with the reaction being conducted under an argon balloon in contrast to a continuous flow of argon.
[c] Determined using Chiracel OD-H HPLC, 0.5 cm^3 min^{-1} [hexane:propan-2-ol (95:5)] (*R* enantiomer) R_t = 14.8 minutes, (*S* enantiomer) R_t = 16.2 minutes [lit.,[126] Chiracel OD-H HPLC, 0.5 cm^3 min^{-1} [hexane:propan-2-ol (95:5)] (*R* enantiomer) R_t = 15.6 minutes, (*S* enantiomer) R_t = 17.7 minutes].
[d] Determined using Chiracel OD-H HPLC, 0.5 cm^3 min^{-1} [hexane:propan-2-ol (95:5)] (*R* enantiomer) R_t = 20.5 minutes, (*S* enantiomer) R_t = 32.6 minutes [lit.,[129] Chiracel OD-H HPLC, 1.0 cm^3 min^{-1} [hexane:propan-2-ol (95:5)] (*R* enantiomer) R_t = 14.0 minutes, (*S* enantiomer) R_t = 23.0 minutes].

In each case the 2*S* configuration of the chiral amino alcohol catalyst **192** effectively controlled the asymmetric addition reactions to consistently afford the predicted enantiomerically enriched *R* alcohol products.

Comparing entries 1 and 2 revealed that increasing the catalyst concentration from 2 mol % to 5 mol % afforded the 1-phenyl-1-propanol product **70** with greater selectivity (15% e.e. *R* versus 50% e.e. *R*) although a slight drop in overall yield was observed (82% to 77%).

Entry 3 was conducted as a direct repeat of entry 2 but unfortunately the latter optimum result could not be reproduced and **70** was obtained in 99% yield and 13% e.e. *R*. Repeating entry 2 using a previously unopened bottle of diethylzinc reagent where the reaction mixture was maintained under an argon balloon (in contrast to a continuous flow of argon) to minimise the moisture absorbed from the argon supply (entry 4) significantly reduced both yield (46%) and enantiocontrol (7% e.e. *R*). Similarly, entry 5 which essentially repeated entry 4 incorporating anhydrous toluene from Aldrich (in contrast to toluene distilled from calcium hydride immediately prior to use) provided **70** in 73% yield and 4% e.e. *R*.

Identical reaction conditions to those detailed in entry 2 were utilised in the addition of diethylzinc to cinnamaldehyde **285** (entry 6, **table 12**) to afford 1-phenyl-1-penten-3-ol **286** in excellent yield (90%) but the material was racemic (1% *R*).

Entries 1-6 highlight the capricious nature of the diethylzinc addition reaction as catalysed by amino alcohol **192** where minor changes in experimental procedure created vast variations in the yields and enantioselectivities of the resultant secondary alcohol products. However, at this stage in the research the 50% enantiomeric excess obtained in entry 2 represented the greatest level of asymmetric induction observed for the solution phase diethylzinc addition reactions. In addition, catalyst **192** exhibited consistent enantiocontrol to afford the *R* alcohol products and appeared to be a stable amino alcohol substrate.[Ψ]

[Ψ] Recovery of catalyst **192** by chromatography of the crude product mixtures or by extraction of the amino alcohol **192** as its hydrochloride salt proved unsuccessful but this could partially be attributed to the small quantities of catalyst employed in the diethylzinc addition reactions.

As such the reproducibility problem was disregarded and the analogous vinyl amino alcohol monomer **167** (**chapter 3.6**) was polymerised (**chapter 4.5.3**) and evaluated as a polymer-bound diethylzinc addition catalyst as discussed in **chapter 6.3**.

6.3 Diethylzinc Reactions Utilising Polymer-Bound Amino Alcohol Catalyst 217

The final series of diethylzinc **68** addition reactions to benzaldehyde **69** and cinnamaldehyde **285** (**scheme 123**) were catalysed by the gel-type chiral polymer-bound amino alcohol **217** (**chapter 4.5.3**), **figure 55**.

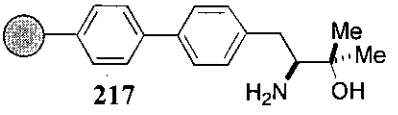

Figure 55

A range of polymer-supported chiral amino alcohols have been investigated as catalysts for the enantioselective addition of dialkylzinc reagents to aldehydes as detailed in **chapter 1.2.4.4.1**. The literature reports highlight the significant variation in enantioselectivity obtained by altering the reaction parameters where the main points are summarised below:

i) The reaction solvent must extensively swell the polymer matrix to allow easy access of the reactants to the catalytic sites where toluene and hexane are commonly utilised as non-polar solvents.[35a]

ii) The polymeric catalyst is typically employed between 3-10 mol %.

iii) The enantiomeric excess of the secondary alcohol product strongly depends on the substrate ratio employed where an excess of the dialkylzinc reagent in relation to the aldehyde provides optimum enantioselectivity.[35d]

iv) As observed for the solution phase reactions, enantioselectivity increases as the reaction temperature is lowered due to the elimination of uncatalysed addition.[35e]

In view of these criteria the asymmetric alkylations were initially conducted in toluene which visually provided maximum swelling of gel-type resin **217**. The catalyst concentration was varied from 5-20 mol % as determined from the loading of resin **217**, and 4.0 equivalents of diethylzinc **68** were used. The small scale reactions were carried out in sintered plastic filtration tubes which allowed simple separation of the soluble chiral products from the resin catalyst **217** by applying a positive pressure of argon. However, as conventional magnetic stirrers cause mechanical breakdown of the polymer beads to produce unusable fines, a horizontal shaker was utilised to ensure mixing, which in turn prevented cooling of the reaction mixtures and as such the experiments were conducted at room temperature.

The general experimental procedure outlined in **method P** of **chapter 8.6** was adapted from literature protocol with initial mixing of the toluene swollen resin **217** and aldehyde at 0 °C followed by addition of diethylzinc **68** and subsequent agitation of the reaction mixture at room temperature over 90 h.

Premixing the polymer-bound amino alcohol **217** with the aldehyde **263** prior to addition of the diethylzinc could potentially aid generation of the supported imine Schiff base **290** which has been shown to enhance the enantiocontrol and consistency obtained in the asymmetric alkylation reactions,[35e] **scheme 126**.

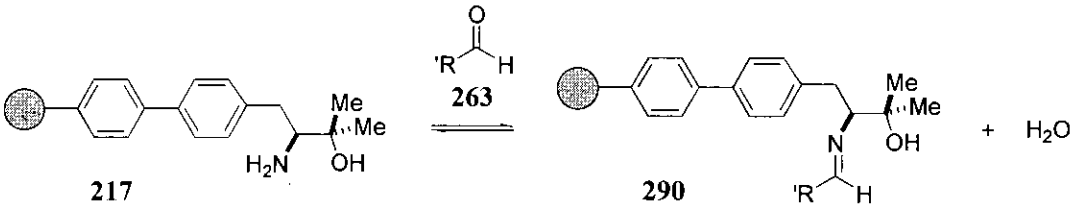

Scheme 126

A summary of the results obtained using the polymer-bound amino alcohol catalyst **217** is depicted in **table 13**.

Table 13 - Diethylzinc Results Utilising Polymer-Bound Amino Alcohol Catalyst 217

Entry	Catalyst (mol %)	Aldehyde substrate	yield (%)	e.e. *S* (%)
1	5	**69**	13	13 [c]
2	10	**69**	72	56 [c]
3	10	**69**	18	52 [c]
4	20	**69**	9	45 [c]
5	10 [a]	**69**	38	20 [c]
6	10 [b]	**69**	80	51 [c]
7	10	**285**	100	45 [d]

[a] Recycled polymer-bound amino alcohol catalyst used for this reaction.
[b] Hexane used as the solvent for this reaction.
[c] Determined using Chiracel OD-H HPLC, 0.5 cm^3 min^{-1} [hexane:propan-2-ol (95:5)] (*R* enantiomer) R_t = 13.6 minutes, (*S* enantiomer) R_t = 14.8 minutes [lit.,[126] Chiracel OD-H HPLC, 0.5 cm^3 min^{-1} [hexane:propan-2-ol (95:5)] (*R* enantiomer) R_t = 15.6 minutes, (*S* enantiomer) R_t = 17.7 minutes].
[d] Determined using Chiracel OD-H HPLC, 0.5 cm^3 min^{-1} [hexane:propan-2-ol (95:5)] (*R* enantiomer) R_t = 22.0 minutes, (*S* enantiomer) R_t = 35.5 minutes [lit.,[129] Chiracel OD-H HPLC, 1.0 cm^3 min^{-1} [hexane:propan-2-ol (95:5)] (*R* enantiomer) R_t = 14.0 minutes, (*S* enantiomer) R_t = 23.0 minutes].

The most striking feature apparent from **table 13** is that the polymeric catalyst **217** generated the *S* enantiomerically enriched alcohol products, whereas the analogous free biaryl amino alcohol catalyst **192** exhibited opposite stereocontrol, thus indicating that the polymer environment surrounding the catalytic sites affected selectivity.

Entry 1 employed 5 mol % of the polymeric catalyst **217** to afford 1-phenyl-1-propanol **70** in 13% yield and 13% e.e. *S*. The resin was subjected to the aqueous acid, aqueous base and solvent washing procedures described by Soai *et al.*[34b] which afforded 95% recovery of the resin with minimal loss of material on transfer. Elemental analysis determined the loading of the recovered resin to be 0.48 $mmolg^{-1}$ which was identical to that of the resin employed in the reaction. Similarly, infra-red analysis provided virtually identical stretching frequencies to those of the original amino alcohol resin, thus confirming the stability of the resin support and the amino alcohol functionality to the reaction conditions.

Entry 2 doubled the catalyst concentration to 10 mol % which dramatically improved the yield (72%) and enantiomeric excess (56% *S*) of the alcohol product **70**, see **appendix** for chiral HPLC trace. An identical repeat of this experiment (entry 3) afforded similar enantiocontrol (52% *S*) but the yield was greatly diminished (18%). Further increasing the catalyst concentration to 20 mol % (entry 4) failed to enhance the yield of **70** (9%) although consistently good selectivity was obtained (45% *S*).

Overall entries 2-4 illustrated that 10-20 mol % of polymeric catalyst **217** provided consistent enantiocontrol (45-56% *S*) in the alkylation of benzaldehyde **69** with diethylzinc **68** although the yields were extremely varied and unoptimised (9-72%).

Entry 5 utilised the recycled polymeric catalyst from entry 1 where the poor yield (38%) and enantiomeric excess (20% *S*) of the addition product **70** could be attributed to inadequate drying of the recovered resin resulting in some quenching of the diethylzinc reagent **68**. Unfortunately, time restraints did not permit further investigation into the recycling potential of polymer-bound amino alcohol catalyst **217**.

Entry 6 employed hexane as the solvent medium which did not affect the chemical yield (80%) or optical yield (51% *S*) of the 1-phenyl-1-propanol **70** product as compared to entry 2 where the reaction was conducted in toluene. This result was unexpected as it was postulated that the lower swelling capacity of the resin in hexane would limit the diffusion of the diethylzinc and aldehyde reagents within the polymer matrix, thus reducing their accessibility to the catalytic sites. This would in turn promote slow uncatalysed alkylation to reduce the overall stereochemical performance of the supported catalyst.

The similar activity of the polymer-bound catalyst **217** observed in toluene (entry 2, **table 13**) and hexane (entry 6, **table 13**) could be attributed to the enhanced mobility of the polymer chains in toluene allowing formation of the homochiral zincoxazine dimer **291** upon addition of diethylzinc, **figure 56 (chapter 6.1)**. If

these site-site interactions were sufficient to serve as cross-links, the overall diffusion of reagents within the polymer could ultimately be comparable to that of the resin swollen in hexane.

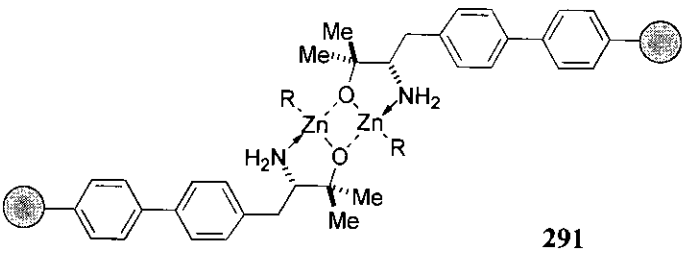

291

Figure 56

Finally, entry 7 details the polymer-bound amino alcohol **217** catalysed addition of diethylzinc **68** to cinnamaldehyde **285** which furnished 1-phenyl-1-penten-3-ol **286** in quantitative yield and 45% e.e. *S* indicating the potential versatility of the polymeric catalyst, see **appendix** for chiral HPLC trace.

6.4 Summary of Chapter 6

Chapter 6 evaluated the activity and selectivity imparted by chiral oxazolidine **194** and a range of model chiral amino alcohols **288**, **149**, **193** and **192** as solution phase catalysts in the asymmetric addition of dialkylzinc reagents to aldehydes. The reaction parameters were modified by variation of the reaction temperature, stoichiometry and source of reagents to obtain consistent results where the stability of the catalyst substrates to the reaction conditions were also investigated.

The optimum catalytic system was subsequently identified as **192** which offered stability and the greatest levels of asymmetric induction (up to 50% e.e.) to consistently afford the enantiomerically enriched *R* secondary alcohol products.

The optimised substitution pattern of the amino alcohol functionality within **192** was replicated in the parent vinyl amino alcohol monomer **167** where polymerisation afforded the gel-type chiral polymer-bound amino alcohol **217** (**chapter 4.5.3**). The functionalised chiral polymer **217** was employed as a catalyst

for the enantioselective addition of dialkylzinc reagents to aldehydes and was found to consistently provide the enantiomerically enriched *S* secondary alcohol products (up to 56% e.e.). The robust polymeric catalyst **217** was effectively recovered intact although time restraints did not permit thorough investigation into the recycling potential of the polymer-bound catalyst **217**.

This development process also explored the extent to which catalyst reactivity and enantioselectivity were affected by introducing the biaryl unit and subsequently binding the amino alcohol to the solid support.

Future work would encompass optimisation of the reaction conditions to attain consistently high chemical and optical yields of the chiral secondary alcohol products. Modifications to the reaction parameters would incorporate a thorough investigation of the effect of reaction temperature and solvent medium on the selectivity of the solid phase asymmetric alkylation reactions. In addition, further evaluation of the recycling potential of the supported catalyst **217** is required and the influence of polymer bead size (100-500 micron versus >500 micron particle size) on the reactivity of the supported dialkylzinc addition catalyst could also be assessed.

Finally, the range of aldehyde substrates could be extended to include aliphatic aldehydes and the polymer-bound amino alcohol **217** could also be employed as a catalyst in the addition of dialkylzinc reagents to complex aldehydes in the synthesis of enantiopure natural product target compounds.

Chapter 7 : Results and Discussion Part 6

Chiral Oxazolidin-2-one Auxiliaries in Asymmetric Synthesis

The highly versatile chiral oxazolidin-2-one auxiliaries **292** and **293** derived from commercially available (*S*)-valinol and (1*S*,2*R*)-norephedrine respectively have been widely used in asymmetric synthesis for controlling a variety of reactions of acyl synthons, **figure 57**.[18] The pioneering methodology developed by Evans *et al.* illustrated that the boron-enolate of an *N*-acylated chiral oxazolidinone can be condensed with aldehydes to obtain high levels of stereocontrol.[18a] Similarly, incorporating lithium-enolate chemistry the *N*-acylated chiral oxazolidinone undergoes enantioselective alkylation with alkyl halides where non-destructive cleavage of the transformed acyl fragment allows recovery of the auxiliary.[18b]

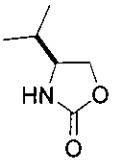

292

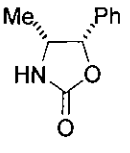

293

Figure 57

7.1 Control of Enolate Geometry

The *N*-propionylated oxazolidinone can exist in two possible conformations **294** and **295** as illustrated in **scheme 127**. The aldol reaction proceeds *via* reaction of the *N*-acylated auxiliary with a dialkylboron reagent in the presence of a weak tertiary amine base where the boron Lewis acid coordinates to the carbonyl acyl group activating the α proton toward removal with the weak base. In a similar manner the metal-enolate which forms an integral part of the alkylation reaction is generated by treatment of the *N*-acylated auxiliary with a metal amide base. In each case deprotonation is highly stereoselective to afford the corresponding *Z*-enolates **296** and **297** where the latter conformation is stabilised by chelation of the metal counter ion, **scheme 127**.

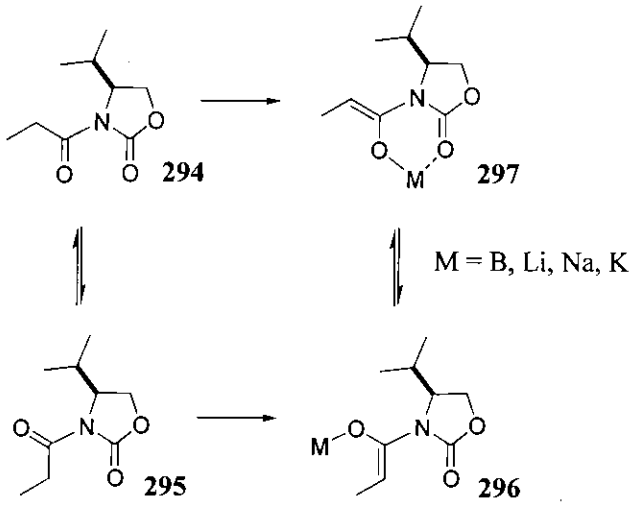

Scheme 127

The enolate geometry is governed by electronic and steric factors as depicted in **scheme 128**. Deprotonation is favoured when the C-H bond which is broken is orthogonal to the plane of the carbonyl acyl group as this conformation creates an overlap between the $\sigma_{C\text{-}H}$ HOMO orbital and the $\pi^*_{C=O}$ LUMO orbital which favours formation of the new enolate π bond. Furthermore, under kinetic control the steric interactions between the large auxiliary (R) and the methyl group of the acyl chain are minimised in the transition state thus exclusively providing the *Z*-enolate.

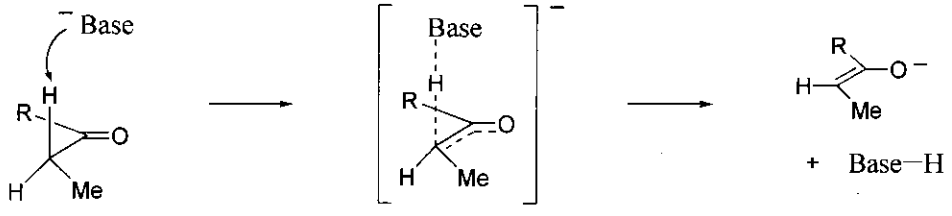

Scheme 128

7.1.1 Asymmetric Aldol Reaction

The asymmetric aldol reaction proceeds *via* the boron-enolate **298** which is typically formed by reaction of the *N*-acylated auxiliary with dibutylboron triflate and triethylamine as previously described. As boron possesses a maximum coordination number of four, the B-O chelation is broken to allow coordination and activation of the aldehyde (RCHO) affording **299**. The chiral auxiliary is now free to adjust its

conformation and rotates through 180° to minimise electronic and steric repulsions providing **300**. Transition state **300** is favoured over **299** as the dipole-dipole repulsion between the oxygen atom of the enolate and the oxygen atom of the chiral auxiliary is minimised, **scheme 129**.

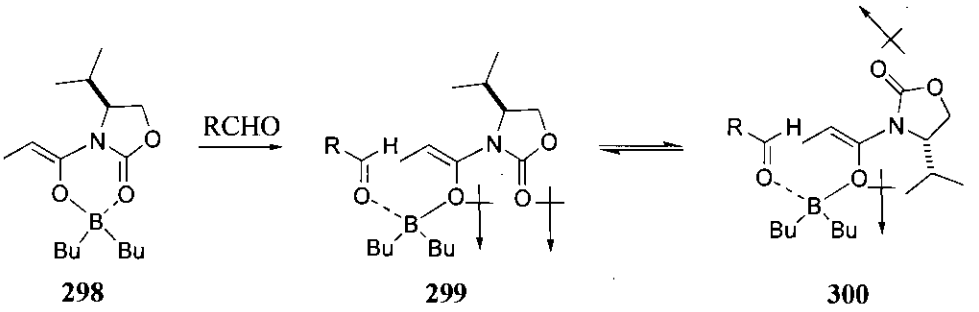

Scheme 129

The reaction proceeds *via* a cyclic six-membered Zimmerman-Traxler type transition state in which the lower face of the enolate attacks the aldehyde due to the steric crowding of the upper face resulting from the isopropyl C-4 substituent of the auxiliary, **figure 58**. Within the favoured model **300** (**scheme 129**) the alkyl group of the aldehyde (R) adopts a pseudo equatorial position as depicted in model **301** thus minimising 1,3-diaxial interactions which are clearly evident in the disfavoured transition state model **302**, **figure 58**.

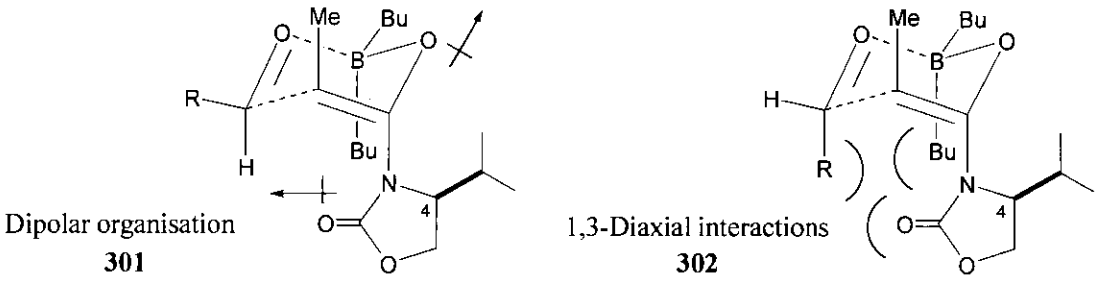

Figure 58

Reaction of the *Z*-boron enolate with the achiral aldehyde RCHO proceeds almost exclusively *via* model **301** to provide the 2',3'-*syn* (Evans *syn*) diastereomer of the aldol adduct **303**. Exceptional levels of stereochemical control can be obtained to virtually exclude generation of the non-Evans *syn* diastereomeric adduct **304** which results from model **302**, **figure 59**.

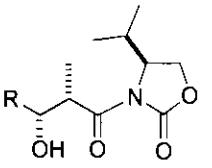

303

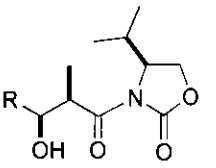

304

Figure 59

7.1.2 Asymmetric Alkylation Reaction

The asymmetric alkylation reaction proceeds *via* the lithium-enolate **305** which is typically formed by deprotonation of the *N*-acylated auxiliary with a lithium amide base as previously described. Chelation effectively holds the enolate with respect to the chiral oxazolidinone such that reaction of the enolate with an alkyl halide (RX) is strongly directed by the C-4 stereochemistry of the auxiliary. In this instance, the upper face of **305** is blocked by the isopropyl group at C-4 inducing high levels of diastereoselectivity with alkylation directed to the lower face affording **306, scheme 130**. Therefore using the same oxazolidinone auxiliary, the chirality induced at C-2' in an alkylation reaction is opposite to that in the aldol reaction of the boron-enolate.

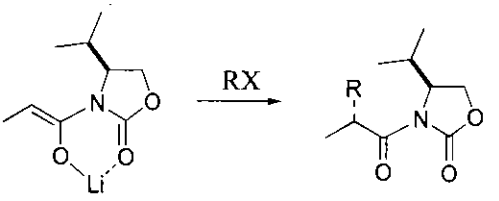

305 306

Scheme 130

The transformed acyl fragment can subsequently be removed under a variety of reaction conditions, for example, hydrolysis ($LiOH$[130] or $LiOOH$[98]), reduction ($NaBH_4$),[22] transesterification ($LiOBn$[18b]) or transamination ($Me_2AlN(OR)R$)[131] allowing the chiral auxiliary to potentially be recovered and re-used.

7.2 "Quat" and "SuperQuat" Auxiliaries

The Evans oxazolidinone auxiliaries **292** and **293** (**figure 57**) can readily be prepared in high yield and optical purity and are stable under enolisation conditions inducing excellent diastereofacial selectivity for a range of asymmetric reactions. However, problematic removal of the transformed acyl fragment under hydrolytic conditions often compromises recovery and recycling of the auxiliary.

The position of nucleophilic cleavage in the *N*-acylated oxazolidinone **307**, for example, is dependant upon steric and electronic requirements. If the acyl derivative is unhindered, nucleophilic cleavage is subject to electronic factors and exocyclic cleavage occurs to provide the required cleaved product **308**, thus regenerating the auxiliary **292**. However, when the R group is large or α-branched, steric factors render the unwanted endocyclic cleavage of the oxazolidinone ring more favourable to afford **309**, **scheme 131**. This undesirable cleavage pathway reduces the yield of cleaved product and limits the recycling capability of the auxiliary.

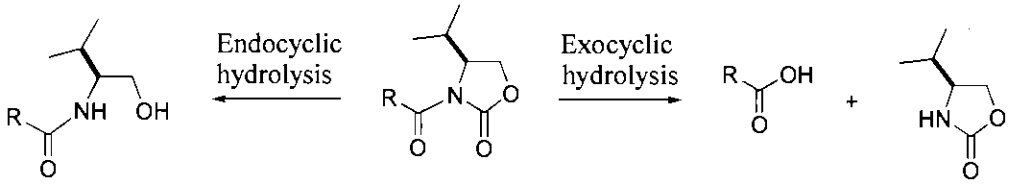

309 **307** **308** **292**

Scheme 131

While the problem of endocyclic cleavage may be overcome by deploying the more nucleophilic hydroperoxide species for hydrolysis which is less susceptible to steric hindrance,[98] the use of this reagent on a large scale may prove hazardous.

Davies *et al.* postulated that a large increase in steric bulk adjacent to the endocyclic carbonyl would favour exocyclic cleavage and subsequently prepared a range of chiral 5-substituted-3,3-dimethyl-2-pyrrolidinone auxiliaries **310** termed "Quat" auxiliaries to explore this concept, **figure 60**.[132a]

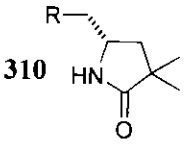

R = $OSiMe_2tBu$, $OCPh_3$, H, Me

Figure 60

Treatment of the corresponding hindered *N*-pivaloyl auxiliaries with lithium hydroxide furnished the "Quat" auxiliaries **310** in excellent yields where no endocyclic cleaved material was observed. The *N*-propionyl derived "Quat" auxiliary **310** (R = H, **figure 60**) was subsequently found to undergo highly stereoselective aldol and alkylation reactions where removal of the auxiliary from the elaborated substrate under a range of conditions proceeded exclusively in an exocyclic manner.[132b]

Ezquerra *et al.* investigated the synthetic utility of the related chiral 4,4-dimethyl pyroglutamate **311** as a "Quat" auxiliary in the asymmetric aldol reaction, **figure 61**. High levels of stereochemical control were obtained where hydrolysis of the aldol adducts allowed recovery of the "Quat" auxiliary **311** with no epimerisation of the pyroglutamate stereogenic centre.[132c] These early reports established that introduction of the geminal dimethyl group adjacent to the ring carbonyl effectively eliminated unwanted endocyclic cleavage.

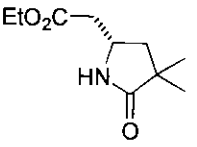

311

Figure 61

Davies *et al.* also developed a series of novel 4-substituted-5,5-dimethyl oxazolidinone auxiliaries termed the "SuperQuat" auxiliaries **205** which incorporated a geminal dimethyl group at the C-5 position, **figure 62**.[97]

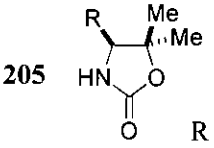

R = Me, Ph, CH_2Ph, *i*Pr

Figure 62

The "SuperQuats" **205** were demonstrated to be effective chiral auxiliaries for stereoselective enolate alkylation and conjugate addition reactions of attached *N*-acyl moieties where the geminal dimethyl group suppressed endocyclic cleavage of the addition products allowing the auxiliaries **205** to be recycled.

Within this series of "SuperQuat" auxiliaries **205** (**figure 62**) the highest yields and diastereoselectivities were obtained when the sterically demanding 4-isopropyl substituent (R = *i*Pr) was incorporated at the C-4 position. Molecular modelling of the corresponding enolate geometry revealed a transition state in accordance with the original mechanism proposed for the Evans auxiliary as detailed in **chapter 7.1.2**. The presence of the geminal dimethyl group at C-5 was shown to be crucial in effectively direct the stereocontrolling isopropyl group at C-4 close to the point of enolate alkylation at C-2' as depicted in **figure 63**, thus increasing stereofacial bias towards incoming electrophiles.[133]

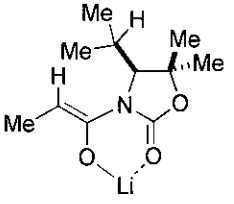

Figure 63

The opposite *R* enantiomer of the 4-phenyl oxazolidinone **205** (R = Ph, **figure 62**) was also employed as an auxiliary to perform highly diastereoselective conjugate addition reactions. This methodology was applied to the asymmetric synthesis of the antifungal (-)-aplysillamide B.[134] The fundamental advantage of the "SuperQuat" auxiliaries **205** (**figure 62**) over the original "Quat" auxiliaries **310** (**figure 60**) resulted from their synthetic accessibility from readily available α-amino acids.[89]

7.3 Polymer-Supported Oxazolidinone Auxiliaries

Few researchers have explored the synthetic utility and potential of attaching chiral oxazolidinone auxiliaries to the solid phase. Examples of asymmetric transformations conducted on the solid phase employing polymer-supported chiral auxiliaries include stereoselective alkylation,[19a, 19b] aldol,[19c, 19d] conjugate addition,[19d] Diels-Alder[19e] and 1,3-dipolar cycloaddition[19f] reactions as discussed in **chapter 1.2.3.3**. The advantages of this approach clearly include simplification of work-up and purification procedures as the polymer-bound auxiliary can be removed from the reaction mixture and potentially recycled. The applications within combinatorial synthesis are also far reaching as the nature of the acyl group, electrophile and cleavage conditions can each be varied to generate vast libraries of compounds.

The gel-type polymer-supported "SuperQuat" chiral oxazolidinone **218** was prepared *via* polymerisation of the parent vinyl monomer **204** as detailed in **chapter 4.5.2, figure 64**.

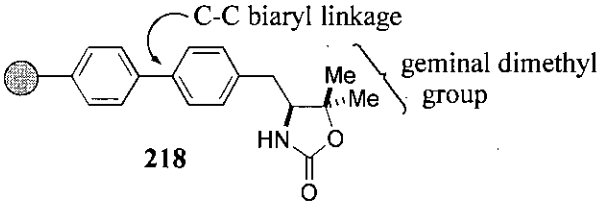

218

Figure 64

It was postulated that the all-carbon backbone would offer increased stability to the system whilst at the same time making it less prone to degradation allowing the resin to be recovered and recycled. The rigid biaryl unit was also incorporated to create a spacer unit between the active site of the auxiliary and the polystyrene, thus reducing steric repulsion to allow a faster rate of reaction.

Another highlighted design feature includes the geminal dimethyl group at the C-5 position as the analogous "SuperQuat" auxiliaries **205** (**figure 62**) employed in the solution phase provided high diastereofacial control exhibiting no endocyclic cleavage of the transformed acyl fragments.

Overall, it was postulated that adaptation of the new family of "SuperQuat" chiral oxazolidinone based auxiliaries to the solid phase would provide a robust auxiliary with enhanced recyclability. The ability to re-use the polymer-bound auxiliary would represent a significant advance within this field of research as only one report to date documents the recycling of a supported oxazolidinone system.[19f]

7.4 "SuperQuat" Oxazolidinone Auxiliary 207

Initial studies focused on the activity and selectivity imparted by the biaryl "SuperQuat" chiral oxazolidinone auxiliary **207** which was prepared and subsequently *N*-propionylated to afford **208** as described in **chapter 3.10.3**, **figure 65**.

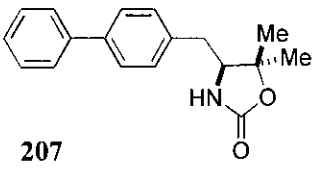

207

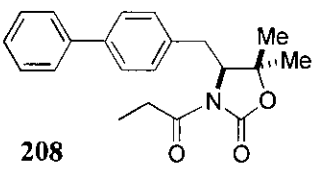

208

Figure 65

Evaluation of **207** as a model auxiliary allowed investigation of the asymmetric aldol and alkylation reactions in the solution phase. The optimised conditions which afforded the cleaved products in optimum chemical and optical yield were then transferred to the solid phase. In addition, infra-red data obtained for **207**, **208** and the alkylated / aldol adducts were used for comparison with the polymer-bound analogues which facilitated the often problematic monitoring of these transformations on the resin. Furthermore, this development process established the extent to which the asymmetric induction imparted by the chiral "SuperQuat" oxazolidinone was affected by attaching the auxiliary to the solid support.

7.4.1 Asymmetric Aldol Reaction Utilising Auxiliary 207

Results published by Heathcock *et al.* illustrated that employing an excess of the dibutylboron triflate Lewis acid results in generation of the *anti* aldol adduct *via*

an open transition state.[135] As such enolisation of the *N*-propionyl oxazolidinone **208** was effected under standard Evans *syn* aldol conditions by reaction with dibutylboron triflate (1.1 equivalents) and triethylamine (1.2 equivalents) where red colouration of the reaction mixture suggested successful formation of the boron-enolate which possesses extended conjugation, **scheme 132**.

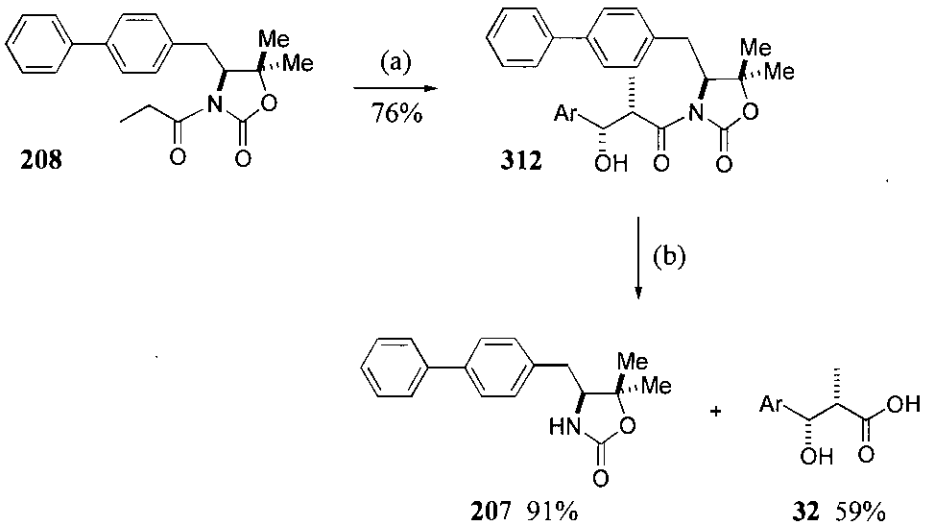

(a) (i) Bu_2BOTf, Et_3N, DCM, 0 °C→-78 °C; (ii) ArCHO, DCM, -78 °C→-25 °C; (iii) pH 7 phosphate buffer, MeOH, H_2O_2, RT; (b) $LiOH{\bullet}H_2O$, H_2O, THF, RT.

Scheme 132

Reaction of the freshly prepared enolate with benzaldehyde discharged the red colouration indicating effective aldol condensation of the two components. The reaction mixture was subsequently quenched with hydrogen peroxide in the presence of phosphate buffer to hydrolyse any complexed boron residues, and chromatographed to afford the aldol adduct **312** in good yield (76%), **scheme 132**.

Analysis of the product material by ^1H NMR indicated the presence of only one diastereomeric product, thus representing a d.e. ≥ 98%. The expected *syn* relative stereochemistry of the aldol adduct **312** was confirmed on the basis of the 4.9 Hz coupling constant measured for H2'-H3'.[Ψ]

[Ψ] In solution β-hydroxy ketones exist in a chair-like conformation due to intramolecular hydrogen bonding. The bulky substituent adopts the favoured equatorial position and the dihedral angle between α and β protons is ~60° for the *syn* arrangement and ~180° for the *anti* arrangement. As a result, the Karplus relationship predicts vicinal coupling constants to be ~3-5 Hz for *syn* and ~7-12 Hz for the *anti* aldol adducts.

The absolute stereochemistry of the two new chiral centres within the aldol adduct **312** were assigned after hydrolytic cleavage of the transformed acyl fragment from the chiral auxiliary. This was effected by exposure of the adduct **312** to lithium hydroxide which afforded the β-hydroxy acid **32** (59%) with good recovery of the chiral auxiliary **207** (91%), **scheme 132**. The moderate yield of acid **32** obtained could be attributed to incomplete base extraction and subsequent back extraction of the acidified aqueous layer into DCM, where the isolation procedure was further hindered by the small scale of the cleavage reaction.

^{1}H NMR analysis of **32** reinforced the exclusive presence of the expected *syn* diastereomer ($J_{H2'\text{-}H3'}$ 3.8 Hz).[136] Comparison of the measured optical rotation of the cleaved β-hydroxy acid **32** $[\alpha]_D$ -33.3 (*c* 0.5, $CHCl_3$), with the literature value[137] for (2*R*,3*R*)-**32** $[\alpha]_D$ +31.0 (*c* 1.1, $CHCl_3$) established the absolute configuration as the expected (2*S*,3*S*) diastereomer.

In summary, the boron-enolate of the conformationally constrained chiral *N*-propionyl "SuperQuat" oxazolidinone **208** underwent efficient aldol condensation with benzaldehyde to furnish the expected *syn* aldol adduct **312** (76%) with excellent diastereofacial selectivity (d.e. ≥ 98%). Exclusive exocyclic hydrolytic cleavage afforded (2*S*,3*S*) β-hydroxy acid **32** as a single diastereomer (59%) allowing recovery of the intact auxiliary **207** (91%).

7.4.2 Asymmetric Alkylation Reaction Utilising Auxiliary 207

Enolisation and subsequent alkylation of the *N*-propionyl auxiliary **208** was primarily attempted employing the reaction conditions reported by Davies *et al.* for the asymmetric alkylation of analogous "SuperQuat" auxiliaries **205** (**figure 62**).[133] Thus, **208** in THF was initially deprotonated with lithium bis(trimethylsilyl)amide (LiHMDS) (1.1 equivalents) at -78 °C, followed by addition of benzyl bromide (3.0 equivalents) where the reaction mixture was allowed to warm to room temperature over a 22 h period. Chromatographic purification of the crude product material [gradient elution hexane:EtOAc (90:10 to 80:20) followed by DCM] afforded

unreacted *N*-acyl oxazolidinone **208** (26%), desired α-benzylated product **313** (5%), auxiliary **207** (36%) and *N*-benzylated auxiliary **314** (40%) as depicted in **scheme 133**.[ξ]

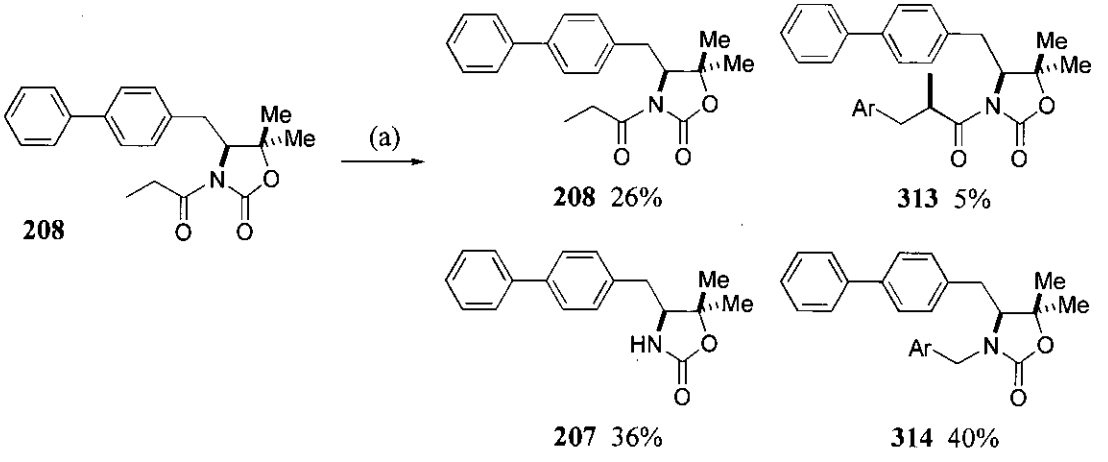

(a) (i) LiHMDS (1.1 equivalents), THF, -78 °C; (ii) $PhCH_2Br$ (3.0 equivalents), -78 °C→RT (22 h).

Scheme 133

Davies *et al.* isolated the analogous series of compounds **315**, **316**, **317** and **318** from treatment of the model achiral *N*-propionyl 5,5-dimethyl "SuperQuat" auxiliary **315** with LiHMDS and benzyl bromide, **scheme 134**.[133]

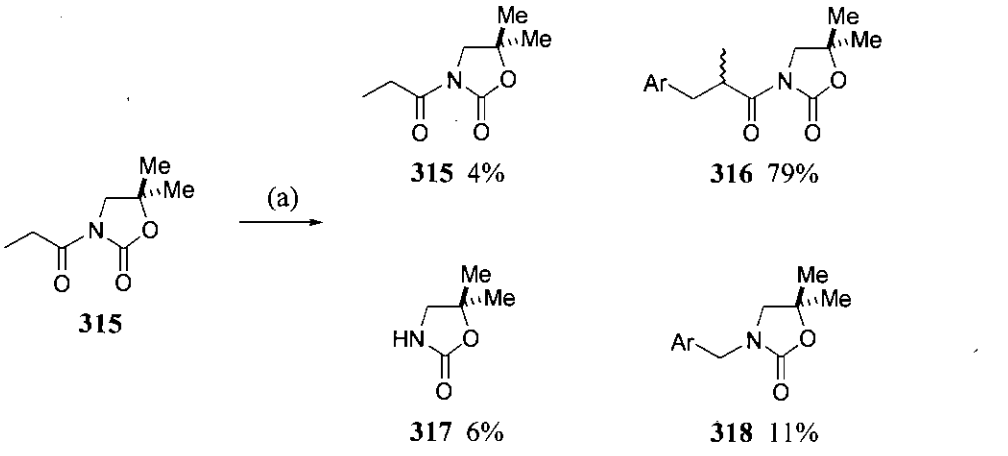

(a) (i) LiHMDS (1.1 equivalents), THF, -78 °C; (ii) $PhCH_2Br$ (3.0 equivalents), -78 °C→RT (22 h).

Scheme 134

[ξ] > 100% recovery of material was attributed to traces of solvent remaining within the various component fractions where the stereochemistry of the α-benzylated product was assumed to be **313** although this could not be accurately assigned due to the small amount of isolated material.

The proposed mechanism involved fragmentation of the intermediate lithium-enolate **319** *via* ketene decomposition to afford the lithiated parent oxazolidinone **320** which subsequently underwent benzylation generating **318, scheme 135**. This theory was reinforced by Evans *et al.* who stated that at temperatures > 0 °C lithium-enolates decompose *via* a ketene pathway.[18b]

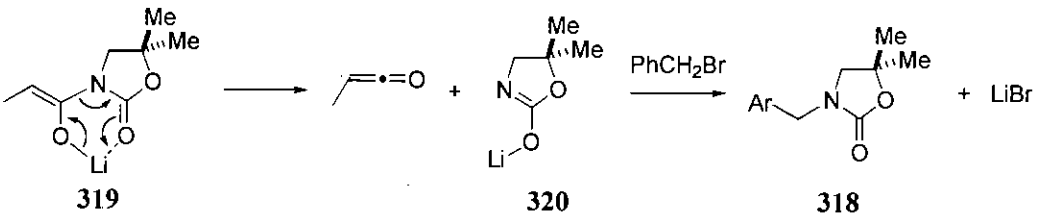

319 **320** **318**

Scheme 135

Davies *et al.* surmised that introduction of the C-5 geminal dimethyl group within the oxazolidinone auxiliary appeared to have an adverse effect on the stability and reactivity of the corresponding *N*-acyl enolates allowing significant levels of decomposition to occur where this alternative mechanism predominated with the *N*-propionyl 5,5-diphenyl "SuperQuat" auxilaries.[133, 138]

Davies *et al.* investigated the use of alternative sodium- or potassium-enolates and reversed the order of addition of the LiHMDS / benzyl bromide but these modifications failed to improve the alkylation yield. Ultimately, decomposition of the lithium-enolate was suppressed by conducting the benzylation in THF at -78 °C incorporating 5.0 equivalents of benzyl bromide.[133]

Unaware and therefore independent of these publications we modified our existing procedure as a result of a report by Burgess *et al.* where asymmetric alkylations on the solid phase using a supported Evans oxazolidinone auxiliary provided maximum yields of the alkylated adduct during the initial stages of the reaction. The observed decrease in yield over time was attributed to loss of the propionyl group from the oxazolidinone prior to cleavage which was reinforced by a diminished intensity of the supported amide at 1701 cm^{-1} by infra-red analysis.[19b]

As such, the asymmetric alkylation of propionylated auxiliary **208** was repeated employing modified reaction conditions adapted from the latter report. Thus, **208** in THF was initially deprotonated with LiHMDS (3.0 equivalents) at -78 °C, followed by addition of benzyl bromide (5.0 equivalents) where the reaction mixture was further stirred at -78 °C for 0.5 h before being warmed to room temperature over 0.75 h. Chromatography of the crude product mixture furnished the target α-benzylated adduct in 79% yield as an inseparable 9:1 mixture of diastereomers **313** and **321** where neither of the decomposition products **207** or **314** (**scheme 133**) were observed, **scheme 136.**

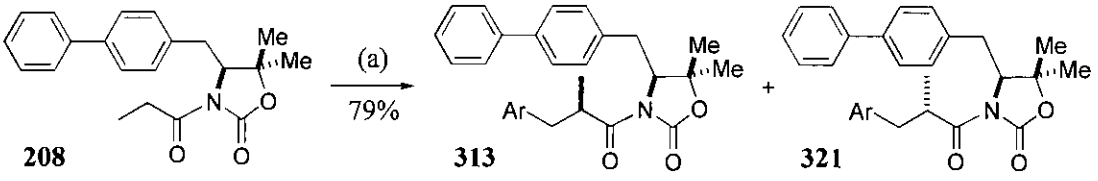

(a) (i) LiHMDS (3.0 equivalents), THF, -78 °C; (ii) $PhCH_2Br$ (5.0 equivalents), -78 °C→RT (1.25 h).

Scheme 136

The major and minor diastereomers were presumed to be the (2'*R*,4*S*) **313** and (2'*S*,4*S*) **321** diastereomers respectively in accordance with the original alkylation mechanism proposed by Evans (**chapter 7.1.2**) where diagnostic peaks from ^{1}H NMR analysis allowed determination of the 80% diastereomeric excess.

313: δ = 4.52 ppm (1H, dd, *J* 9.9, 3.3, C*H*N), δ = 1.18 ppm (3H, d, *J* 7.0, *Me*CHCO).

321: δ = 4.40 ppm (1H, dd, *J* 9.0, 3.0, C*H*N), δ = 0.91 ppm (3H, d, *J* 7.0, *Me*CHCO).

Attempted reductive removal of the transformed acyl fragment with lithium borohydride (10.0 equivalents) gave quantitative recovery of the alkylated adduct mixture **313** and **321**. Lithium aluminium hydride was employed as an alternative hydride reducing agent where the reaction was maintained at 0 °C in an attempt to promote selective cleavage of the alcohol product as reflux conditions effectively hydrolyse the oxazolidinone functionality as discussed in **chapter 5**. The reaction proceeded rapidly with exclusive exocyclic cleavage to furnish the auxiliary **207** (69%) and the alcohol products **26** and *ent*-**26** in a combined 71% yield, **scheme 137**.

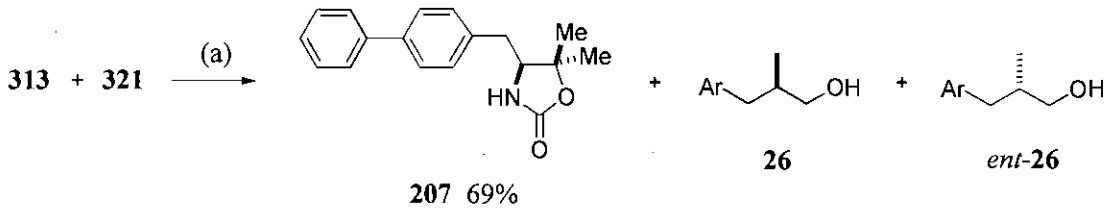

(a) $LiAlH_4$, THF, 0 °C.

Scheme 137

Chiral HPLC analysis of the cleaved alcohol product allowed the enantiomeric excess to be determined as 77% *R* where the retention times for the **26** and *ent*-**26** enantiomers were compared with literature values.[139] ^1H and ^{13}C NMR spectroscopic data for the alcohol product were also in good agreement with literature data.[140]

In summary, the lithium-enolate of the conformationally constrained chiral *N*-propionyl "SuperQuat" oxazolidinone **208** underwent efficient alkylation with benzyl bromide when a short reaction time was employed in 79% yield. The expected (2'*R*,4*S*) adduct **313** was generated in 80% d.e. Exclusive exocyclic reductive cleavage afforded the enantiomerically enriched alcohol product **26** (71% yield and 77% e.e. *R*) allowing recovery of the intact auxiliary **207** (69%).

In order to investigate whether the previously isolated *N*-benzylated auxiliary **314** (**scheme 133**) resulted from ketene decomposition of the lithium-enolate and subsequent benzylation of the lithiated auxiliary as suggested by Davies *et al.*[133] (**scheme 135**) or from alternative cleavage of the α-benzylated acyl fragment during the alkylation reaction where the resulting auxiliary undergoes benzylation as postulated by Burgess *et al.*[19b] the benzylation reaction was repeated under identical reaction conditions to those described above except the final reaction mixture was allowed to warm to room temperature over an extended time period (48 h).

Chromatography of the crude product mixture exclusively afforded the *N*-benzylated auxiliary **314** (82%), **scheme 138**.

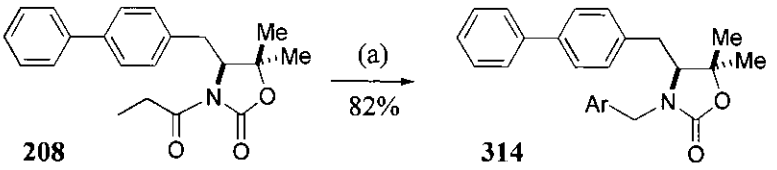

208 314

(a) (i) LiHMDS (3.0 equivalents), THF, -78 °C; (ii) $PhCH_2Br$ (5.0 equivalents), -78 °C→RT (48 h).

Scheme 138

This result indicated that the α-benzylated product **313** generated within the early stages of the alkylation reaction (1.25 h, 79% yield, **scheme 136**) underwent effective conversion to the *N*-benzylated auxiliary **314** (82%, **scheme 138**) when the alkylation reaction time at room temperature was extended (48 h).

Mechanistically, this unwanted side-reaction is unlikely to occur *via* ketene decomposition of the corresponding lithium-enolate of the α-benzylated auxiliary **313** as enolisation of **313** is difficult due to the hindered positioning and resultant stability of the remaining proton at the C-2' position.[121] Yet, this process must involve cleavage of the transformed acyl fragment from **313** to generate the lithiated auxiliary **322**, which subsequently undergoes rapid benzylation as excess benzyl bromide is present in the reaction mixture to afford **314**, **scheme 139**.

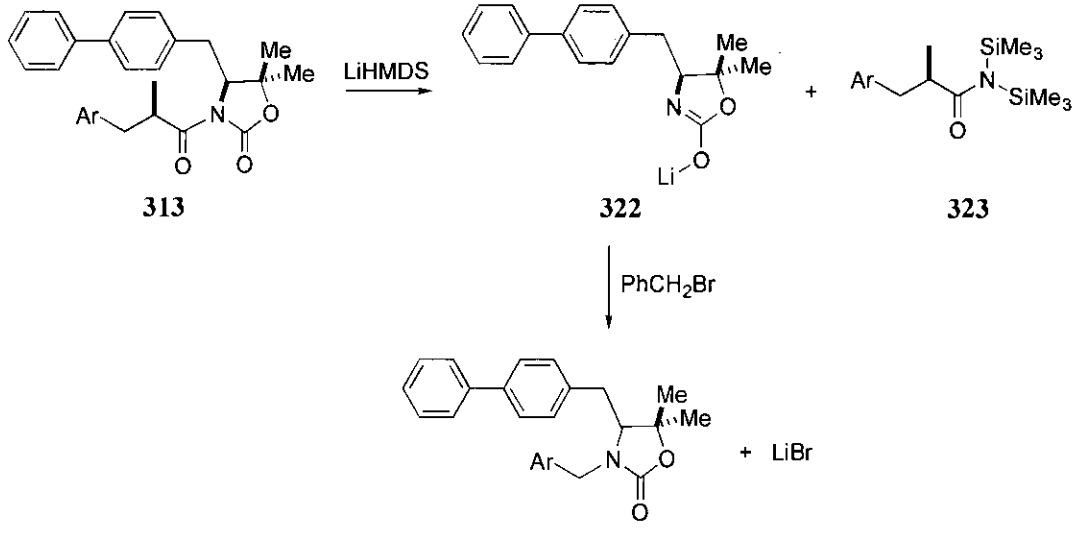

313 322 323

314

Scheme 139

This alternative fragmentation route involving LiHMDS acting as a nucleophile to effectively cleave the transformed acyl component (**scheme 139**) remains highly speculative considering that the steric bulk created by the two trimethylsilylamide ligands renders LiHMDS a non-nucleophilic base. Furthermore, the expected amide by-product **323** was not isolated, although trimethylsilyl signals were evident in the crude ^{1}H NMR spectrum at δ = 0.00 ppm, thus the non-isolation of amide **323** from the reaction mixture could be attributed to rapid elution of this material during the chromatographic purification of the comparatively polar **314**.

7.5 Polymer-Bound "SuperQuat" Oxazolidinone Auxiliary 218

N-propionylation of the gel-type polymer-bound "SuperQuat" oxazolidinone **218** was achieved by initial lithiation using a large excess of *n*-butyllithium[ψ] where red colouration of the beads indicated successful formation of the deprotonated species. Addition of propionyl chloride in excess discharged the red colouration indicating effective acylation of the auxiliary.[101] The polymeric product was collected by filtration, washed, dried and sieved to afford the propionylated oxazolidinone **324** in 78% yield, **scheme 140**.

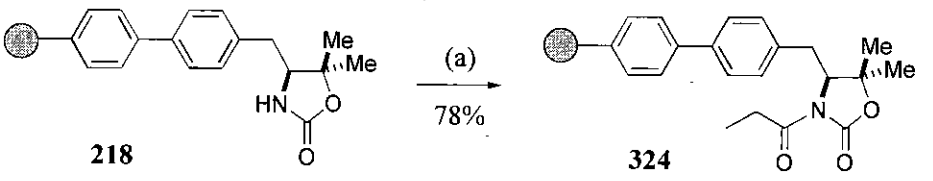

(a) (i) *n*-BuLi, THF, -78 °C, twice; (ii) EtCOCl, THF, -78 °C→RT.

Scheme 140

Note that the reaction mixture was agitated by shaking to minimise loss of the resin as unusable fines which are often obtained from mechanical break-down of the beads when conventional magnetic stirrers are utilised.

[ψ] *n*-Butyllithium and reflux conditions are typically employed in the lithiation of polystyrene,[11] but as the *N*-propionylation reaction was conducted at -78 °C the polystyrene backbone was unaffected.

Infra-red analysis of resin **324** provided distinct bands at 1780 cm^{-1} (C=O, oxazolidinone) and 1704 cm^{-1} (C=O, *N*-acyl) with no NH stretch (see **appendix**), where the analogous biaryl *N*-propionylated oxazolidinone solution phase mimic **208** gave similar stretching frequencies at 1772 cm^{-1} and 1702 cm^{-1}. Elemental analysis determined the loading of the *N*-propionylated resin **324** to be 0.49 $mmolg^{-1}$ which was virtually identical to that of the resin **218** employed in the reaction (0.50 $mmolg^{-1}$). Furthermore, the elemental analysis error margin, which is expressed as the greatest numerical error between those carbon, hydrogen or nitrogen percentage compositions calculated and found, was ± 0.86 % for the *N*-propionylated oxazolidinone polymer **324**, **table 14**.

Table 14 - Elemental Analysis Data for *N*-Propionylated Oxazolidinone Polymer 324

Elemental analysis error margin (Δ%)	C	H	N
Calculated composition assuming quantitative conversion to the *N*-propionylated oxazolidinone polymer **324**	89.31	7.59	0.70
Composition found for the recovered polymer **324**	88.47	8.45	0.68
Difference between calculated and found compositions	0.84	0.86	0.02

7.5.1 Asymmetric Aldol Reaction Utilising Polymer-Bound Auxiliary 218

Enolisation of the gel-type polymer-bound *N*-propionyl oxazolidinone **324** was effected using an excess of dibutylboron triflate and triethylamine where red colouration of the polymer beads suggested successful formation of the boron-enolate which possesses extended conjugation. Note that the resin was thoroughly washed with DCM prior to addition of the benzaldehyde to ensure that excess reagents were removed thus eliminating possible generation of the *anti* aldol adduct *via* an open transition state.[135]

Reaction of the freshly prepared enolate with benzaldehyde discharged the red colouration indicating effective aldol condensation of the two components. The reaction mixture was subsequently quenched with hydrogen peroxide in the presence

of phosphate buffer to hydrolyse any complexed boron residues, where the resin was collected by filtration, washed, dried and sieved to afford the polymer-bound aldol adduct **325** in 83% yield, **scheme 141**.

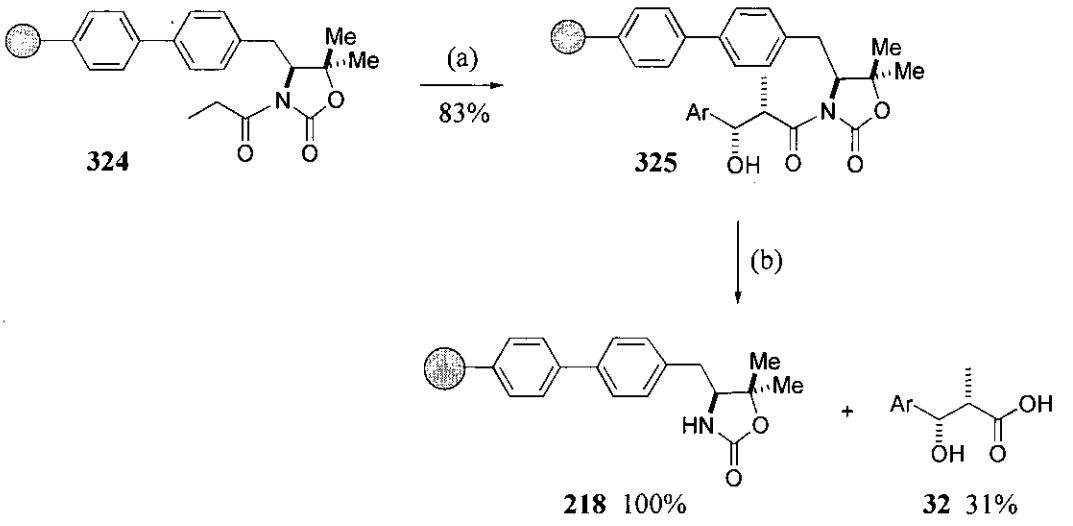

324 **325** **218** 100% **32** 31%

(a) (i) Bu_2BOTf, Et_3N, DCM, 0 °C, polymer washed with DCM, re-swollen in DCM and cooled to -78 °C; (ii) ArCHO, DCM, -78 °C→0 °C; (iii) pH 7 phosphate buffer, MeOH, RT; (b) $LiOH•H_2O$, H_2O, THF, RT.

Scheme 141

Infra-red analysis of resin **325** provided a distinct new broad OH stretch at 3482 cm^{-1} with bands at 1780 cm^{-1} and 1702 cm^{-1} relating to the carbonyl stretches of the oxazolidinone and *N*-acyl moiety (see **appendix**). The analogous biaryl aldol adduct solution phase mimic **312** gave similar stretching frequencies at 3437 cm^{-1}, 1774 cm^{-1} and 1693 cm^{-1} confirming successful generation of the aldol adduct on the solid support. In addition, elemental analysis determined the loading of resin **325** to be 0.50 $mmolg^{-1}$ which was virtually identical to that of the *N*-propionylated resin **324** employed in the reaction (0.49 $mmolg^{-1}$). The elemental analysis error margin expressed as the greatest numerical error between those carbon, hydrogen or nitrogen percentage compositions calculated for the polymer assuming quantitative conversion to the aldol adduct **325** and those found for the recovered polymer was ± 0.99 %.

The absolute stereochemistry of the two new chiral centres within the supported aldol adduct **325** were assigned after hydrolytic cleavage of the

transformed acyl fragment from the resin. Thus, hydrolysis of resin **325** with lithium hydroxide in H_2O / THF at room temperature furnished the β-hydroxy acid **32** (31% yield) with quantitative recovery of the polymer-bound auxiliary **218**, **scheme 141**.

The *syn* relative stereochemistry of the aldol adduct **32** was again determined on the basis of ^1H NMR coupling constants ($J_{H2'-H3'}$ 3.8 Hz).[136] Comparison of the measured optical rotation of the cleaved β-hydroxy acid **32** $[\alpha]_D$ -36.0 (*c* 0.3, $CHCl_3$), with the literature value[137] for (2*R*,3*R*)-**32** $[\alpha]_D$ +31.0 (*c* 1.1, $CHCl_3$) established the absolute configuration as the expected (2*S*,3*S*) diastereomer.

Infra-red analysis of the recovered resin **218** provided bands at 3420 cm^{-1} (NH) and 1772 cm^{-1} (C=O) where the spectrum was virtually identical to that of the original polymer-bound auxiliary **218** (3421 cm^{-1}, 1768 cm^{-1}), thus indicating successful regeneration of the auxiliary on the solid support.

However, elemental analysis of resin **218** was inaccurate suggesting a loading of 0.44 $mmolg^{-1}$ where the loading of the polymer-bound aldol adduct **325** employed was 0.50 $mmolg^{-1}$. Furthermore, the elemental error margin between those percentage compositions previously found for the oxazolidinone polymer **218** prior to *N*-propionylation and aldol adduct formation and those obtained for recovered oxazolidinone polymer **218** was ± 1.24 %.

These discrepancies could be attributed to incomplete washing of the cleaved material from the resin and subsequent drying of the resin, which could in turn account for the poor yield of β-hydroxy acid **32** (31%) obtained. Unfortunately, time restraints did not allow optimisation of the cleavage conditions or recycling of the recovered polymer-bound auxiliary **218**.

In summary, the boron-enolate of the conformationally constrained polymer-bound chiral *N*-propionyl "SuperQuat" oxazolidinone **324** underwent efficient aldol condensation with benzaldehyde to furnish the polymer-supported aldol adduct **325** (83%). Exclusive exocyclic hydrolytic cleavage afforded the (2*S*,3*S*) β-hydroxy acid **32** as a single diastereomer (31%) allowing quantitative recovery of the intact polymer-bound auxiliary **218**.

7.5.2 Asymmetric Alkylation Reactions Utilising Polymer-Bound Auxiliary 218

The gel-type polymer-bound *N*-propionyl oxazolidinone **324** was investigated as an auxiliary for conducting asymmetric alkylation reactions on the solid phase. LiHMDS (3.0 equivalents) was initially employed as the amide base with benzyl bromide (5.0 equivalents) as the alkyl halide thus mimicking the reaction conditions previously optimised for the analogous solution phase benzylation reactions (**chapter 7.4.2**), **scheme 142**. The reaction temperatures and reaction times for the enolisation and subsequent benzylation stages were varied as depicted in **table 15**.

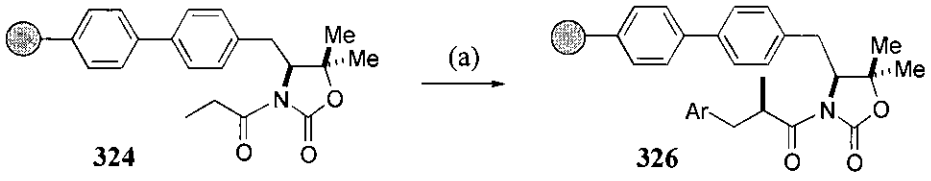

324 **326**

(a) (i) LiHMDS (3.0 equivalents), THF, twice; (ii) $PhCH_2Br$ (5.0 equivalents).

Scheme 142

Table 15 - Benzylation Results Utilising Polymer-Bound *N*-Propionyl Oxazolidinone 324

Entry [a]	Enolisation temperature	Benzylation temperature / time	Infra-red of resin (cm^{-1})	CHN error margin (Δ%) [b]
1	-78 °C	-78 °C, 16 h RT, 6h	3400 1777 (broad) 1702 (weak)	2.22
2	0 °C	0 °C, 22 h RT, 1 h	3400 1774 (broad) 1700 (weak)	1.12
3	0 °C	0 °C, 1 h RT, 0.5 h	3415 1778 1702	1.13

[a] Resin was treated with two separate batches of LiHMDS to promote enolisation where the excess reagent was removed and the resin re-swollen with THF prior to addition of the benzyl bromide.
[b] Elemental analysis error margin was calculated as the difference between those percentage compositions calculated for the polymer assuming quantitative conversion to the alkylated adduct **326** and those found for the recovered resin where the greatest numerical error from the carbon, hydrogen or nitrogen percentages was expressed.

Conducting the enolisation process and the initial stage of the benzylation at -78 °C (entry 1) or 0 °C (entry 2) appeared to have little effect on the outcome of the alkylation reaction. In each case the undefined infra-red spectra of the recovered resins coupled with their inaccurate elemental analysis error margins (up to ± 2.22%) suggested that a range of auxiliary derived species were resin bound.

Analogous alkylation studies employing the *N*-propionylated auxiliary **208** in the solution phase previously illustrated that over prolonged benzylation times the target α-benzylated adduct **313** was prone to deacylation with LiHMDS potentially acting as a nucleophile. The resultant lithiated auxiliary **322** subsequently underwent benzylation to afford the *N*-benzylated auxiliary **314** (**scheme 139**). However, washing the enolised *N*-propionylated resin **324** to remove excess LiHMDS prior to addition of the benzyl bromide should minimise this decomposition pathway.

The diagnostic infra-red stretching frequencies obtained from compounds **208**, **313**, **207** and **314** are depicted in **table 16** in parallel with the analogous supported species **324** and **218**.

Table 16 - Comparison of Infra-red Spectra Obtained from Solution and Solid Phase Studies

	Infra-red diagnostic stretching frequencies (cm^{-1})			
	N-propionylated auxiliary	α-benzylated adduct	Auxiliary	*N*-benzylated auxiliary
Solution phase studies	**208** 1772 (C=O) 1702 (C=O)	**313** 1774 (C=O) 1699 (C=O)	**207** 3449 (NH) 1754 (C=O)	**314** 1745 (C=O)
Solid phase studies	**324** 1780 (C=O) 1704 (C=O)	not isolated	**218** 3421 (NH) 1768 (C=O)	not isolated

As the carbonyl stretching frequencies of the biaryl *N*-propionylated auxiliary and α-benzylated adduct (**208** and **313**) are very similar it was impossible to determine whether the desired alkylated adduct had been generated on the resin. However, infra-red analysis of the resins obtained from entries 1 and 2 (**table 15**)

both provided potential NH stretching bands at 3400 cm^{-1} where the carbonyl stretch resulting from the *N*-acyl moiety was of diminished relative intensity. These observations strongly implied that partial cleavage of the acyl moiety had occurred to afford the polymer-bound auxiliary **218** which could in turn undergo benzylation. Therefore, the broad oxazolidinone carbonyl stretch was feasibly postulated to encompass additional carbonyl signals resulting from the supported auxiliary and *N*-benzylated auxiliary.

Entry 3 (**table 15**) incorporated the 0 °C enolisation and benzylation reaction temperature from entry 2 in an attempt to minimise elemental analysis error margins. Further modifications included reducing the reaction time as shorter reaction times were shown to prevent decomposition of the α-benzylated adduct within the solution phase studies (**chapter 7.4.2**).[19b] Infra-red analysis of the recovered resin provided a potential NH stretch (3415 cm^{-1}), yet the two carbonyl bands were visibly sharper and of approximately equal intensity (1778 cm^{-1} and 1702 cm^{-1}) suggesting minimal cleavage of the *N*-acyl moiety, where the elemental error margin remained consistent at ± 1.13%.

Finally, entry 3 (**table 15**) was repeated in an identical manner substituting freshly prepared lithium diisopropylamide[141] (LDA) as the amide base which is commonly utilised for asymmetric alkylation reactions on the solid phase.[19a, 19b] Unfortunately, infra-red analysis of the recovered resin again suggested deacylation and possible benzylation of the resulting supported auxiliary (3400 cm^{-1}, 1775 cm^{-1} broad, 1700 cm^{-1} weak) where elemental analysis of the resin provided a significant error margin of ± 2.48%.

The recovered resins described above were subjected to various cleavage conditions as depicted in **table 17** in an attempt to quantify the extent to which the original asymmetric benzylation reactions had been successful. The resins were treated with lithium hydroxide as this reagent previously effected cleavage of the aldol adduct from the solid support (**chapter 7.5.1**). Reductive removal of the

transformed acyl fragment with lithium borohydride was also investigated, **scheme 143.**

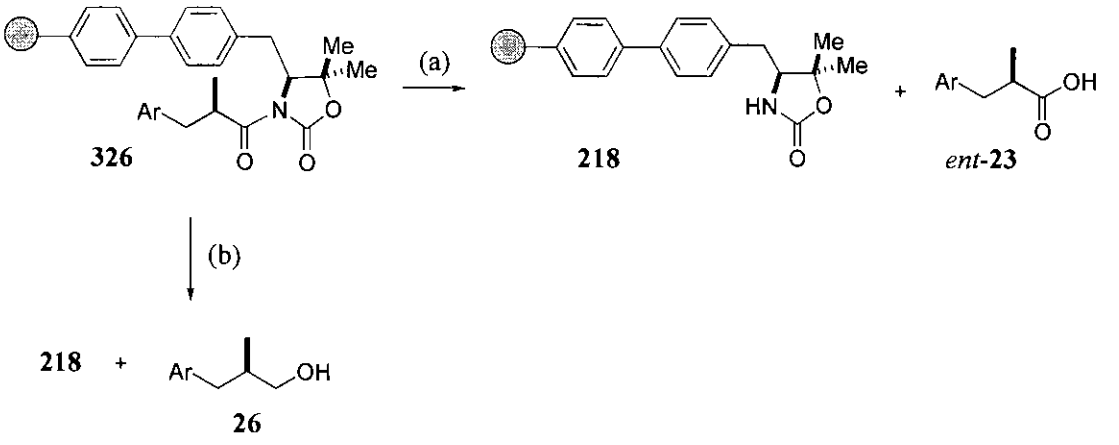

(a) $LiOH{\bullet}H_2O$, H_2O, THF, RT; (b) $LiBH_4$, THF, RT.

Scheme 143

Table 17 - Summary of Cleavage Reaction Results

Entry	Cleavage conditions [c]	Infra-red of resin (cm^{-1})	CHN error margin (Δ%) [d]	Analysis of filtrate
1 [a]	LiOH, 1 h	3400 1777 (broad) 1702 (weak)	not recorded	no cleaved acid *ent*-**23**
2 [a]	LiOH, 66 h	3400 1756	1.70	no cleaved acid *ent*-**23**
3 [a]	$LiBH_4$, 1 h	3422 1755	0.99	trace of cleaved alcohol **26**
4 [b]	$LiBH_4$, 1 h	3400 1773 1700	2.44	no cleaved alcohol **26**

[a] Resin recovered from entry 1, **table 15** employed in cleavage reaction.
[b] Resin recovered from entry 3, **table 15** employed in cleavage reaction.
[c] Stabiliser-free THF was employed in each of the cleavage reactions and subsequent washing procedures to prevent the 2,6-di-*tert*-butyl-4-methylphenol (BHT) stabiliser swamping the cleaved product ^1H NMR spectra.
[d] Elemental analysis error margin was calculated as the difference between those percentage compositions previously found for the oxazolidinone polymer **218** prior to *N*-propionylation and benzyl adduct formation and those obtained for the recovered resin where the greatest numerical error from the carbon, hydrogen or nitrogen percentages was expressed.

Entry 1 employing lithium hydroxide afforded none of the cleaved acid *ent*-**23** and the infra-red spectrum of the recovered polymer was virtually identical to that of the resin employed in the reaction. Entry 2 extended the hydrolysis reaction time where infra-red analysis of the resulting resin suggested possible regeneration of the polymer-bound auxiliary **218** (3400 cm^{-1}, 1756 cm^{-1}), yet the target acid *ent*-**23** was not detected within the filtrate.

Entry 3 investigated reductive cleavage with lithium borohydride where the infra-red spectrum of the recovered resin (3422 cm^{-1}, 1755 cm^{-1}) again contained no *N*-acyl carbonyl stretch indicating effective removal of the *N*-acyl moiety. In this instance, signals consistent with those of the desired alcohol[140] **26** were observed within the ^1H NMR spectrum of the crude concentrated filtrate, but the negligible yield of cleaved material prevented further isolation and characterisation.

Finally, entry 4 utilised the resin recovered from entry 3, **table 15** which appeared to have undergone potential α-benzylation with minimal fragmentation of *N*-acyl moiety. Unfortunately, reductive treatment of the resin generated no alcohol **26** and infra-red analysis of the resin indicated that cleavage had not occurred.

In summary, **chapter 7.5.2** investigated asymmetric alkylation reactions employing the polymer-bound chiral *N*-propionyl "SuperQuat" oxazolidinone **324** incorporating LiHMDS or LDA as the amide base with benzyl bromide as the alkyl halide. Infra-red analysis of the resultant resins indicated possible fragmentation of the *N*-acyl moiety and subsequent benzylation of the polymer-bound auxiliary **218** where decreasing the benzylation time appeared to limit this decomposition process. Ultimately, interpretation of the transformations was severely hindered by the inability to accurately monitor the reactions on the solid phase and subsequent hydrolytic or reductive removal of the *N*-acyl moiety failed to provide the desired cleaved products.

Another factor which could potentially have influenced these asymmetric alkylation reactions on the solid phase relates to the specific environment created around the supported *N*-propionylated auxiliary **324** by the gel-type polymer. A

report by Czarnik stated that deprotonation and reaction of a macroporous polystyrene with LDA and benzyl bromide at -78 °C proceeded in high conversion, whereas the analogous benzylation utilising a gel-type polystyrene gave no reaction.[142] No further information could be obtained regarding the nature of the solid support, yet this example clearly highlights that the resin type exhibits a profound influence over the reactivity of the attached functionality, thus providing another variable to further complicate the process of optimisation on the solid phase.

7.6 Summary of Chapter 7

The work detailed in **chapter 7** provided a tantalising glimpse into the applications of the polymer-bound chiral "SuperQuat" oxazolidinone auxiliary **218**. Clearly, future research would include optimisation of the solid phase aldol and alkylation reaction conditions to attain consistently high chemical and optical yields of the cleaved chiral products. The range of asymmetric transformations employing the supported auxiliary could also be expanded to encompass conjugate addition and Diels-Alder reactions on the solid phase.

Finally, the recycling potential of the recovered supported auxiliary would be evaluated and the methodology could ultimately be adapted to combinatorial synthesis where the nature of the acyl group, electrophile and cleavage conditions could each be varied to generate vast libraries of compounds.

Chapter 8 : Experimental

8.1 General Experimental

^{1}H nuclear magnetic resonance (NMR) spectra were recorded using an internal deuterium lock for the indicated reference at ambient probe temperature on Varian Gemini 200 (200 MHz), Bruker AC250 (250 MHz) or Varian Inova 600 (600 MHz) Fourier transform instruments. The data is presented as follows: chemical shift (in ppm on the δ scale relative to $\delta_{TMS} = 0$), integration, multiplicity (s = singlet, d = doublet, t = triplet, q = quartet, m = multiplet, br = broad), coupling constant and interpretation. ^{13}C nuclear magnetic resonance (NMR) spectra were recorded using an internal deuterium lock for the indicated reference at ambient probe temperature on Varian Gemini 200 (50.3 MHz) or Bruker AC250 (62.9 MHz) instruments and are reported in ppm on the δ scale. ^{19}F nuclear magnetic resonance (NMR) spectra were recorded using an internal deuterium lock for the indicated reference at ambient probe temperature on Bruker AC250 (235.4 MHz) instrument and are reported in ppm on the δ scale.

Infra-red spectra were recorded on a Perkin Elmer Paragon 1000 FT-IR spectrometer instrument using 4 mm sodium chloride plates, 0.1 mm sodium chloride solution cells or *via* the preparation of potassium bromide discs. The wavelengths of maximum absorbance (ν_{max}) are quoted in cm^{-1}.

Fast atom bombardment (FAB) mass spectra were performed on a Kratos MS50TC mass spectrometer. Electron impact (EI) mass spectra were performed on a Finnigan 4500 mass spectrometer. Both FAB and EI high resolution mass spectra (HRMS) are accurate to within 5 ppm. Atmospheric pressure chemical ionisation (APCI) mass spectra were carried out using a Micromass (Platform 2) mass spectrometer. The parent ion M^{+} or fragment of highest mass is quoted, followed by significant fragments and their relative intensities.

Optical rotations were measured on a AA-1000 polarimeter with a path length of 1.0 dm at the sodium D line (589 nm) and are reported as follows: $[\alpha]_D$, concentration (*c* in g/100 cm^3) and solvent. All optical rotations were measured at ambient temperature.

Elemental analysis was carried out using a Perkin Elmer 2400 CHN Elemental analyser.

Thin layer chromatography (t.l.c.) was carried out on Merck 60 F_{254} (0.25 mm) glass backed silica gel plates with visualisation by ultraviolet (UV) and/or potassium permanganate[ξ] and ammonium molybdate[Ψ] stains. Flash chromatography was carried out using Fisher matrix silica 60 gel (particle size 35-70 μm) under positive pressure using a hand pump. Eluent compositions are quoted as v/v ratios.

Preparative high performance liquid chromatography (HPLC) was carried out using a HPLC technology column (internal diameter 20 mm) equipped with a Gilson refractive index detector (model 113). A standard flow rate of 10 cm^3 min^{-1} was used with eluent compositions quoted as v/v ratios.

Unless otherwise stated, chiral HPLC was carried out using a Waters™ instrument equipped with either a Chiracel OD column with a standard flow rate of 0.6 cm^3 min^{-1} or a Chiracel OD-H column with a standard flow rate of 0.5 cm^3 min^{-1}, column internal diameter 4.6 mm, column length 250 mm. In each case a Waters™ 486 tunable absorbance detector (set to 254 nm) was used with [hexane:propan-2-ol (95:5)] as the eluent. All HPLC samples were filtered through 0.20 μm nylon syringe filters prior to analysis and all HPLC solvents were vacuum filtered and degassed prior to use.

[ξ] Potassium permanganate stain prepared as follows: to water (1000 cm^3) was added potassium permanganate (10 g) followed by potassium carbonate (50 g) and sodium hydroxide pellets (ca. 40 pellets). The mixture was stirred until all solid material had dissolved.

[Ψ] Ammonium molybdate stain prepared as follows: to water (950 cm^3) was added concentrated sulphuric acid (50 cm^3) followed by ammonium molybdate (50 g) and ceric sulphate (3 g). The mixture was stirred well until all solid material had dissolved.

Reagents were purified by standard means. Dichloromethane (DCM), toluene, *N*,*N*-dimethylformamide (DMF), triethylamine, pyridine and diisopropylamine were distilled from calcium hydride and stored over calcium hydride under an argon atmosphere. Tetrahydrofuran (THF) and dioxane were distilled from sodium metal/benzophenone and stored under an argon atmosphere. Hexane was distilled and stored over 4Å molecular sieves under an argon atmosphere, ether was dried over sodium wire. Benzaldehyde and cinnamaldehyde were distilled from magnesium sulphate immediately prior to use. Acetyl and propionyl chloride were distilled immediately prior to use. All other reagents were used as supplied.

All experiments were performed in an inert atmosphere of argon under anhydrous conditions using oven dried apparatus cooled in a desiccator or flame dried glassware cooled under argon. Standard techniques for the handling of air sensitive materials were employed.[143]

8.2 Experimental for Results and Discussion Part 1

L-Tyrosine methyl ester hydrochloride *120*

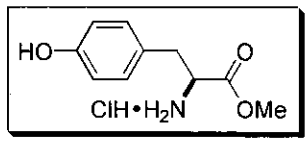

Acetyl chloride (3.92 cm^3, 55.1 mmol) was added dropwise to anhydrous methanol (30 cm^3) at 0 °C, the resulting solution was stirred at 0 °C for 5 minutes. *L*-tyrosine **119** (3.50 g, 19.2 mmol) was added before heating the mixture to reflux for 3 hours. The volatiles were removed under reduced pressure affording the title compound as a white solid (4.44 g, 100%), mp 192-193 °C [lit., (Aldrich) mp 192 °C].

DL-Tyrosine methyl ester hydrochloride *rac-120*

Synthesised in an analogous manner to the (*L*)-isomer, from *DL*-tyrosine. Thus, acetyl chloride (11.28 cm^3, 158.6 mmol), anhydrous methanol (100 cm^3) and *DL*-tyrosine (10.00 g, 55.19 mmol) gave the title compound (12.84 g, 100%) as a white solid, mp 198-199 °C.

L-Tyrosine methyl ester *121*

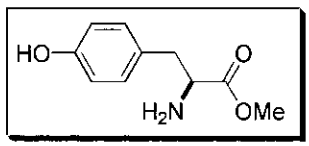

Hydrochloride salt **120** (4.435 g, 19.14 mmol) was dissolved in water (15 cm^3) and the solution was neutralised with solid potassium carbonate (2.650 g. 19.14 mmol). The aqueous suspension was rigorously extracted with EtOAc (5 × 50 cm^3). The combined organic extracts were dried (Na_2SO_4) and concentrated under reduced

pressure affording the title compound as a white crystalline solid (3.330 g, 89%), R_f [DCM:MeOH (90:10)] 0.57; mp 135 °C [lit., (Aldrich) mp 135-139 °C]; δ_H (200 MHz, CD_3OD) 6.98 (2H, d, *J* 8.4, Ar*H*), 6.71 (2H, d, *J* 8.4, Ar*H*), 3.66 (3H, s, O*Me*), 3.64 (1H, t, *J* 6.6, C*H*N), 2.91 (1H, dd, *J* 13.6, 7.0, CH_AH_BAr), 2.81 (1H, dd, *J* 13.6, 6.2, CH_AH_BAr); δ_C (50.3 MHz, CD_3OD) 176.6, 157.6, 131.4 (2C), 128.8, 116.4 (2C), 56.8, 52.8, 40.8.

DL-Tyrosine methyl ester *rac-121*

Synthesised in an analogous manner to the (*L*)-isomer from *rac*-**120**. Thus, *rac*-**120** (12.79 g, 55.20 mmol), water (150 cm^3) and potassium carbonate (7.629 g, 55.20 mmol) gave the title compound as white crystalline solid (8.020 g, 74%), mp 114-116 °C. *NMR spectroscopic data identical to that obtained for* ***121****.*

Methyl (2*S*)-*N*,*N*-2-dimethylamino-3-(*p*-hydroxy)phenyl-propanoate *122*

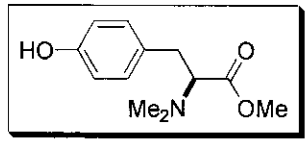

10% activated palladium on charcoal (1.70 g) was added to a mixture of the amino ester **121** (3.33 g, 17.1 mmol) and formaldehyde (2.91 cm^3, 38% aq. solution, 37.3 mmol) in methanol (60 cm^3). The flask was purged with hydrogen and stirred under 1 atm. of hydrogen at room temperature for 24 hours. The reaction mixture was filtered through celite and washed with methanol (10 cm^3). The filtrate was concentrated under reduced pressure affording the title compound as a white solid (3.81 g, 100%). Recrystallisation from acetonitrile provided an analytical sample, R_f [DCM:MeOH (90:10)] 0.70; mp 127-128 °C [lit.,[64] mp 130 °C]; δ_H (200 MHz, $CDCl_3$) 7.00 (2H, d, *J* 8.4, Ar*H*), 6.66 (2H, d, *J* 8.4, Ar*H*), 3.60 (3H, s, O*Me*), 3.41 (1H, dd, *J* 9.2, 6.2, C*H*N), 3.03-2.82 (2H, m, CH_2Ar), 2.40 (6H, s, N*Me* × 2).

(2*S*)-*N*,*N*-2-Dimethylamino-3-(*p*-hydroxy)phenyl-propan-1-ol *123*

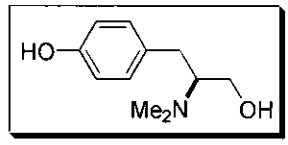

Lithium aluminium hydride (73 mg, 1.9 mmol) was added to a solution of the ester **122** (142 mg, 0.640 mmol) in anhydrous ether (5 cm^3) at -78 °C. The solution was stirred at -78 °C for 4 hours before being quenched with water (2 cm^3). The organic phase was separated and the aqueous phase was extracted with EtOAc (4 × 50 cm^3). The combined organic extracts were dried (Na_2SO_4) and concentrated under reduced pressure. The residue was chromatographed on silica gel [gradient elution DCM:MeOH (95:5 to 65:35)] providing the title compound as a yellow solid (71 mg, 57%), R_f [DCM:MeOH (50:50)] 0.11; mp 138-139 °C; $[\alpha]_D$ +4.0 (*c* 1.0, MeOH); ν_{max} (KBr disc)/cm^{-1} 3151, 2931, 1613, 1592, 1517, 1235, 1041; δ_H (250 MHz, CD_3OD) 7.11 (2H, d, *J* 8.6, Ar*H*), 6.80 (2H, d, *J* 8.6, Ar*H*), 3.58 (2H, d, *J* 5.6, CH_2OH), 2.91-2.77 (2H, m, CH_AH$_B$Ar and C*H*N), 2.56-2.46 (1H, m, CH$_A$$H_B$Ar), 2.46 (6H, s, N*Me* × 2); δ_C (62.9 MHz, CD_3OD) 154.9 (C), 129.8 (C), 129.1 (2 × CH), 114.3 (2 × CH), 67.1 (CH), 59.2 (CH_2), 39.5 (2 × CH_3), 30.1 (CH_2); m/z (APCI) 196 (MH^+, 100%), 178 (10); Anal. Calcd. for $C_{11}H_{17}NO_2$: C, 67.66; H, 8.78; N, 7.17, found C, 67.23; H, 8.75; N, 6.95; single crystal X-ray diffraction: see **appendix**.

(2*S*)-*N*,*N*-2-Dimethylamino-3-(*p*-trifluoromethylsulphonyloxy)phenyl-propan-1-ol *115*

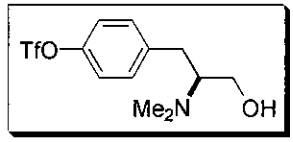

A solution of the diol **123** (35 mg, 0.18 mmol) and *N*-phenyl triflimide (66 mg, 0.18 mmol) in anhydrous DCM (2 cm^3) was cooled to 0 °C. Triethylamine (0.030 cm^3, 0.22 mmol) was added dropwise and the reaction mixture was stirred at 0 °C for 1 hour before being further stirred at room temperature for 17 hours. The solution was diluted with ether (5 cm^3) and the organic phase was washed sequentially with water (2 cm^3), 1N aqueous NaOH (2 × 2 cm^3), water (2 cm^3) and brine (2 cm^3). The organic layer was dried (Na_2SO_4) and concentrated under reduced pressure. The residue was chromatographed on silica gel [gradient elution DCM:MeOH (100:0 to 70:30)] affording title compound as a yellow oil (10 mg, 17%), R_f [DCM:MeOH (90:10)] 0.17; δ_H (200 MHz, $CDCl_3$) 7.16 (4H, s, Ar*H*), 3.45-3.23 (2H, m, CH_2OH), 3.01-2.83 (2H, m, CH_AH$_B$Ar and C*H*N), 2.77-2.52 (2H, br s, CH$_A$$H_B$Ar and O*H*), 2.40 (6H, s, N*Me* × 2); m/z (APCI) 329 (MH^+, 100%), 310 (9), 196 (32).

Methyl (2*S*)-*N*,*N*-2-dimethylamino-3-(*p*-trifluoromethylsulphonyloxy) phenyl-propanoate *124*

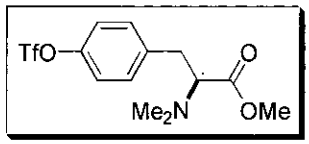

A solution of the phenol **122** (2.78 g, 12.5 mmol) and pyridine (5.00 cm^3, 62.4 mmol) in anhydrous DCM (40 cm^3) was cooled to 0 °C. Trifluoromethanesulphonic anhydride (2.42 cm^3, 14.4 mmol) was added and the resulting orange solution was stirred at 0 °C for 72 hours. The reaction mixture was diluted with water (50 cm^3) and DCM (50 cm^3), the organic phase was separated and washed sequentially with

0.5N aqueous NaOH (50 cm^3), water (50 cm^3), 10% aqueous citric acid solution (2 × 50 cm^3) and water (50 cm^3) and dried (Na_2SO_4). The solvent was removed under reduced pressure affording the title compound as an orange oil (3.85 g, 87%) which was used in subsequent stages without further purification, R_f [DCM:MeOH (90:10)] 0.78; $[\alpha]_D$ +7.0 (*c* 2, $CHCl_3$); ν_{max} (neat)/cm^{-1} 2952, 1733, 1502, 1423, 1250, 889; δ_H (200 MHz, $CDCl_3$) 7.27 (2H, d, *J* 8.8, Ar*H*), 7.16 (2H, d, *J* 8.8, Ar*H*), 3.60 (3H, s, O*Me*), 3.39 (1H, dd, *J* 8.6, 6.2, C*H*N), 3.05 (1H, dd, *J* 13.6 , 8.6, CH_AH_BAr), 2.92 (1H, dd, *J* 13.6, 6.2, CH_AH_BAr), 2.36 (6H, s, N*Me* × 2); δ_C (50.3 MHz, $CDCl_3$) 171.5, 148.1, 138.9, 130.8 (2C), 121.1 (2C), 69.0, 51.0, 41.6 (2C), 34.8, (CF_3 peak missing); δ_F (235.4 MHz, $CDCl_3$) -73.2; m/z (FAB) 356 (MH^+, 100%), 296 (33), 163 (15), 116 (64); HRMS (FAB) $C_{13}H_{17}F_3NO_5S$ (MH^+) requires 356.0780, found 356.0779.

Reduction of *124*: Attempted synthesis of (2*S*)-*N*,*N*-2-Dimethylamino-3-(*p*-trifluoromethylsulphonyloxy)phenyl-propan-1-ol *115*

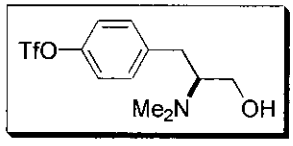

A mixture of silica gel (188 mg, dried at 140 °C under reduced pressure for 3 hours) and lithium aluminium hydride (28 mg, 0.70 mmol) in anhydrous ether (2 cm^3) was stirred at room temperature for 17 hours. Ester **124** (89 mg, 0.25 mmol) was added and the reaction mixture was stirred at room temperature for a further 24 hours before being heated to reflux for 30 minutes. The suspension was quenched with saturated aqueous NH_4Cl (2 cm^3), filtered through celite and washed with ether (20 cm^3). The organic phase was separated, dried (Na_2SO_4) and concentrated under reduced pressure. The remaining residue was chromatographed on silica gel [gradient elution DCM:MeOH (100:0 to 60:40)] affording a range of products:

yellow oil (3 mg, 3% recovery), R_f [DCM:MeOH (90:10)] 0.78; m/z (APCI) 356 (MH^+, 100%), 314 (24), 312 (19), determined to be unreacted ester **124**.

yellow oil (40 mg, 62% of total yield) R_f [DCM:MeOH (90:10)] 0.17 and 0.00, δ_H (200 MHz, $CDCl_3$) found to contain a 1:1 ratio of title compound **115** and the analogous phenol **123** generated by cleavage of the triflate group; m/z (APCI) 328 (MH^+, 96%), 196 (MH^+ 100) reinforcing these findings.

(2*S*)-*N*,*N*-2-Dimethylamino-3-(*p*-hydroxy)phenyl-1-(trifluoromethylsulphonyloxy)-propane *125*

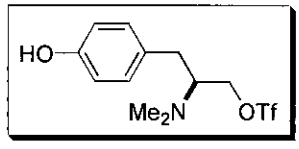

Approximately 30 mg (37% of total yield) of an impurity was isolated from the above crude reaction mixture and subsequently identified as **125**.

Data for **125**:

Obtained as a yellow oil,

R_f [DCM:MeOH (90:10)] 0.11; δ_H (200 MHz, CD_3OD) 7.41 (2H, d, *J* 8.8, Ar*H*), 7.28 (2H, d, *J* 8.8, Ar*H*), 3.53 (2H, d, *J* 4.8, CH_2OTf), 3.02-2.76 (2H, m, CH_AH$_B$Ar and C*H*N), 2.43 (1H, dd, *J* 12.1, 8.4, CH$_A$$H_B$Ar), 2.43 (6H, s, N*Me* × 2); δ_C (62.9 MHz, CD_3OD) 147.6, 140.5, 130.3 (2C), 120.5 (2C), 66.7, 58.9, 39.5 (2C), 30.5, (CF_3 peak missing); δ_F (235.4 MHz, $CDCl_3$) -71.3; m/z (APCI) 328 (MH^+, 100%), 196 (33).

(3*S*)-*N*,*N*-3-Dimethylamino-4-(*p*-hydroxy)phenyl-2-methyl-butan-2-ol *126*

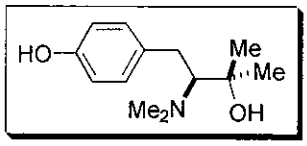

Method A :

A solution of iodomethane (0.840 cm^3, 13.4 mmol) in anhydrous ether (10 cm^3) was slowly added to magnesium turnings (342 mg, 14.1 mmol) and a crystal of iodine. The mixture was heated to reflux for 1 hour and allowed to cool to room temperature before dropwise addition of the ester **122** (150 mg, 0.670 mmol) in anhydrous ether (5 cm^3). The reaction mixture was heated to reflux for 24 hours before being quenched with saturated aqueous NH_4Cl (20 cm^3). The organic phase was separated and the aqueous phase was extracted with DCM (2 × 25 cm^3). The combined organic extracts were dried (Na_2SO_4) and concentrated under reduced pressure. The residue was chromatographed on silica gel [gradient elution DCM:MeOH (96:4 to 93.7)] providing the title compound as a white solid (122 mg, 81%), R_f [DCM:MeOH (90:10)] 0.05; δ_H (200 MHz, $CDCl_3$) 7.09 (2H, d, *J* 8.2, Ar*H*), 6.80 (2H, d, *J* 8.2, Ar*H*), 6.22 (2H, br s, O*H* × 2), 2.87-2.57 (3H, m, C*H*N and CH_2Ar), 2.32 (6H, s, N*Me* × 2), 1.22 (3H, s, *Me*), 1.17 (3H, s, *Me*); δ_C (62.9 MHz, $CDCl_3$) 154.4 (C), 131.6 (C), 129.9 (2 × CH), 115.3 (2 × CH), 74.0 (CH), 71.0 (C), 43.5 (2 × CH_3), 30.6 (CH_2), 29.0 (CH_3), 24.8 (CH_3); m/z (FAB) 224 (MH^+, 59%), 164 (54), 133 (100), 107 (81), 91 (59); HRMS (FAB) $C_{13}H_{22}NO_2$ (MH^+) requires 224.1651, found 224.1660.

Method B :

A solution of the ester **122** (75 mg, 0.34 mmol) in anhydrous THF (5 cm^3) was cooled to -78 °C. Methyl lithium (1.9 cm^3, 1.1 *M* in ether, 2.1 mmol) was added dropwise before stirring the reaction mixture at 0 °C for 40 hours. The reaction

mixture was quenched with saturated aqueous NH_4Cl (10 cm^3), the organic phase was separated and the aqueous phase was extracted with EtOAc (2 × 20 cm^3). The combined organic extracts were washed with brine (20 cm^3), dried (Na_2SO_4) and concentrated under reduced pressure. The residue was chromatographed on silica gel [gradient elution DCM:MeOH (96:4 to 93:7)] affording the title compound as a white solid (58 mg, 77%). *NMR spectroscopic data identical to that obtained for **126** in **Method A**.*

(3*S*)-*N*,*N*-3-Dimethylamino-2-methyl-4-(*p*-trifluoromethylsulphonyloxy) phenyl-butan-2-ol *116*

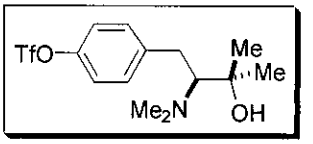

A solution of the diol **126** (22 mg, 0.10 mmol) and *N*-phenyl triflimide (39 mg, 0.11 mmol) in anhydrous DCM (2 cm^3) were cooled to 0 °C. Triethylamine (0.015 cm^3, 0.11 mmol) was added dropwise and the reaction mixture was stirred at 0 °C for 40 hours. The solution was diluted with EtOAC (10 cm^3) and the organic phase was washed with water (2 × 10 cm^3). The organic layer was dried (Na_2SO_4) and concentrated under reduced pressure. The residue was chromatographed on silica gel [DCM:MeOH (96:4)] affording the title compound as a yellow oil (26 mg, 74%). *NMR spectroscopic data identical to that obtained for **116** as given below with some additional similar R_f impurities remaining.*

(3*S*)-*N*,*N*-3-Dimethylamino-2-methyl-4-(*p*-trifluoromethylsulphonyloxy) phenyl-butan-2-ol *116*

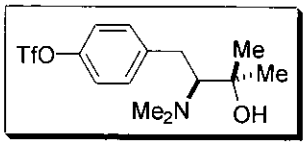

A solution of iodomethane (0.820 cm^3, 13.2 mmol) in anhydrous ether (18 cm^3) was slowly added to magnesium turnings (340 mg, 14.0 mmol) and a crystal of iodine. The mixture was heated to reflux for 1 hour and allowed to cool to room temperature before dropwise addition of the ester **124** (500 mg, 1.41 mmol) in anhydrous ether (9 cm^3). The reaction mixture was heated to reflux for 7 hours and stirred for a further 24 hours at room temperature. The reaction mixture was quenched with saturated aqueous NH_4Cl (45 cm^3), the organic phase was separated and the aqueous phase was extracted with DCM (2 × 50 cm^3). The combined organic extracts were dried (Na_2SO_4) and concentrated under reduced pressure. The residue was chromatographed on silica gel [DCM:MeOH (99:1)] providing the title compound as a yellow oil (68 mg, 14%), R_f [DCM:MeOH (90:10)] 0.42; δ_H (600 MHz, $CDCl_3$) 7.35 (2H, d, *J* 8.7, Ar*H*), 7.21 (2H, d, *J* 8.7, Ar*H*), 2.93 (1H, dd, *J* 14.2, 9.4, CH_AH$_B$Ar), 2.86 (1H, dd, *J* 9.4, 4.0, C*H*N), 2.77 (1H, dd, *J* 14.2, 4.0, CH$_A$$H_B$Ar), 2.33 (6H, s, N*Me* × 2), 1.20 (3H, s, *Me*), 1.16 (3H, s, *Me*); δ_C (62.9 MHz, $CDCl_3$) 147.8 (C), 141.5 (C), 130.6 (2 × CH), 121.2 (2 × CH), 74.1 (CH), 70.9 (C), 43.6 (2 × CH_3), 31.2 (CH_2), 28.8 (CH_3), 25.0 (CH_3), (CF_3 peak missing); δ_F (235.4 MHz, $CDCl_3$) -73.1; m/z (FAB) 356 (MH^+, 100%), 296 (63), 116 (41), 99 (42); HRMS (FAB) $C_{14}H_{21}F_3NO_4S$ (MH^+) requires 356.1143, found 356.1160.

(4*S*)-5,5-Dimethyl-3-methyl-4-(*p*-trifluoromethylsulphonyloxy)benzyl-oxazolidine *127*

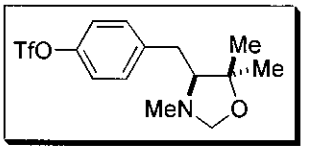

Small traces of a higher R_f compound were isolated during chromatography of the above crude reaction mixture. Approximately 17 mg (3% of total yield) of the impurity were isolated and subsequently identified as **127**.

Data for **127**:

Obtained as a colourless oil,

R_f [DCM:MeOH (95:5)] 0.40; δ_H (200 MHz, $CDCl_3$) 7.33 (2H, d, *J* 8.8, Ar*H*), 7.21 (2H, d, *J* 8.8, Ar*H*), 4.59 (1H, d, *J* 3.1, CH_XH$_Y$O), 3.89 (1H, d, *J* 3.1, CH$_X$$H_Y$O), 2.88 (1H, dd, *J* 14.1, 7.1, CH_AH$_B$Ar), 2.67 (1H, dd, *J* 14.1, 6.4, CH$_A$$H_B$Ar), 2.48 (1H, t, *J* 6.8, C*H*N), 2.18 (3H, s, N*Me*), 1.22 (3H, s, *Me*), 1.07 (3H, s, *Me*); m/z (APCI) 354 (MH^+, 100%), 224 (15).

(2*S*)-2-Amino-3-(*p*-hydroxy)phenyl-propan-1-ol *128*

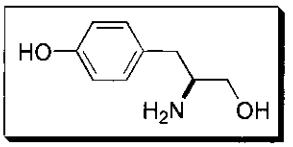

Lithium borohydride (12 mg, 0.55 mmol) in anhydrous THF (1.5 cm^3) was added dropwise to a solution of the ester **121** (50 mg, 0.26 mmol) in anhydrous THF (2 cm^3). The reaction mixture was stirred at room temperature for 72 hours before being quenched with saturated aqueous NH_4Cl (3 cm^3) and extracted with EtOAc (2 × 10 cm^3). The combined organic extracts were washed with brine (3 cm^3), dried (Na_2SO_4) and concentrated under reduced pressure. The white gummy solid was

triturated with ether affording the title compound as a white solid (40 mg, 93%) which was used in subsequent stages without further purification, R_f [DCM:MeOH (90:10)] 0.38; mp 111-113 °C; δ_H (200 MHz, CD_3OD) 7.05 (2H, d, *J* 8.4, Ar*H*), 6.73 (2H, d, *J* 8.4, Ar*H*), 3.69 (1H, dd, *J* 11.4, 3.7, CH_XH$_Y$OH), 3.42 (1H, dd, *J* 11.4, 5.9, CH$_X$$H_Y$OH), 3.01 (1H, dd, *J* 13.0, 4.8, CH_AH$_B$Ar), 2.82-2.76 (1H, m, C*H*N), 2.61 (1H, dd, *J* 13.0, 9.2, CH$_A$$H_B$Ar); δ_C (50.3 MHz, CD_3OD) 157.3, 131.4 (2C), 129.7, 116.5 (2C), 61.7, 61.2, 35.3; m/z (APCI) 168 (MH^+, 53%), 105 (26), 64 (100).

(4*S*)-4-(*p*-Hydroxy)benzyl-oxazolidin-2-one *129*

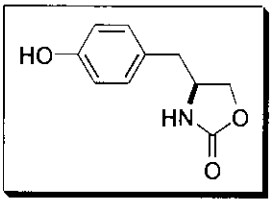

Anhydrous ethanol (2 cm^3) was cautiously added to sodium (~200 mg) generating sodium ethoxide *in situ*. To this was added a solution of the amino alcohol **128** (159 mg, 0.950 mmol) dissolved in anhydrous ethanol (2 cm^3) followed by diethyl carbonate (0.140 cm^3, 1.16 mmol). The mixture was heated to 130 °C for 1 hour before being quenched with water (5 cm^3). The resulting aqueous solution was acidified to pH 1 using 1N aqueous HCl and extracted with EtOAc (2 × 10 cm^3). The combined organic extracts were dried (Na_2SO_4) and concentrated under reduced pressure. Recrystallisation from methanol afforded the title compound as a white crystalline solid (112 mg, 61%), R_f [DCM:MeOH (90:10)] 0.40; mp 184-186 °C; ν_{max} (nujol)/cm^{-1} 3332, 3136, 2929, 1728; δ_H (200 MHz, CD_3OD) 7.04 (2H, d, *J* 8.4, Ar*H*), 6.73 (2H, d, *J* 8.4, Ar*H*), 4.41-4.30 (1H, m, C*H*N), 4.14-4.03 (2H, m, CH_2O), 2.81-2.68 (2H, m, CH_2Ar); δ_C (50.3 MHz, CD_3OD) 162.3, 157.6, 131.5 (2C), 128.3, 116.5 (2C), 70.7, 55.1, 41.0; m/z (APCI) 194 (MH^+, 86%), 168 (100), 150 (10), 107 (10).

(4*S*)-4-(*p*-Trifluoromethylsulphonyloxy)benzyl-oxazolidin-2-one *118*

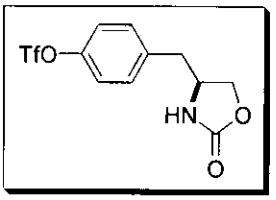

A solution of the oxazolidinone **129** (52 mg, 0.27 mmol) and pyridine (0.11 cm^3, 1.4 mmol) in anhydrous DCM (2 cm^3) was cooled to 0 °C. Trifluoromethanesulphonic anhydride (0.10 cm^3, 0.60 mmol) was added and the resulting orange solution was stirred at 0 °C for 24 hours. The reaction mixture was diluted with water (3 cm^3) and DCM (3 cm^3). The organic phase was separated and washed sequentially with 0.5N aqueous NaOH (3 cm^3), water (3 cm^3), 10% aqueous citric acid solution (2 × 3 cm^3) and water (3 cm^3). The organic extracts were dried (Na_2SO_4) and concentrated under reduced pressure. The residue was chromatographed on silica gel [gradient elution DCM:MeOH (100:0 to 96:4)]. The crude product was subsequently recrystallised from chloroform/petroleum ether (40-60 °C) affording the title compound as a yellow crystalline solid (61 mg, 69%), R_f [DCM:MeOH (90:10)] 0.66; mp 132-133 °C; δ_H (200 MHz, $CDCl_3$) 7.26 (4H, s, Ar*H*), 6.22 (1H, br s, N*H*), 4.44 (1H, t, *J* 10.3, C*H*N), 4.15-4.03 (2H, m, CH_2O), 2.91 (2H, d, *J* 6.2, CH_2Ar); δ_C (50.3 MHz, $CDCl_3$) 159.6, 148.7, 136.6, 130.9 (2C), 121.9 (2C), 69.3, 53.4, 40.5, (CF_3 peak missing); δ_F (235.4 MHz, $CDCl_3$) -73.1; m/z (FAB) 326 (MH^+, 100%), 91 (17); HRMS (FAB) $C_{11}H_{11}F_3NO_5S$ (MH^+) requires 326.0310, found 326.0323.

4-(4,4,5,5-Tetramethyl-1,3,2-dioxaborolyl)toluene *147*

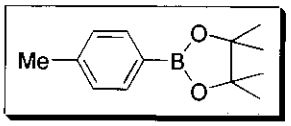

To a solution of $PdCl_2(dppf)•CH_2Cl_2$ (205 mg, 0.251 mmol) in anhydrous dioxane (12 cm^3) was added 4-bromotoluene (860 mg, 5.03 mmol), triethylamine (2.11 cm^3, 15.0 mmol) and pinacolborane (1.09 cm^3, 7.51 mmol). The reaction mixture was

heated to 100 °C for 21 hours before being diluted with water (30 cm^3) and extracted with toluene (2 × 30 cm^3). The organic phase was dried (Na_2SO_4) and concentrated under reduced pressure. The brown residue was purified by Kugelrohr distillation (product found to decompose on silica and alumina) affording the title compound as a yellow oil (763 mg, 70%), R_f [DCM:MeOH (90:10)] 0.93; δ_H (200 MHz, $CDCl_3$) 7.72 (2H, d, *J* 7.7, Ar*H*), 7.19 (2H, d, *J* 7.7, Ar*H*), 2.37 (3H, s, *Me*Ar), 1.34 (12H, s, *Me*); δ_C (50.3 MHz, $CDCl_3$) 141.4, 134.8 (2C), 128.5 (2C), 127.7, 83.6 (2C), 24.8 (4C), 21.7. *NMR spectroscopic data in good agreement with literature data.*[76]

(3*S*)-*N*,*N*-3-Dimethylamino-2-methyl-4-(*p*-tolyl)phenyl-butan-2-ol *150*

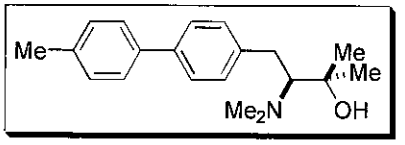

Method C :

Aryl boronic ester **147** (40 mg, 0.18 mmol), triflated amino alcohol **116** (59 mg, 0.18 mmol) and $PdCl_2(dppf)•CH_2Cl_2$ (15 mg, 0.018 mmol) were added to a flask which was purged with argon. 2N aqueous Na_2CO_3 (0.46 cm^3, 0.92 mmol) and DMF (2 cm^3) were added and the mixture was heated to 80 °C for 24 hours. The reaction mixture was diluted with ether (2 × 10 cm^3), the organic phase was separated and washed with water (10 cm^3), brine (10 cm^3), dried (Na_2SO_4) and concentrated under reduced pressure. The residue was chromatographed on silica gel [DCM:MeOH (95:5)] affording the title compound as a yellow oil (40 mg, 50%), R_f [DCM:MeOH (90:10)] 0.36; δ_H (200 MHz, $CDCl_3$) 7.52-7.46 (4H, m, Ar*H*), 7.33-7.20 (4H, m, Ar*H*), 2.97-2.66 (3H, m, C*H*N and CH_2Ar), 2.37 (3H, s, *Me*Ar), 2.32 (6H, s, N*Me* × 2), 1.20 (3H, s, *Me*), 1.17 (3H, s, *Me*); m/z (APCI) 298 (MH^+, 100%), 284 (63).

Methyl (2*S*)-*N*,*N*-2-dimethylamino-3-(*p*-tolyl)phenyl-propanoate *148*

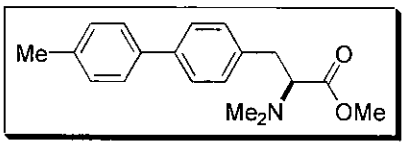

An analogous protocol to that described in Method C was undertaken. Thus, aryl boronic ester **147** (40 mg, 0.18 mmol), triflated ester **124** (59 mg, 0.18 mmol), $PdCl_2(dppf)\bullet CH_2Cl_2$ (15 mg, 0.018 mmol), 2N aqueous Na_2CO_3 (0.46 cm^3, 0.92 mmol) and DMF (2 cm^3) were heated to 80 °C for 72 hours. The residue was chromatographed on silica gel [DCM:MeOH (98:2)] affording the title compound as a yellow oil (33 mg, 66%), R_f [EtOAc] 0.55; ν_{max} (neat)/cm^{-1} 3024, 2946, 1793, 1164, 820; δ_H (250 MHz, $CDCl_3$) 7.52-7.42 (4H, m, Ar*H*), 7.28-7.20 (4H, m, Ar*H*), 3.62 (3H, s, O*Me*), 3.47 (1H, dd, *J* 9.3, 5.8, C*H*N), 3.09 (1H, dd, *J* 13.4, 9.3, CH_AH_BAr), 2.96 (1H, dd, *J* 13.4, 5.8, CH_AH_BAr), 2.40 (6H, s, N*Me* × 2), 2.38 (3H, s, *Me*Ar); δ_C (50.3 MHz, $CDCl_3$) 171.9 (C), 139.2 (C), 138.0 (C), 136.9 (2 × C), 129.4 (4 × CH), 126.9 (2 × CH), 126.8 (2 × CH), 69.5 (CH), 51.0 (CH_3), 41.8 (2 × CH_3), 35.2 (CH_2), 21.0 (CH_3); m/z (FAB) 298 (MH^+, 80%), 238 (38), 116 (100), 91 (25); HRMS (FAB) $C_{19}H_{24}NO_2$ (MH^+) requires 298.1807, found 298.1794.

Method D :

Aryl boronic ester **147** (400 mg, 1.83 mmol), triflated ester **124** (620 mg, 1.74 mmol) and anhydrous potassium carbonate (380 mg, 2.75 mmol) were added to a flask which was purged with argon. Anhydrous DMF (20 cm^3) was added and the solution was stirred for 15 minutes under a flow of argon. $Pd(PPh_3)_4$ (101 mg, 0.0874 mmol) was added and the mixture was heated to 90 °C for 17 hours. The reaction mixture was diluted with EtOAc (20 cm^3). The organic phase was separated and washed sequentially with saturated aqueous $NaHCO_3$ (20 cm^3), water (20 cm^3), 10% aqueous citric acid (20 cm^3), water (20 cm^3) and brine (20 cm^3). The organic phase was dried (Na_2SO_4) and concentrated under reduced pressure. The residue was

chromatographed using preparative HPLC R_t [EtOAc:hexane (70:30)] 10.5 minutes, affording the title compound as a yellow oil (223 mg, 43%). *NMR spectroscopic data identical to that obtained for* ***148*** *in* ***Method C****.*

(2*S*)-*N*,*N*-2-Dimethylamino-3-(*p*-tolyl)phenyl-propan-1-ol *149*

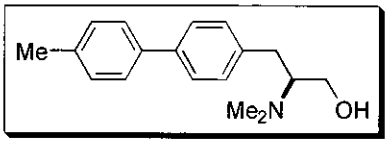

Lithium borohydride (26 mg, 1.1 mmol) in anhydrous THF (10 cm^3) was added dropwise to a solution of the ester **148** (76 mg, 0.26 mmol) in anhydrous THF (2 cm^3). The reaction mixture was stirred at room temperature for 96 hours. The reaction was quenched with saturated aqueous NH_4Cl (5 cm^3), filtered through celite and washed with EtOAc (20 cm^3). The organic phase was separated and washed with brine (5 cm^3), dried (Na_2SO_4) and concentrated under reduced pressure. The residue was chromatographed on silica gel [hexane:EtOAc (50:50)] providing the title compound as a white solid (45 mg, 65%), R_f [hexane:EtOAc (50:50)] 0.64; mp 92-93 °C; δ_H (250 MHz, $CDCl_3$) 7.55-7.46 (4H, m, Ar*H*), 7.31-7.23 (4H, m, Ar*H*), 4.00 (1H, d, *J* 13.3, C$H_X$$H_Y$OH), 3.70 (1H, dd, *J* 13.3, 4.5, $CH_X$$H_Y$OH), 3.29 (1H, d, *J* 12.2, C$H_A$$H_B$Ar), 2.97 (1H, dd, *J* 11.4, 4.5, C*H*N), 2.88 (1H, dd, *J* 12.2, 11.4, $CH_A$$H_B$Ar), 2.79 (3H, s, N*Me*), 2.72 (3H, s, N*Me*), 2.40 (3H, s, *Me*Ar); δ_C (62.9 MHz, $CDCl_3$) 139.5 (C), 137.5 (C), 137.0 (C), 136.5 (C), 129.4 (2 × CH), 129.4 (2 × CH), 127.1 (2 × CH), 126.7 (2 × CH), 73.6 (CH), 59.1 (CH_2), 51.5 (CH_3), 49.2 (CH_3), 31.5 (CH_2), 20.9 (CH_3); m/z (FAB) 282 (100%), 270 (MH^+, 76), 181 (59), 88 (45); HRMS (FAB) $C_{18}H_{24}NO$ (MH^+) requires 270.1858, found 270.1863.

8.3 Experimental for Results and Discussion Part 2

p-Vinylphenylboronic acid *159*

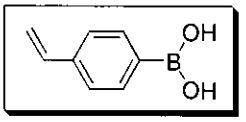

Anhydrous THF (360 cm^3) was added to magnesium turnings (8.77 g, 0.360 mmol) and several crystals of iodine. *p*-Chlorostyrene (43.3 cm^3, 0.360 mmol) was added *via* cannulation ensuring that the reaction mixture maintained a steady rate of reflux. Once addition was complete the solution was heated to reflux for 3 hours and subsequently cooled to -78 °C. Trimethyl borate (41.0 cm^3, 0.360 mmol) was added dropwise with stirring continued at -78 °C for 10 minutes. This afforded a mass of white solid with stirring no longer possible. The reaction mixture was warmed to room temperature and occasionally shaken at room temperature over 72 hours. 10% aqueous NaOH (580 cm^3) was added and stirring resumed for 1 hour at room temperature. The resultant suspension was filtered to remove the insoluble jelly and washed with water (350 cm^3) and ether (350 cm^3). The organic phase was separated and the aqueous phase was extracted with ether (3 × 350 cm^3). The combined organic extracts were dried (Na_2SO_4) and concentrated under reduced pressure. The residue was recrystallised from hexane affording the title compound as a white solid (24.6 g, 46%), R_f [DCM:MeOH (90:10)] 0.71; mp 193-195 °C [lit., (Aldrich) mp 190-193 °C]; δ_H (200 MHz, CD_3OD) 7.66 (2H, d, *J* 8.1, Ar*H*), 7.38 (2H, d, *J* 8.1, Ar*H*), 6.73 (1H, dd, *J* 17.6, 11.0, CH_2=C*H*), 5.80 (1H, d, *J* 17.6, CH_XH$_Y$=CH), 5.24 (1H, d, *J* 11.0, CH$_X$*H*$_Y$=CH). *NMR spectroscopic data in good agreement with literature data.*[84]

Methyl (2*S*)-*N*,*N*-2-dimethylamino-3-[*p*-(*p*-vinylphenyl)phenyl]-propanoate *166*

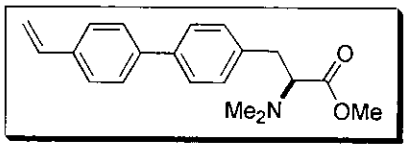

An analogous protocol to that described in Method C (**chapter 8.2**) was undertaken. Thus, vinyl boronic acid **159** (44 mg, 0.30 mmol), triflated ester **124** (100 mg, 0.280 mmol), $PdCl_2(dppf)\bullet CH_2Cl_2$ (23 mg, 0.028 mmol), 2N aqueous Na_2CO_3 (0.70 cm^3, 1.4 mmol) and DMF (4 cm^3) were heated to 80 °C for 21 hours. The residue was chromatographed on silica gel [hexane:EtOAc (75:25)] affording the title compound as a white solid (62 mg, 71%), R_f [DCM:MeOH (90:10)] 0.71; mp 59-60 °C; $[\alpha]_D$ +40.0 (*c* 1.0, $CHCl_3$); ν_{max} ($CHCl_3$ soln.)/cm^{-1} 3025, 2948, 1731, 1628, 1497, 1165, 819; δ_H (200 MHz, $CDCl_3$) 7.58-7.45 (6H, m, Ar*H*), 7.27 (2H, d, *J* 7.7, Ar*H*), 6.76 (1H, dd, *J* 17.6, 10.9, CH_2=C*H*), 5.79 (1H, dd, *J* 17.6, 0.9, CH_XH_Y=CH), 5.27 (1H, dd, *J* 10.9, 0.9, CH_XH_Y=CH), 3.63 (3H, s, O*Me*), 3.49 (1H, dd, *J* 9.5, 5.9, C*H*N), 3.17-2.92 (2H, m, CH_2Ar), 2.42 (6H, s, N*Me* × 2); δ_C (62.9 MHz, $CDCl_3$) 171.7 (C), 140.1 (C), 138.6 (C), 137.2 (C), 136.3 (C), 136.2 (CH), 129.3 (2 × CH), 126.9 (2 × CH), 126.8 (2 × CH), 126.5 (2 × CH), 113.6 (CH_2), 69.3 (CH), 51.0 (CH_3), 41.7 (2 × CH_3), 35.2 (CH_2); m/z (FAB) 310 (MH^+, 18%), 250 (47), 116 (100), 42 (57); HRMS (FAB) $C_{20}H_{24}NO_2$ (MH^+) requires 310.1807, found 310.1794.

(2*S*)-*N*,*N*-2-Dimethylamino-3-[*p*-(*p*-vinylphenyl)phenyl]-propan-1-ol *161*

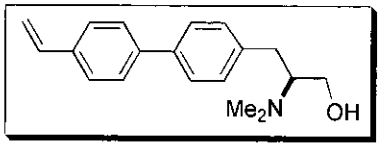

Ester **166** (100 mg, 0.320 mmol) and sodium borohydride (56 mg, 1.5 mmol) were dissolved in anhydrous THF (3 cm^3) and heated to 55 °C. Anhydrous methanol (0.26 cm^3) was added dropwise and the solution was further heated at 55 °C for 38 hours.

The reaction mixture was diluted with water (5 cm^3) and the aqueous layer was extracted with EtOAc (2 × 10 cm^3). The combined organic extracts were washed with brine (10 cm^3), dried (Na_2SO_4) and concentrated under reduced pressure providing the title compound as a white solid (71 mg, 78%), R_f [DCM:MeOH (90:10)] 0.49; mp 109-111 °C; δ_H (250 MHz, $CDCl_3$) 7.57-7.45 and 7.25-7.18 (8H, m, Ar*H*), 6.75 (1H, dd, *J* 17.6, 10.9, CH_2=C*H*), 5.79 (1H, dd, *J* 17.6, 0.9, CH_XH_Y=CH), 5.27 (1H, dd, *J* 10.9, 0.9, CH_XH_Y=CH), 3.47-3.31 (2H, m, CH_2OH), 2.99-2.86 (3H, m, C*H*N and CH_2Ar), 2.37 (6H, s, N*Me* × 2); δ_C (62.9 MHz, $CDCl_3$) 140.1 (C), 138.5 (C), 138.3 (C), 136.3 (C), 136.3 (CH), 129.3 (2 × CH), 126.9 (4 × CH), 126.5 (2 × CH), 113.7 (CH_2), 66.7 (CH), 60.3 (CH_2), 40.0 (2 × CH_3), 30.0 (CH_2); m/z (FAB) 282 (MH^+, 62%), 193 (32), 91 (26), 88 (33); HRMS (FAB) $C_{19}H_{24}NO$ (MH^+) requires 282.1858, found 282.1854.

(3*S*)-*N*,*N*-3-Dimethylamino-2-methyl-4-[*p*-(*p*-vinylphenyl)phenyl]-butan-2-ol *162*

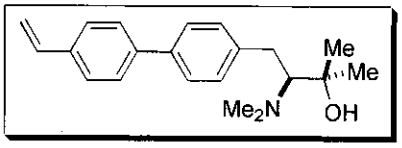

A solution of iodomethane (0.13 cm^3, 2.2 mmol) in anhydrous ether (2 cm^3) was slowly added to magnesium turnings (55 mg, 2.3 mmol) and a crystal of iodine. The mixture was heated to reflux for 1.5 hours and allowed to cool to room temperature before dropwise addition of the ester **166** (67 mg, 0.21 mmol) in anhydrous ether (2 cm^3). The reaction mixture was heated to reflux for 19 hours before being quenched with saturated aqueous NH_4Cl (2 cm^3). The organic phase was separated and the aqueous phase was extracted with DCM (2 × 10 cm^3). The combined organic extracts were dried (Na_2SO_4) and concentrated under reduced pressure. The residue was chromatographed on silica gel [hexane:EtOAc (50:50)] providing the title compound as a white solid (12 mg, 18%), R_f [DCM:MeOH (90:10)] 0.45; δ_H (250 MHz, $CDCl_3$) 7.58-7.25 (8H, m, Ar*H*), 6.75 (1H, dd, *J* 17.6, 10.9, CH_2=C*H*), 5.78

(1H, dd, *J* 17.6, 0.9, C*H*$_X$H$_Y$=CH), 5.26 (1H, dd, *J* 10.9, 0.9, CH$_X$*H*$_Y$=CH), 2.95-2.75 (3H, m, C*H*N and C*H*$_2$Ar), 2.35 (6H, s, N*Me* × 2), 1.22 (3H, s, *Me*), 1.19 (3H, s, *Me*); δ_C (62.9 MHz, $CDCl_3$) 139.9 (C), 139.7 (C), 138.4 (C), 136.4 (C), 136.3 (CH), 129.4 (2 × CH), 126.8 (2 × CH), 126.8 (2 × CH), 126.5 (2 × CH), 113.7 (CH_2), 74.0 (CH), 70.8 (C), 43.6 (2 × CH_3), 31.3 (CH_2), 29.1 (CH_3), 25.0 (CH_3); m/z (FAB) 310 (MH^+, 33%), 250 (48), 193 (50), 116 (77); HRMS (FAB) $C_{21}H_{28}NO$ (MH^+) requires 310.2171, found 310.2173.

Methyl (2*S*)-2-*N*-(*tert*-butoxycarbonyl)-3-(*p*-hydroxy)phenyl-propanoate *179*

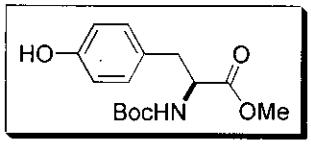

To a solution of the *L*-tyrosine methyl ester **121** (100 mg, 0.512 mmol) and triethylamine (0.139 cm^3, 1.00 mmol) in anhydrous DCM (2 cm^3) at 0 °C was added di-*tert*-butyl dicarbonate (133 mg, 0.609 mmol) dissolved in anhydrous DCM (2 cm^3). The reaction mixture was stirred at room temperature for 17 hours before the addition of water (1 cm^3) with stirring then continued at room temperature for a further 30 minutes. The organic layer was separated and washed sequentially with water (1 cm^3), 0.05N aqueous HCl (1 cm^3), water (1 cm^3) and brine (1 cm^3). The organic phase was then dried (Na_2SO_4) and concentrated under reduced pressure. The residue was chromatographed on silica gel [hexane:EtOAc (80:20)] affording the title compound as a white solid (117 mg, 77%), R_f [DCM:MeOH (90:10)] 0.78; mp 107-108 °C [lit., (Aldrich) mp 100-104 °C]; $[\alpha]_D$ +59.5 (*c* 2.0, $CHCl_3$) [lit., (Aldrich) $[\alpha]_D$ +51.0 (*c* 1.0, $CHCl_3$)]; δ_H (200 MHz, $CDCl_3$) 6.95 (2H, d, *J* 8.4, Ar*H*), 6.72 (2H, d, *J* 8.4, Ar*H*), 6.22 (1H, br s, O*H*), 5.03 (1H, d, *J* 8.4, N*H*), 4.55-4.51 (1H, m, C*H*N), 3.71 (3H, s, O*Me*), 3.00-2.96 (2H, m, C*H*$_2$Ar), 1.41 (9H, s, C(*Me*)$_3$); δ_C (62.9 MHz, $CDCl_3$) 172.7 (C), 155.3 (C), 155.2 (C), 130.3 (2 × CH), 127.4 (C), 115.5 (2 × CH), 80.3 (C), 54.6 (CH), 52.3 (CH_3), 37.5 (CH_2), 28.3 (3 × CH_3); m/z (FAB) 296 (MH^+,

28%), 240 (100), 196 (45), 178 (14), 136 (12); HRMS (FAB) $C_{15}H_{22}NO_5$ (MH^+) requires 296.1500, found 296.1506.

Methyl (2*RS*)-2-*N*-(*tert*-butoxycarbonyl)-3-(*p*-hydroxy)phenyl-propanoate *179*

Synthesised in an analogous manner to the (*S*)-isomer, from *DL*-tyrosine methyl ester. Thus, *DL*-tyrosine methyl ester *rac*-**121** (8.022 g, 41.09 mmol), triethylamine (11.45 cm^3, 82.18 mmol) and di-*tert*-butyl dicarbonate (10.76 g, 49.31 mmol) in anhydrous DCM (210 cm^3) were stirred at room temperature for 44 hours. The residue was chromatographed on silica gel [hexane:EtOAc (80:20)] affording the title compound as a white solid (5.860 g, 48%), mp 140-141 °C. *NMR spectroscopic data identical to that obtained for* ***179***.

Methyl (2*S*)-2-*N*-(*tert*-butoxycarbonyl)-3-(*p*-trifluoromethylsulphonyloxy) phenyl-propanoate *138*

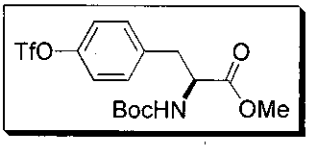

A solution of the phenol **179** (24.36 g, 82.49 mmol) and pyridine (33.29 cm^3, 412.5 mmol) in anhydrous DCM (250 cm^3) was cooled to 0 °C. Trifluoromethanesulphonic anhydride (16.65 cm^3, 98.99 mmol) was added and the resulting orange solution was stirred at 0 °C for 35 hours. The reaction mixture was diluted with water (240 cm^3) and DCM (240 cm^3). The organic phase was separated and washed sequentially with 0.5N aqueous NaOH (240 cm^3), water (240 cm^3), 10% aqueous citric acid solution (2 × 240 cm^3) and water (240 cm^3) and then dried (Na_2SO_4). The solvent was removed under reduced pressure. The residue was chromatographed on silica gel [hexane:EtOAc (88:12)] affording the title compound

as a colourless oil which crystallised on standing (33.88 g, 96%), R_f [DCM] 0.28; mp 49-50 °C [lit.,[50] mp 47-48 °C]; $[\alpha]_D$ +43.0 (*c* 1.0, $CHCl_3$) [lit.,[50] $[\alpha]_D$ +33.6 (*c* 1.0, $CHCl_3$)]; δ_H (250 MHz, $CDCl_3$) 7.20 (4H, s, Ar*H*), 5.03 (1H, d, *J* 7.9, N*H*), 4.58 (1H, m, C*H*N), 3.70 (3H, s, O*Me*), 3.16 (1H, dd, *J* 13.9, 5.8, CH_AH_BAr), 3.01 (1H, dd, *J* 13.9, 6.6, CH_AH_BAr), 1.39 (9H, s, C(*Me*)$_3$); δ_C (62.9 MHz, $CDCl_3$) 171.8 (C), 154.8 (C), 148.5 (C), 136.8 (C), 131.0 (2 × CH), 121.2 (2 × CH), 80.1 (C), 54.1 (CH), 52.3 (CH_3), 37.8 (CH_2), 28.1 (3 × CH_3), (CF_3 peak missing); m/z (FAB) 428 (MH^+, 2%), 372 (34), 328 (82), 268 (28), 57 (100); HRMS (FAB) $C_{16}H_{21}F_3NO_7S$ (MH^+) requires 428.0991, found 428.0971. *NMR spectroscopic data in good agreement with literature data.*[50]

Methyl (*2RS*)-2-*N*-(*tert*-butoxycarbonyl)-3-(*p*-trifluoromethylsulphonyloxy)phenyl-propanoate *138*

Synthesised in an analogous manner to the (*S*)-isomer, from methyl (2*RS*)-2-*N*-(*tert*-butoxycarbonyl)-3-(*p*-hydroxy)phenyl-propanoate **179**. Thus, phenol *rac*-**179** (4.90 g, 16.6 mmol), pyridine (6.70 cm^3, 83.0 mmol), trifluoromethanesulphonic anhydride (3.35 cm^3, 19.9 mmol) in anhydrous DCM (100 cm^3) were stirred at 0 °C for 35 hours. The residue was chromatographed on silica gel [hexane:EtOAc (88:12)] affording the title compound as a colourless oil which crystallised on standing (6.10 g, 86%), mp 78-79 °C. *NMR spectroscopic data identical to that obtained for* ***138***.

Methyl (2*S*)-2-*N*-(*tert*-butoxycarbonyl)-3-[*p*-(*p*-vinylphenyl)phenyl]-propanoate *180*

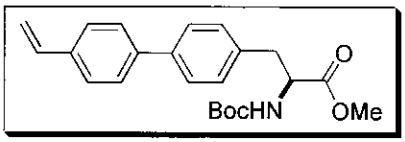

Method E :

$Pd(OAc)_2$ (110 mg, 0.490 mmol) and PPh_3 (370 mg, 1.40 mmol) were dissolved in anhydrous toluene (200 cm^3) and stirred under a flow of argon at room temperature for 1 hour. This mixture was then added dropwise to a suspension of the triflated ester **138** (10.0 g, 23.4 mmol), vinyl boronic acid **159** (6.92 g, 46.8 mmol) and anhydrous potassium carbonate (4.85 g, 35.1 mmol) in anhydrous toluene (150 cm^3) which had also been purged with argon for 15 minutes. The reaction mixture was heated to 85 °C for 20 hours before being filtered through celite and washed with EtOAc (300 cm^3). The combined organic layer was washed sequentially with saturated aqueous $NaHCO_3$ (240 cm^3), water (240 cm^3), 10% aqueous citric acid (240 cm^3), water (240 cm^3) and brine (240 cm^3). The organic phase was dried (Na_2SO_4) and concentrated under reduced pressure. The residue was chromatographed on silica gel [DCM]. The crude product was subsequently recrystallised from hexane affording the title compound as a white solid (5.46 g, 61%), R_f [DCM:MeOH (95:5)] 0.92; mp 110 °C; $[\alpha]_D$ +61.6 (*c* 0.6, $CHCl_3$); ν_{max} ($CHCl_3$ soln.)/cm^{-1} 3429, 3365, 2979, 1740, 1712, 1498, 1366, 1166, 756; δ_H (250 MHz, $CDCl_3$) 7.57-7.44 and 7.25-7.17 (8H, m, Ar*H*), 6.75 (1H, dd, *J* 17.6, 10.9, CH_2=C*H*), 5.78 (1H, dd, *J* 17.6, 0.9, C$H_X$$H_Y$=CH), 5.27 (1H, dd, *J* 10.9, 0.9, $CH_X$$H_Y$=CH), 5.02 (1H, d, *J* 7.7, N*H*), 4.62 (1H, d, *J* 7.9, C*H*N), 3.73 (3H, s, O*Me*), 3.19-3.05 (2H, m, CH_2Ar), 1.42 (9H, s, C(*Me*)$_3$); δ_C (62.9 MHz, $CDCl_3$) 172.2 (C), 155.0 (C), 139.9 (C), 139.3 (C), 136.4 (C), 136.2 (C), 135.0 (CH), 129.6 (2 × CH), 126.9 (4 × CH), 126.5 (2 × CH), 113.8 (CH_2), 79.9 (C), 54.2 (CH), 52.2 (CH_3), 37.8 (CH_2), 28.2 (3 × CH_3); m/z (FAB) 382 (MH^+, 7%), 326 (25), 193 (25), 154 (100), 57 (28); HRMS (FAB) $C_{23}H_{28}NO_4$ (MH^+) requires 382.2018, found 382.2004; chiral

HPLC analysis using HP1100 (Hewlett Packard) instrument equipped with 'Chiralizer' attached to chemstation, HP1100 UV/diode array detector set to 220 nm, Whelk-01 column with a flow rate of 1.0 cm^3 min^{-1}, column internal diameter 4.6 mm, column length 250 mm, [heptane:ethanol (95:5)], (*S* enantiomer) R_t 11.5 minutes, (*R* enantiomer) R_t 12.2 minutes, e.e. ≥ 99.8% *S*.

Methyl (*2RS*)-2-*N*-(*tert*-butoxycarbonyl)-3-[*p*-(*p*-vinylphenyl)phenyl]-propanoate *180*

Synthesised in an analogous manner to the (*S*)-isomer, from methyl (*2RS*)-2-*N*-(*tert*-butoxycarbonyl)-3-(*p*-trifluoromethylsulphonyloxy)phenyl-propanoate **138**. Thus, $Pd(OAc)_2$ (32 mg, 0.14 mmol), PPh_3 (110 mg, 0.419 mmol), triflated ester *rac*-**138** (3.00 g, 7.02 mmol), vinyl boronic acid **159** (2.08 g, 14.0 mmol) and anhydrous potassium carbonate (1.46 g, 10.5 mmol) in anhydrous toluene (80 cm^3) were heated to 85 °C for 16 hours. The residue was chromatographed on silica gel [hexane:EtOAc (90:10)] affording the title compound as a white solid (1.46 g, 55%), mp 118-119 °C; chiral HPLC analysis using HP1100 (Hewlett Packard) instrument equipped with 'Chiralizer' attached to chemstation, HP1100 UV/diode array detector set to 220 nm, Whelk-01 column with a flow rate of 1.0 cm^3 min^{-1}, column internal diameter 4.6 mm, column length 250 mm, [heptane:ethanol (95:5)], (*S* enantiomer) R_t 11.5 minutes, (*R* enantiomer) R_t 12.2 minutes. *NMR spectroscopic data identical to that obtained for* ***180***.

Methyl (2*S*)-3-biphenyl-2-*N*-(*tert*-butoxycarbonyl)-propanoate *195*

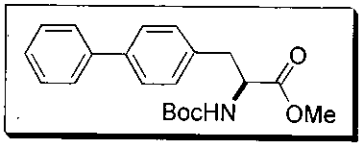

Synthesised in an analogous manner to the vinyl methyl ester **180**, from the Suzuki coupling of phenyl boronic acid and methyl (*2S*)-2-*N*-(*tert*-butoxycarbonyl)-3-(*p*-trifluoromethylsulphonyloxy)phenyl-propanoate **138**. Following the protocol described in Method E, $Pd(OAc)_2$ (32 mg, 0.14 mmol), PPh_3 (110 mg, 0.419 mmol), triflated ester **138** (3.00 g, 7.02 mmol), phenyl boronic acid (1.71 g, 14.0 mmol) and anhydrous potassium carbonate (1.46 g, 10.5 mmol) in anhydrous toluene (80 cm^3) were heated to 85 °C for 16 hours. The residue was chromatographed on silica gel [DCM] affording the title compound as a colourless oil which crystallised on standing (1.37 g, 55%), R_f [DCM] 0.20; mp 85 °C [lit.,[50] mp 83-85 °C]; $[\alpha]_D$ +57.5 (*c* 1.0, $CHCl_3$) [lit.,[50] $[\alpha]_D$ +54.8 (*c* 1.0, $CHCl_3$)]; δ_H (250 MHz, $CDCl_3$) 7.59-7.17 (9H, m, Ar*H*), 5.03 (1H, d, *J* 8.2, N*H*), 4.62 (1H, m, C*H*N), 3.73 (3H, s, O*Me*), 3.19-3.05 (2H, m, CH_2Ar), 1.42 (9H, s, C(*Me*)$_3$); δ_C (62.9 MHz, $CDCl_3$) 172.2 (C), 155.0 (C), 140.7 (C), 139.8 (C), 135.0 (C), 129.6 (2 × CH), 128.7 (2 × CH), 127.2 (3 × CH), 126.9 (2 × CH), 79.9 (C), 54.3 (CH), 52.1 (CH_3), 37.9 (CH_2), 28.2 (3 × CH_3); m/z (FAB) 356 (MH^+, 4%), 300 (43), 256 (100), 238 (73), 167 (59), 57 (75); HRMS (FAB) $C_{21}H_{26}NO_4$ (MH^+) requires 356.1862, found 356.1864. *NMR spectroscopic data in good agreement with literature data.*[50]

(3*S*)-3-*N*-(*tert*-Butoxycarbonyl)-2-methyl-4-[*p*-(*p*-vinylphenyl)phenyl]-butan-2-ol *181*

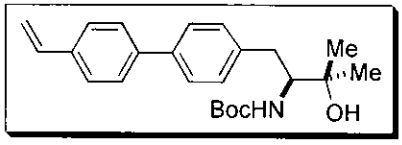

A solution of iodomethane (10.03 cm^3, 161.2 mmol) in anhydrous ether (240 cm^3) was slowly added to magnesium turnings (4.070 g, 167.5 mmol). The mixture was heated to reflux for 1.5 hours and allowed to cool to 40 °C before addition of the ester **180** (6.027 g, 15.80 mmol) in anhydrous ether (180 cm^3) *via* cannulation. The reaction mixture was heated to reflux for 1 hour before being quenched with saturated aqueous NH_4Cl (30 cm^3). The organic phase was separated and the aqueous phase was extracted with DCM (3 × 300 cm^3). The combined organic extracts were dried (Na_2SO_4) and concentrated under reduced pressure. The residue was recrystallised from DCM / hexane providing the title compound as a white solid (4.960 g, 82%), R_f [DCM:MeOH (90:10)] 0.51; mp 150-151 °C; $[\alpha]_D$ -69.0 (*c* 2.0, $CHCl_3$); ν_{max} ($CHCl_3$ soln.)/cm^{-1} 3377, 2980, 1669, 1529, 1172, 757; δ_H (200 MHz, $CDCl_3$) 7.52-7.45 and 7.29-7.26 (8H, m, Ar*H*), 6.76 (1H, dd, *J* 17.5, 10.8, CH_2=C*H*), 5.79 (1H, d, *J* 17.5, CH_XH$_Y$=CH), 5.27 (1H, d, *J* 10.8, CH$_X$$H_Y$=CH), 4.66 (1H, d, *J* 9.2, N*H*), 3.74-3.70 (1H, m, C*H*N), 3.12 (1H, d, *J* 13.8, CH_AH$_B$Ar), 2.68 (1H, d, *J* 13.8, CH$_A$$H_B$Ar), 2.58 (1H, br s, O*H*), 1.30 (15H, m, C(*Me*)$_3$ and 2 × *Me*); δ_C (50.3 MHz, $CDCl_3$) 156.5, 140.4, 138.6, 138.2, 136.4 (2C), 129.6 (2C), 127.0 (2C), 126.8 (2C), 126.6 (2C), 113.8, 79.4, 72.9, 60.3, 35.5, 28.1 (3C), 27.5, 26.5; m/z (FAB) 382 (MH^+, 2%), 373 (5), 309 (9), 301 (14), 193 (43), 57 (100); HRMS (FAB) $C_{24}H_{32}NO_3$ (MH^+) requires 382.2382, found 382.2399; chiral HPLC analysis using HP1100 (Hewlett Packard) instrument equipped with 'Chiralizer' attached to chemstation, HP1100 UV/diode array detector set to 220 nm, Chiracel OD-H column with a flow rate of 1.0 cm^3 min^{-1}, column internal diameter 4.6 mm, column length 250 mm, [heptane:ethanol (95:5)], (*R* enantiomer) R_t 5.6 minutes, (*S* enantiomer) R_t 6.2 minutes, e.e. ≥ 99.8% *S*.

(*3RS*)-3-*N*-(*tert*-Butoxycarbonyl)-2-methyl-4-[*p*-(*p*-vinylphenyl)phenyl]-butan-2-ol *181*

Synthesised in an analogous manner to the (*S*)-isomer, from methyl (*2RS*)-2-*N*-(*tert*-butoxycarbonyl)-3-[*p*-(*p*-vinylphenyl)phenyl]-propanoate **180**. Thus, iodomethane (2.26 cm^3, 36.4 mmol), magnesium turnings (919 mg, 37.8 mmol), ester *rac*-**180** (1.36 g, 3.57 mmol) in anhydrous ether (60 cm^3) were heated to reflux for 16 hours. The residue was chromatographed on silica gel [gradient elution DCM:MeOH (100:0 to 98:2)] providing the title compound as a white solid (750 mg, 55%), mp 158 °C; chiral HPLC analysis using HP1100 (Hewlett Packard) instrument equipped with 'Chiralizer' attached to chemstation, HP1100 UV/diode array detector set to 220 nm, Chiracel OD-H column with a flow rate of 1.0 cm^3 min^{-1}, column internal diameter 4.6 mm, column length 250 mm, [heptane:ethanol (95:5)], (*R* enantiomer) R_t 5.6 minutes, (*S* enantiomer) R_t 6.2 minutes. *NMR spectroscopic data identical to that obtained for **181**.*

(3*S*)-4-Biphenyl-3-*N*-(*tert*-butoxycarbonyl)-2-methyl-butan-2-ol *196*

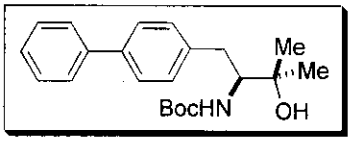

Synthesised in an analogous manner to the vinyl amino alcohol **181**, from the reaction of methyl (2*S*)-2-*N*-(*tert*-butoxycarbonyl)-3-biphenyl-propanoate **195** with methyl Grignard reagent. Thus, iodomethane (1.84 cm^3, 29.9 mmol), magnesium turnings (736 mg, 30.1 mmol), ester **195** (1.00 g, 2.81 mmol) in anhydrous ether (100 cm^3) were heated to reflux for 1 hour. The residue was recrystallised from ether affording the title compound as a white solid (770 mg, 77%), R_f [hexane:EtOAc (80:20)] 0.14; mp 137-138 °C; $[\alpha]_D$ -61.2 (*c* 1.0, $CHCl_3$); ν_{max} ($CHCl_3$ soln.)/cm^{-1} 3442, 2980, 1700, 1503, 1368, 1169; δ_H (250 MHz, $CDCl_3$) 7.58-7.25 (9H, m, Ar*H*), 4.65 (1H, d, *J* 9.6, N*H*), 3.80-3.69 (1H, m, C*H*N), 3.13 (1H, dd, *J* 14.2, 3.4,

C*H*$_A$H$_B$Ar), 2.71 (1H, br s, O*H*), 2.62 (1H, d, *J* 14.2, CH$_A$*H*$_B$Ar), 1.31 (15H, m, C(*Me*)$_3$ and 2 × *Me*); δ_C (62.9 MHz, $CDCl_3$) 156.3 (C), 141.0 (C), 139.0 (C), 137.9 (C), 129.5 (CH), 128.6 (3 × CH), 126.9 (5 × CH), 79.2 (C), 72.8 (C), 60.2 (CH), 35.3 (CH_2), 28.1 (3 × CH_3), 27.4 (CH_3), 26.5 (CH_3); m/z (FAB) 356 (MH^+, 19%), 300 (57), 282 (75), 167 (100), 57 (91); HRMS (FAB) $C_{22}H_{30}NO_3$ (MH^+) requires 356.2225, found 356.2225; Anal. Calcd. for $C_{22}H_{29}NO_3$: C, 74.33; H, 8.22; N, 3.94, found C, 73.82; H, 8.24; N, 4.06.

(3*S*)-3-Amino-2-methyl-4-[*p*-(*p*-vinylphenyl)phenyl]-butan-2-ol *167*

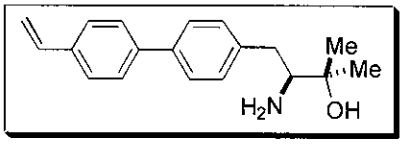

Method F :

3N aqueous HCl (40.0 cm^3, 119 mmol) was added to a solution of the Boc-protected amino alcohol **181** (3.50 g, 9.17 mmol) in acetonitrile (110 cm^3). The reaction mixture was stirred at room temperature for 67 hours before being diluted with water (50 cm^3) and neutralised to pH 7 with saturated aqueous Na_2CO_3. The aqueous layer was extracted with DCM (3 × 200 cm^3) and the combined organic extracts were dried (Na_2SO_4) and concentrated under reduced pressure. The residue was recrystallised from DCM / hexane affording the title compound as a white solid (2.33 g, 87%), R_f [DCM:MeOH (90:10)] 0.23; mp 114-115 °C; $[\alpha]_D$ -44.2 (*c* 0.5, MeOH); ν_{max} ($CHCl_3$ soln.)/cm^{-1} 3402, 3343, 3280, 2976, 1497, 1389; δ_H (200 MHz, CD_3OD) 7.57-7.44 and 7.32-7.28 (8H, m, Ar*H*), 6.75 (1H, dd, *J* 17.8, 10.8, CH_2=C*H*), 5.79 (1H, d, *J* 17.8, C*H*$_X$H$_Y$=CH), 5.22 (1H, d, *J* 10.8, CH$_X$*H*$_Y$=CH), 3.02 (1H, dd, *J* 13.2, 2.7, C*H*$_A$H$_B$Ar), 2.88 (1H, dd, *J* 10.7, 2.7, C*H*N), 2.34 (1H, dd, *J* 13.2, 10.7, CH$_A$*H*$_B$Ar), 1.27 (3H, s, *Me*), 1.23 (3H, s, *Me*); δ_C (62.9 MHz, CD_3OD) 139.6, 138.7, 138.0, 136.0, 135.8, 128.9 (2C), 126.1 (2C), 126.0 (2C), 125.8 (2C), 112.1, 71.5, 61.3, 37.1, 24.7, 22.9; m/z (FAB) 282 (MH^+, 56%), 264 (17), 222 (19), 193 (100), 88 (31), 43

(27); HRMS (FAB) $C_{19}H_{24}NO$ (MH^+) requires 282.1858, found 282.1858; Anal. Calcd. for $C_{19}H_{23}NO$: C, 81.10; H, 8.24; N, 4.98, found C, 80.59; H, 8.16; N, 4.73.

Method G :

Trifluoroacetic acid (0.525 cm^3, 6.82 mmol) was added a solution of the Boc-protected amino alcohol **181** (200 mg, 0.524 mmol) in anhydrous DCM (4 cm^3). The reaction mixture was stirred at room temperature for 1.5 hours before being diluted with water (7 cm^3) and neutralised to pH 7 with saturated aqueous Na_2CO_3. The organic phase was separated and the aqueous phase was extracted with DCM (3 × 20 cm^3). The combined organic extracts were dried (Na_2SO_4) and filtered through celite removing an insoluble jelly presumed to be oligomerised material. The filtrate was concentrated under reduced pressure and the residue was chromatographed on silica gel [DCM] providing the title compound as a white solid (10 mg, 7%). *NMR spectroscopic data identical to that obtained for **167** in **Method F**.*

(3*S*)-3-Amino-4-biphenyl-2-methyl-butan-2-ol *192*

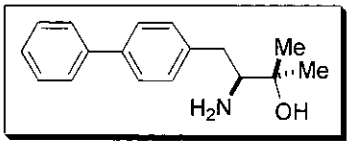

Synthesised in an analogous manner to the vinyl amino alcohol **167**, removing the Boc-protecting group from (3*S*)-4-biphenyl-3-*N*-(*tert*-butoxycarbonyl)-2-methyl-butan-2-ol **196**. Following the protocol described in Method G, Boc-protected amino alcohol **196** (208 mg, 0.585 mmol), trifluoroacetic acid (0.586 cm^3, 7.61 mmol) and anhydrous DCM (4 cm^3) were stirred at room temperature for 1.5 hours affording the title compound as a white solid (130 mg, 87%), R_f [DCM:MeOH (90:10)] 0.23; mp 65-66 °C; $[\alpha]_D$ -40.2 (*c* 1.0, $CHCl_3$); ν_{max} (nujol)/cm^{-1} 3404, 3341, 3270, 1487, 754; δ_H (200 MHz, CD_3OD) 7.60-7.54 and 7.44-7.29 (9H, m, Ar*H*), 3.03 (1H, d, *J* 13.4,

CH_AH_BAr), 2.89 (1H, d, *J* 11.0, C*H*N), 2.35 (1H, dd, *J* 13.4, 11.0, CH_AH_BAr), 1.28 (3H, s, *Me*), 1.24 (3H, s, *Me*); δ_C (50.3 MHz, CD_3OD) 142.3, 140.7 (2C), 130.8 (2C), 129.9 (2C), 128.2 (3C), 127.9 (2C), 73.5, 63.2, 39.0, 26.6, 24.8; m/z (FAB) 256 (MH^+, 85%), 238 (35), 196 (20), 167 (100), 88 (24), 43 (28); HRMS (FAB) $C_{17}H_{22}NO$ (MH^+) requires 256.1701, found 256.1706.

N,N-Dimethylation of *167*: Attempted synthesis of (3*S*)-*N,N*-3-Dimethylamino-2-methyl-4-[*p*-(*p*-vinylphenyl)phenyl]-butan-2-ol *162*

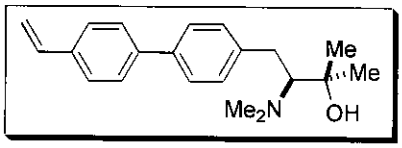

Method H :

Amino alcohol **167** (88 mg, 0.31 mmol) was dissolved in acetonitrile (7 cm^3) and formaldehyde (0.24 cm^3, 38% aq. solution, 3.1 mmol), sodium cyanoborohydride (59 mg, 0.94 mmol) and glacial acetic acid (0.030 cm^3, 0.52 mmol) were added sequentially. The reaction mixture was stirred at room temperature for 10 minutes before being diluted with water (5 cm^3). The aqueous layer was extracted with ether (3 × 15 cm^3) and the combined organic extracts were washed with 1N aqueous NaOH (3 × 10 cm^3) and brine (10 cm^3). The organic phase was dried (Na_2SO_4) and concentrated under reduced pressure affording 112 mg of a yellow oil. A ^1H NMR spectrum ($CDCl_3$) of the yellow oil gave the ratio of title compound **162** : oxazolidine by-product **183** as 11:1 with other impurities present. The material was dissolved in formic acid (2.0 cm^3, 53 mmol) and heated to reflux for 16 hours. The reaction mixture was basified to pH 9 with 10% aqueous ammonia and extracted with EtOAc (3 × 10 cm^3). The combined organic extracts were washed with water (10 cm^3), brine (10 cm^3), dried (Na_2SO_4) and concentrated under reduced pressure affording a yellow oil (88 mg, 45% of total yield). ^1H NMR analysis determined that

this material was not the title compound **162**. The impurity was subsequently identified as the diastereomeric oligomerised product dimer **189**.

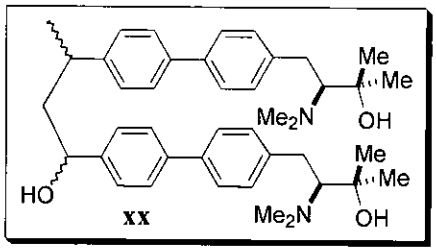

xx

Data for **189**:

δ_H (200 MHz, $CDCl_3$) 7.59-7.26 (16H, m, Ar*H*), 6.47 (0.9H, br s, O*H*), 6.38 (0.1H, br s, O*H*), 3.80-3.30 (1H, m, C*H*OH), 3.03-2.68 (7H, m, CH_2Ar × 2 and C*H*N × 2 and ArC*H*Me), 2.35 (12H, s, N*Me* × 4), 1.63 (0.3H, d, *J* 7.0, ArCH*Me*), 1.52 (2.7, d, *J* 7.0, ArCH*Me*), 1.41-1.19 (2H, m, ArCHCH_2), 1.22 (6H, s, *Me* × 2), 1.19 (6H, s, *Me* × 2).

(3*S*)-4-Biphenyl-*N*,*N*-3-dimethylamino-2-methyl-butan-2-ol *193*

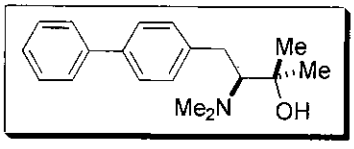

Synthesised in an analogous manner to the vinyl *N*,*N*-dimethylated amino alcohol **162**, from the *N*,*N*-dimethylation of (3*S*)-3-amino-4-biphenyl-2-methyl-butan-2-ol **192**. Following the protocol described in Method H, amino alcohol **192** (200 mg, 0.783 mmol), formaldehyde (0.606 cm^3, 38% aq. solution, 7.83 mmol), sodium cyanoborohydride (148 mg, 2.35 mmol), glacial acetic acid (0.080 cm^3, 1.4 mmol) and acetonitrile (10 cm^3) were stirred at room temperature for 10 minutes. A ^1H NMR spectrum ($CDCl_3$) of the yellow oil obtained (230 mg) gave the ratio of title compound **193** : oxazolidine by-product **201** as 8:1 with other impurities present. The material was dissolved in formic acid (2.00 cm^3, 53.0 mmol) and heated to reflux for 16 hours. The residue obtained was chromatographed on silica gel

[DCM:MeOH (95:5)] affording the title compound as a white solid (202 mg, 91%), R_f [DCM:MeOH (90:10)] 0.46; mp 57-58 °C; $[\alpha]_D$ -42.1 (*c* 1.0, $CHCl_3$); ν_{max} ($CHCl_3$ soln.)/cm^{-1} 3268, 2977, 1603, 1489, 1387; δ_H (200 MHz, $CDCl_3$) 7.73-7.26 (9H, m, Ar*H*), 3.01-2.69 (3H, m, CH_2Ar and C*H*N), 2.35 (6H, s, N*Me* × 2), 1.23 (3H, s, *Me*), 1.20 (3H, s, *Me*); δ_C (50.3 MHz, $CDCl_3$) 140.8, 139.9, 139.0, 129.5 (2C), 128.7 (2C), 127.1 (3C), 126.9 (2C), 74.0, 70.9, 43.6 (2C), 31.3, 29.1, 25.0; m/z (FAB) 284 (MH^+, 81%), 224 (100), 167 (86), 116 (54); HRMS (FAB) $C_{19}H_{26}NO$ (MH^+) requires 284.2014, found 284.2014; Anal. Calcd. for $C_{19}H_{25}NO$: C, 80.52; H, 8.89; N, 4.94, found C, 80.39; H, 9.04; N, 5.08.

Method I :

Anhydrous potassium carbonate (352 mg, 2.55 mmol) was added to a solution of the amino alcohol **192** (130 mg, 0.509 mmol) in anhydrous acetonitrile (4 cm^3). The reaction mixture was stirred vigorously for 15 minutes before dropwise addition of iodomethane (0.127 cm^3, 2.04 mmol). The suspension was further stirred at room temperature for 20 hours before being diluted with water (10 cm^3). The aqueous layer was extracted with EtOAc (3 × 20 cm^3) and the combined organic extracts were dried (Na_2SO_4) and concentrated under reduced pressure. The residue was chromatographed on silica gel [DCM:MeOH (95:5)] affording the title compound as a white solid (47 mg, 33%). *NMR spectroscopic data identical to that obtained for **193** in **Method H**.*

(3*S*)-4-Biphenyl-2-methyl-*N*,*N*,*N*-3-trimethylamino-butan-2-ol iodide salt *200*

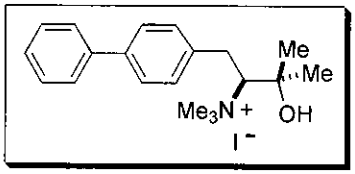

Small traces of a lower R_f compound were isolated during chromatography of the above crude reaction mixture. Approximately 17 mg (8% of total yield) of the impurity were isolated and subsequently identified as **200**.

Data for **200**:

Obtained as a white solid,

R_f [DCM:MeOH:Et_3N (90:5:5)] 0.47; δ_H (200 MHz, $CDCl_3$) 7.62-7.33 (9H, m, Ar*H*), 4.51-4.40 (1H, m, C*H*N), 4.32 (1H, br s, O*H*), 3.48 (9H, s, N*Me* × 3), 3.41-3.03 (2H, m, CH_2Ar), 1.66 (3H, s, *Me*), 1.59 (3H, s, *Me*).

(4*S*)-2,2-Dimethyl-5,5-dimethyl-4-[*p*-(*p*-vinylphenyl)benzyl]-oxazolidine *168*

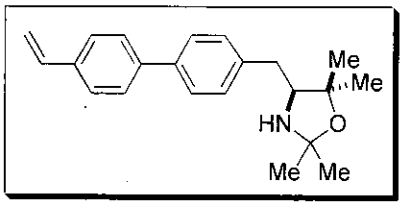

Amino alcohol **167** (25 mg, 0.098 mmol) was dissolved in acetone (5 cm^3) and stirred at room temperature for 20 hours. The reaction mixture was concentrated under reduced pressure affording the title compound as a white solid (29 mg, 100%), R_f [DCM:MeOH (90:10)] 0.64 (compound decomposes to amino alcohol **167** on t.l.c. plate giving predominantly R_f 0.23 material); mp 67-68 °C; $[\alpha]_D$ +5.0 (*c* 1.0, $CHCl_3$); ν_{max} ($CHCl_3$ soln.)/cm^{-1} 3400, 2971, 1628, 1498, 754; δ_H (200 MHz, $CDCl_3$)

7.49-7.37 and 7.28-7.17 (8H, m, Ar*H*), 6.67 (1H, dd, *J* 17.6, 10.8, CH_2=C*H*), 5.70 (1H, d, *J* 17.6, CH_XH$_Y$=CH), 5.19 (1H, d, *J* 10.8, CH$_X$*H*$_Y$=CH), 3.31 (1H, t, *J* 7.0, C*H*N), 2.66 (2H, d, *J* 7.3, CH_2Ar), 1.95 (1H, br s, N*H*), 1.36 (3H, s, *Me*CNH), 1.23 (3H, s, *Me*CNH), 1.11 (3H, s, *Me*), 1.03 (3H, s, *Me*); δ_C (50.3 MHz, $CDCl_3$) 140.3, 138.8, 138.2, 136.4 (2C), 129.1 (2C), 127.0 (4C), 126.6 (2C), 113.8, 92.8, 80.6, 67.0, 35.5, 29.5, 28.4, 27.3, 23.2; m/z (FAB) 322 (MH^+, 97%), 264 (50), 193 (100), 128 (72), 70 (33); HRMS (FAB) $C_{22}H_{28}NO$ (MH^+) requires 322.2171, found 322.2172.

(4*S*)-2,2-Dimethyl-5,5-dimethyl-4-[*p*-(phenyl)benzyl]-oxazolidine *194*

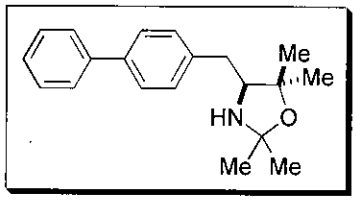

Synthesised in an analogous manner to the vinyl oxazolidine **168**, from the reaction of (3*S*)-3-amino-4-biphenyl-2-methyl-butan-2-ol **192** with acetone. Thus, amino alcohol **192** (50 mg, 0.20 mmol) was dissolved in acetone (10 cm^3) and stirred at room temperature for 21 hours. The reaction mixture was concentrated under reduced pressure affording the title compound as a white solid (58 mg, 100%), R_f [DCM:MeOH (90:10)] 0.64 (compound decomposes to amino alcohol **192** on t.l.c. ν_{max} ($CHCl_3$ soln.)/cm^{-1} 3391, 2978, 1602, 1489, 1268; δ_H (200 plate giving predominantly R_f 0.23 material); mp 58-59 °C; $[\alpha]_D$ +5.1 (*c* 1.0, $CHCl_3$); MHz, $CDCl_3$) 7.62-7.55 and 7.48-7.34 (9H, m, Ar*H*), 3.42 (1H, t, *J* 7.0, C*H*N), 2.76 (2H, d, *J* 7.0, CH_2Ar), 1.47 (3H, s, *Me*CNH), 1.34 (3H, s, *Me*CNH), 1.21 (3H, s, *Me*), 1.13 (3H, s, *Me*); δ_C (50.3 MHz, $CDCl_3$) 140.9 (C), 139.3 (C), 138.2 (C), 129.1 (2 × CH), 128.8 (2 × CH), 127.3 (2 × CH), 127.1 (CH), 127.0 (2 × CH), 92.9 (C), 80.7 (C), 67.0 (CH), 35.5 (CH_2), 29.5 (CH_3), 28.5 (CH_3), 27.3 (CH_3), 23.2 (CH_3); m/z (FAB) 296 (MH^+, 69%), 238 (63), 167 (100), 128 (64), 70 (47); HRMS (FAB) $C_{20}H_{26}NO$ (MH^+) requires 296.2014, found 296.2014.

(2*S*)-2-*N*-(*tert*-Butoxycarbonyl)-3-[*p*-(*p*-vinylphenyl)phenyl]-propan-1-ol

206

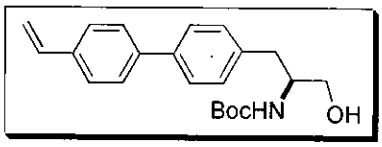

Ester **180** (100 mg, 0.26 mmol) and sodium borohydride (22 mg, 0.59 mmol) were dissolved in anhydrous THF (2 cm^3) and heated to 55 °C. Anhydrous methanol (0.21 cm^3) was added dropwise and the solution was further heated at 55 °C for 21 hours. The reaction mixture was diluted with water (4 cm^3) and the aqueous layer was extracted with EtOAc (2 × 10 cm^3). The combined organic extracts were washed with brine (10 cm^3), dried (Na_2SO_4) and concentrated under reduced pressure. Recrystallisation from hexane provided the title compound as a white solid (83 mg, 89%), R_f [DCM:MeOH (95:5)] 0.32; δ_H (200 MHz, $CDCl_3$) 7.57-7.45 and 7.30-7.26 (8H, m, Ar*H*), 6.75 (1H, dd, *J* 17.4, 10.9, CH_2=C*H*), 5.79 (1H, dd, *J* 17.4, 0.9 CH_XH_Y=CH), 5.27 (1H, dd, *J* 10.9, 0.9, CH_XH_Y=CH), 4.80 (1H, d, *J* 8.2, N*H*), 3.90 (1H, m, C*H*N), 3.74-3.54 (2H, m, CH_2OH), 2.88 (2H, d, *J* 7.2, CH_2Ar), 1.42 (9H, s, C(*Me*)$_3$); δ_C (62.9 MHz, $CDCl_3$) 156.0 (C), 140.0 (C), 138.8 (C), 136.9 (C), 136.4 (C), 136.2 (CH), 129.6 (2 × CH), 126.9 (4 × CH), 126.5 (2 × CH), 113.7 (CH_2), 79.7 (C), 64.1 (CH_2), 53.6 (CH), 37.0 (CH_2), 28.2 (3 × CH_3); m/z (FAB) 354 (MH^+, 5%), 193 (10), 154 (100); HRMS (FAB) $C_{22}H_{28}NO_3$ (MH^+) requires 354.2069, found 354.2072.

(4*S*)-4-[*p*-(*p*-Vinylphenyl)benzyl]-oxazolidin-2-one *203*

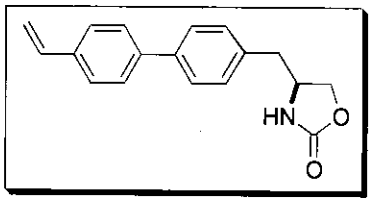

Thionyl chloride (0.049 cm^3, 0.68 mmol) was added dropwise to a solution of the Boc-protected amino alcohol **206** (30 mg, 0.085 mmol) in anhydrous THF (4 cm^3) at 0 °C. The reaction mixture was stirred at 0 °C for 98 hours before being concentrated under reduced pressure. The residue was recrystallised from $CHCl_3$ / hexane affording the title compound as a white solid (16 mg, 67%), R_f [DCM:MeOH (90:10)] 0.58; mp 180-182 °C; δ_H (250 MHz, $CDCl_3$) 7.58-7.45 and 7.26-7.22 (8H, m, Ar*H*), 6.75 (1H, dd, *J* 17.6, 10.9, CH_2=C*H*), 5.79 (1H, dd, *J* 17.6, 0.8, C$H_X$$H_Y$=CH), 5.51 (1H, br s, N*H*), 5.28 (1H, dd, *J* 10.9, 0.8, $CH_X$$H_Y$=CH), 4.48 (1H, t, *J* 7.7, C*H*N), 4.21-4.05 (2H, m, CH_2O), 2.91 (2H, d, *J* 6.6, CH_2Ar); δ_C (62.9 MHz, $CDCl_3$) 159.0 (C), 139.7 (C), 136.7 (C), 136.2 (C and CH), 134.9 (C), 129.3 (2 × CH), 127.4 (2 × CH), 126.9 (2 × CH), 126.6 (2 × CH), 113.9 (CH_2), 69.5 (CH_2), 53.6 (CH), 41.0 (CH_2); m/z (FAB) 280 (MH^+, 91%), 193 (62), 91 (100), 73 (52), 57 (70); HRMS (FAB) $C_{18}H_{18}NO_2$ (MH^+) requires 280.1338, found 280.1338.

(4*S*)-5,5-Dimethyl-4-[*p*-(*p*-vinylphenyl)benzyl]-oxazolidin-2-one *204*

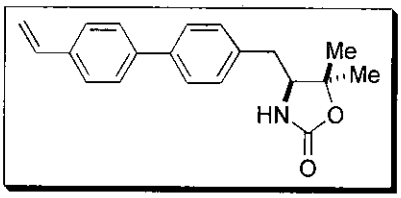

Potassium *tert*-butoxide (1.928 g, 17.18 mmol) was added to a solution of the Boc-protected amino alcohol **181** (4.370 g, 11.45 mmol) in anhydrous THF (100 cm^3) at 0 °C. The reaction mixture was further stirred at 0 °C for 1 hour before being quenched with saturated aqueous NH_4Cl (35 cm^3). The aqueous layer was extracted

with EtOAc (3 × 100 cm^3) and the combined organic extracts were washed with brine (2 × 35 cm^3) and dried (Na_2SO_4). Concentration under reduced pressure afforded the title compound as a pale yellow solid (3.480 g, 99%) which was used in subsequent stages without further purification, R_f [DCM:MeOH (90:10)] 0.79; mp 193-194 °C; $[\alpha]_D$ -139.0 (*c* 1.0, $CHCl_3$); ν_{max} (KBr disc)/cm^{-1} 3441, 3238, 2979, 1753, 1496, 1303, 820; δ_H (200 MHz, $CDCl_3$) 7.59-7.46 and 7.27-7.23 (8H, m, Ar*H*), 6.76 (1H, dd, *J* 17.7, 10.9, CH_2=C*H*), 5.80 (1H, d, *J* 17.7, C$H_X$$H_Y$=CH), 5.28 (1H, d, *J* 10.9, C$H_X$$H_Y$=CH), 5.18 (1H, br s, N*H*), 3.72 (1H, dd, *J* 10.3, 4.4, C*H*N), 2.91-2.66 (2H, m, CH_2Ar), 1.48 (3H, s, *Me*), 1.46 (3H, s, *Me*); δ_C (50.3 MHz, $CDCl_3$) 158.0, 139.8, 139.6, 136.7, 136.3, 136.0, 129.3 (2C), 127.5 (2C), 127.0 (2C), 126.7 (2C), 114.0, 83.2, 62.9, 36.7, 27.5, 21.9; m/z (FAB) 308 (MH^+, 84%), 193 (100), 114 (10), 70 (12); HRMS (FAB) $C_{20}H_{22}NO_2$ (MH^+) requires 308.1651, found 308.1661; single crystal X-ray diffraction: see **appendix**.

(4*S*)-5,5-Dimethyl-4-[*p*-(phenyl)benzyl]-oxazolidin-2-one *207*

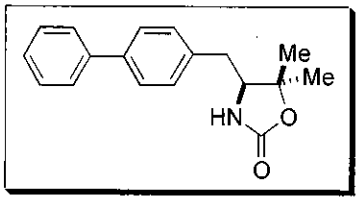

Synthesised in an analogous manner to the vinyl oxazolidinone **204**, from the reaction of (3*S*)-4-biphenyl-3-*N*-(*tert*-Butoxycarbonyl)-2-methyl-butan-2-ol **196** with potassium *tert*-butoxide. Thus, Boc-protected amino alcohol **196** (1.54 g, 4.33 mmol), potassium *tert*-butoxide (729 mg, 6.50 mmol) in anhydrous THF (60 cm^3) were stirred at 0 °C for 30 minutes affording the title compound as a pale yellow solid (1.16 g, 95%) which was used in subsequent stages without further purification, R_f [DCM:MeOH (90:10)] 0.79; mp 146-147 °C; $[\alpha]_D$ -125.7 (*c* 1.0, $CHCl_3$); ν_{max} ($CHCl_3$ soln.)/cm^{-1} 3449, 3011, 2987, 1754, 1488, 1404, 1376, 1300; δ_H (250 MHz, $CDCl_3$) 7.59-7.23 (9H, m, Ar*H*), 5.13 (1H, br s, N*H*), 3.72 (1H, dd, *J* 10.4, 4.1, C*H*N), 2.87 (1H, dd, *J* 13.4, 4.1, C$H_A$$H_B$Ar), 2.72 (1H, dd, *J* 13.4, 10.4, C$H_A$$H_B$Ar),

1.48 (3H, s, *Me*), 1.46 (3H, s, *Me*); δ_C (62.9 MHz, $CDCl_3$) 157.8 (C), 140.3 (C), 140.0 (C), 135.8 (C), 129.1 (2 × CH), 128.7 (2 × CH), 127.6 (2 × CH), 127.3 (CH), 126.8 (2 × CH), 83.1 (C), 62.9 (CH), 36.6 (CH_2), 27.4 (CH_3), 21.8 (CH_3); m/z (FAB) 282 (MH^+, 79%), 167 (100), 154 (49), 136 (36); HRMS (FAB) $C_{18}H_{20}NO_2$ (MH^+) requires 282.1494, found 282.1494.

(4*S*)-5,5-Dimethyl-3-(1'-oxopropyl)-4-[*p*-(phenyl)benzyl]-oxazolidin-2-one *208*

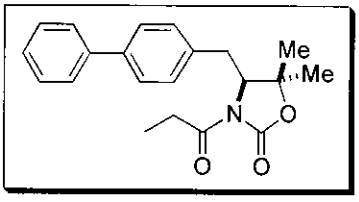

Butyllithium (0.26 cm^3, 1.6 *M* in hexane, 0.42 mmol) was added to a solution of the biaryl oxazolidinone **207** (78 mg, 0.28 mmol) in anhydrous THF (4 cm^3) at -78 °C. The reaction mixture was further stirred at -78 °C for 20 minutes before addition of propionyl chloride (0.036 cm^3, 0.42 mmol) in anhydrous THF (2 cm^3). The solution was stirred at -78 °C for 30 minutes and subsequently for 1 hour at room temperature before being quenched with saturated aqueous NH_4Cl (1 cm^3). The aqueous phase was extracted with EtOAc (3 × 10 cm^3) and the combined organic extracts were dried (Na_2SO_4). Concentration under reduced pressure afforded the title compound as a white solid (80 mg, 85%) which was used in subsequent stages without further purification, R_f [hexane:EtOAc (90:10)] 0.20; mp 106-107 °C; $[\alpha]_D$ -52.4 (*c* 1.0, $CHCl_3$); ν_{max} ($CHCl_3$ soln.)/cm^{-1} 3036, 2987, 1772, 1702, 1489, 1376; δ_H (200 MHz, $CDCl_3$) 7.60-7.26 (9H, m, Ar*H*), 4.54 (1H, dd, *J* 9.5, 3.5, C*H*N), 3.20 (1H, dd, *J* 14.3, 3.5, CH_AH_BAr), 3.01-2.86 (3H, m, CH_AH_BAr and CH_3CH_2), 1.41 (3H, s, *Me*), 1.39 (3H, s, *Me*), 1.16 (3H, t, *J* 7.3, CH_3CH_2); δ_C (62.9 MHz, $CDCl_3$) 174.2 (C), 152.5 (C), 140.4 (C), 139.5 (C), 135.9 (C), 129.3 (2 × CH), 128.6 (2 × CH), 127.2 (3 × CH), 126.8 (2 × CH), 82.1 (C), 63.4 (CH), 34.9 (CH_2), 29.2 (CH_2), 28.5 (CH_3), 22.2 (CH_3), 8.2 (CH_3); m/z (FAB) 338 (MH^+, 100%), 337 (40), 167 (27); HRMS (FAB)

$C_{21}H_{24}NO_3$ (MH^+) requires 338.1757, found 337.1756; single crystal X-ray diffraction: see **appendix**.

8.4 Experimental for Results and Discussion Part 3

1% Cross-linked 4 mmolg^{-1} chloromethylpolystyrene gel resin *3*

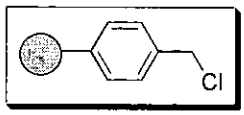

Method J :

General polymerisation methodology adapted from literature precedent.[4a] A dry 250 cm^3 3-necked flask equipped with overhead stirrer, condenser and septum was charged with distilled water (160 cm^3) which was subsequently degassed and purged with argon. PVA (1.60 g, 87-89% hydrolysed, average MW = 85000-146000) was added and the reaction mixture was stirred at 125 °C for 10 minutes before being cooled to room temperature. A second dry flask was charged with AIBN (250 mg, 1.52 mmol), styrene (6.38 cm^3, 55.7 mmol), divinylbenzene (0.428 cm^3, 2.40 mmol) and vinylbenzyl chloride (8.75 cm^3, 62.1 mmol) and flushed with argon. The monomer phase was added *via* cannulation over a period of 10 minutes to the aqueous phase which was stirred at 188 RPM. The reaction mixture was stirred at 188 RPM at room temperature for a further 10 minutes before being heated to 80 °C with constant stirring under argon for 18 hours. The polymer beads were collected by filtration through a 100 micron mesh sieve and washed with water (250 cm^3), THF (250 cm^3) and methanol (250 cm^3). The polymeric material was then dried under reduced pressure at 40 °C to constant mass affording the title polymer as white free flowing beads (5.81 g, 37%), ν_{max} (KBr disc)/cm^{-1} 3024, 2922, 1601, 1493, 1452, 759, 647; Anal. Calcd. for polymer: C, 79.19; H, 6.64; N, 0.00, found C, 79.33; H, 6.58; N, 0.00, loading = 3.97 mmolg^{-1}; Anal. Calcd. for polymer: Cl, 14.17, found Cl, 15.48, loading = 4.37 mmolg^{-1}; N_2 BET adsorption < 10 m^{2}g^{-1}; resin swelled to 4.0 times its own volume in DCM.

12% Cross-linked 0.5 mmolg^{-1} chloromethylpolystyrene macroporous resin *3*

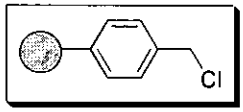

Method K :

A dry 500 cm^3 3-necked flask equipped with overhead stirrer, condenser and septum was charged with distilled water (160 cm^3) which was subsequently degassed and purged with argon. PVA (800 mg, 87-89% hydrolysed, average MW = 85000-146000) was added and the reaction mixture was stirred at 125 °C for 10 minutes before being cooled to room temperature. A second dry flask was charged with AIBN (250 mg, 1.52 mmol), styrene (11.9 cm^3, 102 mmol), divinylbenzene (6.22 cm^3, 34.9 mmol), vinylbenzyl chloride (1.09 cm^3, 7.76 mmol), THF (60 cm^3) and toluene (60 cm^3) and flushed with argon. The monomer phase was added *via* cannulation over a period of 10 minutes to the aqueous phase which was stirred at 350 RPM. The height of the paddle impeller was positioned ~ 3 cm below the surface of the reaction mixture as this depth was found to visually reduce horizontal flow. Stirring was then continued at room temperature for 10 minutes. The reaction mixture was then heated to 80 °C with constant stirring at 350 RPM under argon for 18 hours. The polymer beads were collected by filtration through a 100 micron mesh sieve and washed with water (500 cm^3), THF (500 cm^3) and methanol (500 cm^3). The polymeric material was then dried under reduced pressure at 40 °C to constant mass and sieved between 500 and 100 micron mesh sieves affording the title polymer as white free flowing beads (6.50 g, 40%), ν_{max} (KBr disc)/cm^{-1} 3024, 2922, 1601, 1493, 1452, 759, 647; Anal. Calcd. for polymer: C, 90.62; H, 7.60; N, 0.00, found C, 90.66; H, 7.54; N, 0.00, loading = 0.51 mmolg^{-1}; resin swelled to 3.5 times its own volume in DCM.

12% Cross-linked 0.5 mmolg^{-1} chloromethylpolystyrene macroporous resin *3*

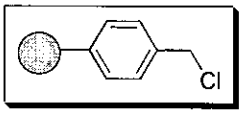

Method L :

A dry 500 cm^3 3-necked flask equipped with overhead stirrer, condenser and septum was charged with distilled water (160 cm^3) which was subsequently degassed and purged with argon. PVA (800 mg, 87-89% hydrolysed, average MW = 85000-146000) was added and the reaction mixture was stirred at 125 °C for 10 minutes before being cooled to 0 °C. A second dry flask was charged with THF (60 cm^3) and toluene (60 cm^3) and this was also degassed and purged with argon. AIBN (250 mg, 1.52 mmol), styrene (11.8 cm^3, 103 mmol), divinylbenzene (6.22 cm^3, 34.9 mmol) and vinylbenzyl chloride (1.09 cm^3, 7.76 mmol) were added to the THF / toluene solution with each of the monomers being washed with 1% aqueous NaOH (10 cm^3) and water (2 × 10 cm^3) immediately prior to use. The monomer phase was added *via* cannulation over a period of 10 minutes to the cooled aqueous phase which was stirred at 350 RPM. The height of the paddle impeller was positioned ~ 3 cm below the surface of the reaction mixture as this depth was found to visually reduce horizontal flow. Stirring was then continued at 0 °C for 1 hour. The reaction mixture was then heated to 80 °C with constant stirring at 350 RPM under argon for 18 hours. The polymer beads were collected by filtration through a 100 micron mesh sieve and washed with water (500 cm^3), THF (500 cm^3) and methanol (500 cm^3). The polymeric material was then dried under reduced pressure at 40 °C to constant mass and sieved between 500 and 100 micron mesh sieves affording the title polymer as white free flowing beads (4.99 g, 30%), ν_{max} (KBr disc)/cm^{-1} 3024, 2922, 1601, 1493, 1452, 759, 647; Anal. Calcd. for polymer: C, 90.62; H, 7.60; N, 0.00, found C, 90.42; H, 7.82; N, 0.00, loading = 0.50 mmolg^{-1}; resin swelled to 6.7 times its own volume in DCM.

12% Cross-linked 0.5 mmolg^{-1} oxazolidinone polymer *218*

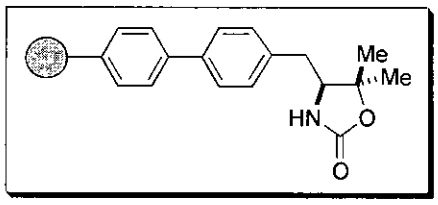

A dry 500 cm^3 3-necked flask equipped with overhead stirrer, condenser and septum was charged with distilled water (160 cm^3) which was subsequently degassed and purged with argon. PVA (800 mg, 87-89% hydrolysed, average MW = 85000-146000) was added and the reaction mixture was stirred at 125 °C for 10 minutes before being cooled to 0 °C. Two further dry flasks were separately charged with THF (60 cm^3) and toluene (60 cm^3), each being degassed and purged with argon. The oxazolidinone monomer **204** (2.39 g, 7.76 mmol) was added to the THF ensuring dissolution before addition of the toluene. AIBN (250 mg, 1.52 mmol), styrene (11.8 cm^3, 103 mmol) and divinylbenzene (6.22 cm^3, 34.9 mmol) were then added to the organic phase with each of the monomers being washed with 1% aqueous NaOH (10 cm^3) and water (2 × 10 cm^3) immediately prior to use. The monomer phase was added *via* cannulation over a period of 10 minutes to the cooled aqueous phase which was stirred at 350 RPM. The height of the paddle impeller was positioned ~ 3 cm below the surface of the reaction mixture as this depth was found to visually reduce horizontal flow. Stirring was then continued at 0 °C for 1 hour. The reaction mixture was then heated to 80 °C with constant stirring at 350 RPM under argon for 18 hours. The polymer beads were collected by filtration through a 100 micron mesh sieve and washed with water (500 cm^3), THF (500 cm^3) and methanol (500 cm^3). The polymeric material was then dried under reduced pressure at 40 °C to constant mass and sieved between 500 and 100 micron mesh sieves affording the title polymer as pale yellow free flowing beads (7.67 g, 43%), ν_{max} (KBr disc)/cm^{-1} 3421, 3023, 2918, 1768, 1600, 1492, 1452, 698; Anal. Calcd. for polymer: C, 90.09; H, 7.61; N, 0.70, found C, 89.32; H, 7.92; N, 0.67, loading = 0.48 mmolg^{-1}; N_2 BET adsorption = 2 m^{2}g^{-1}; resin swelled to 7.4 times its own volume in DCM.

12% Cross-linked 0.5 mmolg^{-1} amino alcohol polymer *217*

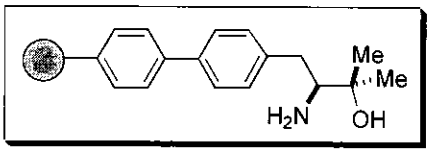

A dry 500 cm^3 3-necked flask equipped with overhead stirrer, condenser and septum was charged with distilled water (135 cm^3) which was subsequently degassed and purged with argon. PVA (675 mg, 87-89% hydrolysed, average MW = 85000-146000) was added and the reaction mixture was stirred at 125 °C for 10 minutes before being cooled to 0 °C. Two further dry flasks were separately charged with THF (50 cm^3) and toluene (50 cm^3), each being degassed and purged with argon. The amino alcohol monomer **167** (1.84 g, 6.55 mmol) was added to the THF ensuring dissolution before addition of the toluene. AIBN (211 mg, 1.28 mmol), styrene (9.94 cm^3, 86.7 mmol) and divinylbenzene (5.25 cm^3, 29.5 mmol) were then added to the organic phase with each of the monomers being washed with 1% aqueous NaOH (10 cm^3) and water (2 × 10 cm^3) immediately prior to use. The monomer phase was added *via* cannulation over a period of 10 minutes to the cooled aqueous phase which was stirred at 350 RPM. The height of the paddle impeller was positioned ~ 3 cm below the surface of the reaction mixture as this depth was found to visually reduce horizontal flow. Stirring was then continued at 0 °C for 1 hour. The reaction mixture was then heated to 80 °C with constant stirring at 350 RPM under argon for 18 hours. The polymer beads were collected by filtration through a 100 micron mesh sieve and washed with water (500 cm^3), THF (500 cm^3) and methanol (500 cm^3). The polymeric material was then dried under reduced pressure at 40 °C to constant mass and sieved between 500 and 100 micron mesh sieves affording the title polymer as white free flowing beads (3.40 g, 23%), ν_{max} (KBr disc)/cm^{-1} 3446, 3025, 2923, 1601, 1493, 1452, 758, 698; Anal. Calcd. for polymer: C, 90.69; H, 7.81; N, 0.70, found C, 89.74; H, 8.05; N, 0.67, loading = 0.48 mmolg^{-1}; N_2 BET adsorption < 10 m^{2}g^{-1}; resin swelled to 5.2 times its own volume in DCM.

A significant proportion of the polymeric product was found to contain larger white beads mixed with plastic residue which were retained in the 500 micron mesh sieve (4.34 g, 30%), ν_{max} (KBr disc)/cm^{-1} 3446, 3025, 2918, 1601, 1493, 1452, 758, 699; Anal. Calcd. for polymer: C, 90.69; H, 7.81; N, 0.70, found C, 89.89; H, 8.08; N, 0.70, loading = 0.50 $mmolg^{-1}$; N_2 BET adsorption < 10 m^2g^{-1}; resin swelled to 4.7 times its own volume in DCM.

8.5 Experimental for Results and Discussion Part 4

(3*S*)-4-Biphenyl-2-methyl-*N*-3-methylamino-butan-2-ol *223*

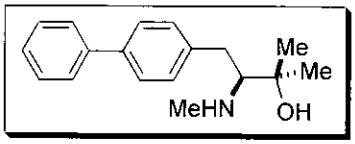

Lithium aluminium hydride (24 mg, 0.64 mmol) was dissolved in anhydrous THF (2 cm^3) and cooled to 0 °C. Oxazolidinone **207** (90 mg, 0.32 mmol) was added in one portion and the resultant mixture was heated to reflux for 3.5 hours. The reaction mixture was diluted with water (0.10 cm^3), 15% aqueous NaOH (0.10 cm^3), water (0.30 cm^3) and DCM (5 cm^3) before being filtered through celite. The celite was washed with further DCM (3 × 10 cm^3). The combined organic layer was extracted into 1N aqueous HCl (3 × 10 cm^3) isolating the title compound as the hydrochloride salt in the aqueous layer. The combined aqueous phase was then basified to pH 14 using NaOH pellets regenerating the non-protonated title compound which was insoluble in the aqueous phase. The aqueous phase was then extracted with DCM (3 × 20 cm^3) and the combined organic layer was dried (Na_2SO_4) and concentrated under reduced pressure affording the title compound as a white crystalline solid (43 mg, 50%), R_f [DCM:MeOH (90:10)] 0.17; mp 44-45 °C; $[\alpha]_D$ -27.0 (*c* 1.0, $CHCl_3$); ν_{max} ($CHCl_3$ soln.)/cm^{-1} 3406, 2971, 1601, 1487, 1377; δ_H (200 MHz, $CDCl_3$) 7.54-7.17 (9H, m, Ar*H*), 3.00-2.84 (1H, m, C*H*N), 2.49-2.33 (2H, m, CH_2Ar), 2.11 (3H, s, N*Me*), 1.18 (3H, s, *Me*), 1.07 (3H, s, *Me*); δ_C (50.3 MHz, $CDCl_3$) 141.6, 140.8, 139.1, 129.4 (2C), 128.8 (2C), 127.2 (3C), 126.9 (2C), 71.6, 70.5, 37.7, 37.4, 27.3, 24.1; m/z (FAB) 270 (MH^+, 100%), 210 (30), 167 (60), 102 (22); HRMS (FAB) $C_{18}H_{24}NO$ (MH^+) requires 270.1858, found 270.1857.

(4*S*)-5,5-Dimethyl-3-methyl-4-(*p*-phenyl)benzyl-oxazolidine *201*

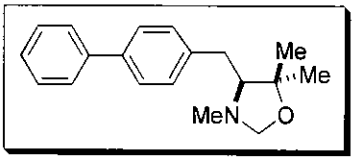

Amino alcohol **223** (39 mg, 0.14 mmol) was dissolved in toluene (2 cm^3) and formaldehyde (0.013 cm^3, 38% aq. solution, 0.16 mmol) was added dropwise. The reaction mixture was stirred for 30 minutes before being diluted with water (5 cm^3) and extracted with DCM (3 × 10 cm^3). The combined organic layer was washed with brine (15 cm^3), dried (Na_2SO_4) and concentrated under reduced pressure. The residue was chromatographed on silica gel [hexane:EtOAc (80:20)] providing the title compound as a white crystalline solid (34 mg, 83%), R_f [DCM:MeOH (90:10)] 0.54; mp 48-49 °C; $[\alpha]_D$ +52.0 (*c* 1.0, $CHCl_3$); ν_{max} ($CHCl_3$ soln.)/cm^{-1} 3012, 2976, 1488; δ_H (200 MHz, $CDCl_3$) 7.55-7.18 (9H, m, Ar*H*), 4.54 (1H, d, *J* 2.9, CH_XH_YO), 3.81 (1H, d, *J* 2.9, CH_XH_YO), 2.87 (1H, dd, *J* 13.9, 6.6, CH_AH_BAr), 2.61 (1H, dd, *J* 13.9, 7.0, CH_AH_BAr), 2.46 (1H, t, *J* 7.0 C*H*N), 2.17 (3H, s, N*Me*), 1.19 (3H, s, *Me*), 1.01 (3H, s, *Me*); δ_C (50.3 MHz, $CDCl_3$) 140.8, 139.1, 138.1, 129.5 (2C), 128.8 (2C), 127.2, 127.1 (2C), 127.0 (2C), 86.2, 82.4, 74.3, 38.5, 35.1, 27.3, 23.2; m/z (FAB) 282 (MH^+, 76%), 280 (78), 167 (93), 114 (100), 84 (83), 43 (92); HRMS (FAB) $C_{19}H_{24}NO$ (MH^+) requires 282.1858, found 282.1858.

(*E*)-Methyl 3-(*p*-hydroxy)phenyl-prop-2-enoate *230*

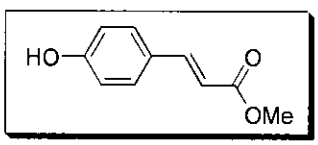

A solution of *m*-chloroperbenzoic acid (49 mg, 86% w/w, 0.28 mmol) in anhydrous DCM (3 cm^3) was added dropwise to a solution of the methyl ester **124** (100 mg, 0.28 mmol) in anhydrous DCM (2 cm^3) at 0 °C. The reaction mixture was warmed to room temperature and further stirred for 5 hours before being diluted with DCM

(30 cm^3). The organic layer was washed with water (2 × 20 cm^3), 1N aqueous NaOH (20 cm^3), brine (20 cm^3), dried (Na_2SO_4) and concentrated under reduced pressure. The residue was chromatographed on silica gel [DCM] affording the title compound as a yellow oil (39 mg, 91%), R_f [DCM] 0.79; δ_H (200 MHz, $CDCl_3$) 7.66 (1H, d, *J* 16.1, C*H*), 7.60 (2H, d, *J* 8.8, Ar*H*), 7.30 (2H, d, *J* 8.8, Ar*H*), 6.44 (1H, d, *J* 16.1, C*H*), 3.81 (3H, s, O*Me*); m/z (APCI) 179 (MH^+, 100%), 178 (58).

(*E*)-4-Biphenyl-2-methyl-3-buten-2-ol *232*

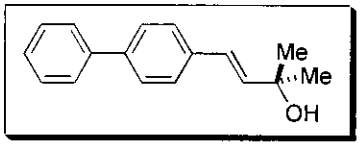

A solution of *m*-chloroperbenzoic acid (21 mg, 46% w/w, 0.12 mmol) in anhydrous DCM (2 cm^3) was added dropwise to a solution of the amino alcohol **193** (35 mg, 0.12 mmol) in anhydrous DCM (2 cm^3) at 0 °C. The reaction mixture was warmed to room temperature and further stirred for 1.5 hours before being diluted with DCM (10 cm^3). The organic layer was washed with water (2 × 10 cm^3), 1N aqueous NaOH (10 cm^3), brine (10 cm^3), dried (Na_2SO_4) and concentrated under reduced pressure. The residue was chromatographed on silica gel [DCM] providing the title compound as a white solid (10 mg, 74%), R_f [DCM:MeOH (90:10)] 0.72; δ_H (200 MHz, $CDCl_3$) 7.63 -7.31 (9H, m, Ar*H*), 6.64 (1H, d, *J* 16.1, C*H*), 6.40 (1H, d, *J* 16.1, C*H*), 1.45 (6H, s, 2 × *Me*).

Title compound **232** was found to undergo acid catalysed dehydration on standing in $CDCl_3$ affording (*E*)-1-biphenyl-3-methyl-1,3-butadiene **233**.

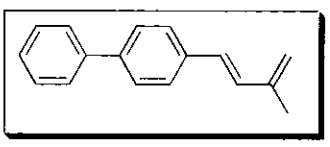

Data for **233**:

δ_H (200 MHz, $CDCl_3$) 7.56-7.23 (9H, m, Ar*H*), 6.86 (1H, d, *J* 16.4, C*H*), 6.50 (1H, d, *J* 16.4, C*H*), 5.04 (2H, d, *J* 8.9, CH_2), 1.92 (3H, s, CH_3).

(3*S*)-4-Biphenyl-*N*,*N*-3-dimethylamino-2-methyl-butan-2-ol *N*-oxide *246*

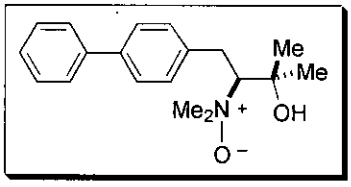

A dried NMR tube was charged with the amino alcohol **193** (16 mg, 0.056 mmol) and CD_2Cl_2 (0.50 cm^3) and cooled to 0 °C. *m*-Chloroperbenzoic acid (21 mg, 46% w/w, 0.056 mmol) was dissolved in CD_2Cl_2 (0.50 cm^3) and cooled to 0 °C before being added dropwise to the NMR tube. The reaction mixture was maintained at 0 °C for 10 minutes before a ^1H NMR spectrum revealed complete conversion of the amino alcohol **193** to the *N*-oxide **246**, R_f [DCM:MeOH (90:10)] 0.46; δ_H (200 MHz, CD_2Cl_2) 7.61-7.40 (9H, m, Ar*H*), 4.40-4.15 (1H, m, C*H*N), 3.61 (3H, s, N*Me*), 3.35 (3H, s, N*Me*), 3.30-3.04 (2H, m, CH_2Ar), 1.61 (3H, s, *Me*), 1.38 (3H, s, *Me*).

8.6 Experimental for Results and Discussion Part 5

(1*RS*)-1-Phenyl-1-propanol *70*

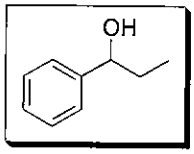

Method M :

Ethylmagnesium bromide (18.9 cm^3, 1.0 *M* in THF, 18.9 mmol) was slowly added to a solution of benzaldehyde (0.191 cm^3, 1.88 mmol) in anhydrous ether (10 cm^3). The reaction mixture was heated to 70 °C for 1 hour before being quenched with saturated aqueous NH_4Cl (5 cm^3) and diluted with water (10 cm^3). The organic phase was separated and the aqueous phase was extracted with DCM (2 × 30 cm^3). The combined organic extracts were dried (Na_2SO_4) and concentrated under reduced pressure. The residue was chromatographed on silica gel [hexane:EtOAc (95:5)] affording the title compound as a colourless oil (254 mg, 99%), R_f [hexane:EtOAc (80:20)] 0.54; ν_{max} (neat)/cm^{-1} 3369, 3029, 2964, 1454, 700; δ_H (200 MHz, $CDCl_3$) 7.40-7.22 (5H, m, Ar*H*), 4.58 (1H, t, *J* 6.6, C*H*OH), 2.03 (1H, br s, O*H*), 1.94-1.63 (2H, m, CH_2), 0.91 (3H, t, *J* 7.3, CH_3); δ_C (50.3 MHz, $CDCl_3$) 144.6, 128.4 (2C), 127.5, 126.0 (2C), 76.0, 31.8, 10.0; m/z (EI) 136 (M^+, 5%), 107 (46), 79 (100), 77 (74), 29 (39); HRMS (EI) $C_9H_{12}O$ (M^+) requires 136.0888, found 136.0890; Chiracel OD-H HPLC, 0.5 cm^3 min^{-1} [hexane:propan-2-ol (95:5)] (*R* enantiomer) R_t = 14.9 minutes, (*S* enantiomer) R_t = 16.2 minutes, [lit.,[126] Chiracel OD-H HPLC, 0.5 cm^3 min^{-1} [hexane:propan-2-ol (95:5)] (*R* enantiomer) R_t = 15.6 minutes, (*S* enantiomer) R_t = 17.7 minutes].

(3*RS*)-1-Phenyl-1-penten-3-ol *286*

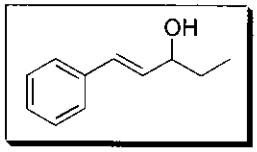

An analogous protocol to that described in Method M was undertaken. Thus, ethylmagnesium bromide (15.1 cm^3, 1.0 *M* in THF, 15.1 mmol) and *trans*-cinnamaldehyde (0.190 cm^3, 1.51 mmol) in anhydrous ether (10 cm^3) gave, after chromatography on silica gel [hexane:EtOAc (95:5)] the title compound (241 mg, 98%) as a yellow oil, R_f [hexane:EtOAc (80:20)] 0.46; ν_{max} (neat)/cm^{-1} 3386, 3026, 2965, 1698, 1493, 1450, 966, 748, 693; δ_H (200 MHz, $CDCl_3$) 7.41-7.13 (5H, m, Ar*H*), 6.58 (1H, d, *J* 15.8, ArC*H*), 6.22 (1H, dd, *J* 15.8, 6.6, ArCHC*H*) 4.26-4.17 (1H, m, C*H*OH), 1.82 (1H, br s, O*H*), 1.75-1.56 (2H, m, CH_2), 0.98 (3H, t, *J* 7.3, CH_3); δ_C (50.3 MHz, $CDCl_3$) 136.8, 132.2, 130.4, 128.5 (2C), 127.5, 126.4 (2C), 74.3, 30.1, 9.6; m/z (EI) 162 (M^+, 47%), 133 (100), 105 (74), 91 (61), 55 (62); HRMS (EI) $C_{11}H_{14}O$ (M^+) requires 162.1045, found 162.1045; Chiracel OD-H HPLC, 0.5 cm^3 min^{-1} [hexane:propan-2-ol (95:5)] (*R* enantiomer) R_t = 22.1 minutes, (*S* enantiomer) R_t = 35.6 minutes, [lit.,[129] Chiracel OD-H HPLC, 1.0 cm^3 min^{-1} [hexane:propan-2-ol (95:5)] (*R* enantiomer) R_t = 14.0 minutes, (*S* enantiomer) R_t = 23.0 minutes].

Enantioselective addition of diethylzinc to benzaldehyde utilising amino alcohol catalyst *149* affording 1-phenyl-1-propanol *70*

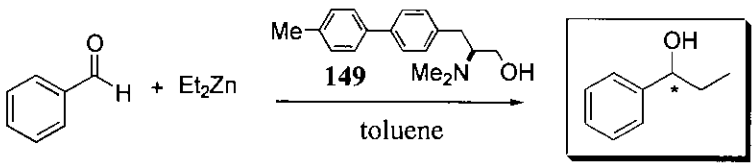

Method N :

Diethylzinc (7.4 cm^3, 1.1 *M* in toluene, fresh batch of reagent, 8.1 mmol) was added to a solution of the amino alcohol **149** (24 mg, 0.089 mmol, 2 mol%) in anhydrous toluene (9 cm^3) and stirred for 15 minutes at room temperature. The reaction mixture was cooled to -78 °C and benzaldehyde (0.46 cm^3, 4.5 mmol) was added before stirring the solution at 0 °C for 72 hours. Further diethylzinc (7.4 cm^3, 8.1 mmol) was added and stirring was then continued at room temperature for 24 hours. The reaction mixture was quenched with saturated aqueous NH_4Cl (14 cm^3), diluted with water (20 cm^3) and filtered through celite which was washed with water (20 cm^3) and EtOAc (2 × 30 cm^3). The organic phase was separated and the aqueous phase was extracted with EtOAc (2 × 30 cm^3). The combined organic extracts were dried (Na_2SO_4) and concentrated under reduced pressure. The residue was chromatographed on silica gel [hexane:EtOAc (95:5)] affording the title compound as a clear oil (480 mg, 78%), Chiracel OD HPLC, 0.6 cm^3 min^{-1} [hexane:propan-2-ol (95:5)] (*R* enantiomer) R_t = 12.6 minutes, (*S* enantiomer) R_t = 13.9 minutes, e.e. 34% *R* [lit.,[127] Chiracel OD HPLC, 0.5 cm^3 min^{-1} [hexane:ethanol (95:5)] (*R* enantiomer) R_t = 14.2 minutes, (*S* enantiomer) R_t = 16.1 minutes]. *NMR spectroscopic data identical to that obtained for **70** as given above.*

Enantioselective addition of diethylzinc to cinnamaldehyde utilising amino alcohol catalyst *149* affording 1-phenyl-1-penten-3-ol *286*

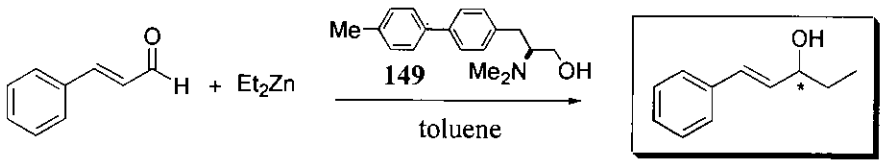

An analogous protocol to that described in Method N was undertaken. Thus, amino alcohol **149** (24 mg, 0.089 mmol, 2 mol%), diethylzinc (7.4 cm^3, 1.1 *M* in toluene, fresh batch of reagent, 8.1 mmol) and *trans*-cinnamaldehyde (0.57 cm^3, 4.5 mmol) in anhydrous toluene (9 cm^3) were stirred at 0 °C for 72 hours. Further diethylzinc (7.4 cm^3, 8.1 mmol) was added and stirring was then continued at room temperature for 24 hours. The residue was chromatographed on silica gel [hexane:EtOAc (95:5)] affording the title compound as a yellow oil (221 mg, 30%), Chiracel OD HPLC, 0.6 cm^3 min^{-1} [hexane:propan-2-ol (95:5)] (*R* enantiomer) R_t = 18.8 minutes, (*S* enantiomer) R_t = 31.2 minutes, e.e. 12% *R* [lit.,[128] Chiracel OD HPLC, 1.0 cm^3 min^{-1} [hexane:propan-2-ol (95:5)] (*R* enantiomer) R_t = 16.9 minutes, (*S* enantiomer) R_t = 27.2 minutes]. *NMR spectroscopic data identical to that obtained for **286** as given above.*

Diethylzinc reactions utilising oxazolidine catalyst *194*

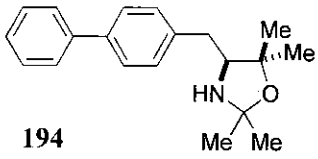

194

Method O :

Diethylzinc (1.3 cm^3, 1.1 *M* in toluene, 1.4 mmol) was added to a solution of oxazolidine **194** (10 mg, 0.034 mmol, 5 mol%) in anhydrous toluene (2 cm^3) and heated at 80 °C for 1 hour. The reaction mixture was cooled to -78 °C and benzaldehyde (0.071 cm^3, 0.70 mmol) was added before stirring the solution at 0 °C

for 112 hours. Further diethylzinc (1.3 cm^3, 1.4 mmol) was added and stirring was then continued at 0 °C for 24 hours. The reaction mixture was quenched with saturated aqueous NH_4Cl (2 cm^3), diluted with water (5 cm^3) and filtered through celite which was washed with water (10 cm^3) and EtOAc (2 × 15 cm^3). The organic phase was separated and the aqueous phase was extracted with EtOAc (2 × 15 cm^3). The combined organic extracts were dried (Na_2SO_4) and concentrated under reduced pressure. The residue was chromatographed on silica gel [hexane:EtOAc (95:5)] affording the title compound as a clear oil (61 mg, 65%), Chiracel OD-H HPLC, 0.5 cm^3 min^{-1} [hexane:propan-2-ol (95:5)] (*R* enantiomer) R_t = 14.8 minutes, (*S* enantiomer) R_t = 16.2 minutes, e.e 20% *R* [lit.,[126] Chiracel OD-H HPLC, 0.5 cm^3 min^{-1} [hexane:propan-2-ol (95:5)] (*R* enantiomer) R_t = 15.6 minutes, (*S* enantiomer) R_t = 17.7 minutes]. *NMR spectroscopic data identical to that obtained for* ***70*** *as given above.*

Diethylzinc reactions utilising polymer-bound amino alcohol catalyst *217*

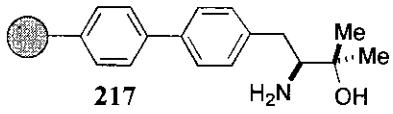

217

Method P :

The polymer-bound amino alcohol catalyst **217** (84 mg, 0.040 mmol, 5 mol% based on loading of amino alcohol = 0.48 $mmolg^{-1}$) was weighed into a sintered filtration tube. The reaction vessel was sealed with a septum, flushed with argon and subsequently maintained under a balloon of argon. The polymer was swollen in anhydrous toluene (6 cm^3) and cooled to 0 °C. Benzaldehyde (0.072 cm^3, 0.71 mmol) was added and the mixture was then shaken at 0 °C for 15 minutes. Diethylzinc (1.3 cm^3, 1.1 *M* in toluene, previously unopened bottle, 1.4 mmol) was added dropwise with the reaction mixture then being shaken at room temperature for 66 hours. Further diethylzinc (1.3 cm^3, 1.4 mmol) was added and shaking was

continued at room temperature for 24 hours before quenching the reaction mixture with 1N aqueous HCl (3 cm^3). The filtrate was removed by filtration through the sinter using a positive pressure of argon. The polymer was subsequently washed with DCM (20 cm^3) and water (20 cm^3) with the filtrate being isolated in the same manner. The organic phase was separated and the aqueous phase was extracted with DCM (2 × 20 cm^3). The combined organic extracts were dried (Na_2SO_4) and concentrated under reduced pressure. The residue was chromatographed on silica gel [hexane:EtOAc (95:5)] affording the title compound as a clear oil (13 mg, 13%), Chiracel OD-H HPLC, 0.5 cm^3 min^{-1} [hexane:propan-2-ol (95:5)] (*R* enantiomer) R_t = 13.6 minutes, (*S* enantiomer) R_t = 14.8 minutes, e.e 13% *S* [lit.,[126] Chiracel OD-H HPLC, 0.5 cm^3 min^{-1} [hexane:propan-2-ol (95:5)] (*R* enantiomer) R_t = 15.6 minutes, (*S* enantiomer) R_t = 17.7 minutes]. *NMR spectroscopic data identical to that obtained for* ***70*** *as given above.*

Polymer recovery protocol :

The recovered polymer catalyst was partially swollen in THF:2N aqueous HCl (4:1, 10 cm^3) and shaken for 4 hours at room temperature. The polymer was separated by filtration and sequentially washed with water (2 × 10 cm^3) and further THF:2N aqueous HCl (4:1, 10 cm^3). The polymer was then partially swollen in THF:2N aqueous NaOH (4:1, 10 cm^3) and shaken for 4 hours at room temperature. The polymer was separated by filtration and sequentially washed with water (2 × 10 cm^3), methanol (2 × 10 cm^3), THF (2 × 10 cm^3), water:THF (1:1, 2 × 10 cm^3), THF (2 × 10 cm^3), methanol (2 × 10 cm^3). The polymeric material was then dried under reduced pressure at 50 °C for 7 hours affording the polymer-bound amino alcohol as white beads (80 mg, 95% recovery), ν_{max} (KBr disc)/cm^{-1} 3447, 3024, 2921, 1601, 1493, 1452, 758, 673; Anal. found for polymer **217**: C, 89.74; H, 8.05; N, 0.67, found for recovered polymer **217** C,89.18; H, 7.87; N, 0.67.

8.7 Experimental for Results and Discussion Part 6

(2'*S*,3'*S*,4*S*)-5,5-Dimethyl-3-(3'-hydroxy-2'-methyl-1'-oxopropyl-3'-phenyl)-4-[*p*-(phenyl)benzyl]-oxazolidin-2-one *312*

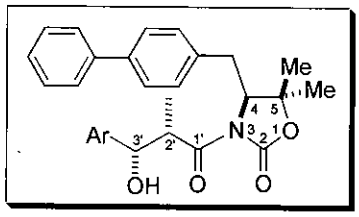

Acylated oxazolidinone auxiliary **208** (200 mg, 0.59 mmol) was dissolved in anhydrous DCM (4 cm^3) and cooled to 0 °C. Dibutylboron triflate (0.65 cm^3, 1.0 *M* in DCM, 0.65 mmol) was added dropwise followed by triethylamine (0.10 cm^3, 0.71 mmol). Stirring was continued at 0 °C for a further 20 minutes and the reaction mixture was then cooled to -78 °C. A solution of benzaldehyde (0.30 cm^3, 3.0 mmol) in anhydrous DCM (2 cm^3) was added and the reaction mixture was stirred at -78 °C for a further 1.5 hours. The reaction mixture was then warmed to between -30 °C and -20 °C for a further 2.5 hours before being quenched with pH 7 aqueous phosphate buffer (5 cm^3), methanol (8.5 cm^3) and a solution of methanol:H_2O_2 (1:1, 10 cm^3). The resulting solution was stirred vigorously for 1 hour, extracted into DCM (3 × 20 cm^3), the organic layer was dried (Na_2SO_4) and concentrated under reduced pressure. The residue was chromatographed on silica gel [DCM] affording the title compound as a white foaming solid (200 mg, 76%), R_f [DCM] 0.23; $[\alpha]_D$ -28.8 (*c* 1.0, $CHCl_3$); ν_{max} ($CHCl_3$ soln.)/cm^{-1} 3437, 1774, 1693, 1488, 756; δ_H (250 MHz, $CDCl_3$) 7.60-7.21 (14H, m, Ar*H*), 5.02 (1H, d, *J* 4.9, ArC*H*OH), 4.44 (1H, dd, *J* 9.0, 4.6, C*H*N), 4.17 (1H, dq, *J* 6.9, 4.9, MeC*H*CO), 3.07 (1H, dd, *J* 14.3, 4.6, CH_AH_BAr), 2.97 (1H, br s, O*H*), 2.92 (1H, dd, *J* 14.3, 9.0 CH_AH_BAr), 1.38 (3H, s, *Me*), 1.18 (3H, d, *J* 6.9, *Me*CHCO), 1.15 (3H, s, *Me*); δ_C (62.9 MHz, $CDCl_3$) 176.4 (C), 152.0 (C), 141.3 (C), 140.4 (C), 139.6 (C), 135.5 (C), 129.4 (2 × CH), 128.6 (2 × CH), 128.2 (2 × CH), 127.5 (CH), 127.2 (3 × CH), 126.8 (2 × CH), 126.2 (2 × CH), 82.1 (C), 74.0 (CH), 63.1 (CH), 44.4 (CH), 34.9 (CH_2), 27.9 (CH_3), 22.0 (CH_3), 11.6

(CH_3); m/z (FAB) 444 (MH^+, 2%), 426 (40), 167 (100), 145 (77); HRMS (FAB) $C_{28}H_{30}NO_4$ (MH^+) requires 444.2175, found 444.2176.

(2*S*,3*S*)-3-Hydroxy-2-methyl-3-phenyl-propanoic acid *32*

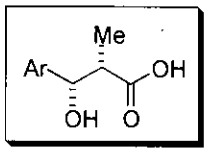

Aldol adduct **312** (146 mg, 0.33 mmol) was dissolved in stabiliser-free THF (9 cm^3) and cooled to 0 °C. Lithium hydroxide monohydrate (30 mg, 0.72 mmol) dissolved in water (3 cm^3) was added with vigorous stirring which was continued at room temperature for 2 hours. The reaction mixture was concentrated under reduced pressure and the residue was partitioned between DCM (15 cm^3) and saturated aqueous $NaHCO_3$ (15 cm^3). The organic layer was separated and further extracted with saturated aqueous $NaHCO_3$ (2 × 15 cm^3). The combined aqueous extracts were acidified to pH 1 using 6N aqueous HCl and extracted with DCM (3 × 20 cm^3). The combined organic layer was dried (Na_2SO_4) and concentrated under reduced pressure affording the title compound as a white solid (35 mg, 59%), R_f [DCM:MeOH:AcOH (94:5:1)] 0.38; mp 62-63 °C; $[\alpha]_D$ -33.3 (*c* 0.5, $CHCl_3$) [lit.,[137] 2*R*,3*R* diastereomer $[\alpha]_D$ +31.0 (*c* 1.1, $CHCl_3$)]; δ_H (200 MHz, $CDCl_3$) 7.35-7.30 (5H, m, Ar*H*), 6.16 (2H, br s, O*H* and CO_2H), 5.17 (1H, d, *J* 3.8, ArC*H*OH), 2.87-2.74 (1H, m, MeC*H*CO), 1.13 (3H, d, *J* 7.2, *Me*); δ_C (62.9 MHz, $CDCl_3$) 180.8 (C), 140.9 (C), 128.2 (2 × CH), 127.5 (CH), 125.8 (2 × CH), 73.2 (CH), 46.0 (CH), 10.1 (CH_3); m/z (EI) 180 (M^+, 19%), 163 (29), 105 (46), 79 (100), 29 (48); HRMS (EI) $C_{10}H_{12}O_3$ (M^+) requires 180.0786, found 180.0787. *NMR spectroscopic data in good agreement with literature data.*[136]

(2'*R*,4*S*)-5,5-Dimethyl-3-(2'-methyl-1'-oxopropyl-3'-phenyl)-4-[*p*-(phenyl) benzyl]-oxazolidin-2-one *313* and (2'*S*,4*S*)-5,5-Dimethyl-3-(2'-methyl-1'-oxopropyl-3'-phenyl)-4-[*p*-(phenyl)benzyl]-oxazolidin-2-one *321*

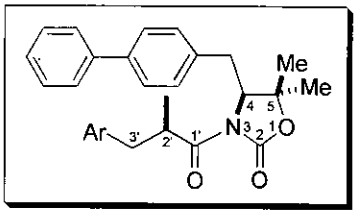

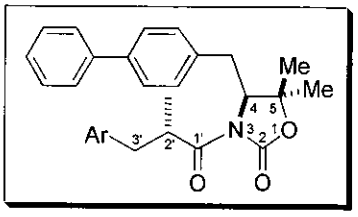

Acylated oxazolidinone auxiliary **208** (50 mg, 0.15 mmol) was dissolved in anhydrous THF (5 cm^3) and cooled to -78 °C. Lithium bis(trimethylsilyl)amide (0.42 cm^3, 1.06 *M* in THF, 0.44 mmol) was added dropwise with stirring continued at -78 °C for 30 minutes before addition of benzyl bromide (0.088 cm^3, 0.74 mmol). The reaction mixture was further stirred at -78 °C for 30 minutes and subsequently warmed to room temperature for 45 minutes. The resulting solution was quenched with saturated aqueous NH_4Cl (5 cm^3) and extracted with EtOAc (3 × 20 cm^3). The combined organic extracts were washed with brine (20 cm^3), dried (Na_2SO_4) and concentrated under reduced pressure. The residue was chromatographed on silica gel [hexane:EtOAc (80:20)] providing the title compounds as an inseparable 9:1 mixture of diastereomers (2'*R*,4*S*):(2'*S*,4*S*) as a colourless oil (50 mg, 79%), R_f [hexane:EtOAc (80:20)] 0.45 (2'*R*,4*S*) and 0.60 (2'*S*,4*S*); $[\alpha]_D$ -92.2 (*c* 0.9, $CHCl_3$); ν_{max} (neat)/cm^{-1} 3028, 2976, 1774, 1699, 1695, 1489; m/z (FAB) 428 (MH^+, 96%), 167 (100), 147 (39), 119 (50), 91 (77); HRMS (FAB) $C_{28}H_{30}NO_3$ (MH^+) requires 428.2226, found 428.2225.

NMR spectroscopic data for major diastereomer (2'*R*,4*S*) **313**:

δ_H (200 MHz, $CDCl_3$) 7.60-7.17 (14H, m, Ar*H*), 4.52 (1H, dd, *J* 9.9, 3.3, C*H*N), 4.22-4.07 (1H, m, MeC*H*CO), 3.11 (1H, dd, *J* 13.6, 7.0, CH_XH_YCHCO), 2.99 (1H, dd, *J* 14.6, 3.3, CH_AH_BAr), 2.75-2.58 (2H, m, CH_XH_YCHCO and CH_AH_BAr), 1.35 (6H, s, 2 × *Me*), 1.18 (3H, d, *J* 7.0, *Me*CHCO); δ_C (50.3 MHz, $CDCl_3$) 177.1, 152.4,

140.6, 139.7, 139.2, 136.1, 129.5 (2C), 129.3 (2C), 128.8 (2C), 128.3 (2C), 127.3 (3C), 127.0 (2C), 126.3, 81.9, 63.6, 39.9, 39.5, 34.5, 28.6, 22.3, 16.5.

^{1}H NMR (200 MHz, $CDCl_3$) diagnostic peaks for minor diastereomer (2'*S*,4*S*) **321** at 4.40 (1H, dd, *J* 9.0, 3.0, C*H*N) and 0.91 (3H, d, *J* 7.0, *Me*CHCO).

(2*R*)-2-Methyl-3-phenyl-propan-1-ol *26*

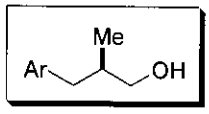

The inseparable mixture of diastereomeric alkylated adducts **313** and **321** (40 mg, 0.094 mmol) was dissolved in stabiliser-free anhydrous THF (2 cm^3), cooled to 0 °C and added dropwise to a 0 °C solution of lithium aluminium hydride (7 mg, 0.19 mmol) in stabiliser-free anhydrous THF (2 cm^3). The reaction mixture was stirred at 0 °C for a further 15 minutes before being diluted with water (0.1 cm^3), 15% aqueous NaOH (0.1 cm^3), water (10 cm^3) and DCM (10 cm^3). The organic layer was separated and the aqueous layer was further extracted with DCM (3 × 10cm^3). The combined organic phase was dried (Na_2SO_4), filtered though celite and concentrated under reduced pressure. The residue was chromatographed [hexane:EtOAc (90:10)] affording the title compounds as a 9:1 mixture of enantiomers (2*R*):(2*S*) as a pale yellow oil (10 mg, 71%), R_f [hexane:EtOAc (80:20)] 0.20; $[\alpha]_D$ +10.0 (*c* 0.3, $CHCl_3$); δ_H (250 MHz, $CDCl_3$) 7.31-7.15 (5H, m, Ar*H*), 3.57-3.43 (2H, m, CH_2OH), 2.75 (1H, dd, *J* 13.4, 6.4, CH_AH$_B$Ar), 2.42 (1H, dd, *J* 13.4, 8.0, CH$_A$$H_B$Ar), 1.98-1.90 (1H, m, C*H*Me), 1.58 (1H, br s, O*H*), 0.91 (3H, d, *J* 6.7, *Me*); δ_C (62.9 MHz, $CDCl_3$) 140.5 (C), 129.0 (2 × CH), 128.2 (2 × CH), 125.8 (CH), 67.6 (CH_2), 39.6 (CH_2), 37.7 (CH), 16.4 (CH_3); m/z (EI) 150 (M^+, 12%), 117 (37), 91 (100), 41 (42), 31 (40); HRMS (EI) $C_{10}H_{14}O$ (M^+) requires 150.1045, found 150.1046; Chiracel OD-H HPLC, 0.9 cm^3 min^{-1} [hexane:propan-2-ol (95:5)] (*S* enantiomer) R_t = 8.7 minutes, (*R* enantiomer) R_t = 10.2 minutes, e.e. 77% *R* [lit.,[139] Chiracel OD HPLC, 0.9 cm^3 min^{-1} [hexane:propan-2-ol (95:5)] (*S* enantiomer) R_t = 14.5 minutes, (*R* enantiomer)

R_t = 18.9 minutes]. *NMR spectroscopic data in good agreement with literature data.*[140]

(4*S*)-3-Benzyl-5,5-dimethyl-4-[*p*-(phenyl)benzyl]-oxazolidin-2-one *314*

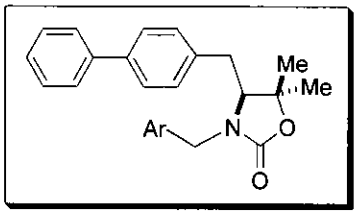

Acylated oxazolidinone auxiliary **208** (50 mg, 0.15 mmol) was dissolved in anhydrous THF (5 cm^3) and cooled to -78 °C. Lithium bis(trimethylsilyl)amide (0.42 cm^3, 1.06 *M* in THF, 0.44 mmol) was added dropwise with stirring continued at -78 °C for 30 minutes before addition of benzyl bromide (0.088 cm^3, 0.74 mmol). The reaction mixture was stirred at -78 °C for a further 30 minutes and subsequently warmed to room temperature for 48 hours. The resulting solution was quenched with saturated aqueous NH_4Cl (5 cm^3) and extracted with EtOAc (3 × 20 cm^3). The combined organic layer was washed with brine (20 cm^3), dried (Na_2SO_4) and concentrated under reduced pressure. The residue was chromatographed on silica gel [hexane:EtOAc (80:20)] providing the title compound as a white solid (45 mg, 82%), R_f [hexane:EtOAc (80:20)] 0.16; mp 95-96 °C; $[\alpha]_D$ -10.2 (*c* 0.6, $CHCl_3$); ν_{max} ($CHCl_3$ soln.)/cm^{-1} 3027, 2980, 1745, 1488, 1412; δ_H (200 MHz, $CDCl_3$) 7.61-7.26 (10H, m, Ar*H*), 7.13-7.09 (4H, m, Ar*H*), 4.82 (1H, d, *J* 15.4, NCH_XH$_Y$), 3.90 (1H, d, *J* 15.4, NCH$_X$$H_Y$), 3.58 (1H, dd, *J* 8.1, 6.4, C*H*N), 3.04 (1H, dd, *J* 14.3, 6.4, CH_AH$_B$Ar), 2.77 (1H, dd, *J* 14.3, 8.1, CH$_A$$H_B$Ar), 1.40 (3H, s, *Me*), 1.14 (3H, s, *Me*); δ_C (62.9 MHz, $CDCl_3$) 157.6 (C), 140.3 (C), 139.7 (C), 135.8 (C), 135.7 (C), 129.2 (2 × CH), 128.7 (2 × CH), 128.6 (2 × CH), 128.0 (2 × CH), 127.7 (CH), 127.3 (3 × CH), 126.8 (2 × CH), 80.9 (C), 63.9 (CH), 46.4 (CH_2), 34.6 (CH_2), 27.7 (CH_3), 22.1 (CH_3); m/z (FAB) 372 (MH^+, 92%), 204 (15), 167 (74), 91 (100); HRMS (FAB) $C_{25}H_{26}NO_2$ (MH^+) requires 372.1964, found 372.1965.

12% Crosslinked 0.5 mmolg^{-1} *N*-propionylated oxazolidinone polymer *324*

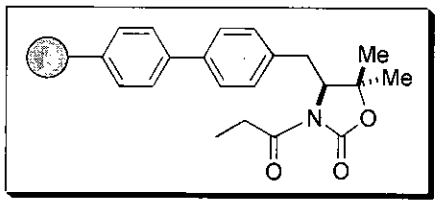

Oxazolidinone polymer **218** (2.47 g, 1.24 mmol, loading of oxazolidinone = 0.50 mmolg^{-1}) was swollen in anhydrous THF (40 cm^3) and cooled to -78 °C. *n*-Butyllithium (9.26 cm^3, 1.6 *M* in hexane, 14.8 mmol) was added and reaction mixture was shaken occasionally at -78 °C for 1 hour. Further *n*-butyllithium (9.26 cm^3, 1.6 *M* in hexane, 14.8 mmol) was added and shaking was continued at -78 °C for a further 1 hour. Propionyl chloride (4.02 cm^3, 46.3 mmol) was added dropwise with the reaction mixture being held at -78 °C for 16 hours. The polymer beads were collected by filtration through a 100 micron mesh sieve and washed with THF (100 cm^3), THF:water (3:2, 100 cm^3), water (100 cm^3), THF (100 cm^3) and DCM (100 cm^3). The polymeric material was then dried under reduced pressure at 40 °C to constant mass and sieved between 500 and 100 micron mesh sieves affording the title polymer as white free flowing beads (1.99 g, 78%), ν_{max} (KBr disc)/cm^{-1} 3025, 2923, 1780, 1704, 1601, 1493, 1452; Anal. Calcd. for polymer assuming quantitative conversion to *N*-propionylated oxazolidinone **324**: C, 89.31; H, 7.59; N, 0.70, found C, 88.47; H, 8.45; N, 0.68; N_2 BET adsorption < 10 m^{2}g^{-1}; resin swelled to 6.7 times its own volume in DCM.

Polymer-bound aldol adduct *325*

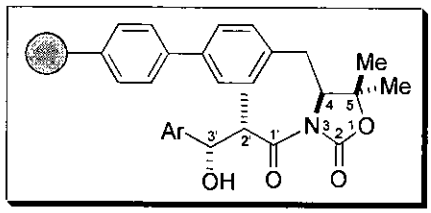

Polymer-bound acylated oxazolidinone auxiliary **324** (1.49 g, 0.730 mmol, loading of auxiliary = 0.49 mmolg^{-1}) was weighed into a sintered filtration tube. The reaction vessel was sealed with a septum, flushed with argon and subsequently maintained under a balloon of argon. The polymer was swollen in anhydrous DCM (30 cm^3) and cooled to 0 °C. Dibutylboron triflate (10.2 cm^3, 1.0 *M* in DCM, 10.2 mmol) was added dropwise followed by triethylamine (1.62 cm^3, 11.7 mmol). The reaction mixture was occasionally shaken at 0 °C over 2 hours before removing excess reagents and DCM *via* filtration through the sinter using a positive pressure of argon. The polymer was subsequently washed with anhydrous DCM (2 × 20 cm^3) with the filtrate being removed in the same manner. The polymer was then re-swollen in anhydrous DCM (20 cm^3) and cooled to -78 °C. A solution of benzaldehyde (1.31 cm^3, 12.9 mmol) in anhydrous DCM (10 cm^3) was added and the reaction mixture was shaken at -78 °C for a further 3 hours. The reaction mixture was then warmed to 0 °C for a further 15 hours before being quenched with pH 7 aqueous phosphate buffer (8 cm^3) and methanol (16 cm^3). The reaction mixture was shaken vigorously at room temperature for 1.5 hours. The polymer beads were collected by filtration through a 100 micron mesh sieve and washed with THF (200 cm^3), THF:water (3:2, 200 cm^3), water (200 cm^3), THF (200 cm^3) and DCM (200 cm^3). The polymeric material was then dried under reduced pressure at 40 °C to constant mass and sieved between 500 and 100 micron mesh sieves affording the title polymer as pale yellow free flowing beads (1.30 g, 83%), ν_{max} (KBr disc)/cm^{-1} 3482, 3025, 2922, 1780, 1702, 1601, 1493, 1452, 759; Anal. Calcd. for polymer assuming quantitative conversion to aldol adduct **325**: C, 88.69; H, 7.49; N, 0.69, found C, 87.70; H, 6.75; N, 0.70.

(2*S*,3*S*)-3-Hydroxy-2-methyl-3-phenyl-propanoic acid *32*

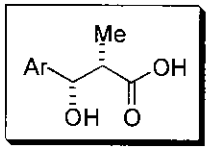

Polymer-bound aldol adduct **325** (494 mg, 0.247 mmol, loading of aldol adduct = 0.50 mmolg^{-1}) was weighed into a sintered filtration tube, swollen in stabiliser-free THF (10 cm^3) and cooled to 0 °C. Lithium hydroxide monohydrate (118 mg, 2.80 mmol) dissolved in water (3 cm^3) was added with the reaction mixture then being maintained at 0 °C for 30 minutes. Vigorous shaking was then continued at room temperature for 69 hours. The reaction mixture was acidified to pH 7 using 6N aqueous HCl and then the filtrate was removed by filtration through the sinter using a positive pressure of argon. The polymer was washed sequentially with water (2 × 30 cm^3) and DCM (2 × 30 cm^3) with the filtrate being removed in the same manner. The organic layer from the combined polymer washings was separated and the aqueous layer was further extracted with DCM (2 × 30 cm^3). The combined organic extracts were dried (Na_2SO_4) and concentrated under reduced pressure. The residue was chromatographed on silica gel [DCM:MeOH:AcOH (99:0:1 to 97:2:1)] affording the title compound as a white solid (14 mg, 31%), $[\alpha]_D$ -36.0 (*c* 0.3, $CHCl_3$) [lit.,[137] 2*R*,3*R* diastereomer $[\alpha]_D$ +31.0 (*c* 1.1, $CHCl_3$)]. *NMR spectroscopic data identical to that obtained for **32** as given above where product was cleaved from the analogous aldol adduct in the solution phase.*

Polymer recovery protocol :

The recovered oxazolidinone polymer was washed with THF (50 cm^3), THF:water (3:2, 50 cm^3), water (50 cm^3), THF:water (3:2, 50 cm^3), THF (50 cm^3) and DCM (50 cm^3). The polymeric material was then dried under reduced pressure at 50 °C for 7 hours affording the oxazolidinone polymer as pale yellow beads (454 mg, 100% recovery), ν_{max} (KBr disc)/cm^{-1} 3420, 3024, 2921, 1772, 1600, 1493, 1452, 698; Anal. previously found for oxazolidinone polymer **218** prior to *N*-propionylation and

aldol adduct formation: C, 89.70; H, 7.77; N, 0.70, found for recovered oxazolidinone polymer C, 88.46; H, 8.47; N, 0.62.

References

[1] R. B. Merrifield, *J. Am. Chem. Soc.*, **1963**, *85*, 2149.

[2a] S. J. Shuttleworth, S. M. Allin, P. K. Sharma, *Synthesis*, **1997**, 1217; [2b] S. J. Shuttleworth, S. M. Allin, R. D. Wilson, D. Nasturica, *Synthesis*, **2000**, 1035.

[3] G. Bhalay, A. Dunstan, A. Glen, *Synlett*, **2000**, 1846.

[4a] P. Hodge, D. C. Sherrington, *Polymer-supported Reactions in Organic Synthesis*, **1980**, John Wiley and Sons, New York; [4b] J. M. J. Fréchet, *Tetrahedron*, **1981**, *37*, 663; [4c] A. Akelah, D. C. Sherrington, *Chem. Rev.*, **1981**, *81*, 557.

[5] G. Bhalay, *Chemistry in Britain*, **1999**, *3*, 25.

[6a] P. H. H. Hermkens, H. C. J. Ottenheijm, D. Rees, *Tetrahedron*, **1996**, *52*, 4527; [6b] J. Christopher, C. McCusker, F. McKerlie, T. Wildman, J. Tierney, B. Wathey, *J. Chem. Soc., Perkin Trans. 1, Abstracts*, **2000**, *11*, xi.

[7] R. C. D. Brown, *J. Chem. Soc., Perkin Trans. 1*, **1998**, 3293.

[8] L. Pu, *Tetrahedron: Asymmetry*, **1998**, *9*, 1457.

[9] G. Terfloth, G. Blaschke, *Macromol. Chem. Phys.*, **1994**, *195*, 3863.

[10] J. M. G. Cowie, *Polymers: Chemistry and Physics of Modern Materials*, **1991**, Blackie Academic and Professional, Glasgow.

[11] M. J. Farrall, J. M. J. Fréchet, *J. Org. Chem.*, **1976**, *41*, 3877.

[12] P. H. Toy, T. S. Reger, K. D. Janda, *Aldrichimica Acta*, **2000**, *33*, 87.

[13] M. Kawana, S. Emoto, *Tetrahedron Lett.*, **1972**, 4855.

[14] P. M. Worster, C. R. McArthur, C. C. Leznoff, *Angew. Chem., Int. Ed. Engl.*, **1979**, *18*, 221.

[15] A. I. Meyers, *J. Heterocyclic. Chem.*, **1998**, *35*, 991.

[16] A. R. Colwell, L. R. Duckwall, R. Brooks, S. P. McManus, *J. Org. Chem.*, **1981**, *46*, 3097.

[17a] H. Moon, N. E. Schore, M. J. Kurth, *J. Org. Chem.*, **1992**, *57*, 6088; [17b] H.-S. Moon, N. E. Schore, M. J. Kurth, *Tetrahedron Lett.*, **1994**, *35*, 8915.

[18a] D. A. Evans, J. Bartroli, T. L. Shih, *J. Am. Chem. Soc.*, **1981**, *103*, 2127; [18b] D. A. Evans, M. D. Ennis, D. J. Mathre, *J. Am. Chem. Soc.*, **1982**, *104*, 1737.

[19a] S. M. Allin, S. J. Shuttleworth, *Tetrahedron Lett.*, **1996**, *37*, 8023; [19b] K. Burgess, D. Lim, *Chem. Commun.*, **1997**, 785; [19c] A. Purandare, S. Natarajan, *Tetrahedron Lett.*, **1997**, *38*, 8777; [19d] C. W. Phoon, C. Abell, *Tetrahedron Lett.*, **1998**, *39*, 2655; [19e] J. D. Winkler, W. McCoull, *Tetrahedron Lett.*, **1998**, *39*, 4935; [19f] G. Faita, A. Paio, P. Quadrelli, F. Rancati, P. Seneci, *Tetrahedron Lett.*, **2000**, *41*, 1265.

[20] E. Vedejs, M. Gingras, *J. Am. Chem. Soc.*, **1994**, *116*, 579.

[21a] M. Reggelin, V. Brenig, *Tetrahedron Lett.*, **1996**, *37*, 6851; [21b] M. Reggelin, V. Brenig, C. Zur, *Organic Lett.*, **2000**, *2*, 531.

[22] M. Prashad, D. Har, H.-Y. Kim, O. Repic, *Tetrahedron Lett.*, **1998**, *39*, 7067.

[23a] B. B. De, B. B. Lohray, S. Sivaram, P. K. Dhal, *Tetrahedron: Asymmetry*, **1995**, *6*, 2105; [23b] B. B. De, B. B. Lohray, S. Sivaram, P. K. Dhal, *J. Polym. Sci., Polym. Chem.*, **1997**, *35*, 1809; [23c] F. Minutolo, D. Pini, P. Salvadori, *Tetrahedron: Asymmetry*, **1996**, *7*, 2293; [23d] F. Minutolo, D. Pini, P. Salvadori, *Tetrahedron Lett.*, **1996**, *37*, 3375.

[24] L. Canali, E. Cowan, H. Deleuze, C. L. Gibson, D. C. Sherrington, *Chem. Commun.*, **1998**, 2561.

[25] T. S. Reger, K. D. Janda, *J. Am. Chem. Soc.*, **2000**, *122*, 6929.

[26] I. F. J. Vankelecom, D. Tas, R. F. Parton, V. Vyver, P. A. Jacobs, *Angew. Chem., Int. Ed. Engl.*, **1996**, *35*, 1346.

[27a] L. Canali, J. K. Karjalainen, D. C. Sherrington, O. Hormi, *Chem. Commun.*, **1997**, 123; [27b] J. K. Karjalainen, D. C. Sherrington, O. Hormi, *Tetrahedron: Asymmetry*, **1998**, *9*, 1563.

[28] D. C. Sherrington, *Catalysis Today*, **2000**, *57*, 87.

[29] I. Cazaux, C, Cazé, *Reactive Polymers*, **1993**, *20*, 87.

[30] H. Han, K. D. Janda, *J. Am. Chem. Soc.*, **1996**, *118*, 7632.

[31] C. Bolm, A. Maischak, A. Gerlach, *Chem. Commun.*, **1997**, 2353.

[32] C. Bolm, A. Maischak, *Synlett*, **2001**, 93.

[33a] K. Soai, S. Niwa, M. Watanabe, *J. Org. Chem.*, **1988**, *53*, 927; [33b] K. Soai, S. Niwa, M. Watanabe, *J. Chem. Soc., Perkin Trans. 1*, **1989**, 109; [33c] S. Itsuno, J. M. J.

Fréchet, *J. Org. Chem.*, **1987**, *52*, 4140; [33d] K. Soai, M. Watanabe, A. Yamamoto, *J. Org. Chem.*, **1990**, *55*, 4832.

[34a] K. Soai, M. Watanabe, *Tetrahedron: Asymmetry*, **1991**, *2*, 97; [34b] M. Watanabe, K. Soai, *J. Chem. Soc., Perkin Trans. 1*, **1994**, 837.

[35a] D. W. L. Sung, P. Hodge, P. W. Stratford, *J. Chem. Soc., Perkin Trans. 1*, **1999**, 1463; [35b] D. W. L. Sung, P. Hodge, P. W. Stratford, *J. Chem. Soc., Perkin Trans. 1*, **1999**, 2335; [35c] T. Suzuki, N. Narisada, T. Shibata, K. Soai, *Polym. Adv. Technol.*, **1999**, *10*, 30; [35d] C. Dreisbach, G. Wischnewski, U. Kragl, C. Wandrey, *J. Chem. Soc., Perkin Trans. 1*, **1995**, 875; [35e] S. Itsuno, Y. Sakurai, K. Ito, T. Maruyama, S. Nakahama, J. M. J. Fréchet, *J. Org. Chem.*, **1990**, *55*, 304.

[36] P. J. Comina, A. K. Beck, D. Seebach, *Organic Process Research & Development*, **1998**, *2*, 18.

[37a] H. Sellner, D. Seebach, *Angew. Chem., Int. Ed. Engl.*, **1999**, *38*, 1918; [37b] D. Seebach, R. E. Marti, T. Hintermann, *Helv. Chim. Acta*, **1996**, *79*, 1710.

[38a] X.-W. Yang, J.-H. Sheng, C.-S. Da, H.-S. Wang, W. Su, R. Wang, A. S. C. Chan, *J. Org. Chem.*, **2000**, *65*, 295; [38b] X. Yang, W. Su, D. Liu, H. Wang, J. Shen, C. Da, R. Wang, A. S. C. Chan, *Tetrahedron*, **2000**, *56*, 3511.

[39a] Q.-S. Hu, W.-S. Huang, L. Pu, *J. Org. Chem.*, **1998**, *63*, 2798; [39b] W.-S. Huang, Q.-S. Hu, L. Pu, *J. Org. Chem.*, **1999**, *64*, 7940.

[40] C. Bolm, C. L. Dinter, A. Seger, H. Höcker, J. Brozio, *J. Org. Chem.*, **1999**, *64*, 5730.

[41a] S. Itsuno, M. Nakano, K. Ito, A. Hirao, M. Owa, N. Kanda, S. Nakahama, *J. Chem. Soc., Perkin Trans. 1*, **1985**, 2615; [41b] S. Itsuno, K. Ito, T. Maruyama, N. Kanda, A. Hirao, S. Nakahama, *Bull. Chem. Soc. Jpn.*, **1986**, *59*, 3329.

[42a] C. Franot, G. B. Stone, P. Engeli, C. Spöndlin, E. Waldvogel, *Tetrahedron: Asymmetry*, **1995**, *16*, 2755; [42b] C. Caze, N. E. Moualij, P. Hodge, C. J. Lock, J. Ma, *J. Chem. Soc., Perkin Trans. 1*, **1995**, 345.

[43] G. Giffels, J. Beliczey, M. Felder, U. Kragl, *Tetrahedron: Asymmetry*, **1998**, *9*, 691.

[44a] R. Halle, E. Schulz, M. Lemaire, *Synlett*, **1997**, 1257; [44b] D. J. Bayston, C. B. Travers, M. E. C. Polywka, *Tetrahedron: Asymmetry*, **1998**, *9*, 2015.

[45] K. Kamahori, K. Ito, S. Itsuno, *J. Org. Chem.*, **1996**, *61*, 8321.

[46] J. K. Stille, *Reactive Polymers*, **1989**, *10*, 165.

[47] A. Giroux, Y. Han, P. Prasit, *Tetrahedron Lett.*, **1997**, *22*, 3841.

[48] Y. Satoh, C. Gude, K. Chan, F. Fiirooznia, *Tetrahedron Lett.*, **1997**, *38*, 7645.

[49] S. R. Piettre, S. Baltzer, *Tetrahedron Lett.*, **1997**, *38*, 1197.

[50] W.-C. Shieh, J. A. Carlson, *J. Org. Chem.*, **1992**, *57*, 379.

[51a] J. W. Tilley, R. Sarabu, R. Wagner, K. Mulkerins, *J. Org. Chem.*, **1990**, *55*, 906;

[51b] R. E. Dolle, S. J. Schmidt, L. I. Kruse, *J. Chem. Soc., Chem. Commun.*, **1987**, 904.

[52] M. A. Huffman, N. Yasuda, *Synlett*, **1999**, 471.

[53] S. A. Metwally, H. H. Coenen, G. Stöcklin, *Bull. Chem. Soc. Jpn.*, **1987**, *60*, 4437.

[54] H. Lei, M. S. Stoakes, K. P. B. Herath, J. Lee, A. W. Schwabacher, *J. Org. Chem.*, **1994**, *59*, 4206.

[55] B. A. Lorsbach, M. J. Kurth, *Chem. Rev.*, **1999**, *99*, 1549.

[56a] S. Wendeborn, S. Berteina, W. K.-D. Brill, A. Mesmaeker, *Synlett*, **1998**, 671; [56b] M. Larhed, G. Lindeberg, A. Hallberg, *Tetrahedron Lett.*, **1996**, *37*, 8219; [56c] J. W. Guiles, S. G. Johnson, W. V. Murray, *J. Org. Chem.*, **1996**, *61*, 5169; [56d] R. Frenette, R. W. Friesen, *Tetrahedron Lett.*, **1994**, *35*, 9177; [56e] B. J. Backes, J. A. Ellman, *J. Am. Chem. Soc.*, **1994**, *116*, 11171.

[57] J. K. Stille, *Angew. Chem., Int. Ed. Engl.*, **1986**, *25*, 508.

[58] S. Marquais, M. Arlt, *Tetrahedron Lett.*, **1996**, *37*, 5491.

[59] M, Rottländer, P. Knochel, *Synlett*, **1997**, 1084.

[60] H. Nakamura, M. Fujiwara, Y. Yamamoto, *J. Org. Chem.*, **1998**, *63*, 7529.

[61] H. Nakamura, M. Fujiwara, Y. Yamamoto, *Bull. Chem. Soc. Jpn.*, **2000**, *73*, 231.

[62] F. Firooznia, C. Gude, K. Chan, Y. Satoh, *Tetrahedron Lett.*, **1998**, *39*, 3985.

[63] F. Firooznia, C. Gude, K. Chan, N. Marcopulos, Y. Satoh, *Tetrahedron Lett.*, **1999**, *40*, 213.

[64] R. L. Huguenin, R. A. Boissonnas, *Helv. Chim. Acta*, **1961**, *44*, 213.

[65] H. C. Brown, S. Narasimhan, Y. M. Choi, *J. Org. Chem.*, **1982**, *47*, 4702.

[66] M. D. Drew, N. J. Lawrence, D. Fontaine, L. Sehkri, *Synlett*, **1997**, 989.

[67] J. M. Defauw, M. M. Murphy, G. E. Jagdmann, J. H. Hu, J. W. Lampe, S. P. Hollinshead, T. J. Mitchell, H. M. Crane, J. M. Heerding, J. S. Mendoza, J. E. Davis, J. W. Darges, F. R. Hubbard, S. E. Hall, *J. Med. Chem.*, **1996**, *39*, 5215.

[68] M. J. Kornet, *J. Heterocyclic. Chem.*, **1990**, *27*, 2125.

[69] Y. Kamitori, M. Hojo, R. Masuda, T. Inoue, T. Izumi, *Tetrahedron Lett.*, **1983**, *24*, 2575.

[70] F. Sato, T. Jinbo, M. Sato, *Tetrahedron Lett.*, **1980**, *21*, 2175.

[71] R. E. Gawley, G. C. Hart, L. J. Bartolotti, *J. Org. Chem.*, **1989**, *54*, 175.

[72] A. Suzuki, *Pure Appl. Chem.*, **1985**, *57*, 1749.

[73] G. B. Smith, G. C. Dezeny, D. L. Hughes, A. O. King, T. R. Verhoeven, *J. Org. Chem.*, **1994**, *59*, 8151.

[74a] D. W. Old, J. P. Wolfe, S. L. Buchwald, *J. Am. Chem. Soc.*, **1998**, *120*, 9722; [74b] J.-C. Galland, M. Savignac, J.-P. Genêt, *Tetrahedron Lett.*, **1999**, *40*, 2323; [74c] A. Zapf, M. Beller, *Chem. Eur, J.* **2000**, *6*, 1830.

[75] P. J. Hajduk, J. Dinges, G. F. Miknis, M. Merlock, T. Middleton, D. J. Kempf, D. A. Egan, K. A. Walter, T. S. Robins, S. B. Shuker, T. F. Holzman, S. W. Fesik, *J. Med. Chem.*, **1997**, *40*, 3144.

[76] M. Murata, S. Watanabe, Y. Masuda, *J. Org. Chem.*, **1997**, *62*, 6458.

[77] T. Ishiyama, M. Murate, N. Miyaura, *J. Org. Chem.*, **1995**, *60*, 7508.

[78] M. Murata, T. Oyama, S. Watanabe, Y. Masuda, *J. Org. Chem.*, **2000**, *65*, 164.

[79] H. Nöth, *Z. Naturforsch*, **1984**, 1463.

[80] G. M. Kapteijn, P. J. Baesjou, P. L. Alsters, D. M. Grove, W. J. J. Smeets, H. Kooijman, A. L. Spek, G. Koten, *Chem. Ber. Recueil.*, **1997**, *130*, 35.

[81] T. Oh-e, N. Miyaura, A. Suzuki, *J. Org. Chem.*, **1993**, *58*, 2201.

[82] S. Itsuno, Y. Sakurai, K. Ito, A. Hirao, S. Nakahama, *Polymer*, **1987**, *28*, 1005.

[83a] A. Huth, I. Beetz, I. Schumann, *Tetrahedron*, **1989**, *45*, 6679; [83b] G. Marck, A. Villiger, R. Buchecker, *Tetrahedron Lett.*, **1994**, *35*, 3277; [83c] A. F. Littke, C. Dai, G. C. Fu, *J. Am. Chem. Soc.*, **2000**, *122*, 4020.

[84] H. Kamogawa, S. Shiraki, *Macromolecules*, **1991**, *24*, 4224.

[85] Y.-H. Lai, *Synthesis*, **1981**, 585.

[86] J. R. Leebrick, H. E. Ramsden, *J. Org. Chem.*, **1958**, *23*, 935.

[87] K.R. K. Prasad, N. N. Joshi, *J. Org. Chem.*, **1997**, *62*, 3770.

[88a] X. Wei, R. J. K. Taylor, *Chem. Commun.*, **1996**, 187; [88b] X. Wei, P. Johnson, R. J. K. Taylor, *J. Chem. Soc., Perkin Trans. 1*, **2000**, 1109.

[89] S. D. Bull, S. G. Davies, S. Jones, M. E. C. Polywka, R. S. Prasad, H. J. Sanganee, *Synlett*, **1998**, 519.

[90] M. C. Pirrung, S. W. Shuey, *J. Org. Chem.*, **1994**, *59*, 3890.

[91a] J. P. Wolfe, R. A. Singer, B. H. Yang, S. L. Buchwald, *J. Am. Chem. Soc.*, **1999**, *121*, 9550; [91b] M. Watanabe, M. Nishiyama, T. Yamamoto, Y. Koie, *Tetrahedron Lett.*, **2000**, *41*, 481; [91c] M. Sasaki, H. Fuwa, M. Inoue, K. Tachibana, *Tetrahedron Lett.*, **1998**, *39*, 9027; [91d] N. Yasuda, L. Xavier, D. L. Rieger, Y. Li, A. E. DeCamp, U.-H. Dolling, *Tetrahedron Lett.*, **1993**, *34*, 3211.

[92] B. B. Snider, H. Lin, *J. Am. Chem. Soc.*, **1999**, *121*, 7778.

[93] T. Hayashi, M. Konishi, M. Fukushima, K. Kanehira, T. Hioki, M. Kumada, *J. Org. Chem.*, **1983**, *48*, 2195.

[94] R. F. Borch, A. I. Hassid, *J. Org. Chem.*, **1972**, *37*, 1673.

[95] P. C. B. Page, H. Heaney, G. A. Rassias, S. Reignier, E. P. Sampler, S. Talib, *Synlett*, **2000**, 104.

[96] J. Beliczey, G. Giffels, U. Kragl, C. Wandrey, *Tetrahedron: Asymmetry*, **1997**, *8*, 1529.

[97] S. G. Davies, H. J. Sanganee, *Tetrahedron: Asymmetry*, **1995**, *6*, 671.

[98] D. A. Evans, T. C. Britton, J. A. Ellman, *Tetrahedron Lett.*, **1987**, *28*, 6141.

[99] K. Soai, H. Oyamada, M. Takase, *Bull. Chem. Soc. Jpn.*, **1984**, *57*, 2327.

[100] H. Matsunaga, T. Ishizuka, T. Kunieda, *Tetrahedron*, **1997**, *53*, 1275.

[101] J. R. Gage, D. A. Evans, *Org. Synth.*, **1989**, *68*, 83.

[102] D. C. Sherrington, *Chem. Commun.*, **1998**, 2275.

[103] D. C. Sherrington, *British Polymer Journal*, **1984**, *16*, 164.

[104] D. C. Sherrington, *Macromolecular Syntheses*, **1982**, *8*, 69.

[105] B. Carboni, C. Pourbaix, F. Carreaux, H. Deleuze, B. Maillard, *Tetrahedron Lett.*, **1999**, *40*, 7979.

[106] J. A. Riddick, W. B. Burger, *Techniques of Chemistry, Volume III*, **1970**, John Wiley and Sons, New York.

[107] T. A. Crabb, M. J. Hall, R. O. Williams, *Tetrahedron*, **1973**, *29*, 3389.

[108] M. Huche, J. Aubouet, G. Pourcelot, J. Berlan, *Tetrahedron Lett.*, **1983**, *24*, 585.

[109] D. R. Wright, L. B. Sims, A. Fry, *J. Am. Chem. Soc.*, **1983**, *105*, 3714.

[110] J. C. Craig, K. K. Purushothaman, *J. Org. Chem.*, **1970**, *35*, 1721.

[111] D. H. Williams, I. Fleming, *Spectroscopic Methods in Organic Chemistry*, **1995**, McGraw-Hill Publishing Company, London.

[112] S.-K. Kang, S.-C. Choi, H.-C. Ryu, T. Yamaguchi, *J. Org. Chem.*, **1998**, *63*, 5748.

[113] G. Roussi, J. Zhang, *Tetrahedron*, **1991**, *47*, 5161.

[114] A. Goosen, C. W. McCleland, A. M. Sipamla, *J. Chem. Research (S)*, **1995**, 18.

[115] A. R. Gangloff, T. M. Judge, P. Helquist, *J. Org. Chem.*, **1990**, *55*, 3679.

[116] J. P. Ferris, R. D. Gerwe, G. R. Gapski, *J. Org. Chem.*, **1968**, *33*, 3493.

[117] K. Gollnick, J. H. E. Lindner, *Tetrahedron Lett.*, **1973**, *21*, 1903.

[118] R. Noyori, M. Kitamura, *Angew. Chem., Int. Ed. Engl.*, **1991**, *30*, 49.

[119] M. Kitamura, S. Suga, K. Kawai, R. Noyori, *J. Am. Chem. Soc.*, **1986**, *108*, 6071.

[120a] M. Kitamura, S. Okada, S. Suga, R. Noyori, *J. Am. Chem. Soc.*, **1989**, *111*, 4028;

[120b] E. J. Corey, F. J. Hannon, *Tetrahedron Lett.*, **1987**, *28*, 5237.

[121] G. Procter, *Asymmetric Synthesis*, **1996**, Oxford University Press, New York.

[122] D. Heller, H.-J. Drexler, C. Fischer, H. Buschmann, W. Baumann, B. Heller, *Angew. Chem., Int. Ed. Engl.*, **2000**, *39*, 495.

[123] P. A. Chaloner, E. Langadianou, *Tetrahedron Lett.*, **1990**, *31*, 5185.

[124] M. Laspéras, N. Bellocq, D. Brunel, P. Moreau, *Tetrahedron: Asymmetry*, **1998**, *9*, 3053.

[125] M. J. McKennon, A. I. Meyers, *J. Org. Chem.*, **1993**, *58*, 3568.

[126] D. Guijarro, P. Pinho, P. G. Andersson, *J. Org. Chem.*, **1998**, *63*, 2530.

[127] M. Palmer, T. Walsgrove, M. Willis, *J. Org. Chem.*, **1997**, *62*, 5226.

[128] C. L. Gibson, *Tetrahedron: Asymmetry*, **1999**, *10*, 1551.

[129] G. Bringmann, M. Breuning, *Tetrahedron: Asymmetry*, **1998**, *9*, 667.

[130] D. A. Evans, J. A. Ellman, R. L. Dorow, *Tetrahedron Lett.*, **1987**, *28*, 1123.

[131] D. A. Evans, E. B. Sjogren, J. Bartroli, R. L. Dow, *Tetrahedron Lett.*, **1986**, *27*, 4957.

[132a] S. G. Davies, G. J.-M. Doisneau, J. C. Prodger, H. J. Sanganee, *Tetrahedron Lett.*, **1994**, *35*, 2369; [132b] S. G. Davies, G. J.-M. Doisneau, J. C. Prodger, H. J. Sanganee, *Tetrahedron Lett.*, **1994**, *35*, 2373; [132c] J, Ezquerra, A. Rubio, J. Martín, J. L. G. Navío, *Tetrahedron: Asymmetry*, **1997**, *8*, 669.

[133] S. D. Bull, S. G. Davies, S. Jones, H. J. Sanganee, *J. Chem. Soc., Perkin Trans. 1*, **1999**, 387.

[134] S. G. Davies, H. J. Sanganee, P. Szolcsanyi, *Tetrahedron*, **1999**, *55*, 3337.

[135] H, Danda, M. H. Hansen, C. H. Heathcock, *J. Org. Chem.*, **1990**, *55*, 173.

[136] D. A. Evans, J. V. Nelson, E. Vogel, T. R. Taber, *J. Am. Chem. Soc.*, **1981**, *103*, 3099.

[137] S. Masamune, W. Choy, F. A. J. Kerdesky, B. Imperiali, *J. Am. Chem. Soc.*, **1981**, *103*, 1566.

[138] T. Hintermann, D. Seebach, *Helv. Chim. Acta*, **1998**, *81*, 2093.

[139] F. Langer, K. Püntener, R. Stürmer, P. Knochel, *Tetrahedron: Asymmetry*, **1997**, *8*, 715.

[140] A. D. Hughes, D. A. Price, N. S. Simpkins, *J. Chem. Soc., Perkin Trans. 1*, **1999**, 1295.

[141] T. Harada, H. Kurakawa, Y. Kagamihara, S. Tanaka, A. Inoue, A. Oku, *J. Org. Chem.*, **1992**, *57*, 1412.

[142] A. W. Czarnik, *Biotechnol. Bioeng.*, (*Comb Chem*), **1998**, *61*, 77.

[143] J. Leonard, B. Lygo, G. Procter, *Advanced Practical Organic Chemistry*, **1990**, Blackie, London.

HPLC Traces for Ester 180

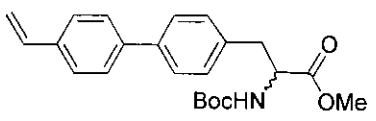

rac-**180**

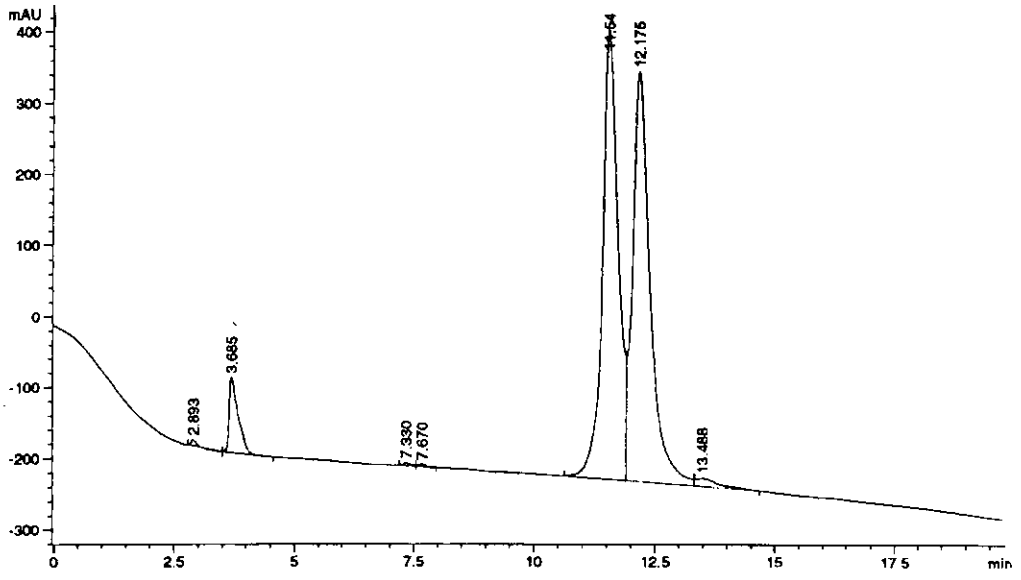

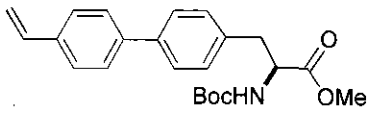

180

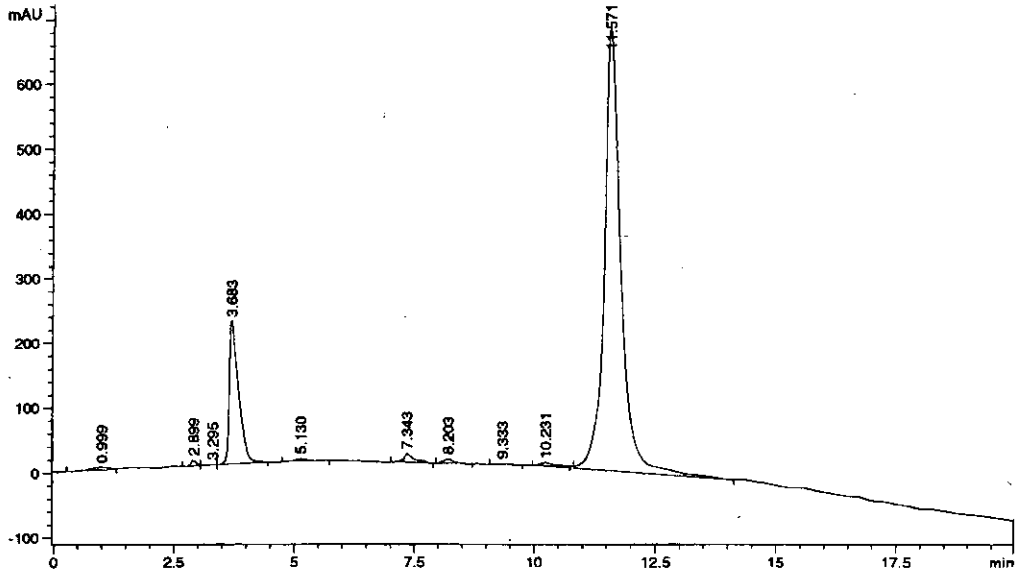

HPLC Traces for Alcohol 181

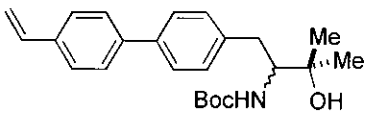

rac-**181**

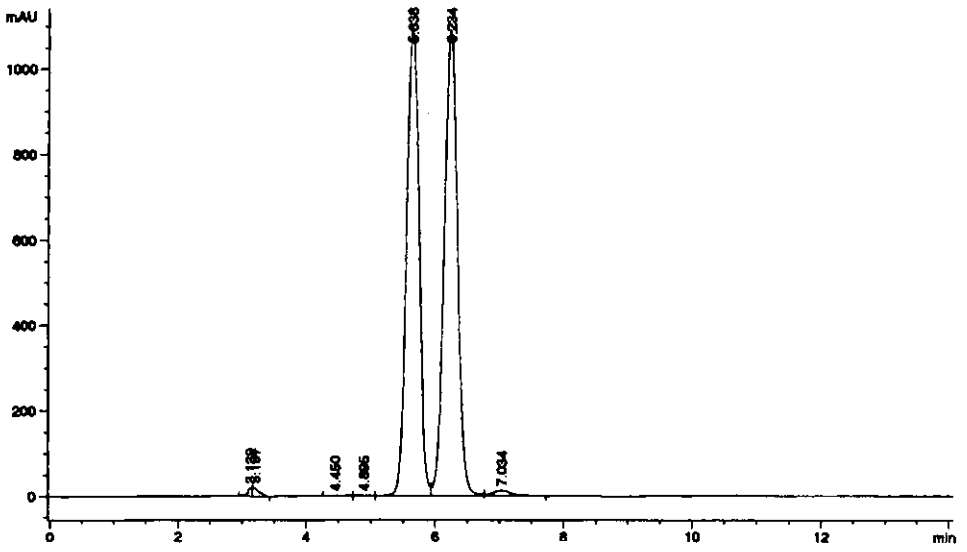

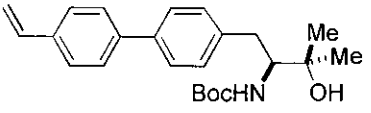

181

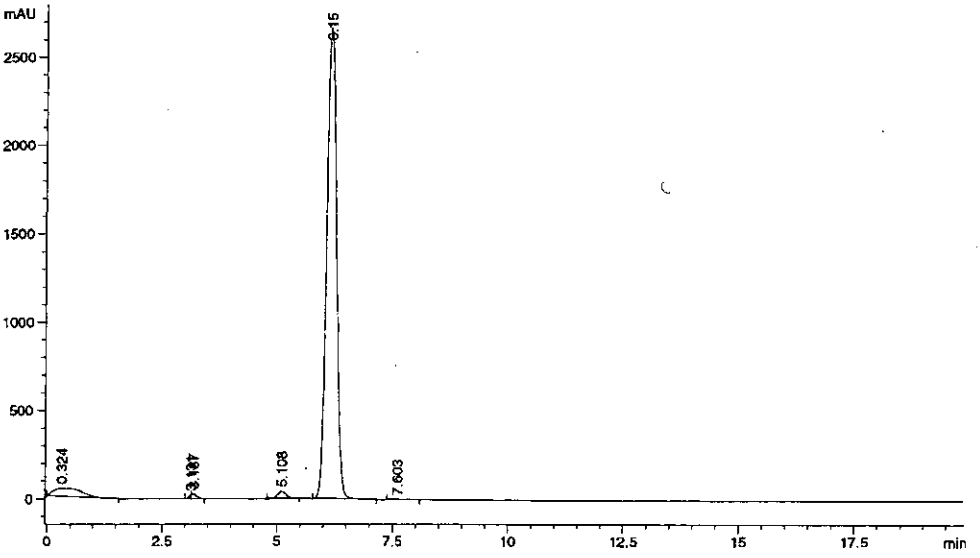

HPLC Traces for Alcohol 70

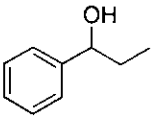

rac-**70**

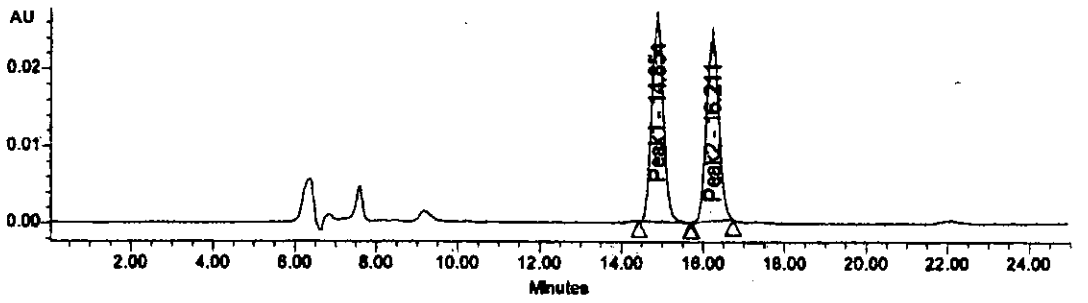

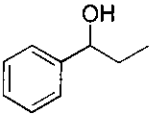

70 (56% e.e. *S*)

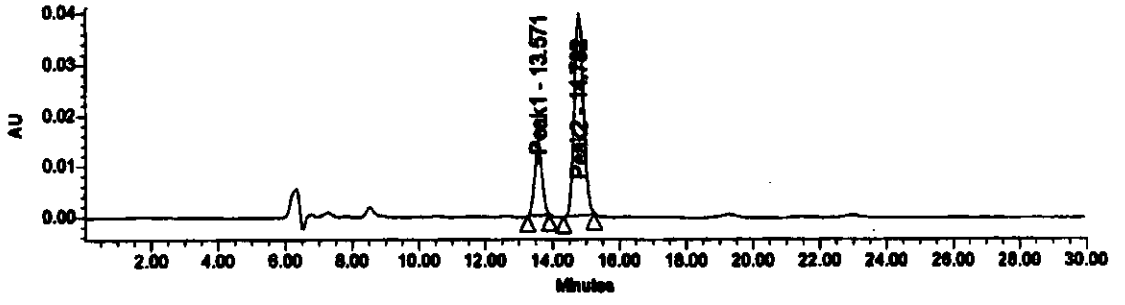

HPLC Traces for Alcohol 286

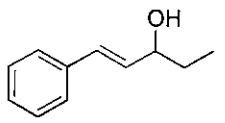

rac-**286**

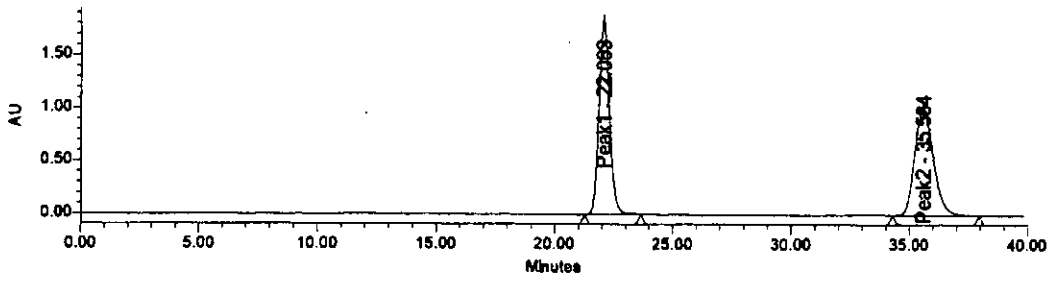

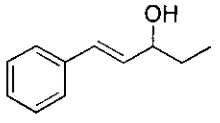

286 (45% e.e. *S*)

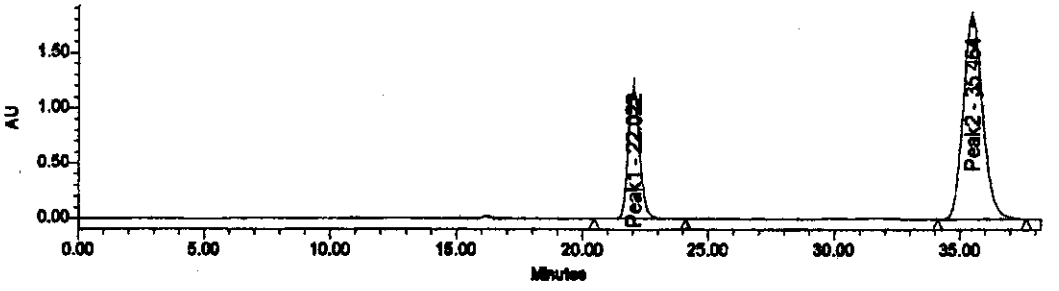

Infra-red Spectrum of Polymer-Bound Oxazolidinone 218

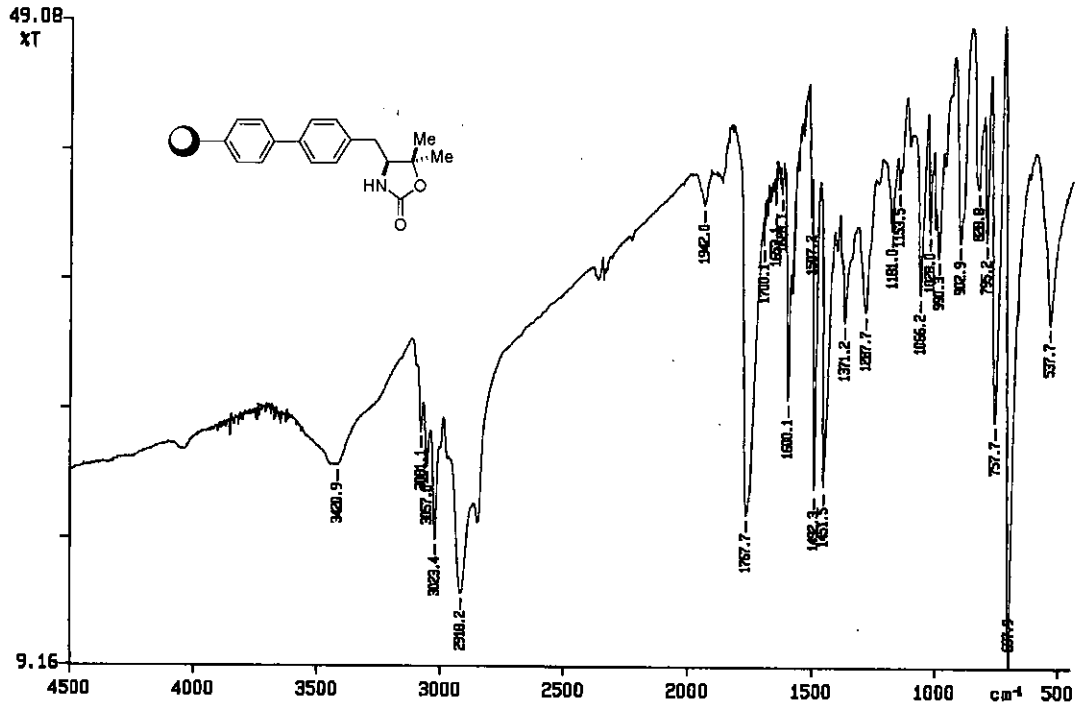

Infra-red Spectrum of Polymer-Bound *N*-Propionylated Oxazolidinone 324

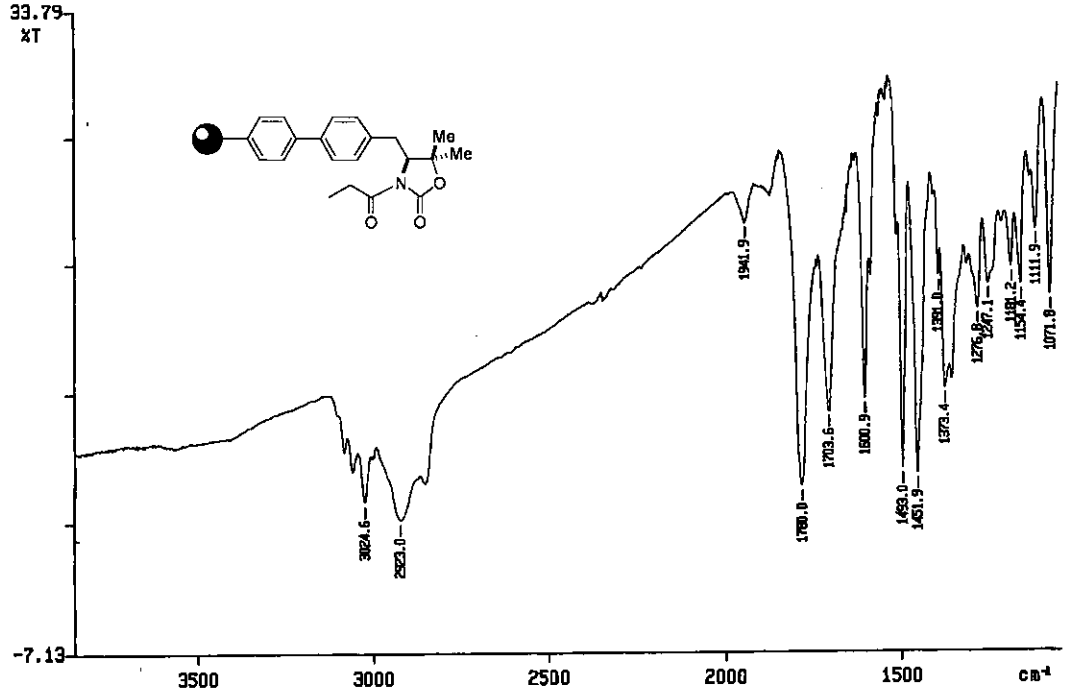

Infra-red Spectrum of Polymer-Bound Aldol Adduct 325

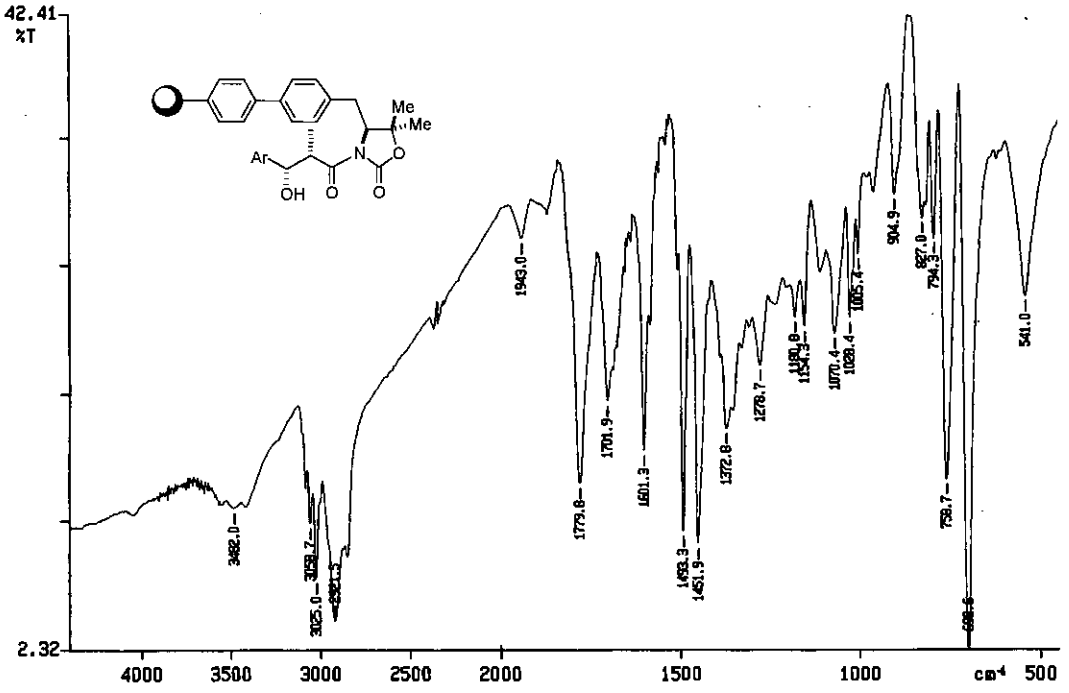

X-ray Crystal Structure of 123

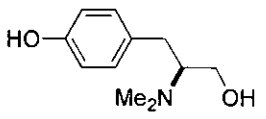

123

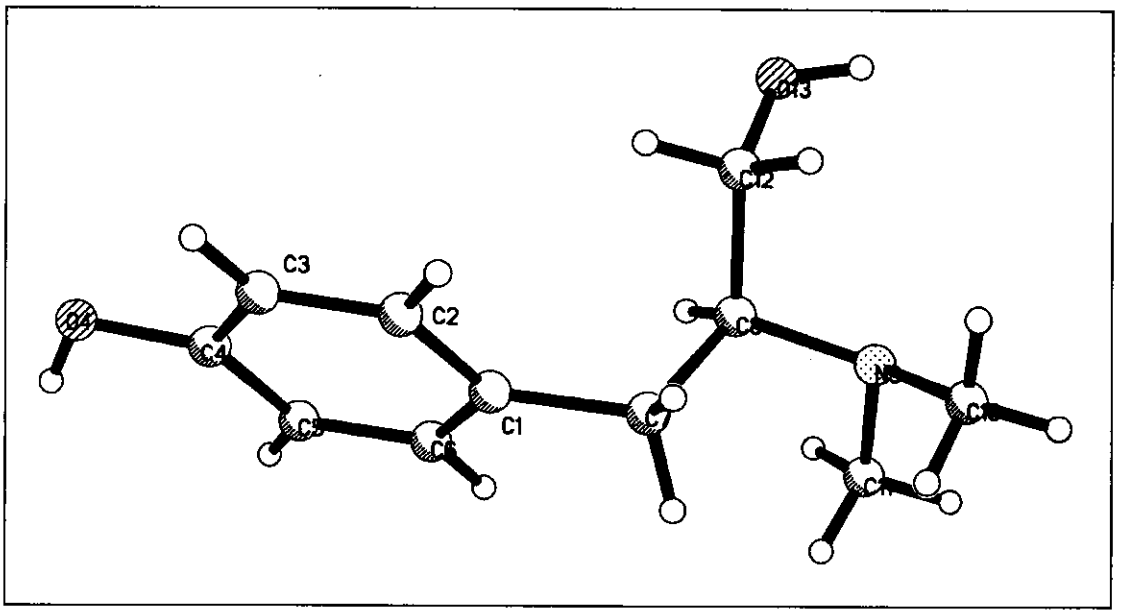

Table 1 - Crystal data and structure refinement for **123**.

Part A: Crystal data	
Empirical formula	$C_{11}H_{17}NO_2$
Formula weight	195.26
Wavelength	0.71073 / 1.54184 / 2.2909 Å
Temperature	273 (2) K
Crystal system	Orthorhombic
Space group	P21212
Unit cell dimensions	a = 9.6449 (5) Å alpha = 90 deg. b = 19.9559 (11) Å beta = 90 deg. c = 5.7812 (4) Å gamma = 90 deg.
Volume	1112.72 (11) $Å^3$
Number of reflections for cell	4826 (2 < theta < 27.5 deg.)
Z	4
Density (calculated)	1.166 Mg / m^3
Absorption coefficient	0.640 mm^{-1}
F (000)	424
Part B: Data collection	
Crystal description	Colourless plate
Crystal size	0.89 × 0.78 × 0.12 mm
Theta range for data collection	2.04 to 74.85 deg.
Index ranges	$-10 \leq h \leq 12$, $0 \leq k \leq 26$, $0 \leq l \leq 7$
Independent reflections	4168 [R (int) = 0.0000]
Part C: Solution and refinement	
Solution	direct (SHELXS-97 (Sheldrick, 1990))
Refinement type	Full-matrix least squares on F^2
Program used for refinement	SHELXL-97
Hydrogen atom placement	geometric
Hydrogen atom treatment	riding
Data / restraints / parameters	4168 / 0 / 134

Goodness of fit on F^2	1.035
Conventional R [F>4sigma (F)]	R1 = 0.0531 [3724 data]
Weighted R (F^2 and all data)	wR2 = 0.1554
Absolute structure parameters	0.0 (2)
Extinction coefficient	0.0057 (9)
Final maximum delta / sigma	0.027
Weighting scheme	calc w = 1 / [\s^2^(Fo^2^) + (0.01294P)^2^ + 0.0000P] where P = (Fo^2^ + 2Fc^2^) / 3
Largest diff. peak and hole	0.181 and -0.186 e.Å^-3

Table 2 - Atomic coordinates ($\times 10^4$) and equivalent isotropic displacement parameters ($Å^2 \times 10^3$) for **123**. U(eq) is defined as one third of the trace of the orthogonalised Uij tensor.

	x	**y**	**z**	**U (eq)**
C (1)	2148 (2)	7702 (1)	13787 (2)	44 (1)
C (2)	1248 (2)	7171 (1)	14144 (3)	57 (1)
C (3)	1186 (2)	6639 (1)	12646 (3)	62 (1)
O (4)	1885 (1)	6078 (1)	9263 (2)	68 (1)
C (4)	2014 (2)	6617 (1)	10694 (3)	50 (1)
C (5)	2943 (2)	7136 (1)	10319 (2)	50 (1)
C (6)	2991 (2)	7670 (1)	11830 (2)	48 (1)
C (7)	2192 (2)	8296 (1)	15398 (2)	50 (1)
C (8)	1419 (1)	8914 (1)	14415 (2)	40 (1)
N (9)	1872 (1)	9564 (1)	15347 (2)	51 (1)
C (10)	1862 (3)	9591(1)	17858 (3)	86 (1)
C (11)	3260 (2)	9741 (1)	14461 (5)	84 (1)
C (12)	-130 (2)	8826 (1)	14686 (3)	52 (1)
O (13)	-890 (1)	9267 (1)	13226 (2)	57 (1)

Table 3 - Bond lengths (Å) for **123**.

Bond	Length (Å)
C(1)-C(2)	1.3843 (19)
C(1)-C(6)	1.3951 (19)
C(1)-C(7)	1.5088 (17)
C(2)-C(3)	1.371 (2)
C(3)-C(4)	1.383 (2)
O(4)-C(4)	1.3633 (17)
C(4)-C(5)	1.3867 (18)
C(5)-C(6)	1.3778 (17)
C(7)-C(8)	1.5474 (16)
C(8)-N(9)	1.4722 (16)
C(8)-C(12)	1.512 (2)
N(9)-C(10)	1.452 (2)
N(9)-C(11)	1.476 (2)
C(12)-O(13)	1.4239 (16)

Table 4 - Bond angles (degrees) for **123**.

Bond	Angle (degrees)
C(2)-C(1)-C(6)	116.82 (12)
C(2)-C(1)-C(7)	121.82 (12)
C(6)-C(1)-C(7)	121.34 (12)
C(3)-C(2)-C (1)	121.70 (13)
C(2)-C(3)-C(4)	121.00 (13)
O(4)-C(4)-C(3)	117.90 (12)
O(4)-C(4)-C(5)	123.66 (13)
C(3)-C(4)-C(5)	118.43 (13)
C(6)-C(5)-C(4)	120.04 (12)
C(5)-C(6)-C(1)	121.97 (12)

C(1)-C(7)-C(8)	112.71 (11)
N(9)-C(8)-C(12)	110.93 (10)
N(9)-C(8)-C(7)	115.15 (10)
C(12)-C(8)-C(7)	110.21 (11)
C(10)-N(9)-C(8)	113.34 (13)
C(10)-N(9)-C(11)	110.13 (18)
C(8)-N(9)-C(11)	110.64 (14)
O(13)-C(12)-C(8)	112.07 (12)

X-ray Crystal Structure of 204

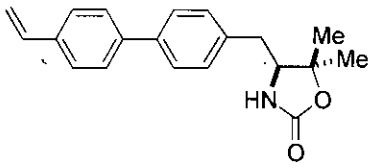

204

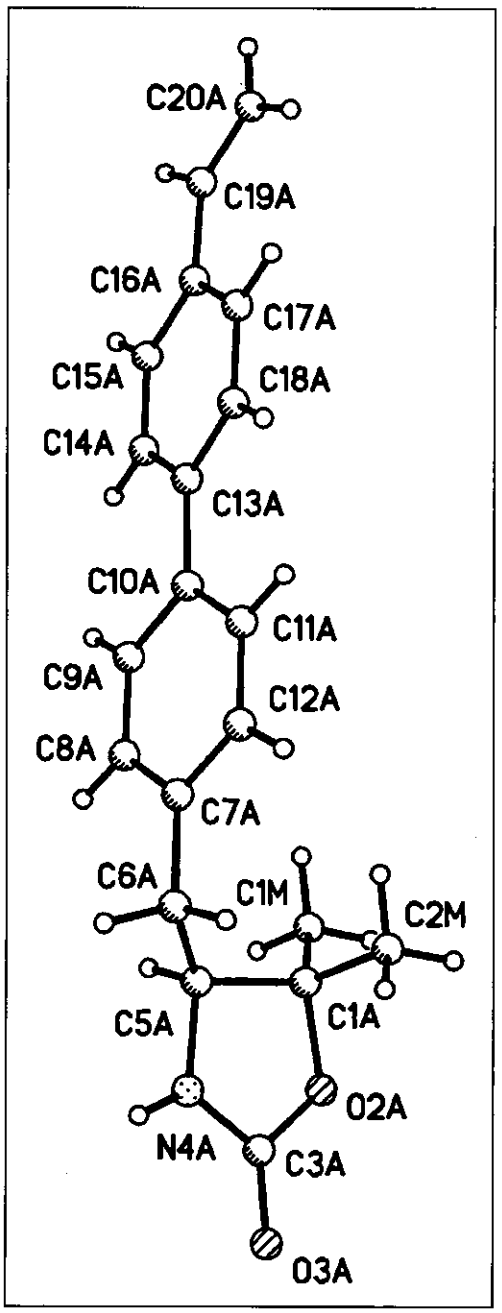

Table 1 - Crystal data and structure refinement for **204**.

Part A: Crystal data	
Empirical formula	$C_{20}H_{21}NO_2$
Formula weight	307.38
Wavelength	1.54178 Å
Temperature	150 (2) K
Crystal system	Monoclinic
Space group	P21
Unit cell dimensions	a = 6.121 (3) Å alpha = 90 deg. b = 31.556 (10) Å beta = 103.05 (2) deg. c = 8.649 (5) Å gamma = 90 deg.
Volume	1627.6 (13) $Å^3$
Number of reflections for cell	17 (20 < theta < 22 deg.)
Z	4
Density (calculated)	1.254 Mg / m^3
Absorption coefficient	0.637 mm^{-1}
F (000)	656
Part B: Data collection	
Crystal description	Colourless block
Crystal size	0.38 × 0.35 × 0.12 mm
Theta range for data collection	2.80 to 60.04 deg.
Index ranges	$-6 \leq h \leq 6, -15 \leq k \leq 35, -2 \leq l \leq 9$
Reflections collected	2548
Independent reflections	2425 [R (int) = 0.0476]
Scan type	Omega-theta
Part C: Solution and refinement	
Solution	direct (SIR92)
Refinement type	Full-matrix least squares on F^2
Program used for refinement	SHELXL-97
Hydrogen atom placement	calc

Hydrogen atom treatment	riding
Data / restraints / parameters	2425 / 495 / 412
Goodness of fit on F^2	1.005
Conventional R [F>4sigma (F)]	R1 = 0.0858 [1095 data]
Weighted R (F^2 and all data)	wR2 = 0.2359
Absolute structure parameters	0.2 (11)
Final maximum delta / sigma	0.006
Weighting scheme	calc w = 1 / [\s^2^(Fo^2^) + (0.1038P)^2^ + 0.0000P] where P = (Fo^2^ + 2Fc^2^) / 3
Largest diff. peak and hole	0.244 and -0.244 e.Å^-3

Table 2 - Atomic coordinates ($\times 10^4$) and equivalent isotropic displacement parameters ($Å^2 \times 10^3$) and site occupancies for **204**. U(eq) is defined as one third of the trace of the orthogonalised Uij tensor.

	x	y	z	U (eq)	Occ
C (1A)	7250 (20)	5544 (4)	1734 (13)	53 (3)	1
C (1M)	9633 (19)	5491 (4)	1558 (16)	62 (3)	1
C (2M)	5560 (20)	5415 (4)	274 (14)	62 (4)	1
O (2A)	6910 (14)	5997 (3)	1999 (9)	55 (2)	1
O (3A)	4896 (16)	6376 (3)	3384 (9)	59 (2)	1
C (3A)	5680 (20)	6044 (4)	3108 (14)	59 (4)	1
N (4A)	5594 (18)	5673 (3)	3845 (11)	57 (3)	1
C (5A)	6920 (20)	5339 (3)	3307 (14)	57 (3)	1
C (6A)	5690 (20)	4917 (3)	3156 (15)	56 (3)	1
C (7A)	6840 (20)	4547 (4)	2674 (14)	48 (3)	1
C (8A)	8950 (20)	4429 (4)	3423 (13)	56 (3)	1
C (9A)	10070 (20)	4091 (4)	2967 (14)	56 (3)	1
C (10A)	9014 (18)	3833 (3)	1681 (13)	42 (3)	1

C (11A)	6890 (20)	3954 (4)	939 (15)	53 (3)	1
C (12A)	5830 (20)	4301 (4)	1380 (13)	52 (3)	1
C (13A)	10140 (20)	3448 (3)	1236 (15)	49 (3)	1
C (14A)	12380 (20)	3356 (4)	1860 (14)	48 (3)	1
C (15A)	13380 (20)	3006 (4)	1404 (15)	59 (3)	1
C (16A)	12280 (20)	2728 (4)	264 (15)	52 (3)	1
C (17A)	10000 (20)	2817 (4)	-343 (16)	62 (4)	1
C (18A)	8900 (20)	3159 (4)	121 (14)	57 (3)	1
C (19A)	13380 (20)	2368 (4)	-278 (15)	65 (4)	1
C (20A)	12610 (30)	2109 (4)	-1417 (16)	68 (4)	1
C (1B)	19480 (20)	1440 (4)	-7901 (12)	50 (3)	1
C (3M)	18470 (20)	1566 (4)	-9659 (14)	71 (4)	1
C (4M)	21953 (18)	1433 (4)	-7477 (15)	62 (4)	1
O (2B)	18704 (15)	1006 (3)	-7737 (9)	62 (2)	1
O (3B)	17400 (16)	636 (3)	-5933 (10)	67 (3)	1
C (3B)	17940 (20)	973 (4)	-6372 (15)	59 (3)	1
N (4B)	17907 (19)	1358 (3)	-5734 (11)	58 (3)	1
C (5B)	18280 (20)	1699 (3)	-6796 (14)	50 (3)	1
C (6B)	19610 (20)	2078 (4)	-5967 (16)	63 (4)	1
C (7B)	18320 (20)	2423 (4)	-5397 (15)	54 (3)	1
C (8B)	18870 (20)	2835 (4)	-5604 (14)	59 (3)	1
C (9B)	17860 (20)	3166 (4)	-5054 (14)	59 (3)	1
C (10B)	16080 (20)	3111 (4)	-4298 (15)	53 (3)	1
C (11B)	15490 (30)	2691 (4)	-4099 (17)	70 (4)	1
C (12B)	16610 (20)	2355 (4)	-4631 (17)	69 (4)	1
C (13B)	14970 (20)	3475 (4)	-3676 (14)	56 (3)	1
C (14B)	15620 (20)	3897 (4)	-3845 (14)	62 (3)	1
C (15B)	14490 (30)	4222 (4)	-3328 (15)	74 (4)	1
C (16B)	12650 (30)	4168 (4)	-2697 (16)	74 (4)	1
C (17B)	12070 (20)	3745 (4)	-2501 (14)	72 (4)	1

C (18B)	13140 (20)	3410 (4)	-2976 (15)	63 (3)	1
C (19B)	11670 (60)	4564 (7)	-2320 (50)	80 (6)	0.50
C (20B)	10060 (40)	4611 (8)	-1670 (30)	47 (7)	0.50
C (21B)	11260 (60)	4474 (7)	-2100 (50)	80 (6)	0.50
C (22B)	11190 (60)	4866 (7)	-2260 (40)	98 (11)	0.50

Table 3 - Bond lengths (Å) for **204**.

Bond	**Length (Å)**
C(1A)-O(2A)	1.470 (12)
C(1A)-C(2M)	1.496 (14)
C(1A)-C(1M)	1.510 (14)
C(1A)-C(5A)	1.560 (14)
O(2A)-C(3A)	1.355 (11)
O(3A)-C(3A)	1.201 (12)
C(3A)-N(4A)	1.338 (13)
N(4A)-C(5A)	1.467 (12)
C(5A)-C(6A)	1.523 (14)
C(6A)-C(7A)	1.474 (14)
C(7A)-C(8A)	1.357 (14)
C(7A)-C(12A)	1.388 (13)
C(8A)-C(9A)	1.372 (14)
C(9A)-C(10A)	1.411 (13)
C(10A)-C(11A)	1.367 (14)
C(10A)-C(13A)	1.490 (13)
C(11A)-C(12A)	1.372 (13)
C(13A)-C(14A)	1.385 (14)
C(13A)-C(18A)	1.417 (15)
C(14A)-C(15A)	1.364 (14)
C(15A)-C(16A)	1.375 (15)

C(16A)-C(17A)	1.404 (16)
C(16A)-C(19A)	1.453 (14)
C(17A)-C(18A)	1.378 (14)
C(19A)-C(20A)	1.284 (15)
C(1B)-O(2B)	1.464 (12)
C(1B)-C(4M)	1.477 (14)
C(1B)-C(3M)	1.559 (14)
C(1B)-C(5B)	1.560 (14)
O(2B)-C(3B)	1.369 (12)
O(3B)-C(3B)	1.199 (12)
C(3B)-N(4B)	1.338 (13)
N(4B)-C(5B)	1.466 (12)
C(5B)-C(6B)	1.530 (13)
C(6B)-C(7B)	1.495 (14)
C(7B)-C(8B)	1.367 (14)
C(7B)-C(12B)	1.371 (14)
C(8B)-C(9B)	1.355 (14)
C(9B)-C(10B)	1.401 (14)
C(10B)-C(11B)	1.393 (14)
C(10B)-C(13B)	1.494 (14)
C(11B)-C(12B)	1.396 (14)
C(13B)-C(14B)	1.406 (14)
C(13B)-C(18B)	1.407 (15)
C(14B)-C(15B)	1.368 (15)
C(15B)-C(16B)	1.369 (16)
C(16B)-C(17B)	1.403 (16)
C(16B)-C(19B)	1.453 (18)
C(16B)-C(21B)	1.455 (18)
C(17B)-C(18B)	1.356 (15)
C(19B)-C(20B)	1.253 (19)

C(21B)-C(22B)	1.25 (2)

Table 4 - Bond angles (degrees) for **204**.

Bond	**Angle (degrees)**
O(2A)-C(1A)-C(2M)	107.5 (10)
O(2A)-C(1A)-C(1M)	107.2 (9)
C(2M)-C(1A)-C(1M)	112.6 (10)
O(2A)-C(1A)-C(5A)	102.4 (8)
C(2M)-C(1A)-C(5A)	115.0 (10)
C(1M)-C(1A)-C(5A)	111.2 (10)
C(3A)-O(2A)-C(1A)	109.8 (9)
O(3A)-C(3A)-N(4A)	127.5 (11)
O(3A)-C(3A)-O(2A)	123.2 (12)
N(4A)-C(3A)-O(2A)	109.2 (10)
C(3A)-N(4A)-C(5A)	113.1 (9)
N(4A)-C(5A)-C(6A)	111.0 (10)
N(4A)-C(5A)-C(1A)	99.8 (8)
C(6A)-C(5A)-C(1A)	116.5 (10)
C(7A)-C(6A)-C(5A)	117.2 (10)
C(8A)-C(7A)-C(12A)	115.9 (11)
C(8A)-C(7A)-C(6A)	123.2 (11)
C(12A)-C(7A)-C(6A)	120.9 (11)
C(7A)-C(8A)-C(9A)	123.9 (12)
C(8A)-C(9A)-C(10A)	120.3 (11)
C(11A)-C(10A)-C(9A)	115.3 (10)
C(11A)-C(10A)-C(13A)	123.5 (10)
C(9A)-C(10A)-C(13A)	121.2 (10)
C(10A)-C(11A)-C(12A)	123.5 (12)
C(11A)-C(12A)-C(7A)	121.0 (11)

C(14A)-C(13A)-C(18A)	117.4 (11)
C(14A)-C(13A)-C(10A)	123.0 (11)
C(18A)-C(13A)-C(10A)	119.6 (10)
C(15A)-C(14A)-C(13A)	121.7 (12)
C(14A)-C(15A)-C(16A)	123.1 (12)
C(15A)-C(16A)-C(17A)	115.1 (11)
C(15A)-C(16A)-C(19A)	122.9 (12)
C(17A)-C(16A)-C(19A)	122.0 (12)
C(18A)-C(17A)-C(16A)	123.9 (12)
C(17A)-C(18A)-C(13A)	118.7 (12)
C(20A)-C(19A)-C(16A)	129.0 (14)
O(2B)-C(1B)-C(4M)	107.4 (10)
O(2B)-C(1B)-C(3M)	105.5 (9)
C(4M)-C(1B)-C(3M)	113.9 (10)
O(2B)-C(1B)-C(5B)	102.9 (8)
C(4M)-C(1B)-C(5B)	116.9 (10)
C(3M)-C(1B)-C(5B)	109.0 (10)
C(3B)-O(2B)-C(1B)	109.7 (9)
O(3B)-C(3B)-N(4B)	130.0 (11)
O(3B)-C(3B)-O(2B)	121.0 (11)
N(4B)-C(3B)-O(2B)	109.0 (10)
C(3B)-N(4B)-C(5B)	112.9 (9)
N(4B)-C(5B)-C(6B)	114.9 (10)
N(4B)-C(5B)-C(1B)	99.2 (8)
C(6B)-C(5B)-C(1B)	115.1 (10)
C(7B)-C(6B)-C(5B)	117.3 (10)
C(8B)-C(7B)-C(12B)	116.8 (12)
C(8B)-C(7B)-C(6B)	118.9 (11)
C(12B)-C(7B)-C(6B)	124.3 (11)
C(9B)-C(8B)-C(7B)	122.7 (12)

C(8B)-C(9B)-C(1OB)	122.2 (12)
C(11B)-C(1OB)-C(9B)	115.2 (11)
C(11B)-C(1OB)-C(13B)	122.3 (11)
C(9B)-C(1OB)-C(13B)	122.4 (11)
C(1OB)-C(11B)-C(12B)	121.4 (12)
C(7B)-C(12B)-C(11B)	121.6 (12)
C(14B)-C(13B)-C(18B)	116.9 (11)
C(14B)-C(13B)-C(1OB)	121.9 (11)
C(18B)-C(13B)-C(1OB)	121.0 (11)
C(15B)-C(14B)-C(13B)	120.2 (13)
C(14B)-C(15B)-C(16B)	124.0 (14)
C(15B)-C(16B)-C(17B)	114.9 (13)
C(15B)-C(16B)-C(19B)	113.7 (15)
C(17B)-C(16B)-C(19B)	131.4 (17)
C(15B)-C(16B)-C(21B)	131.3 (16)
C(17B)-C(16B)-C(21B)	113.8 (16)
C(19B)-C(16B)-C(21B)	17.8 (16)
C(18B)-C(17B)-C(16B)	123.6 (14)
C(17B)-C(18B)-C(13B)	120.3 (13)
C(20B)-C(19B)-C(16B)	128 (2)
C(22B)-C(21B)-C(16B)	129 (3)

Note, two crystallographically unique molecules within the structure due to rotation of vinyl moiety.

X-ray Crystal Structure of 208

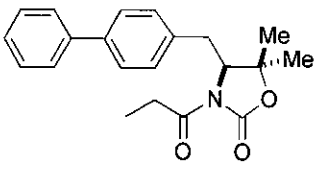

208

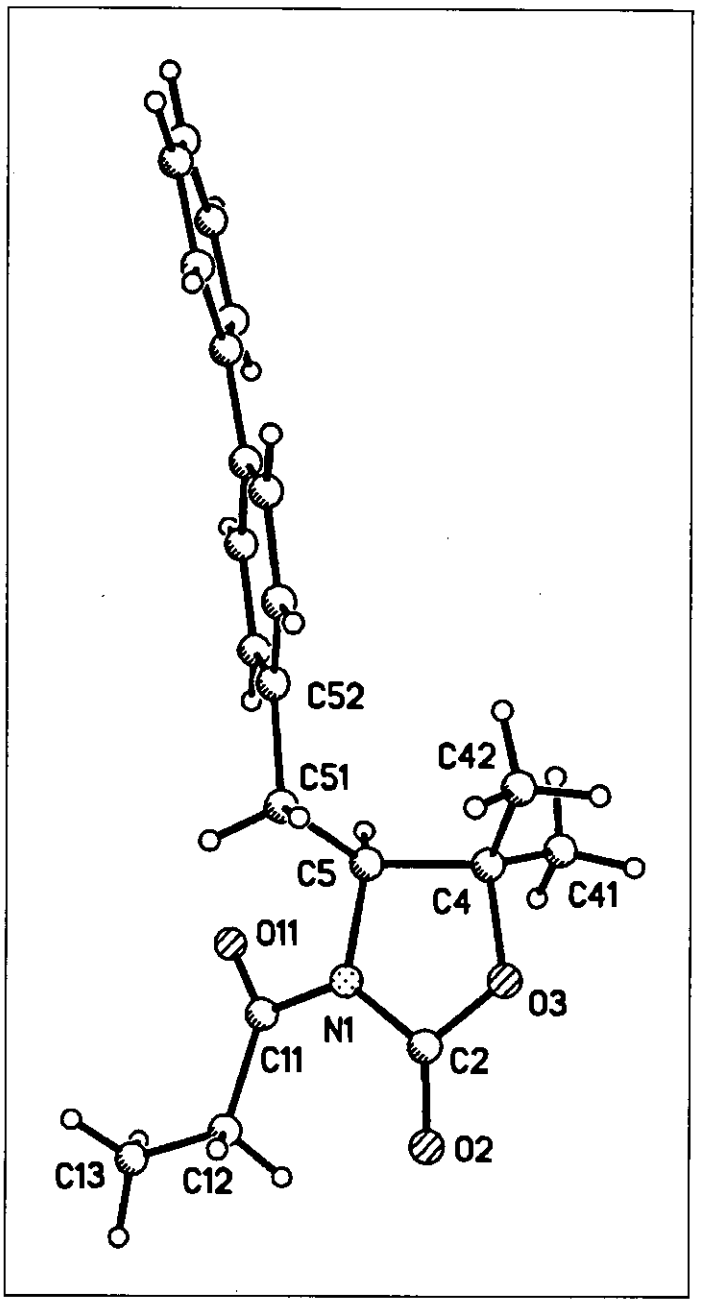

Table 1 - Crystal data and structure refinement for **208**.

Part A: Crystal data	
Empirical formula	$C_{21}H_{23}NO_3$
Formula weight	337.40
Wavelength	0.71073 Å
Temperature	150 (2) K
Crystal system	Orthorhombic
Space group	P212121
Unit cell dimensions	a = 5.7118 (10) Å alpha = 90 deg. b = 8.5309 (15) Å beta = 90 deg. c = 37.011 (6) Å gamma = 90 deg.
Volume	1803.4 (5) $Å^3$
Number of reflections for cell	4874 (2.5 < theta < 29 deg.)
Z	4
Density (calculated)	1.243 Mg / m^3
Absorption coefficient	0.083 mm^{-1}
F (000)	720
Part B: Data collection	
Crystal description	Colourless plate
Crystal size	0.18 × 0.15 × 0.05 mm
Instrument	CCD area detector
Theta range for data collection	1.10 to 25.00 deg.
Index ranges	$-6 \leq h \leq 6$, $-9 \leq k \leq 10$, $-44 \leq l \leq 42$
Reflections collected	9333
Independent reflections	3176 [R (int) = 0.0317]
Scan type	phi and omega scans
Absorption correction	Sadabs (Tmin = 0.839, Tmax = 1)
Part C: Solution and refinement	
Solution	direct (SHELXS-97 (Sheldrick, 1990))
Refinement type	Full-matrix least squares on F^2

Program used for refinement	SHELXL-97
Hydrogen atom placement	geometric
Hydrogen atom treatment	riding
Data / restraints / parameters	3176 / 11 / 253
Goodness of fit on F^2	1.244
Conventional R [F>4sigma (F)]	R1 = 0.0586 [3038 data]
Weighted R (F^2 and all data)	wR2 = 0.1286
Absolute structure parameters	1 (2) (meaningless)
Final maximum delta / sigma	0.089
Weighting scheme	calc w = 1 / [\s^2^(Fo^2^) + (0.0372P)^2^ + 0.8353P] where P = (Fo^2^ + 2Fc^2^) / 3
Largest diff. peak and hole	0.275 and -0.305 e.Å^-3

Table 2 - Atomic coordinates ($\times 10^4$) and equivalent isotropic displacement parameters ($Å^2 \times 10^3$) and site occupancies for **208**. U(eq) is defined as one third of the trace of the orthogonalised Uij tensor.

	x	y	z	U (eq)	Occ
N (1)	1395 (3)	2175 (2)	645 (1)	40 (1)	1
C (11)	1560 (7)	549 (3)	616 (1)	80 (1)	1
O (11)	214 (9)	-165 (4)	819 (1)	96 (2)	0.50
C (12)	3301 (11)	-77 (6)	343 (1)	78 (2)	0.50
C (13)	3831 (17)	-1672 (6)	353 (2)	124 (3)	0.50
O (11')	1039 (9)	-287 (4)	874 (1)	65 (1)	0.50
C (12')	2763 (12)	-160 (7)	285 (1)	142 (3)	0.50
C (13')	4774 (11)	-906 (11)	418 (2)	159 (3)	0.50
C (2)	2029 (3)	3284 (2)	392 (1)	31 (1)	1
O (2)	3119 (3)	3110 (2)	118 (1)	47 (1)	1
O (3)	1289 (2)	4683 (2)	505 (1)	34 (1)	1

C (4)	-260 (3)	4539 (2)	822 (1)	30 (1)	1
C (41)	-2736 (4)	4651 (3)	685 (1)	48 (1)	1
C (42)	362 (5)	5875 (2)	1071 (1)	43 (1)	1
C (5)	272 (4)	2864 (2)	962 (1)	30 (1)	1
C (51)	1807 (4)	2707 (2)	1300 (1)	33 (1)	1
C (52)	435 (3)	2823 (2)	1651 (1)	29 (1)	1
C (53)	-1435 (4)	1818 (2)	1719 (1)	32 (1)	1
C (54)	-2592 (3)	1860 (2)	2048 (1)	31 (1)	1
C (55)	-1969 (3)	2898 (2)	2320 (1)	26 (1)	1
C (56)	-99 (4)	3915 (2)	2246 (1)	31 (1)	1
C (57)	1068 (4)	3868 (2)	1920 (1)	32 (1)	1
C (58)	-3148 (3)	2888 (2)	2679 (1)	27 (1)	1
C (59)	-5329 (4)	2175 (3)	2732 (1)	35 (1)	1
C (60)	-6356 (4)	2131 (3)	3069 (1)	39 (1)	1
C (61)	-5270 (4)	2814 (3)	3363 (1)	38 (1)	1
C (62)	-3130 (4)	3532 (2)	3319 (1)	37 (1)	1
C (63)	-2086 (4)	3571 (2)	2981 (1)	34 (1)	1

Table 3 - Bond lengths (Å) for **208**.

Bond	**Length (Å)**
N(1)-C(2)	1.379 (3)
N(1)-C(11)	1.394 (3)
N(1)-C(5)	1.462 (2)
C(11)-O(11')	1.229 (4)
C(11)-O(11)	1.236 (5)
C(11)-C(12)	1.515 (5)
C(11)-C(12')	1.528 (6)
C(12)-C(13)	1.394 (6)
C(12')-C(13')	1.401 (7)

C(2)-O(2)	1.200 (2)
C(2)-O(3)	1.333 (2)
O(3)-C(4)	1.473 (2)
C(4)-C(41)	1.504 (3)
C(4)-C(42)	1.509 (3)
C(4)-C(5)	1.551 (3)
C(5)-C(51)	1.532 (3)
C(51)-C(52)	1.521 (3)
C(52)-C(57)	1.384 (3)
C(52)-C(53)	1.392 (3)
C(53)-C(54)	1.386 (3)
C(54)-C(55)	1.387 (3)
C(55)-C(56)	1.403 (3)
C(55)-C(58)	1.491 (2)
C(56)-C(57)	1.378 (3)
C(58)-C(63)	1.398 (3)
C(58)-C(59)	1.400 (3)
C(59)-C(60)	1.380 (3)
C(60)-C(61)	1.380 (3)
C(61)-C(62)	1.377 (3)
C(62)-C(63)	1.385 (3)

Table 4 - Bond angles (degrees) for **208**.

Bond	**Angle (degrees)**
C(2)-N(1)-C(11)	127.79 (18)
C(2)-N(1)-C(5)	112.60 (16)
C(11)-N(1)-C(5)	119.44 (18)
O(11')-C(11)-O(11)	24.5 (3)
O(11')-C(11)-N(1)	120.1 (3)

O(11)-C(11)-N(1)	113.7 (3)
O(11')-C(11)-C(12)	118.2 (3)
O(11)-C(11)-C(12)	129.8 (3)
N(1)-C(11)-C(12)	116.5 (3)
O(11')-C(11)-C(12')	120.1 (3)
O(11)-C(11)-C(12')	124.9 (4)
N(1)-C(11)-C(12')	119.1 (3)
C(12)-C(11)-C(12')	14.4 (4)
C(13)-C(12)-C(11)	118.0 (5)
C(13')-C(12')-C(11)	105.6 (5)
O(2)-C(2)-O(3)	122.73 (19)
O(2)-C(2)-N(1)	128.7 (2)
O(3)-C(2)-N(1)	108.55 (15)
C(2)-O(3)-C(4)	111.44 (15)
O(3)-C(4)-C(41)	107.03 (15)
O(3)-C(4)-C(42)	106.37 (16)
C(41)-C(4)-C(42)	112.25 (19)
O(3)-C(4)-C(5)	103.05 (15)
C(41)-C(4)-C(5)	110.80 (18)
C(42)-C(4)-C(5)	116.39 (16)
N(1)-C(5)-C(51)	111.63 (16)
N(1)-C(5)-C(4)	100.76 (14)
C(51)-C(5)-C(4)	117.82 (16)
C(52)-C(51)-C(5)	113.34 (16)
C(57)-C(52)-C(53)	117.85 (17)
C(57)-C(52)-C(51)	121.43 (18)
C(53)-C(52)-C(51)	120.65 (17)
C(54)-C(53)-C(52)	120.59 (18)
C(53)-C(54)-C(55)	122.10 (18)
C(54)-C(55)-C(56)	116.60 (17)

C(54)-C(55)-C(58)	121.83 (17)
C(56)-C(55)-C(58)	121.51 (17)
C(57)-C(56)-C(55)	121.45 (18)
C(56)-C(57)-C(52)	121.41 (19)
C(63)-C(58)-C(59)	117.16 (17)
C(63)-C(58)-C(55)	120.94 (17)
C(59)-C(58)-C(55)	121.89 (17)
C(60)-C(59)-C(58)	121.01 (19)
C(61)-C(60)-C(59)	120.7 (2)
C(62)-C(61)-C(60)	119.60 (19)
C(61)-C(62)-C(63)	119.9 (2)
C(62)-C(63)-C(58)	121.6 (2)

Abbreviations

Ac	acetyl
AIBN	2,2'-azobis-(2-methyl-propionitrile)
APCI	atmospheric pressure chemical ionisation
aq.	aqueous
Ar	aryl
atm	atmosphere
BHT	2,6-di-*tert*-butyl-4-methylphenol
Boc	*tert*-butoxycarbonyl
Bu	butyl
*t*BuOOH	*tert*-butyl hydroperoxide
d	density
DAIB	3-*exo*-(dimethylamino)isoborneol
DCM	dichloromethane
d.e.	diastereomeric excess (i.e. % of major diastereomer - % of minor diastereomers)
DIBAL-H	diisobutylaluminium hydride
DIPEA	diisopropylethylamine
DME	ethylene glycol dimethyl ether
DMF	*N*,*N*-dimethylformamide
DMSO	dimethyl sulphoxide
dppf	1,1'-bis(diphenyl-phosphino)ferrocene
ds	diastereoselectivity
e.e.	enantiomeric excess
EI	electron impact ionisation
Et	ethyl
Ether	diethyl ether
FAB	fast atom bombardment
HPLC	high performance liquid chromatography
HRMS	high resolution mass spectrum

Hz	Hertz
IR	infra-red
L	unspecified ligand
LDA	lithium diisopropylamide
LiHMDS	lithium bis(trimethylsilyl)amide
M	mol dm^{-3}
*m*CPBA	*meta*-chloroperbenzoic acid
Me	methyl
MS	mass spectrometry
MW	molecular weight
NMR	nuclear magnetic resonance
Ph	phenyl
PMHS	polymethylhydrosiloxane
ppm	parts per million
Pr	propyl
PVA	poly(vinyl alcohol)
RedAl	sodium bis(2-methoxyethoxy)aluminium hydride
RPM	revolutions per minute
R_t	retention time for HPLC
TBAF	tetrabutylammonium fluoride
TBDPS	*tert*-butyldiphenylsilyl
Tf	trifluoromethylsulphonate
TFA	trifluoro acetic acid
THF	tetrahydrofuran
t.l.c.	thin layer chromatography
TMS	trimethylsilyl